New Jersey Institute of Technology
Digital Commons @ NJIT

Dissertations | Theses and Dissertations

Spring 1994

Biological denitrification : fundamental kinetic studies, and process analysis for sequencing batch reactor operation

Jun-Hsien Wang
New Jersey Institute of Technology

Follow this and additional works at: https://digitalcommons.njit.edu/dissertations

 Part of the Chemical Engineering Commons

Recommended Citation
Wang, Jun-Hsien, "Biological denitrification : fundamental kinetic studies, and process analysis for sequencing batch reactor operation" (1994). *Dissertations*. 1095.
https://digitalcommons.njit.edu/dissertations/1095

This Dissertation is brought to you for free and open access by the Theses and Dissertations at Digital Commons @ NJIT. It has been accepted for inclusion in Dissertations by an authorized administrator of Digital Commons @ NJIT. For more information, please contact digitalcommons@njit.edu.

Copyright Warning & Restrictions

The copyright law of the United States (Title 17, United States Code) governs the making of photocopies or other reproductions of copyrighted material.

Under certain conditions specified in the law, libraries and archives are authorized to furnish a photocopy or other reproduction. One of these specified conditions is that the photocopy or reproduction is not to be "used for any purpose other than private study, scholarship, or research." If a, user makes a request for, or later uses, a photocopy or reproduction for purposes in excess of "fair use" that user may be liable for copyright infringement,

This institution reserves the right to refuse to accept a copying order if, in its judgment, fulfillment of the order would involve violation of copyright law.

Please Note: The author retains the copyright while the New Jersey Institute of Technology reserves the right to distribute this thesis or dissertation

Printing note: If you do not wish to print this page, then select "Pages from: first page # to: last page #" on the print dialog screen

NJIT New Jersey's Science & Technology University

The Van Houten library has removed some of the personal information and all signatures from the approval page and biographical sketches of theses and dissertations in order to protect the identity of NJIT graduates and faculty.

INFORMATION TO USERS

This manuscript has been reproduced from the microfilm master. UMI films the text directly from the original or copy submitted. Thus, some thesis and dissertation copies are in typewriter face, while others may be from any type of computer printer.

The quality of this reproduction is dependent upon the quality of the copy submitted. Broken or indistinct print, colored or poor quality illustrations and photographs, print bleedthrough, substandard margins, and improper alignment can adversely affect reproduction.

In the unlikely event that the author did not send UMI a complete manuscript and there are missing pages, these will be noted. Also, if unauthorized copyright material had to be removed, a note will indicate the deletion.

Oversize materials (e.g., maps, drawings, charts) are reproduced by sectioning the original, beginning at the upper left-hand corner and continuing from left to right in equal sections with small overlaps. Each original is also photographed in one exposure and is included in reduced form at the back of the book.

Photographs included in the original manuscript have been reproduced xerographically in this copy. Higher quality 6" x 9" black and white photographic prints are available for any photographs or illustrations appearing in this copy for an additional charge. Contact UMI directly to order.

UMI

University Microfilms International
A Bell & Howell Information Company
300 North Zeeb Road, Ann Arbor, MI 48106-1346 USA
313/761-4700 800/521-0600

Reproduced with permission of the copyright owner. Further reproduction prohibited without permission.

Order Number 9427000

Biological denitrification: Fundamental kinetic studies, and process analysis for sequencing batch reactor operation

Wang, Jun-Hsien, Ph.D.

New Jersey Institute of Technology, 1994

Copyright ©1994 by Wang, Jun-Hsien. All rights reserved.

U·M·I
300 N. Zeeb Rd.
Ann Arbor, MI 48106

Reproduced with permission of the copyright owner. Further reproduction prohibited without permission.

ABSTRACT

BIOLOGICAL DENITRIFICATION: FUNDAMENTAL KINETIC STUDIES, AND PROCESS ANALYSIS FOR SEQUENCING BATCH REACTOR OPERATION

by
Jun-Hsien Wang

This study dealt with a detailed investigation of biological denitrification of nitrate and nitrite by a pure culture of *Pseudomonas denitrificans* (ATCC 13867), under anaerobic conditions.

In the first part of the study, the kinetics of denitrification were studied in serum-bottle experiments. It was found that reduction of both nitrate and nitrite follows inhibitory expressions of the Andrews type. It was also found that when nitrite is present at levels above 15 mg/L, nitrite and nitrate are involved in a cross-inhibitory, non-competitive, interaction pattern. Analysis of the kinetic data has shown that the culture used has severe maintenance requirements, which can be described by the model proposed by Herbert. Experiments at different temperatures have revealed that the optimum temperature is around 38 °C. Activation energies have been determined as 8.6 Kcal/mole for nitrate, and 7.21 Kcal/mole for nitrite reduction. Studies on the effect of pH have shown that the optimal value is about 7.5.

Based on the detailed kinetic expressions determined in the first part of the study, denitrification of nitrite and nitrate/nitrite mixtures was theoretically analyzed and experimentally investigated in a continuously operated sequencing batch reactor. The theoretical analysis was based on the bifurcation theory for forced systems. The different types of the dynamical behavior of the system were found, and are presented in the form

Reproduced with permission of the copyright owner. Further reproduction prohibited without permission.

of bifurcation diagrams and two-dimensional operating diagrams. The analysis predicts that there are domains in the operating parameter space where the system can reach different periodic patterns which are determined by the conditions under which the process is started-up. The analysis also predicts that improper selection of operating parameters can lead to high nitrite accumulation in the reactor. The predictions of the theory were tested in experiments with a specially designed system. The unit involved a fully automated 2-liter reactor which operated under different inlet flowrate and concentration conditions. During the experiments the system was perfectly sealed and the medium kept under a helium atmosphere of pressure slightly higher than 1 atm. In all cases, a remarkably good agreement was found between theoretical predictions and experimental data.

The experimentally validated model can be used in process optimization studies, and preliminary scale-up calculations.

Reproduced with permission of the copyright owner. Further reproduction prohibited without permission.

BIOLOGICAL DENITRIFICATION: FUNDAMENTAL KINETIC STUDIES, AND PROCESS ANALYSIS FOR SEQUENCING BATCH REACTOR OPERATION

by
Jun-Hsien Wang

A Dissertation
Submitted to the Faculty of
New Jersey Institute of Technology
in Partial Fulfillment of the Requirements for the Degree of
Doctor of Philosophy

Department of Chemical Engineering,
Chemistry, and Environmental Science

May 1994

Reproduced with permission of the copyright owner. Further reproduction prohibited without permission.

Copyright © 1994 by Jun-Hsien Wang
ALL RIGHTS RESERVED

Reproduced with permission of the copyright owner. Further reproduction prohibited without permission.

APPROVAL PAGE

**BIOLOGICAL DENITRIFICATION:
FUNDAMENTAL KINETIC STUDIES, AND PROCESS ANALYSIS FOR
SEQUENCING BATCH REACTOR OPERATION**

Jun-Hsien Wang

Dr. Bacil C. Baltzis, Dissertation Advisor — Date
Professor of Chemical Engineering, Chemistry, and Environmental Science, NJIT

Dr. Gordon A. Lewandowski, Dissertation Advisor — Date
Professor of Chemical Engineering, Chemistry, and Environmental Science, NJIT

Dr. Ching-Rong Huang, Committee Member — Date
Professor of Chemical Engineering, Chemistry, and Environmental Science, NJIT

Dr. Piero M. Armenante, Committee Member — Date
Professor of Chemical Engineering, Chemistry, and Environmental Science, NJIT

Dr. L. Y. Young, Committee Member — Date
Professor of Microbiology, Rutgers University (New Brunswick, NJ)

Reproduced with permission of the copyright owner. Further reproduction prohibited without permission.

BIOGRAPHICAL SKETCH

Author: Jun-Hsien Wang

Degree: Doctor of Philosophy in Chemical Engineering

Date: May 1994

Undergraduate and Graduate Education:

- Doctor of Philosophy in Chemical Engineering
  New Jersey Institute of Technology, New Jersey, 1994
- Master of Science in Chemical Engineering
  National Cheng Kung University, Tainan, Taiwan, R.O.C., 1982
- Bachelor of Science in Chemical Engineering
  Feng Chia University, Taichung, Taiwan, R.O.C., 1976

Major: Chemical Engineering

Presentations and Publications:

Ting-Chia Huang and Jun-Hsien Wang. "A Study of Ionic Transfer in Electrodialysis Process with Laminar Flow." *Canadian J. Chem. Eng.*, **67:** 385-391 (1989)

B. C. Baltzis, G. A. Lewandowski, and J. H. Wang. "Denitrification with a Strain of *Pseudomonas denitrificans*: Fundamental Kinetic Studies and Their Implications for Bioreactor Design." 205th ACS National Meet-ing, Division of Biochemical Technology, Denver, CO (March 28 - April 2, 1993)

B. C. Baltzis, G. A. Lewandowski, and J. H. Wang. "Biodenitrification Studies with a Bioreactor Operating in a Periodic Mode." First International Symposium on Bioprocess Engineering, Cuernavaca, Mexico (June 1994)

Reproduced with permission of the copyright owner. Further reproduction prohibited without permission.

This dissertation is dedicated to
my parents

Reproduced with permission of the copyright owner. Further reproduction prohibited without permission.

ACKNOWLEDGEMENT

The author would like to express his sincere gratitude to his dissertation advisors, Dr. Basil C. Baltzis and Dr. Gordon A. Lewandowski, for their moral encouragement and valuable advice during his graduate research and education. Without the support from both of them, this work would not have been finished.

The author would like to sincerely thank Dr. Stavro Pavlou (University of Patras, Greece) for his kind help in numerical analysis of Sequencing Batch Reactors (SBRs). His gentle suggestion gave the valuable direction in fulfillment of the theoretical analysis of the denitrification in SBRs.

The author would also like to express his sincere thanks to Dr. Ching-Rong Huang, Dr. Piero M. Armenante, and Dr. Lily Y. Young for their kind serving as the Committee Members.

As for the accessibility of research instruments, the author would like to express his special thanks to Ms. Gwendolyn San Agustin and Mr. Clint Brockway, the Hazardous Substance Management Research Center (HSMRC) of NJIT, for their enthusiastic assistances in the operation of Ion Chromatograph and Coulter Counter, material selection for the installation of Gas Chromatograph and the helium purge system. Without their eager help, the kinetic studies of this work would not have achieved the fruitful results.

The author had acquired a lot of encouragement and assistance during this study. To these friendly people, the author would like to give his deep appreciation. The followings are some of them: Socrates Ioannides, Zarook Shareefdeen, Mr. Bill Guzy, Dr. Hanesian, and Ms. Gwendolyn San Agustin.

Finally, the author would like to express his appreciation to his wife for her timeless patience and carefulness, and to his parents for their considerate support and enduring patience through the study at New Jersey Institute of Technology.

Reproduced with permission of the copyright owner. Further reproduction prohibited without permission.

TABLE OF CONTENTS

Reproduced with permission of the copyright owner. Further reproduction prohibited without permission.

Chapter **Page**

Reproduced with permission of the copyright owner. Further reproduction prohibited without permission.

LIST OF TABLES

Reproduced with permission of the copyright owner. Further reproduction prohibited without permission.

Table **Page**

Reproduced with permission of the copyright owner. Further reproduction prohibited without permission.

Table **Page**

Reproduced with permission of the copyright owner. Further reproduction prohibited without permission.

LIST OF FIGURES

Reproduced with permission of the copyright owner. Further reproduction prohibited without permission.

Figure **Page**

Reproduced with permission of the copyright owner. Further reproduction prohibited without permission.

Figure **Page**

Reproduced with permission of the copyright owner. Further reproduction prohibited without permission.

Figure **Page**

Reproduced with permission of the copyright owner. Further reproduction prohibited without permission.

Nomenclature Used in Chapter 6

b biomass concentration in the reactor (g m^{-3})

b_o initial biomass concentration in the reactor (g m^{-3})

K_j constant in the specific growth rate expression μ_j (g m^{-3})

K_{Ij} inhibition constant in the specific growth rate expression μ_j (g m^{-3})

K_{ij} cross-inhibition constant expressing the effect of substrate i on the removal of substrate j (g m^{-3})

Q exit flowrate of treated waste from the SBR (m^3 h^{-1})

Q_f flowrate at which untreated waste is fed into the SBR (m^3 h^{-1})

Q' dimensionless flowrate of stream exiting from the SBR

Q_f' dimensionless flowrate of waste stream fed into the SBR

Q_f^* reference flowrate, defined as the feed flowrate during the fill-phase (m^3 h^{-1})

s concentration of nitrate in the reactor (g m^{-3})

s_f concentration of nitrate in the untreated waste stream (g m^{-3})

s_o nitrate concentration in the SBR at the start-up conditions (g m^{-3})

t time (h)

t_1 time indicating the end of the fill-phase in a SBR cycle (h)

t_2 time indicating the beginning of the draw-down phase in a SBR cycle (h)

t_3 time indicating the end of a SBR cycle (h)

u concentration of nitrite in the reactor (g m^{-3})

u_f concentration of nitrite in the untreated waste stream (g m^{-3})

u_o nitrite concentration in the SBR at the start-up conditions (g m^{-3})

V volume of SBR contents (m^3)

V' dimensionless volume of SBR contents

V_{max} maximum volume of SBR contents; value of V for $t_1 \le t \le t_2$ (m^3)

V_o minimum volume of SBR contents; value of V for $t = 0$ and $t = t_3$ (m^3)

x dimensionless biomass concentration in the SBR

x_o dimensionless biomass concentration in the SBR at the start-up conditions

y dimensionless nitrate concentration in the SBR

y_f dimensionless nitrate concentration in the untreated waste stream

y_o dimensionless nitrate concentration in the SBR at the start-up conditions

Y_j true yield coefficient on substrate j (g biomass/g substrate, j =1: nitrate; j = 2: nitrite)

z dimensionless nitrite concentration in the SBR

z_f dimensionless nitrite concentration in the untreated waste stream

z_o dimensionless nitrite concentration in the SBR at the start-up conditions

Reproduced with permission of the copyright owner. Further reproduction prohibited without permission.

Nomenclature Used in Chapter 6
(Continued)

Greek symbols

α conversion factor, (g nitrite produced/g nitrate consumed)

β dimensionless measure of the hydraulic residence time

γ_j dimensionless inhibition constant, defined as K_1/K_{Ij}; (j =1: nitrate; j = 2: nitrite).

δ ratio of minimum to maximum volume of SBR contents

$\Delta(s)$ delta function; equal to 1 if $s > 0$, and 0 if $s = 0$

$\Delta(u)$ delta function; equal to 1 if $u > 0$, and 0 if $u = 0$

$\Delta(y)$ delta function; equal to 1 if $y > 0$, and 0 if $y = 0$

$\Delta(z)$ delta function; equal to 1 if $z > 0$, and 0 if $z = 0$

ε_j dimensionless cross-inhibition constant

η ratio of yield coefficients defined as Y_1/Y_2

θ dimensionless time

θ_j dimensionless time corresponding to t_j, j = 1,...,3

λ_j dimensionless maintenance rate defined as $\mu_{cj}/\hat{\mu}_2$

μ_{cj} expression for the biomass specific maintenance rate referring to substrate j (h^{-1})

$\mu_j(s,u)$ expression for the biomass specific growth rate expression on substrate j (h^{-1})

$\mu_j(y,z)$ dimensionless form of expression $\mu_j(s,u)$

$\hat{\mu}_j$ constant in expression $\mu_j(s,u)$; (h^{-1})

σ_j fraction of cycle time devoted to phase j of the SBR cycle (j = 1,...,3)

φ dimensionless constant defined as $\hat{\mu}_1/\hat{\mu}_2$

ω dimensionless constant defined as K_1/K_2

Reproduced with permission of the copyright owner. Further reproduction prohibited without permission.

CHAPTER 1

INTRODUCTION

Biological methods for treatment of municipal and industrial wastes have been in use for many years. As the increased awareness of the public regarding environmental issues has led the local and federal regulatory agencies to impose stricter limits on the amounts of hazardous and toxic chemicals that can be released to the environment, industry needs to either develop new technologies, or to modify existing ones, through process optimization, in order to meet the regulatory standards in an economical fashion.

A technology which has been successfully used in treating liquid wastes involves the use of sequencing batch reactors (SBRs). Irvine and his co-workers [e.g., Irvine and Bush, 1979] have made pioneering contributions to the development of SBR technology. SBRs operate in a semicontinuous mode which involves a cyclic operation. Each cycle is comprised of five distinct periods: fill-, react-, settle-, draw-down-, and idle-period. SBRs offer a number of advantages (Arora et al., 1985; Chang, 1987; Dikshitulu et al., 1993), among which are flexibility in operation, ability to alternate between aerobic and anoxic conditions, no need of a separate clarifier, better ability to meet effluent concentration requirements, and higher productivity when compared to equivalent continuous flow reactors (CSTRs). Classical SBR technology usually involves large idle periods which in actuality make SBRs discontinuous systems where each cycle is almost independent of the others. In the recent years, the group of Baltzis and Lewandowski (e.g., Chang, 1987; Baltzis et al., 1987 and 1990; Sanyal, 1990; Dikshitulu, 1993; Dikshitulu et al., 1993), has demonstrated that SBRs can be further optimized when they operate continuously following a self-repeated pattern. This approach is based on taking advantage of the kinetic characteristics of the process, and on finding proper operating parameter regimes through a detailed analysis of the dynamics of the system. This approach has been primarily applied to, and experimentally demonstrated for aerobic processes. The results

Reproduced with permission of the copyright owner. Further reproduction prohibited without permission.

show substantial advantages of this mode of operation when proper operating conditions are identified through analysis, and have revealed types of behavior which could explain SBR response to operational upsets. These results have created an interest in examining SBR optimal design for anaerobic operations. Among anaerobic (anoxic) processes, denitrification is of great interest and importance.

Nitrogen is an essential chemical for a variety of processes associated with life. It is required for fish and crop production, poutry operations and livestock feeding, as well as for synthesis of proteins. Due to increasing demands to feed the increasing population around the world, chemical fertilizers have been used in large quantities (Atlas 1988). Nitrogen, in the form of nitrate and nitrite, has also been used widely for many years as a food preservative and color fixative in meat products. Nitrogen containing compounds are also used in munitions manufacturing (Sanyal, 1990).

The wide use of nitrogen-containing compounds leads to serious environmental problems, and potential hazards to human health. Nitrogen fertilization of farm lands (Nyamapfene and Mtetwa, 1987), urban runoff, and municipal wastes appear to be factors in the eutrophication of some lakes and rivers. Nitrogen also enhances the growth of aquatic vegetation, and excessive growth of algal species affects water quality and use. Furthermore, some forms of nitrogen can be toxic to animals. For example, nitrite that reaches the bloodstream reacts directly with hemoglobin to produce methemoglobin, with consequent impairment of oxygen transport. Nitrate itself is relatively nontoxic to mammals, being readily absorbed and readily excerted. Under certain circumstances, however, nitrate can be reduced in the gastrointestinal tract to nitrite. Thus, the methemoglobin response is dependent upon either preformed nitrite, or nitrite formation in the body. It has been found that the reaction of nitrite with hemoglobin is inconsequential in adults, but it can be troublesome in infants (US National Research Council, 1972; Nyamapfene and Mtetwa, 1987; Lee and Dahab, 1988). Methemoglobinemia in infants has been related to a high level of nitrate in drinking water. Furthermore, the possible

Reproduced with permission of the copyright owner. Further reproduction prohibited without permission.

presence of nitrosamines (organic compounds that are carcinogenic, teratogenic, and mutagenic) in meats, vegetables, and canned foods has aroused concern. Nitrate, nitrite, as well as secondary and tertiary amines are precursors of nitrosamines, and this has led to concern over the nitrate and nitrite food additives.

Microbial organisms have the ability to reduce various forms of nitrogen-containing compounds to nitrogen. These transformations involve production of gaseous intermediates such as nitric oxide (NO) and nitrous oxide (N_2O). The upward diffusion of these chemical species has been considered as a major contributor to ozone depletion in the stratosphere (Payne, 1981; Klingensmith and Alexander, 1983).

Twenty years ago, the concern over the accumulation of various nitrogen-containing compounds (especially nitrate), in the environment led to the formation of a special committee by the US National Research Council. The committee, headed by Martin Alexander, investigated the various problems and, for the most part, acknowledged that there were not enough data for unequivocal conclusions to be reached (US National Research Council, 1972).

The drinking-water standard set by the US Environmental Protection Agency for nitrate is 10 mg/L, as nitrate-nitrogen (Gayle et al., 1989; Lee and Dahab, 1988; van der Hoek, 1987, 1988). In the European Community the same standard is 50 mg/L, as nitrate (11.3 mg/L, as nitrate-nitrogen).

As nitrogen is a major constituent of the earth's atmosphere, and an essential chemical for life, it is involved in a global cycle which includes assimilatory nitrification and dissimilatory denitrification by microorganisms (Atlas, 1988; Payne, 1981). In the former pathway, inorganic nitrogen oxides are converted to ammonia while in the latter, they are reduced to nitrogen gas. The enzymes involved in these pathways are assimilatory and dissimilatory reductases. These are different proteins which are encoded by different genes. On the basis of proton translocation, these enzymes are associated

Reproduced with permission of the copyright owner. Further reproduction prohibited without permission.

with cytoplasmic membranes, and are found in inner membrane face locations (Payne, 1981; Krul and Veeningen, 1977).

The existence of microorganisms which are capable of transforming nitrogen containing compounds to innocuous forms, is the basis of the technology for denitrification of wastes. Denitrification is the result of the ability of bacteria to utilize nitrogen oxides as terminal electron acceptors, in the absence of oxygen. Among the bacteria having such capabilities, the *Pseudomonas* and *Alcaligenes* genera appear to be of the greatest significance. As reviewed by Payne (1981), Knowles (1982), and Painter (1970), there are many factors affecting the denitrification rate. Among them, the most important are the identity of the nitrogen oxides, the source of the organic carbon used for the bacteria, temperature, pH, dissolved oxygen, and the presence of inhibitors.

Because of the importance of microbial denitrification, a number of fundamental studies have been performed (Payne, 1981; Knowles, 1982; Painter, 1970; Iwasaki et al., 1955, 1956, 1958, 1960, 1962, 1963; Suzuki and Iwasaki, 1962; Miyata et al., 1968, 1969a, 1969b; Matsubara and Mori, 1968; Matsubara, 1970, 1971) using sediments, activated sludges, suspended pure cultures, and even cell-free extracts (Ohnishi, 1963; Bryan et al., 1983). Some efforts have been also undertaken in simultaneous removal of nitrogen oxides and organic wastes (Nozawa and Maruyama, 1988; Hsu, 1986; Evans et al., 1992). These studies have generated a lot of valuable information but for the most part, they have not revealed detailed kinetic expressions which could be used for engineering analysis of the denitrification process. From an engineering point of view, the denitrification kinetics and the dynamics of reactors used are of paramount importance for developing feasible and economic processes for nitrogen removal from wastes (Fredrickson and Tsuchiya, 1977; Bailey, 1973; Bailey and Ollis, 1986).

Despite the fact that detailed kinetic expressions for the denitrification process are lacking, a number of processes have been evaluated (Gayle et al., 1989), based primarily on empirical and semi-empirical approaches. Processes that have been considered include

Reproduced with permission of the copyright owner. Further reproduction prohibited without permission.

ion exchange, reverse osmosis, conventional batch (Jones, 1990a) and CSTR reactors (Francis and Mankin, 1977), an upflow sludge blanket reactor (Klapwijk et al., 1981,), a moving bed upflow sand filter (Biswas and Warnock, 1971; Timberlake, et al., 1988; Koopman et al., 1990), a fluidized bed biofilm reactor (Mulcahy and Shieh, 1987; Schügerl, 1989), an anaerobic filter (Strand, et al., 1985; Polprasert and Park, 1986), a packed bed reactor (Przytocka-Jusiak et al., 1984; Lee and Dahab, 1988), a plug flow activated sludge system (US EPA, 1979), sequencing batch reactors (Irvine and Busch, 1979), or more complex processes (Hamilton et al., 1992; Jain et al., 1992). The complex processes include combined nitrification/denitrification (US EPA, 1979; Silverstein and Schroeder, 1983; Rittmann and Langeland, 1985; Henze, 1987; Timberlake et al., 1988; Jones et al., 1990b), and ion exchange/biological denitrification (van der Hoek et al., 1987, 1988) processes. In nitrification/denitrification processes nitrogen removal is achieved by oxidation of the ammonium (NH_4^+) to nitrate (NO_3^-) followed by the dissimilatory nitrate reduction to nitrogen. In ion exchange involving processes, nitrate is removed from ground water by ion exchange, and the regeneration of the resins is carried out in a biological denitrification reactor.

As mentioned earlier in this introduction, detailed analysis of the dynamics of SBRs can lead to optimal process design. For denitrification, there are indications (Sanyal, 1990) that SBR operation can lead to interesting results. The study of Sanyal can be viewed only as a preliminary one, since it was based on assumed kinetic expressions, and did not involve experiments.

The topic of the present dissertation is a detailed analysis of the dynamics of denitrification in SBRs. Since detailed kinetic expressions are required for such an analysis, the first part of the dissertation involves fundamental kinetic studies with a culture which was subsequently used in SBR experiments. The SBR experiments were designed based on the results of the analysis of the dynamics of the process.

Reproduced with permission of the copyright owner. Further reproduction prohibited without permission.

CHAPTER 2

LITERATURE REVIEW

In this chapter, the pertinent literature is reviewed. Due to the diversity of the topic, the review is organized in four sections. The first section refers to studies regarding the key factors which affect denitrification. In the second section, a brief discussion of studies on the mechanism of denitrification is presented. In the third section, a brief review of studies with sequencing batch reactors is presented, especially of studies dealing directly, or indirectly with denitrification. Since proper monitoring of a variety of aqueous and gaseous compounds is essential for a systematic study of denitrification, the fourth and final section of this chapter deals with assay methods for the various compounds encountered in bio-denitrification.

2.1 Important Factors Controlling Biodenitrification

2.1.1 Nitrogen Oxides

Dissimilatory reduction of nitrogen oxides is a process in which organisms use these oxides (nitrate, nitrite, nitric oxide, nitrous oxide) as terminal electron acceptors instead of molecular oxygen. Painter (1970) pointed out that for dissimilation most organisms require a period of adaptation to nitrate and anaerobic conditions, while the assimilation process does not normally require such adaptation. In a review paper, Knowles (1982) summarized that the gaseous oxides (nitric oxide, NO, and nitrous oxide, N_2O) are not reported to affect the reduction of ionic oxides (nitrate, NO_3^-, and nitrite, NO_2^-). Ionic oxides are usually preferentially reduced before the gaseous oxides, causing the often observed transient accumulation of denitrification intermediates. For *Pseudomonas denitrificans*, nitrite has been reported not to affect the reduction rate of nitrate but to cause partial uncoupling of the energy metabolism. At low concentrations, nitrate seems to control the rate of the denitrification reaction with first-order kinetics. At high

Reproduced with permission of the copyright owner. Further reproduction prohibited without permission.

concentrations, it may inhibit the enzymatic reduction of NO and cause nitrite accumulation; it may also inhibit the reduction of N_2O and thus, cause a greater N_2O mole fraction presence in the products. Evans et al. (1992) described three types of denitrification profiles as follows. Type 1 is illustrated by a *Flavobacterium sp.* that does not transiently accumulate nitrite during nitrate reduction to nitrous oxide and nitrogen (Betlach and Tiedje, 1981). Nitrate and nitrite reduction occurs simultaneously, and at equal rates. Type 2 is illustrated by *Pseudomonas fluorescens* that leads to nitrite accumulation such that its maximal concentration is 50 per cent of the initial concentration of nitrate (Betlach and Tiedje, 1981). From a mole balance, it was concluded that nitrous oxide or nitrogen must be formed simultaneously with the accumulation of nitrite. These data indicate that the reduction of nitrate and nitrite occurs also simultaneously, although at different rates. Type 3 is exhibited by a *Pseudomonas sp.* strain KB740 that degrades 2-aminobenzoic acid under denitrifying conditions. This bacterium leads to nitrite accumulation at a concentration equal to 90 per cent of the initial nitrate concentration, indicating that nitrite reduction to nitrogen occurs predominantly after nitrate is reduced to nitrite. Kodama et al. (1969), also observed the Type 3 denitrification profile with anaerobic growth of *Pseudomonas stutzeri,* and characterized it as biphasic growth (or diauxie phenomenon). They concluded that nitrate inhibits nitrite reduction in two ways, by repressing formation of the nitrite-reducing system to some extent, and by competiting with nitrite as an electron acceptor. Nakajima et al. (1984b), performed studies with sludge from an oxidation ditch. Their data suggest that the denitrification rate on nitrate follows a Monod model while the nitrite reduction rate follows an Andrews inhibitory expression. In another paper the same researchers (Nakajima et al., 1984a), studied denitrification with sediments of an eutrophic lake. The data from this study imply that an Andrews inhibitory model should be used for both nitrate and nitrite reduction. Timmermans et al. (1983), studied the effect of nitrate on the nitrite reductase activity in *Hyphomicrobium sp.*, as described by Kodama et al., and found identical growth rates

Reproduced with permission of the copyright owner. Further reproduction prohibited without permission.

when using either nitrate- or nitrite- nitrogen. Their results suggest that nitrate to nitrite reduction is the rate limiting step of the process. They also observed some inhibition by high concentrations of nitrite on the nitrate reduction. This seems to imply that nitrate and nitrite are involved in a cross-inhibition interaction pattern.

Delwiche (1959) quoted observations of Sacks and Barker that under some circumstances the utilization of nitrous oxide by nitrate adapted cells of *Pseudomonas denitrificans* showed a lag, indicating that adaptation to nitrate did not necessarily include adaptation to nitrous oxide. The same result was obtained by Delwiche himself. He further observed that the length of the lag period was dependent on the concentration of the nitrate ion in the growth medium used. Low levels of nitrate ion resulted in a short lag period, while higher levels in a lag period considerably longer. Mastubara and Mori (1968) concluded that nitrous oxide is an obligatory precursor in the formation of nitrogen from nitrite by a strain of *Pseudomonas denitrificans*, which is different from the conclusions of Delwiche, and Sacks and Barker (1949).

2.1.2 Temperature

On the basis of the temperature range in which growth can occur, bacteria are usually divided into three categories: thermophiles, mesophiles, and psychrophiles (sometimes called cryophiles, or rhigophiles). The effect of temperature on bacterial growth rate is often described by the Arrhenius expression (Ingraham, 1958; Ng, 1969; Atlas 1988). Because of protein denaturation at elevated temperatures and the resultant change in membrane fluidity, there is an upper temperature limit for microbial growth. At temperatures above that limit, microorganisms are unable to survive because they cannot carry out their life-supporting metabolic activities. Dawson and Murphy (1972) reported that for biological denitrification of a defined medium by a dominant culture of *Pseudomonas denitrificans*, the specific denitrification rate can be closely approximated by an Arrhenius temperature relationship. They found an activation energy for the

Reproduced with permission of the copyright owner. Further reproduction prohibited without permission.

denitrification rate equal to 16,800 calories per mole at temperature ranges from 5 to 27°C, and pH 7.0. Nakajima et al. (1984a) reported activation energies of nitrate and nitrite reduction as 39 and 34 Kilo-joules per mole (i.e. 9.32 and 8.13 Kilo-calories per mole), respectively, for mixed cultures present in the sediments of an eutrophic lake. In another paper the same researchers (Nakajima et al., 1986b) found the activation energies of nitrate and nitrite reduction to be 53 and 59 Kilo-joules per mole (i.e. 12.67 and 14.10 Kilo-calories per mole), respectively, for mixed cultures present in the sludge from an oxidation ditch. They also showed that the nitrite removal rate was always higher than the nitrate removal rate.

Antoniou et al. (1990) assumed an Arrhenius type dependence for the net specific growth rate of nitrifying bacteria of the genus *Nitrosomonas*. The net specific growth rate is defined as the difference between the actual specific growth rate and the specific rate of biomass consumption for purposes of endogenous metabolism (maintenance).

The endogenous metabolism of microorganisms is an important issue and has been studied by many researchers (Lamanna, 1963; Dawes and Ribbons, 1962, 1964). It may be defined as the total metabolic reactions that occur within the living cell when it is held without compounds or elements that may serve as specific exogenous substrates (Dawes and Ribbons 1962, 1964). Some products of endogenous metabolism may be released into the surrounding medium and are often utilized by the cells, sometimes resulting in regrowth. Dawes and Ribbons (1962) pointed out that endogenous metabolism may continue in the presence of exogenous substrates. Maintenance has been described mathematically by two categories of models. Herbert (1958) assumed that maintenance requirements are satisfied by self-oxidation of biomass, while Marr et al. (1963) and Pirt (1965) described maintenance by special consumption of the energy-yielding substrate for non-growth purposes.

Although most approaches for describing the temperature dependence of growth use an overall Arrhenius expression, Topiwala (1971) has showed that each kinetic

Reproduced with permission of the copyright owner. Further reproduction prohibited without permission.

constant involved in a Monod expression has its own temperature dependence. In addition, he showed that the specific rate of maintenance, which he described according to Herbert's model, has also a separate temperature dependence. He found that over certain temperature ranges the maximum specific growth rate, and the specific rate for maintenance can be expressed via an Arrhenius expression, while the half-saturation constant exhibits an inverse Arrhenius expression.

Ng (1969) and Topiwala (1971) have pointed out that increasing the temperature of the culture may change its physical properties appreciably and hence, indirectly affect cell metabolism. Palumbo and Witter (1969) studied the influence of temperature on the conversion of glucose into cell material and into energy for maintenance by *Pseudomonas fluorescens;* they found that the yield and specific maintenance rate decreased with decreasing temperature. Topiwala (1971) reported that the temperature has no effect on the yield coefficient.

2.1.3 pH

Microbial growth rates are greatly influenced by pH as its value affects the nature of proteins (Atlas, 1988). Because charge interactions between the amino acids of a polypeptide chain greatly influence the structure and function of proteins, enzymes are normally inactive at very high and very low pH values. Painter (1970) summarized the effect of pH on denitrification as follows. The optimum value depends on the concentration of nitrate, age of culture, and the organism concerned. *P. aerugenosa* denitrified at values varying from 5.8 to 9.2, with an optimum value between pH 7.0 and 8.2. Knowles (1982) after reviewing the literature, concluded that in pure cultures, as well as in natural systems, the denitrification rate is positively related to pH, with an optimum in the range of 7.0 to 8.0. Denitrification may occur in wastes at pH values as high as 11. At low pH values, the nitrogen oxide reductases, especially that which reduces N_2O, are progessively inhibited so that the overall rate of denitrification decreases. As the

Reproduced with permission of the copyright owner. Further reproduction prohibited without permission.

pH decreases the amount of N_2O produced increases, and at pH 4.0 N_2O may be the major product. In acid peat, the low pH of 3.5 was reported to be the only factor which prevented the occurance of denitrification. Timmermans and Van Haute (1983) found that the optimal pH for denitrification by *Hyphomicrobium sp.* was 8.3, with methanol as the carbon source, and used a non-competitive inhibition model proposed by Hartmann and Laubenberger (1968) to express the pH-denitrification rate relationship. Antoniou et al. (1990) used analogs of the Michaelis pH functions (Bailey and Ollis, 1986; Dixon and Webb, 1979) for enzymes, to describe the relationship between the net specific growth rate of *Nitrosomonas* and pH.

2.1.4 Dissolved Oxygen (DO)

Painter (1970) summarized the effect of dissolved oxygen on denitrification as follows. Most denitrifying enzyme systems have first to be induced by growth of the organism in the presence of nitrate and absence of oxygen. *Pseudomonas denitrificans* grown under vigorously-agitated conditions using a gas mixture of 1 per cent oxygen and 99 per cent nitrogen possessed about two-thirds the nitrate-reducing capacity of cells grown anaerobically (Sacks and Barker, 1949). When the oxygen content was raised to 5 per cent, the cells had no activity. *Pseudomonas denitrificans* reduced nitrite in a mixture of 6 per cent oxygen and 94 per cent nitrogen at about one-sixth the rate in 100 per cent nitrogen, but no dissolved oxygen measurements were made. At concentrations of dissolved oxygen above 0.2 - 0.4 mg per liter no nitrate was reduced. When the head space in the reaction vessel was filled with commercial nitrogen known to contain oxygen, nitrate was reduced but oxygen could not be detected in the solution. The occurance of nitrate dissimilation in the presence of a positive, though low, dissolved-oxygen concentration may be the result of an oxygen gradient in the culture such that some cells are actually at zero dissolved oxygen and are thus able to reduce nitrate. Knowles (1982) reported that the nitrogen oxide reductases are repressed by O_2 and that, when this gas is

Reproduced with permission of the copyright owner. Further reproduction prohibited without permission.

removed, even in the absence of nitrogen oxides, the reductase enzymes are derepressed within a period of 40 minutes to 3 hours. Nakajima and his coworkers (1984a, 1984b) reported that the reduction rates of both nitrate and nitrite were high at dissolved oxygen concentrations lower than 20 - 30 μM, and decreased sharply to zero for dissolved oxygen concentrations higher than 30 μM. Simpkin and Boyle (1988) showed that in nitrifying activated-sludge systems, repression of enzyme synthesis by oxygen was not complete, and that the enzymes were synthesized to at least 50 per cent of their maximum level; hence they concluded that inhibition of the enzyme activity by oxygen, and not repression of enzyme synthesis must be the most important effect oxygen has on denitrification in activated sludge systems. Hernandez and Rowe (1987) indicated that at least for *Pseudomonas aeruginosa* the inhibitory effect is immediate and reversible. Furthermore, inhibition appeared to be at the level of nitrate uptake, since it was observed in whole-cell preparations but not in cell extracts. The degree of oxygen inhibition was dependent on the concentration of oxygen, and increasing nitrate concentrations could not overcome the inhibition. The inhibition effect of oxygen was maximal at approximately 0.2 per cent oxygen saturation. The inhibition appeared to be specific for nitrate uptake. Nitrite uptake was not affected at low levels of aeration, and its reduction was only partially inhibited in the presence of oxygen.

2.1.5 Carbon Source

The availability of electrons in organic carbon compounds is one of the most important factors controlling the activity of heterotrophs. Under some conditions of denitrification, organic carbon addition has no effect on the process (Payne 1981), indicating that this factor is not rate limiting. It has been also reported that with abundant carbon and completely anaerobic conditions, reduction proceeds significantly towards NH_4^+ rather than the gaseous products (Knowles 1982). A remarkable variety of electron donors other than methanol have been tested (Payne 1981) [e.g., acetate, acetone, citrate, ethanol,

Reproduced with permission of the copyright owner. Further reproduction prohibited without permission.

glucose, lactate, sucrose and bakery sludge, brewery waste, chemical industry's waste, milk solids, corn starch, fish meal, and fruit juices]. None was preferable to methanol. The usefulness of this compound in the denitrification process is determined first of all by economic considerations (Grabinska-Loniewska et al., 1985; Manoharan et al., 1989; Dahab and Lee, 1988). McCarty et al. (1969), and Narkis et al. (1979), have concluded that the ideal methanol : nitrate ratio is 2.47 mg/mg. The equation:

$$C_m = 2.47\ NO_3^-\text{-}N + 1.53\ NO_2^-\text{-}N + 0.87\ DO$$

provides a convenient means of calculating the amount of methanol required for a given denitrification process.

McCarty and his coworkers observed a somewhat different response of microbes to different carbon substrates. In some cases, a large quantity of nitrite intermediate was formed, while in others this was not the case. Their fed-batch experiments indicated that a molar consumption ratio of about 1.3 to 1.4 could be expected for acetate, ethanol, acetone, and methanol.

Based on currently available biochemical knowledge of nitrate reduction and assimilation, methanol oxidation and assimilation, and the energy yield and requirements for these reactions, Nurse (1980) developed a theoretical equation to describe the stoichiometry of denitrification with methanol by *Hyphomicrobium*, and found a molar consumptive ratio of 1.31 which agrees with the results of McCarty and his coworkers.

Dahab and Lee (1988) demonstrated near total removal of nitrate at a molar C/N ratio of 1.5 by operating a static-bed upflow reactor for 10 months with a feed concentration of 100 mg-NO_3 per liter, and acetic acid as carbon source.

Narkis et al. (1979), found that when the concentration of the organic matter is expressed as BOD, a critical ratio of (mg BOD / mg ΣNO_x-N) = 2.3 ensures 100 per cent denitrification.

Timmermans and Van Haute (1983), modified the stoichiometry proposed by McCarty et al. (1969), and used a methanol to nitrate-N weight ratio of 2.55 for

Reproduced with permission of the copyright owner. Further reproduction prohibited without permission.

denitrification by *Hyphomicrobium sp.* Beccari and his coworkers (1983) used an equivalent methanol consumption ratio of 2.7 mg CH_3OH / mg NO_3-N. Koopman et al. (1990) suggested that the minimum methanol dosage required for complete denitrification, in a moving bed upflow sand filter, was in the range of 3.3 to 3.5 g CH_3OH / g NO_3-N_{eq}.

2.2 The Mechanism of Denitrification

In the denitrification performed by *Pseudomonas denitrificans*, nitrate is reduced stepwise to nitrogen gas via nitrite, nitric oxide, and nitrous oxide as intermediates (Matsubara and Mori, 1968; Miyata and Mori, 1968; Painter, 1970; Payne et al., 1971; Payne, 1981; Nurse 1980). In each step, reduction is initiated by a specific enzyme (Painter 1970, Payne et al., 1971; Payne, 1981; Knowles, 1982; Atlas, 1988). However, the role of NO and the existence of NOR, nitric oxide reductase, remain debatable (Knowles, 1982). Knowles pointed out that the above denitrification pathway is present in *Paracoccus denitrificans*, and is not necessarily applicable to other organisms. The products of NO_2^- reduction by whole cells are mainly N_2O and N_2 (Matsubara and Mori, 1968; Matsubara, 1970; Nakajima et al., 1984a and 1984b); with enzyme preparations of varying purity, NO is commonly a major product (Miyata and Mori, 1968, 1969a). The evidence for the participation of a NO-binding complex in the reduction of NO_2^- to N_2O is conflicting. Attempts to clarify the role of NO by means of isotope-trapping experiments (Weeg-Aerssens et al., 1987, 1988; Garber and Hollocher, 1981; Bryan et al., 1983) have also given conflicting results. Knowles has suggested that with *Pseudomonas denitrificans*, nitrite reduction occurs predominantly via a NO-free pathway.

Reproduced with permission of the copyright owner. Further reproduction prohibited without permission.

2.3 Studies with Sequencing Batch Reactors (SBRs)

As discussed in the introduction, sequencing batch reactors (SBRs) have been used in a number of studies and applications. The great majority of these studies deal with aerobic treatment of wastes, utilizing unidentified mixed cultures. In most cases, the SBR mode involves cycles separated by substantial idle periods which make the operation practically discontinuous. Most of the applications are for municipal wastes and lecheates from landfills.

An early overview of SBRs was given by Irvine and Busch (1979). Dennis and Irvine (1979) showed that there is an optimal ratio of fill- to react-time in SBR operation. Various applications involving municipal wastes, petrochemical wastes, and wastes containing high phosphorus loads have been discussed in the literature (Irvine et al., 1979; Hsu, 1986; Ketchum and Liao, 1979; Irvine et al., 1987). Ketchum et al. (1979) performed a cost analysis of SBR systems and concluded that they are more economical than conventional ones. SBR systems may be comprised of a single or multiple tanks.

The fact that SBRs could have great advantages in denitrifying operations can be judged from the following early studies. Moore and Schroeder (1970) studied the effect of residence time on anaerobic bacterial denitrification in a continuous flow system (CFS) and showed that bacterial physiology is an important consideration in bacterial denitrification, and is a function of feed rate and feed composition. They also concluded that a definite optimal operating range exists for the denitrification process, so that nitrite buildup is not a problem. In studying the effect of loading rate on batch-activated sludge effluent quality, Hoepker and Schroeder (1979) pointed out that batch or semibatch operation led to better effluent quality. The semibatch systems were considerably more stable in terms of dispersed growth, and the authors found a positive correlation between this type of growth and the volumetric efficiency of the reactor. Semibatch operation is essentially a SBR mode of operation.

Reproduced with permission of the copyright owner. Further reproduction prohibited without permission.

SBRs have been studied for nitrification/denitrification processes (Alleman and Irvine, 1980; Irvine et al., 1983; Silverstein and Schroeder, 1983; Palis and Irvine, 1985; Jones et al., 1990a, 1990b). Abufayed and Schroeder (1986a, 1986b) studied denitrification in SBRs by using a primary sludge as carbon source and got excellent results. Wilderer et al. (1987) studied the effect of population shifts during SBR denitrifying operations, and concluded that nitrite accumulation could be explained by the loss of denitrifying organisms from the culture.

The fact that continuous SBR operation may lead, depending on the operating conditions, to population shifts has been theoretically and experimentally shown in a study involving aerobic phenol degradation by two competing species (Dikshitulu et al., 1993).

Modeling studies with SBRs used in denitrification processes, have shown that multiple outcomes (culture washout or survival) are possible under certain conditions of operation (Sanyal, 1990; Baltzis et al., 1990).

2.4 Assay Methods for Monitoring Denitrification

2.4.1 Nitrogen Oxides

Burns (Streuli and Averell, 1970) evaluated a number of analytical techniques employing classical and instrumental methods to detect, determine, and characterize nitrogen-oxygen compounds. Along with the improvement of analytical technologies, advanced intruments provide more precise measurements. Ion Chromatography (IC) is capable of measuring nitrate and nitrite at ppb levels. Recently, Ju et al. (1991), and Ju and Triveri (1992) have presented a technique for an on-line measurement of NO_3^- and NO_2^- concentrations during bio-denitrification. This technique is based on the fluorescence of the culture used in the process. To monitor gaseous components, care must be taken in selecting an effective Gas Chromatography (GC) column, a sensitive detector, and proper GC operating conditions. For denitrification, gaseous components of concern are O_2, N_2, NO, N_2O, CO_2. Valuable information concerning the selection of the carrier gas, and the

Reproduced with permission of the copyright owner. Further reproduction prohibited without permission.

porous polymer packing material for the GC column are available from the National Bureau of Standards (Bruno and Paris 1986). To obtain better resolution in analyzing low boiling-point components, use of a reduced temperature is strongly recommended (Szulczewski and Higuchi, 1957; Drew and McNesby, 1957; Marvillet and Tranchant, 1960). Use of a thermal conductivity dectector (TCD) is recommended for measurements of low boiling-point components (Drew and McNesby, 1957; Smith et al., 1958). The carrier gas must be an inert gas having a large conductivity difference with each one of the components of concern (Bruno and Paris, 1986). Argon is inadequate for two reasons; first, it has a thermal conductivity value (1.90×10^{-2} W/m/K) close to those of carbon dioxide (1.83×10^{-2} W/m/K), nitrogen (2.75×10^{-2} W/m/K), and oxygen (2.85×10^{-2} W/m/K); second, it is more expensive than helium. Hence, helium is a proper carrier gas. Mindrup (1978) has presented a review on column selection. Based on this review, it turns out that a Porapak-Q column is able to separate most of the gases of concern, except oxygen. The latter can be separated from nitrogen by the use of a molecular sieve 5A column. The quantities of dissolved gases in the solution can be estimated by assuming gas-liquid equilibrium, and using Henry's law. Henry's constants are available in the literature (US National Research Council, 1928; Grayson, 1980).

2.4.2 Methanol

Methanol which is the most common carbon source for denitrification, can be monitored by a method available from the ASTM standards (ASTM, 1989).

2.4.3 Biomass

Biomass concentration can be determined readily by measuring the absorbance (optical density) at a specific wavelength of visible light by a spectrophotometer (Atlas, 1988; Chang, 1987). Frame and Hu (1990) have shown that there is a proportionality between

Reproduced with permission of the copyright owner. Further reproduction prohibited without permission.

the volume of the cells and their dry weight. Hence, a Coulter Counter can be also used for biamass concentration measurements.

Reproduced with permission of the copyright owner. Further reproduction prohibited without permission.

CHAPTER 3

OBJECTIVES

The key objective of this study was to systematically investigate the biological reduction of nitrate and nitrite containing media (wastes) in continuously operated sequencing batch reactors. This objective could not be met unless accurate kinetic expressions were available for describing the complex system which involves long-lived intermediates. Such expressions are not available in the literature, hence they had to be determined during the course of the present study.

Continuous operation of biological systems involving mixed cultures leads to variations in the biomass composition depending on the conditions of operation. These variations are due to microbial interactions which, unless they are specifically investigated and described, lead to changes in the apparent kinetic expressions determined in batch experiments with the mixed culture. In order to avoid such further complications in an already complex system, it was decided to use a pure culture of *Pseudomonas denitrificans*.

In view of the above, the specific objectives set for this study were the following.

I. Detailed determination of the kinetics of biological reduction of nitrate and nitrite, under various temperature and pH conditions.

This objective was met by performing a significant number of series of batch experiments (in serum bottles). In each series of experiments the temperature and the pH were kept constant. Some series of experiments involved media containing either only nitrite, or only nitrate, while others involved mixtures of the two electron acceptors. Liquid and gaseous samples were frequently taken from the bottles and analyzed for monitoring the presence of various reaction participants as a function of time. The data were subjected to

Reproduced with permission of the copyright owner. Further reproduction prohibited without permission.

detailed mathematical analysis, and led to the derivation of kinetic expressions describing the reaction rates as functions of NO_3^- and NO_2^- concentrations, temperature, and pH.

II. Description of biological reduction of nitrate/nitrite-containing media in continuously operated SBRs and analysis for predicting the different types of behavior of the process.

This objective was met by deriving a general model describing biological reduction of media containing either nitrate, or nitrite only, as well as media containing NO_3^- / NO_2^- mixtures. This model was based on the kinetic expressions revealed after objective I was met. An advanced methodology based on the bifurcation theory of forced systems was used in analyzing the model equations in two cases; one in which a simpler system containing nitrite only is considered, and one in which the full system involving NO_3^- / NO_2^- mixtures is investigated.

III. Validation of the model predictions through SBR experiments.

This objective was met through experiments with a fully automated continuous unit which was designed specifically for this study. Conditions of SBR operation were selected in different regimes of the operating parameter space, regimes in which theory predicted that the system behaves differently. Two classes of experiments were performed to correspond to the two cases analyzed in meeting objective II. Theoretically predicted outcomes were experimentally realized at both the qualitative and quantitative level, with media containing either NO_2^- only, or mixtures of NO_3^- and NO_2^- .

The results of the work performed in meeting objective I, are analyzed and discussed in Chapter 5. Both the theoretical, and experimental work performed in meeting objectives II and III is shown, analyzed, and discussed in Chapter 6.

Reproduced with permission of the copyright owner. Further reproduction prohibited without permission.

CHAPTER 4

MATERIALS AND METHODS

4.1 Materials and Apparatus

4.1.1 Chemicals Used

Potassium nitrate, KNO_3 (Baker's Analyzed, J. T. Baker, Phillipsburg, NJ) and potassium nitrite, KNO_2 (General Chemical, New York, NY), were used as sources of nitrate and nitrite, respectively.

For preparing the primary growth medium on which the inocula were developed before they were used in the actual experiments, the following chemicals were employed: Bacto-Peptone (Difco certified; Difco, Detroit, MI), yeast extract (Y-4000, Sigma Chemical Co., St. Louis, MO), and sodium chloride, NaCl (EM Science, purchased from CMS, Morris Plains, NJ).

The kinetic runs for determining the denitrification kinetics, as well as the SBR experiments were performed with a synthetic medium which contained, sodium chloride, NaCl; potassium monobasic phosphate anhydrous, KH_2PO_4 (Certified A.C.S., Fisher Scientific, Fair Lawn, NJ); potassium dibasic phosphate anhydrous, K_2HPO_4 (Certified A.C.S., Fisher Scientific, Fair Lawn, NJ); magnesium sulfate, $MgSO_4 \cdot 7H_2O$ (Certified A.C.S., Fisher Scientific, Fair Lawn, NJ); calcium chloride, $CaCl_2 \cdot 2H_2O$ (Certified A.C.S., Fisher Scientific, Fair Lawn, NJ); manganese sulfate, $MnSO_4$ (Certified A.C.S., Fisher Scientific, Fair Lawn, NJ); cupric sulfate, $CuSO_4$ (Certified A.C.S., Fisher Scientific, Fair Lawn, NJ); ferric chloride, $FeCl_3$ (Matheson Coleman & Bell, East Rutherford, NJ); sodium molybdate, $Na_2MoO_4 \cdot 2H_2O$ (Baker's Analyzed, J. T. Baker, Phillipsburg, NJ). In all runs methanol (Certified A.C.S., Fisher Scientific, Fair Lawn, NJ) was used as the carbon source for biomass growth.

As dissolved oxygen indicator, resazurin (MRX0010-1, EM Science, purchased

Reproduced with permission of the copyright owner. Further reproduction prohibited without permission.

from CMS, Morris Plains, NJ) was used.

4.1.2 Microbial Culture

All experiments performed in the present study, employed a pure culture of *Pseudomonas denitrificans* (ATCC 13867). The culture was obtained from the American Type Culture Collection (Rockville, MD) as a freeze-dried pellet. The culture was sealed in a closed glass tube, and kept inside a refrigerator.

4.2 Culture Development

Inocula of the culture obtained from ATCC were first grown on a primary substrate medium as follows.

In a 1 L flask, 10 g peptone, 1 g yeast extract, 10 g of NaCl and 500 mL deionized water were added. The flask was closed, and shaken until the solids dissolved in the water. At that point, another 500 mL deionized water were added in the flask. In a 160 mL serum bottle (Wheaton "400", Wheaton, Millville, NJ), 125 mL of the growth medium were transferred. The bottle was sealed with a rubber stopper and an aluminum clamp, and placed in an autoclave (Harward/LTE series 300, Harvard Co., South Natick, MA) at 121 °C, 2.25 psig for 20 minutes. The sterilized medium was then inoculated with *P. denitrificans*, and the bottle was placed in an incubator (Precision Model 6, Precision Scientific, purchased from Fisher Scientific, Pittsburgh, PA), at 30 °C for two weeks. When the culture grew on this medium, samples of it were used for the actual experiments.

4.3 Kinetic Experiments

4.3.1 Medium Composition and Preparation

The medium used in the kinetic (and SBR) experiments was prepared by slightly modifying the recipe reported by Koike and Hattori (1975a, 1975b).

Reproduced with permission of the copyright owner. Further reproduction prohibited without permission.

In a 1L flask, 1.5 g KH_2PO_4 , 5 g K_2HPO_4 , 5 g NaCl, 0.2 $MgSO_4 \cdot 7H_2O$, 0.2 g $CaCl_2 \cdot 2H_2O$, and 500 mL deionized water were placed and shaken till all solids were dissolved. A drop of a trace metal mixture was also added, before the solution was diluted with another 500 mL of deionized water. To the final solution, 0.3 mL of a resazurin solution was added. The resazurin solution contained the reagent at 0.1 %. The amounts of KH_2PO_4 and K_2HPO_4 added, were such that the final medium solution was of pH = 7.1. The trace metal mixture contained $MnSO_4$, $CuSO_4$, $FeCl_3$, and $Na_2MoO_4 \cdot 2H_2O$ in water; each of the aforementioned chemicals was present at 0.5 % (W/V) in the trace metal mixture solution.

Kinetic experiments were performed in 160 mL closed serum bottles. Each experiment was prepared as follows. In a clean serum bottle, 125 mL of synthetic medium were transferred using a graduated cylinder. The bottle was closed with a rubber stopper, and sealed with an aluminum clamp. The sealed bottle was purged with helium gas (zero grade, Liquid Carbonic Specialty Gases, Bethlehem, PA), as follows. Helium gas was injected into the bottle at a pressure of 5 psig. The bottle was vigorously shaken for 1 min, and then its gaseous contents were removed by applying a vacuum system (-18" Hg) for 3 min. To enhance the removal of dissolved oxygen, the bottle was immersed in an ultrasonicator (Solid State/Ultrasonic FS-14, Fischer Scientific, Pittsburgh, PA) during the period of vacuum application. The purge-evacuation cycle was repeated three times. The purge-evacuation system was installed in a hood, and a schematic of it, is given in Figure A-1. After the third gas evacuation of the bottle, helium was added again so that the liquid was kept under a helium atmosphere. The bottle was then placed in an autoclave at 121 °C, 2.25 psig for 20 min, for the medium to get sterilized. Due to the presence of resazurin, the liquid had a blue color before autoclaving. If the color remained blue after autoclaving, it was an indication that dissolved oxygen was not present, and the bottle was used for a kinetic run as explained in the next section. If after autoclaving, the color of the medium changed to pink, the bottle was not used because the color change implied

Reproduced with permission of the copyright owner. Further reproduction prohibited without permission.

dissolved oxygen presence. It should be mentioned that a change from blue to pink at room temperature (in case dissolved oxygen is present), takes a long time.

For the kinetic runs, the autoclaved medium in the serum bottles had to be injected with nitrate and/or nitrite, methanol, and biomass. Nitrate/methanol, and nitrite/methanol stock solutions were prepared as follows. A water solution of KNO_3 containing 10,000 mg NO_3^-/L was prepared, and placed in serum bottles (125 mL solution in a 160 mL bottle). The bottles were purged with helium as described above for the medium solutions, and autoclaved. Subsequently an amount of methanol was added so that its mole ratio to nitrate was 2 : 1. The bottles were then stored for use in the kinetic experiments. The same procedure was repeated for preparing the nitrite-containing stock solution. In this case KNO_2 was used for preparing a solution carrying 10,000 mg NO_2^- /L. Methanol was again added (2 moles methanol/mole NO_2^-). The bottles were stored for later use.

4.3.2 Procedures for the Kinetic Runs

In each serum bottle carrying the autoclaved solution containing all constituents of the medium except methanol and nitrate/nitrite, 1.25 mL of the nitrate, or nitrite stock solution were added by a 5 mL disposable syringe (Becton Dickinson, Rutherford, NJ). The color of the resulting solution remained light blue. Using another 5 mL disposable syringe, an amount of biomass suspension grown on the primary substrate (see section 4.2) was added to the serum bottle. The amount of biomass suspension added to each bottle varied, depending on the nitrate or nitrite concentration at which the actual kinetic run was to be performed. The intent was for each kinetic run to last long enough so that growth could be monitored, but also to be completed in a matter of a few hours. The inoculated serum bottles showed a pink color almost immediately upon addition of the biomass suspension. This was an indication that a reaction involving electron exchange was taking place. The inoculated bottles were placed in an incubator shaker for at last 24

Reproduced with permission of the copyright owner. Further reproduction prohibited without permission.

hours without being sampled. If at the end of this incubation period the color of the suspension changed from pink to transparent, it was an indication that nitrate, or nitrite were depleted under anaerobic conditions. Depletion of nitrate, or nitrite was confirmed through ion chromatographic (IC) analysis of a sample. If after 24 hours the color remained pink, a sample was taken and subjected to IC analysis. If the results indicated a consumption of nitrate, or nitrite incubation was continued for a few more hours. If the results of the IC analysis showed no, or minimal nitrate, or nitrite consumption after 24 hours, or after the extended incubation period, the bottle was discarded since the results implied that the reaction was suppressed probably due to oxygen presence. The bottles which turned from blue to transparent were used in the actual kinetic runs.

Depending on its biomass content, each bottle was injected with an amount of nitrate, or nitrite stock solution so that each run was performed at a different initial NO_3^-, or NO_2^- concentration. During each kinetic run, the liquid phase and the head-space of the bottle were frequently sampled. The volumes of the samples were carefully monitored and recorded, so that eventually an accurate nitrogen balance could be performed as explained and discussed in Chapter 5.

Gas samples were taken with a 0.1 mL gas tight syringe (Pressure-Lok series A-2, 2 mL, AllTech Associates, Avondale, PA), and subjected to gas chromatographic analysis for monitoring the nitrogen, nitrous oxide, and oxygen presence in the headspace of the bottle. Before its use, the gas syringe was rinsed three times with helium gas.

Liquid samples were taken for monitoring the biomass concentration via optical density measurements, and the nitrate/nitrite concentrations via ion chromatographic analysis, as explained in subsequent sections of this chapter. The liquid sample used for OD measurements, was also used for measuring the pH value, via a pH electrode (Orion, Boston, MA).

Experiments were performed at different temperatures in the range of 30 to 40 °C. During each kinetic run, the temperature was maintained constant by placing the serum

Reproduced with permission of the copyright owner. Further reproduction prohibited without permission.

bottle in a Gyrotary Water Bath Shaker (New Brunswick Scientific, New Brunswick, NJ).

Most experiments were performed at a pH value of 7.1. For these experiments, the medium had the composition discussed in section 4.3.1. However, experiments were also performed under other pH values. In such cases, the pH of the medium was adjusted by the addition of calculated precise amounts of either 0.5 N acetic acid, or 0.5 N sodium hydroxide solution.

4.4 SBR Experiments

4.4.1 Design and Components of the SBR Unit

The SBR experiments were performed in a laboratory-scale microprocessor controlled unit, a detailed process and instrumentation diagram (P & ID) of which, is shown in Figure A-2.

The heart of the unit was a 3 L fermentor (BioFlo II, New Brunswick Scientific, New Brunswick, NJ), accompanied by a time sequence controller (Model SCY-PO, Omron, Peabody, MA).

The fermentor unit was equipped with microprocessors for controlling the pH, dissolved oxygen (DO), agitation speed, temperature, nutrient feed rate, and foam formation. The vessel was made of thick walled flanged glass tube, covered by a stainless steel head plate. The vessel was placed on the top of a jacketed dished-head for temperature control purposes. The head plate of the vessel had a number of ports allowing for inoculation, sampling, feed, as well as for immersing temperature, pH, and DO sensors.

A steam sterilizable 8" long Galvanic Oxygen Electrode (Ingold, purchased from New Brunswick Scientific, New Brunswick, NJ) was used for DO monitoring. The pH was monitored via a steam sterilizable combined electrode (Type 465, Ingold, purchased from New Brunswick Scientific, New Brunswick, NJ).

SBR operation implies feeding the reactor, and decanting parts of its contents at

Reproduced with permission of the copyright owner. Further reproduction prohibited without permission.

different time intervals. A schematic of the variation of the reactor contents volume during a SBR cycle is shown in Figure A-3. To experimentally realize this mode of operation, pumps and valves activated at different instants of time need to be used.

In the experimental unit, flowrates of various streams were determined and controlled by three Masterflex® tubing pump drives (Masterflex® L/S "Unified" Drives Model 7520-35, Cole-Parmer, Niles, IL), and three pump-heads (Masterflex® Easy-Load® Pump Head Model 7518-10, Cole-Parmer, Niles, IL). The calibration curve for the pumps is shown in Figure A-5. Five Skinner valves (Honeywell, New Britain, CT) were used for implementing the signals from the time sequence controller, and determining (based on the on/off position) the flows of the liquid and gaseous streams.

The feed tank was a 20 L polypropylene container having a rubber seal.

The whole system was sealed and pressurized (~3 psig) with helium gas during the experiments in order to maintain anaerobic conditions. A sensitive gas leak detector (TEKMAR GLD, Model 15, Fischer Scientific, Pittsburgh, PA) was used for checking the existence of any leakage from the system.

To continuously operate a pressurized system requires special care for avoiding leaks. During the fill-phase, pumps P1 and P3, and the corresponding valves V1, V3, and V5 were activated by the time sequence controller. As medium was fed into the reactor, the volume of the head-space decreased and thus the pressure, increased in the reactor, and decreased in the feed tank. For this reason, valve V3 was activated to remove an amount of gas from the reactor; this was done through a water seal in order to prevent back flow of air. Similarly, valve V5 was activated so that helium gas was supplied to the feed tank. This way, the pressure inside the system was kept constant. During the "react"-phase, the reactor operated in the batch mode. Only valve V4 was active for allowing supply, as needed, of helium gas into the reactor so that the pressure was again kept constant. During the draw-down phase, an amount of the reactor contents were decanted by the use of pump P2. The exit stream, through valve V2, was collected into a

Reproduced with permission of the copyright owner. Further reproduction prohibited without permission.

waste container. During this phase, the pressure in the reactor would decrease if valve V4 was not kept on so that helium gas was supplied to the reactor. During this period, and in preparation for the fill-phase, the feed tank was purged with helium gas through valve V5. A schematic of the on/off position of pumps and valves during a SBR cycle is shown in Figure A-4.

4.4.2 Procedures for SBR Experiments

The medium used in the SBR experiments had the same composition as the one used in the kinetic experiments (section 4.3.1). Initially no nitrate, nitrite, or methanol was added to the medium. Each time, 15 L of medium were prepared in six 2.5 L glass bottles. Each bottle carried the various chemicals at amounts 2.5 times those reported in section 4.3.1 for the preparation of 1 L of solution. Deionized Milli-Q® water was used. After dissolving the chemicals, the solution was filtered with filter membranes (Type HV, 0.45 μm pore size, Millipore, Bedford, MA) to remove any undissolved solids which would interfere with the optical density measurements for biomass concentration monitoring. The vacuum applied for the filtration process, led also to removal of the dissolved oxygen from the medium. To enhance the DO removal, the filtrate was placed in an ultrasonicator (Solid State/Ultrasonic FS-28, Fisher Scientific, Pittsburgh, PA). The bottles carrying the filtered medium were sealed with caps and placed in the autoclave. After pasterization, amounts of nitrate and/or nitrite stock solutions (see section 4.3.1) were added in the bottles so that the desired NO_3^-/NO_2^- concentration for the particular SBR run was obtained. Subsequently, the contents of the bottles were transferred into the feed tank which had been cleaned and sterilized.

Before each run, the reactor vessel with the DO and pH electrodes, was rinsed and sterilized in the autoclave. After sterilization, the pH electrode was calibrated with two standard buffer solutions of pH 7.0 and 10.0. The procedure for calibrating the DO probe was as follows. The probe was disconnected for 1 min to set the zero point. An amount

Reproduced with permission of the copyright owner. Further reproduction prohibited without permission.

of deionized water was placed in the vessel, and air was sparged through it for 30 min. The water was kept at 30 °C and was agitated at 100 rpm. After 30 min, the reading of the DO probe was taken and set at 100 %. The reactor was drained, and vacuum was applied through the three-way valve shown in Figure A-2 in order to remove the air. Subsequently, the time sequence controller was used for activating valves V3 or V4 so that helium gas was supplied, and then removed from the reactor. This helium gas rinsing procedure lasted for several hours. During this period, the system was checked with the leak detector to ensure that it was perfectly sealed.

After rinsing the reactor with helium gas, 1 L of medium was brought into the reactor from the feed tank. The solution in the feed tank had already been purged with helium gas for 30 min. If the DO reading was not zero, the reactor and the feed tank were purged with helium gas again.

Once the DO reading was zero, the 1 L medium present in the reactor was inoculated through the appropriate port, with a calculated amount of primary biomass suspension (see section 4.2). The culture was left in the reactor for a period of 24 h for activation of its denitrification enzyme system. After this period, the suspension present in the reactor was sampled; biomass, NO_3^-, and NO_2^- concentrations were measured. Their values in the reactor were adjusted to the desired start-up conditions by the addition of water or medium. After this adjustment which was made so that the system was close to its predicted steady cycle, the time sequence controller was programmed, activated, and the SBR experiment started.

During SBR runs the gas phase of the reactor was not sampled for analysis. Liquid samples (about 10 mL) were collected through the sampling valve shown in Figure A-2. The positive pressure in the reactor allowed sampling by just opening the valve. The sample was used for optical density, and nitrate and/or nitrite concentration measurements through the methodologies described in the following sections.

Reproduced with permission of the copyright owner. Further reproduction prohibited without permission.

4.5 Analytical Methods

Concentrations of various constituents of the liquid phase, and of the gas phase (in the case of the kinetic runs), were monitored via the following methodologies.

4.5.1 Nitrate and Nitrite Assays

The concentrations of nitrate and nitrite in the liquid phase were monitored through ion chromatographic (IC) analysis. The IC unit used consisted of a Waters 600E system controller, a Waters 715 Ultra WISP Sample Processor, an IC-PAK A HC 150 x 4.6 mm 10 μm Column, a Waters 431 Conductivity Detector, and a Waters 484 Turnable Absorbance Detector, all components made by a division of the Millipore Co. (Waters Chromatograph Division, Milford, MA). The unit was also equipped with a Chromatography Server (VG Data Systems Ltd., purchased from Fisons Co., Denvers, MA). The data were handled by the MiniChrom (version 1.5, VG Data Systems Ltd., purchased also from Fisons Co., Denvers, MA) software package which was installed in a CompuAdd 325 PC/AT 486 (CompuAdd, Austin, TX) unit.

Analysis of samples containing nitrate and/or nitrite followed the US EPA/Waters method A-102. The procedure for preparing the borate/gluconate eluent and working standards followed the Waters IC Manual. The unit operated under the following conditions:

Eluent: Borate/Gluconate	**Injection:** 100 μL of sample
Pump: 600E Solvent Delivery Module	**Detection:** 484 UV/Vis at 214 nm
Injector: 715 Ultra WISP	**Range:** 500 μS[1]
Column: IC-PAK Anion HC	**Temperature:** On
Data: Chromatography Server	**Polarity:** +
Flow rate: 2.0 mL/min.	**Background:** 274 μS

[1] 1 μS (one microSiemen) = 1 ohm^{-1} = 1 mho.

Reproduced with permission of the copyright owner. Further reproduction prohibited without permission.

The preparation of samples for IC analysis was done as follows. An amount of 4.5 mL deionized water was measured and added to a 10 mL polypropylene sampling vial. A suspension sample of about 0.6 mL was taken from the reactor (serum bottle or SBR), with a 1 mL disposable syringe (Luer-Lock tip, J & H Berge, purchased from AllTech, Deerfield, IL). The syringe was erected with the tip up, and gently knocked with the fingers to remove the gas bubble which was usually trapped inside the syringe. The plunger of the syringe was pushed, and the liquid discarded, until the 0.5 mL mark on the syringe was reached. This 0.5 mL sample was transferred into a polypropylene sampling vial which already contained 4.5 mL water as discussed above. The vial was covered, and its contents mixed for 10 sec. A clean 5 mL disposable syringe (Luer-Lock Tip, Becton Dickinson, Rutherford, NJ), without the needle was used in uptaking about 4 mL of the diluted sample. On the syringe tip, a plastic Swinney filter holder (13 mm OD, Gelman No. 4317, Gelman, Ann Arbor, MI) containing a Nylaflo nylon membrane filter (0.2 μm pore size, 13 mm OD, Gelman No. 66600, Gelman, Ann Arbor, MI) was adapted. The filter allowed for removal of the biomass present in the sample. During the filtering process, the first 2 mL were discarded in order to allow saturation of the nylon membrane. Subsequently, an amount of filtrate (about 1 mL) was collected in a clean sepcap IC vial (96 positions, National Scientific Company, Lawrenceville, GA), and placed in the IC autosampler for analysis. Although the biomass was removed, the samples were analyzed immediately after preparation in order to exclude the possibility of further NO_3^- / NO_2^- reduction due to potential presence of extracellular active enzymes.

The IC unit was equipped with both a conductivity and a UV/Vis detector, and in principle, either detector can be used for measuring nitrate and/or nitrite concentrations. The UV/Vis detector was selected for the following reasons. The samples contained phosphate and chloride ions. The retention time of nitrate (about 11 min), is very close to that of the phosphate ion (about 13 min). In addition, the retention time of nitrite (about 6 min), is very close to that of the chloride ion (about 5 min). Since the conductivity

Reproduced with permission of the copyright owner. Further reproduction prohibited without permission.

detector is very sensitive to temperature variations, it may affect the accuracy of IC measurements. Furthermore, the positive peaks of the aforementioned anions were so close that there was an overlap of peaks. On the other hand, the UV/Vis detector is not very sensitive to temperature variations, and in addition, the UV absorbencies of the chloride and phosphate ions are negligible. Thus, the UV/Vis detector allowed for a more accurate determination of NO_3^- and NO_2^- concentrations.

The IC calibration curves for nitrate and nitrite are given in Figures A-6 and A-7, respectively. These curves were prepared from readings on a series of standard solutions, for nitrate and for nitrite. The series contained the component of interest at 0.5, 1.0, 5.0, 10.0 and 20.0 mg/L. The IC system was conditioned for at least 30 min with the borate/gluconate eluent, until the temperature and pressure reached steady state conditions. An IC sample vial containing Mill-Q® water[2], was used as a blank. The blank sample was run through the system three times to perfectly rinse the needle and the flow system. Subsequently, 100 µL samples of the standard solutions were injected into the unit, starting with samples containing the lowest concentration of the component of interest. The length of each run was 17 min so that the last peak (that of phosphate) was detected. The appropriate parameters were selected for the data acquisition software, the IC peaks were stored, and their areas measured. From the values of the appropriate peaks, and the known concentrations of the standards, the calibration curves were prepared. Calibration was repeated every time the IC unit was used for processing samples from experimental runs.

As mentioned earlier, actual samples of 0.5 mL were diluted with 4.5 mL water for preparing the samples processed in the IC unit. This was done in order to avoid overloading the IC column with inorganic salts. The maximum column capacity was 100 mg - total salts / L.

---

[2] Milli-Q® water: Water which was filtrated by the Milli-Q® water system (Millipore Co.). It provides an electric resistance of 18 megaohm (MΩ).

Reproduced with permission of the copyright owner. Further reproduction prohibited without permission.

In order to avoid inaccuracies due to nitrate/nitrite retained by the needle of the autosampler, the system was frequently rinsed by running Milli-Q® water samples through it. When samples containing high nitrate/nitrite concentrations were processed, the rinsing procedure was repeated after processing each individual sample.

A final comment needs to be made regarding the preparation of the standard solutions for calibration. The very low concentration containing standards are hard to prepare directly, since even an electronic balance cannot be used in weighing minute quantities of KNO_3 and KNO_2. For this reason, these standard solutions were prepared via dilution, using a precision liquid pipette (Pipetman, Gilson, France), of precise volumes of standard solutions containing the components of interest at higher concentration levels.

4.5.2 Biomass Assay

As mentioned in the previous section, samples of biomass suspension were diluted, and then filtered for preparing the samples processed for determining the NO_3^- and/or NO_2^- concentration via IC analysis. It was also mentioned that the pore size of the membrane filter was 0.2 μm. This size was selected after the particle size distribution of *P. denitrificans* cells was determined via a Coulter® Counter (Coulter Scientific, Luton, Beds, England). Cells were grown, and samples of the suspension were processed for size distribution analysis. The analysis showed that cell sizes ranged between 0.1 and 0.5 μm, and about 98 % of them had sizes greater than 0.2 μm; hence, the pore size for the membrane filter was selected to be 0.2 μm. The Coulter® Counter unit consisted primarily of a Coulter® Sampling Stand II, and a Coulter® Multisizer (Coulter Scientific, Luton, Beds, England). The balance electrolyte solution used, was ISOTON® II (Coulter Scientific, Luton, Beds, England). Calibration and operation of the unit followed the procedures described in the manuals provided by the manufacturer of the unit.

Biomass concentration during kinetic and SBR runs was monitored by measuring the optical density of samples at a wavelength of 540 nm in a Varian DMS 200 UV-

Reproduced with permission of the copyright owner. Further reproduction prohibited without permission.

Visible spectrophotometer (Varian Scientific, San Fernando, CA)

The calibration procedure for the OD measurements was as follows. Synthetic medium of composition as that described in section 4.3.1, was placed in 8 serum bottles. Each bottle was spiked with 1 mL of a solution containing nitrate, or nitrite at 100 mg/L, and methanol at levels twice those of NO_3^- or NO_2^-, on a molar basis. The bottles were inoculated with an amount of biomass prepared as discussed in section 4.2, and placed in an incubator shaker (Series 25, New Brunswick Scientific, New Brunswick, NJ) for 24 hours. The bottles were spiked with NO_3^- / NO_2^- / methanol until a relatively thick suspension was obtained. The contents of the 8 bottles were then transferred in a 1 L flask, and mixed for 3 min. A 4 mL sample was placed in a cuvette. Its absorbance was measured at a wavelength of 540 nm, and found to be 0.254 units of OD. Other samples were first diluted with precisely measured quantities of deionized water, and the OD of samples from the resulting solutions was measured at 540 nm. The unused amount of the original biomass suspension was centrifuged (MSE Mistreal 3000i, purchased from CMS, Morris Plains, NJ), at 30 °C, 5000 rpm for 15 sec. The concentrated biomass was rinsed with deionized water for three times in order to remove any salts absorbed on it. Finally, it was placed in two pre-weighed plastic tubes. The weight of the filled tubes was determined, before they were placed in a decanter where they stayed for a period of one week. The weight of the dry biomass containing tubes was measured again. The weight of the empty tubes was subtracted from these readings, and thus the amount of dry biomass contained in the volume of the suspension which was centrifuged was determined, and from it, the biomass concentration of the samples having an OD of 0.254. The values of the various weights mentioned above are shown in Table A-1. Knowing the biomass concentration of the original suspension, and the dilution factor in all other samples used in OD measurements, a calibration curve was prepared and is shown in Figure A-8. From the regression of biomass versus UOD data, a response factor of 256.3 mg-dry-biomass/L/ UOD was found.

Reproduced with permission of the copyright owner. Further reproduction prohibited without permission.

During the kinetic experiments, 3.4 mL samples were taken with a 5 mL disposable syringe, placed in a cuvette, and immediately processed in the UV/Visible spectrophotometer. The absorbance values were recorded over a period of up to 3 min; the average of these values was taken as the biomass concentration in the serum bottle at the time of sampling. During SBR experiments samples were obtained through the sampling valve, and then processed as the samples from the serum bottles.

4.5.3 Gaseous Components Assay

During the kinetic runs, the head space of the serum bottles was sampled for monitoring the concentrations of N_2, O_2, and N_2O. Nitrogen and nitrous oxide are products of the reactions, while oxygen measurements were made in order to detect leakage of air into the bottles. The gas samples were subjected to gas chromatographic (GC) analysis in a Carle Gas AGH 111H unit (Carle Instruments, Inc., Tulsa, OK), which was connected to a HP 3396A chromatography integrator (Hewlett-Packard, Avondale, PA). The procedures for installation, calibration, and operation of the GC and the integrator followed the guidelines given in the manufacturer's manuals. A schematic of the GC flow system is shown in Figure A-10. Since nitrogen was one of the products to be monitored, helium was used as the carrier gas. For measuring the N_2O moles, a Porapak Q column, 80/100 mesh, 12' x 1/8" (Supelco, Bellefonte, PA) was used. Nitrogen and oxygen moles were monitored through the use of a Molecular Sieve 5A column, 60/80 mesh, 9' x 1/8" (Supelco, Bellefonte, PA). When one column was used for processing a sample, the other served as a reference for the TCD detector. The flow rates of the carrier gas were regulated by an adjustable flow controller (Model 202, UICI ConDyne, Inc., AllTech, Deerfield, IL), and checked by an on-line flow meter (Flow Check, AllTech, Deerfield, IL). The column temperature was maintained at 30 °C. The conditions of operation were:

Reproduced with permission of the copyright owner. Further reproduction prohibited without permission.

Attenuation: 1	**Output:** 16
Chart Speed: 0.3	**Columns:** 60/80 Molecular Sieve 5A, 80/100 Porapak Q
Area Rejection: 0	**Column Temperature, °C:** 30
Threshold: 0	**Injection Temperature:** On
Peak Width: 0.01	**Helium Flow Rate, mL/min:** 25
Bridge Setting: 3	**Bottle Pressure, psig:** 5

Under these operating conditions, the retention times for nitrogen, oxygen, and nitrous oxide were 1.28, 1.47, and 4.5 min, respectively.

Calibration of the GC for N_2, O_2, and N_2O mole measurements was done as follows. Several air samples of 0.025, 0.1, and 0.2 mL were taken by a 2 mL gas-tight syringe (Pressure Lok Series A-2, AllTech, Deerfield, IL), and injected to the GC for analysis. The areas of the peaks were determined, and attributed to a number of moles based on the volume of the sample, and by assuming ideal gas behavior. Typical values for the peak areas obtained for N_2 and O_2 calibration are shown in Tables A-2 and A-3, respectively. The calibration curves are shown in Figure A-9.

For N_2O GC calibration, the standard gas was N_2O contained in a 99 % Lecture Bottle (Liquid Carbonic, Bethlehem, PA). The lecture Bottle was used instead of helium in the unit schematically shown in Figure A-1. A single stage pressure regulator (CGA 580, Max. Del. 15 psig, Max. Inlet 3000 psig, J & H. Berge, purchased from AllTech, Deerfield, IL) was used for a better control of the pressure in the serum bottle. The serum bottle was pressurized with N_2O gas and then evacuated for several times, before it was finally filled with N_2O gas at 5 psig. A number of 0.025, 0.050, and 0.075 mL samples were taken from the bottle and analyzed in the GC, as in the cases of N_2 and O_2 discussed above. Table A-4 shows typical values of peak areas obtained, and Figure A-9 shows the calibration curve.

During the kinetic runs, 0.1 mL samples were taken from the head space of the serum bottles and injected to the appropriate GC port for N_2 and O_2 analysis. When this

Reproduced with permission of the copyright owner. Further reproduction prohibited without permission.

sample had been processed, another 0.1 mL sample was taken, again with a gas-tight syringe, and injected in the other GC port which led to N_2O moles determination. The sampling procedure was repeated at frequent time intervals. The GC calibration was checked on a weekly basis during the period of the kinetic experiments.

Reproduced with permission of the copyright owner. Further reproduction prohibited without permission.

CHAPTER 5

DENITRIFICATION KINETIC STUDIES

5.1 General Approach

In this chapter the results of a detailed kinetic study of biological nitrate and/or nitrite reduction are presented. The experiments involved reduction of nitrate, nitrite, and nitrate/nitrite mixtures by *P. denitrificans* (ATCC 13867), under anaerobic conditions. Methanol was used as the carbon source for the organisms. The medium was formulated in such a way that only nitrate and nitrite would exert kinetic limitation on the growth of the culture. The study entailed finding the dependence of reduction kinetics on nitrate and nitrite concentration, temperature, and pH. Experiments were performed in small scale, in serum bottles of 160 mL, as explained in the preceding chapter.

The general experimental protocol was as follows. The first class of experiments involved three series of runs under a constant temperature of 30 °C and a pH of 7.1 ± 0.1. In the first, the medium contained nitrite only at different initial concentrations. The second series involved experiments with nitrate containing medium at various concentrations. The third series of experiments was performed with media containing both nitrate and nitrite at different relative concentrations. The second class of experiments examined the effect of temperature while the pH was again maintained at 7.1 ± 0.1. Isothermal conditions were maintained during runs at 32.5, 35, and 38 °C with media which originally contained either nitrite, or nitrate at various concentrations. Experiments with media originally containing both nitrate and nitrite were performed at 37 and 38 °C. The third class of experiments involved investigation of the effect of pH at a temperature of 30 °C. There were two series of runs. The first involved media containing nitrite only at 50 mg/L, and the second was with media carrying nitrate only at 50 mg/L.

Reproduced with permission of the copyright owner. Further reproduction prohibited without permission.

Within each series, experiments were performed under constant pH values in the range from 6 to 12.

The experimental data from all runs were analyzed in order to derive detailed analytical expressions for the denitrification rates.

5.2 Modeling of Kinetics Under Constant Temperature and pH

When a microbial culture grows in a batch system under conditions of constant temperature and pH, and when growth is kinetic limited by the availability of a single substrate, the process can be described by two mass balances: one on the biomass, and one on the rate-limiting substrate. These two equations can assume the following form:

$$\frac{ds}{dt} = -\frac{1}{Y}\mu(s)b \qquad (5.1)$$

$$\frac{db}{dt} = [\mu(s) - \mu_c]\, b = \mu_{net}\, b \qquad (5.2)$$

where, s and b are concentrations of the substrate and biomass, respectively; Y is the true yield coefficient of the biomass on the rate limiting substrate; $\mu(s)$ is the specific growth rate of the biomass on the rate limiting substrate; t is time; and μ_c is the specific rate of biomass self oxidation for fulfillment of energy needs for maintenance.

Equation (5.2) adopts the model of Herbert (1958), for maintenance. When the substrate which limits growth is also directly used for maintenance purposes, then equation (5.1) needs to be modified with the inclusion of one more consumption term. In the latter case, the substrate should be the energy source; if the specific rate of substrate consumption is assumed constant, the modification of equation (5.1) assumes the form proposed by Pirt (1965) and Marr et al. (1963). The modification according to Pirt is based on concepts discussed by Schulze and Lipe (1964), but is problematic as it predicts negative substrate concentrations. Maintenance is an integral part of the endogenous metabolism of microorganisms, a topic which has been reviewed by various authors [e.g., Dawes and Ribbons, 1962 and 1964].

Reproduced with permission of the copyright owner. Further reproduction prohibited without permission.

Equations (5.1) and (5.2) imply that biomass and substrate concentration measurements during a run can be used in determining an apparent yield coefficient (Y_{app}), since,

$$Y_{app} = \frac{db}{-ds} \tag{5.3}$$

Values of Y_{app} can be used in determining Y and μ_c as follows. Taking into consideration the fact that

$$\mu(s) = \mu_{net} + \mu_c \tag{5.4}$$

equation (5.1) can be written as

$$\frac{ds}{dt} = -\frac{1}{Y}(\mu_{net} + \mu_c)\, b \tag{5.5}$$

From equations (5.2), (5.3), and (5.5) one gets

$$Y_{app} = \frac{Y \cdot \mu_{net}}{\mu_{net} + \mu_c} \tag{5.6}$$

which can be rearranged as

$$\frac{1}{Y_{app}} = \frac{1}{Y} + \frac{\mu_c}{Y}\frac{1}{\mu_{net}} \tag{5.7}$$

Since during the logarithmic phase of growth $\mu(s)$ is constant, and μ_c is assumed constant, μ_{net} is also constant and is the slope of the ln b versus t line. Experimental data from runs with different initial substrate concentrations can be used in generating pairs of (Y_{app}, μ_{net}) values. When the reciprocal of these values are plotted against each other, according to equation (5.7), they fall on a straight line which has a slope equal to μ_c/Y and intercept 1/Y. Thus, the values of Y and μ_c can be revealed.

It should be mentioned that in many instances maintenance requirements are not important, and can be neglected. In the classical work of Monod (1942) for example, it is reported that maintenance requirements during growth of *Escherichia coli* on glucose are insignificant. In such cases, equations (5.1) and (5.2) are still valid by simply setting μ_c

Reproduced with permission of the copyright owner. Further reproduction prohibited without permission.

equal to zero; consequently, the true and the apparent yield coefficients are identical, something which can be seen from either equation (5.6), or (5.7).

The specific growth rate $\mu(s)$, which appears in equations (5.1) and (5.2) can take various forms among which, the most common are those proposed by Monod (1942) [expression (5.8)], and Andrews (1968) [expression (5.9)]

$$\mu(s) = \frac{\mu_m s}{K_m + s} \tag{5.8}$$

$$\mu(s) = \frac{\hat{\mu}\ s}{K + s + \frac{s^2}{K_I}} \tag{5.9}$$

In expression (5.8) μ_m is the maximum specific growth rate and has units of inverse time; K_m has units of concentration -same as s- and is known as the half-saturation constant by analogy to the Michaelis-Menten kinetics for enzymatic reactions (Bailey and Ollis, 1986; Shuler and Kargi, 1992). Expression (5.9) involves three kinetic constants which do not really have a physical significance; K and K_I have units of concentration -same as s- and $\hat{\mu}$ has units of inverse time; constant K_I is known as the inhibition constant; K is not a saturation constant and cannot be compared to K_m. In many instances, $\hat{\mu}$ is referred to in the literature as the maximum specific growth rate; this is not correct. In fact, expression (5.9) predicts a maximum specific growth rate given by expression (5.10).

$$\text{when } s = \sqrt{K \cdot K_I},\ \mu(s) = \mu_{max} = \frac{\hat{\mu}}{1 + 2\sqrt{\frac{K}{K_I}}} \tag{5.10}$$

Expression (5.9) implies that high substrate concentrations inhibit growth, and according to Shuler and Kargi (1992), it could imply a noncompetitive substrate inhibition pattern when $K_I >> K$.

For the case of nitrite reduction by a culture in a batch system, one could use equations (5.1) and (5.2) to describe the process based on the following reasoning. It is

Reproduced with permission of the copyright owner. Further reproduction prohibited without permission.

known that under anaerobic conditions, nitrite serves as the terminal electron acceptor in the respiratory chain. It can also serve as the nitrogen source for biomass growth. If respiration is assumed to be growth associated, and if nitrogen availability limits the growth, then equations (5.1) and (5.2) can be used. In this case, the physical significance of Y is not that of the amount of biomass produced per unit amount of substrate consumed for growth purposes, but rather it represents the amount of biomass produced per unit amount of substrate consumed for growth and respiratory purposes. It is recognized that nitrite reduction (during respiration) may lead to formation of nitric oxide and/or nitrous oxide before the final reduction product (N_2) is formed. Consequently, the use of equations (5.1) and (5.2) to describe reduction of nitrite, also implies that the potential intermediate products do not interfere with the kinetics of nitrite biological elimination.

As discussed in the literature survey, reduction of nitrate leads to nitrite accumulation in many cases. This suggests that nitrite, an intermediate of nitrate reduction, is not short-lived and thus, it affects the process of nitrate eventual reduction to nitrogen. As a result, when a medium contains nitrate only, and if nitrate is used as the nitrogen source for growth, as well as for respiratory purposes (in a growth associated pattern), equations (5.1) and (5.2) cannot be used, except at the very beginning of an experiment when nitrite accumulation has not yet reached any significant levels. To describe completely, the biological elimination of nitrate, as well as of nitrate/nitrite mixtures, one could use the following equations.

Balance on nitrate:

$$\frac{ds}{dt} = -\frac{1}{Y_1}\mu_1(s,u)b \tag{5.11}$$

Balance on nitrite:

$$\frac{du}{dt} = \alpha\frac{1}{Y_1}\mu_1(s,u)b - \frac{1}{Y_2}\mu_2(u,s)b \tag{5.12}$$

Reproduced with permission of the copyright owner. Further reproduction prohibited without permission.

Balance on biomass:

$$\frac{db}{dt} = [\mu_1(s,u)+\mu_2(u,s)]b - (\mu_{c1}+\mu_{c2})b$$
$$= (\mu_{1net} + \mu_{2net})b \qquad (5.13)$$

with,

$$\mu_{1net} = \mu_1(s, u) - \mu_{C1} \text{ and } \mu_{2net} = \mu_2(u, s) - \mu_{C2} \qquad (5.14)$$

where s and u are the nitrate and nitrite concentrations, respectively; b is the biomass concentration; $\mu_1(s, u)$ and $\mu_2(u, s)$ are the specific growth rates of biomass on nitrate and nitrite, respectively; Y_1 and Y_2 are the amounts of biomass produced per unit amount of nitrate and nitrite, respectively, consumed for both growth and respiration; α is a constant denoting the amount of nitrite produced per unit amount of nitrate consumed; and, μ_{c1} and μ_{c2} are specific maintenance rates associated, respectively, with nitrate and nitrite biological elimination.

The assumptions under which model equations (5.11) - (5.13) are valid, are as follows. Nitrate and nitrite serve as electron acceptors and participate in the respiration process. In addition, both nitrate and nitrite can serve as nitrogen sources for biomass growth, and the availability of each one of them exerts limitation on the growth rate. The culture uses nitrate and nitrite for growth purposes, simultaneously and without any preference, thus the overall specific growth rate is simply the sum of the two individual specific growth rates. Maintenance requirements associated with nitrate elimination are different from those associated with nitrite depletion. This could be explained by assuming that maintenance requirements are associated with synthesis of reductases, and that they are different for nitrate reductase and nitrite reductase. Regarding constant α, it can be calculated from a balance on the nitrogen atoms based on the following equations:

Nitrate (NO_3^-)	$\rightarrow$	Nitrite (NO_2^-)	+	Biomass (N-containing)
1 g		α g		Y_1 g
1/62 g-atom N		α/46 g-atom N		$Y_1\pi$/M g-atom N

Reproduced with permission of the copyright owner. Further reproduction prohibited without permission.

where M is the "molecular weight" of biomass, and π is the number of nitrogen atoms in the "molecular formula" of the biomass.

A simple nitrogen-atom balance yields

$$\alpha = 46\left[\frac{1}{62} - \frac{Y_1\pi}{M}\right] \tag{5.15}$$

The specific growth rate expressions for the biomass on both nitrate and nitrite, in equations (5.11) - (5.13), are indicated to be functions of both nitrate and nitrite concentrations. This is done because there are reports -discussed in the literature review chapter- (Kodama et al., 1969; Timmermans and Van Haute, 1983), indicating that nitrate and nitrite may be involved in inhibitory kinetic interactions. Particular expressions which can be used for $\mu_1(s, u)$ and $\mu_2(u, s)$ are

$$\mu_1(s, u) = \frac{\hat{\mu}_1 \; s}{K_1 + s + \frac{s^2}{K_{I1}} + K_{21}\, u\, s} \tag{5.16}$$

$$\mu_2(u, s) = \frac{\hat{\mu}_2 \; u}{K_2 + u + \frac{u^2}{K_{I2}} + K_{12}\, s\, u} \tag{5.17}$$

Constants K_{12} and K_{21} have units of inverse concentration and can be called cross-inhibition constants; their magnitude indicates the intensity of the kinetic interaction between the two substrates (nitrate and nitrite). If K_{21} and/or K_{12} are equal to zero, expressions (5.16) and/or (5.17) reduce to the Andrews model. If the two substrates do not interact, and K_{I1} and/or K_{I2} are very large, expressions (5.16) and/or (5.17) reduce to the Monod model. As discussed in Chapter 2 there are reports indicating that nitrite biological elimination follows inhibitory kinetics. Regarding nitrate, although most researchers have used Monod-type kinetics, there are reports -sometimes by the same researches- indicating that depending on the culture, nitrate may follow Monod-, or inhibitory-type kinetics (e.g., Nakajima et al., 1984a and 1984b). Shuler and Kargi (1992)

Reproduced with permission of the copyright owner. Further reproduction prohibited without permission.

indicate how the specific growth rate expression of a culture on a particular substrate can be altered due to the presence of an inhibitor. Various expressions are proposed depending on the pattern of inhibition, and they are all adaptations from principles of enzyme kinetics inhibition (Dixon and Webb, 1979). Expressions (5.16) and (5.17), can be viewed as modified rates due to noncompetitive inhibition by another substrate.

5.3 Results and Discussion

5.3.1 Studies at 30 °C and pH = 7.1 ± 0.1

Experiments with medium which contained nitrate only (as nitrogen source, and terminal electron acceptor), were performed at a number of different initial nitrate concentrations, and the data are reported in full detail in Table B-1. In this table, values of the liquid phase nitrate, nitrite, and biomass concentrations along with gas phase concentrations of nitrous oxide, and nitrogen are reported. In Table B-1, V_o stands for the initial volume of liquid (biomass suspension) in the 160 mL vial. Similarly, data from experiments with nitrite are reported in Table B-2. With the exception of nitrate, which was absent, Table B-2 reports measured values for the quantities reported in Table B-1 for the first series of experiments.

The biomass concentration data from each experimental run reported in Tables B-1 and B-2 were plotted semilogarithmically versus time. An example (from run 22A), is shown in Figure 1. The initial points (usually from the first hour of the run), in the ln b versus t plane were regressed to a straight line as shown in Figure 1. For the regression, the method of least squares was used. The slope of the line was taken as the μ_{net} at the initial nitrate or nitrite concentration of the run. This approach assumes that equation (5.2) is valid, and that μ_{net} is constant during the exponential growth phase. There is no problem with the validity of equation (5.2) for the experiments with nitrite, while with

Reproduced with permission of the copyright owner. Further reproduction prohibited without permission.

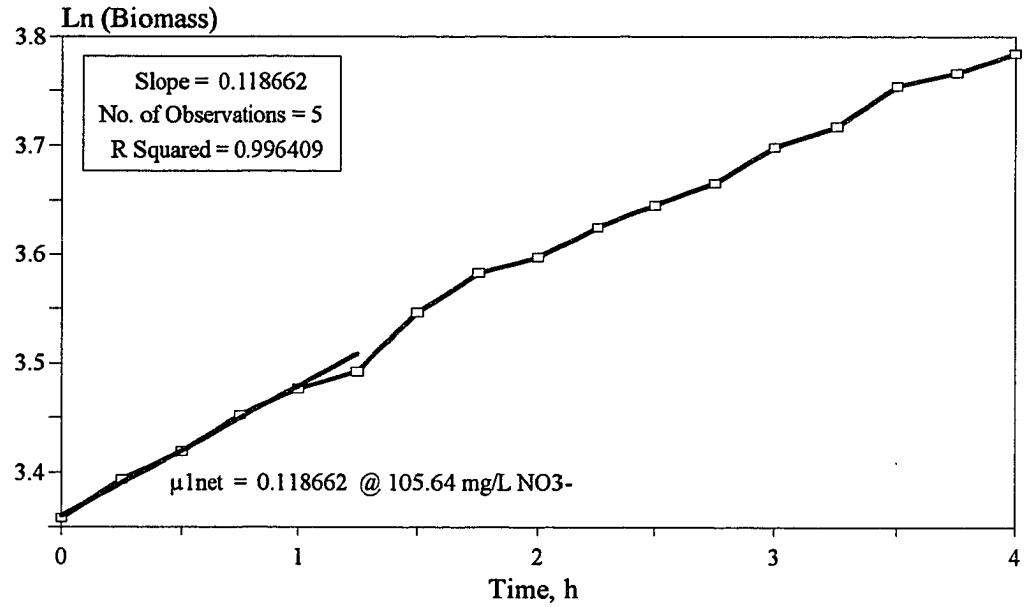

Figure 1 Determination of the net specific growth rate of biomass on nitrate from run 22A.

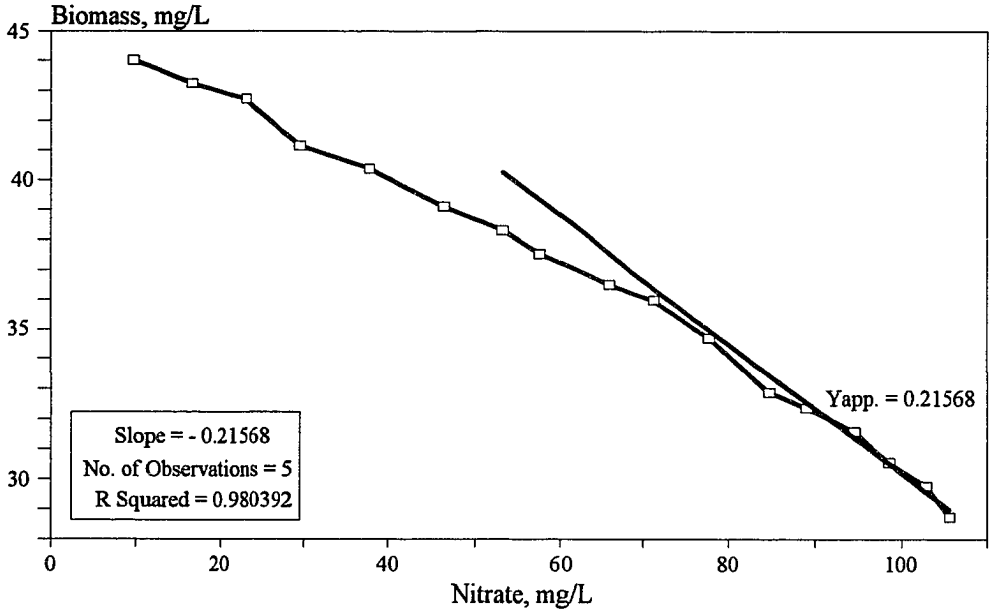

Figure 2 Determination of the apparent yield coefficient of biomass on nitrate from run 22A.

Reproduced with permission of the copyright owner. Further reproduction prohibited without permission.

nitrate one can again use it with confidence since [see Table B-1], in the great majority of the runs, and at least for the first hour, nitrite presence did not exceed the level of 2 mg/L. If maintenance were not important, then μ_{net} would be the real specific growth rate. Values of μ_{1net} and μ_{2net} for all experimental runs are reported in Tables B-3 and B-4.

Biomass and nitrate, or nitrite concentration data from each run reported in Table B-1 and B-2 were plotted against each other on an arithmetic scale, as shown [data from run 22A], in Figure 2. If Y_{app} were constant, equation (5.3) would imply that *b* versus *s*, or *b* versus *u* data fall on a straight line. This was not the case as can be seen from Figure 2. Only data from the initial phase of each run appeared to be falling on a straight line. Consequently, for each experimental run, only the biomass data which were semilogarithmically regressed to a straight line versus time, were also linearly regressed versus the corresponding substrate concentration values. The slope of the resulting line was taken, according to equation (5.3), as $-Y_{app}$, and was attributed to the μ_{net} value which was determined as explained in the preceding paragraph. Values of Y_{app}, corresponding to the beginning of all experimental runs, are given for nitrate in Table B-3, and for nitrite in Table B-4.

The fact that Y_{app} was not constant implied that maintenance requirements cannot be neglected. The inverse values of Y_{1app} were plotted versus the inverse values of μ_{1net} (values in Table B-3), as shown in Figure 3. Similarly, inverse values of Y_{2app} were plotted, in Figure 4, versus the corresponding inverse values of μ_{2net} (data in Table B-4). Simple visual inspection of the data shown in Figures 3 and 4, leads to the conclusion that they fall on a straight line. Consequently, a linear regression was performed by the method of least squares, and -as dictated by equation (5.7)- the values of the true yield coefficients, and the specific maintenance rates were determined from the intercept and slope of the line. The yield coefficients on nitrate and nitrite were found to be equal; more specifically, a value of 0.3093 was determined for nitrate, and a value of 0.3090 was found for nitrite. The specific rates for maintenance were found to be different; in fact, it was

Reproduced with permission of the copyright owner. Further reproduction prohibited without permission.

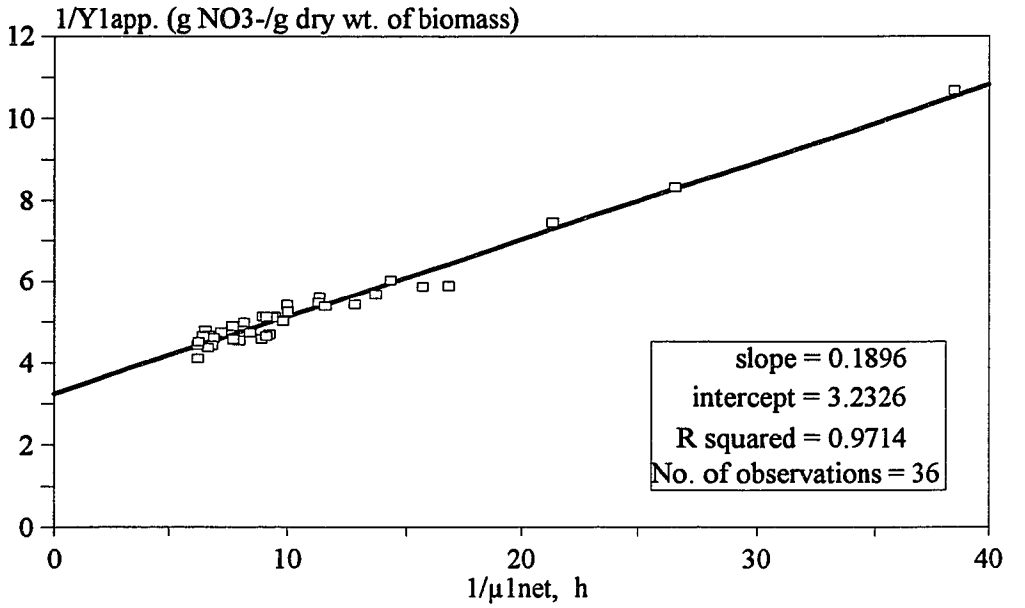

Figure 3 Reciprocal of the apparent yield coefficient on nitrate as a function of the reciprocal net specific growth rate. Data from experiments at 30 °C and pH 7.1 ± 0.1. Slope = μ_{c_1}/Y_1; intercept = the reciprocal of true yield coefficient, Y_1.

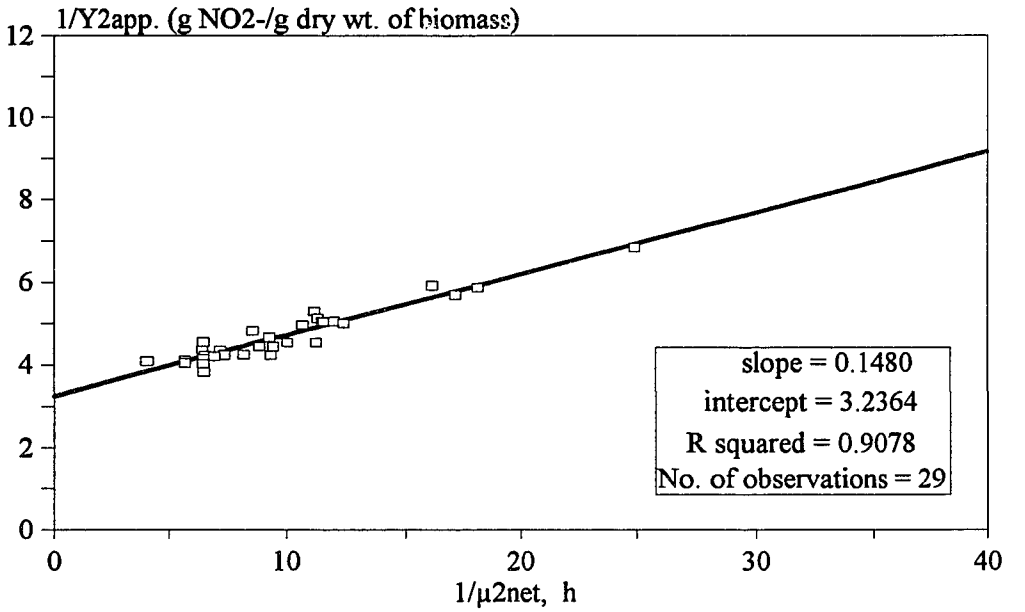

Figure 4 Reciprocal of the apparent yield coefficient on nitrite as a function of the reciprocal net specific growth rate. Data from experiments at 30 °C and pH 7.1 ± 0.1. Slope = μ_{c_2}/Y_2; intercept = the reciprocal of true yield coefficient, Y_2.

Reproduced with permission of the copyright owner. Further reproduction prohibited without permission.

found that $\mu_{c1} = 0.0586\ h^{-1}$, and $\mu_{c2} = 0.0457\ h^{-1}$.

It is always desirable to compare the results one gets from a study, to those reported by other researchers in the literature. On the other hand, biological systems are so complex, and conditions of experiments vary so significantly from one study to the other, that results of comparisons should be taken with a good amount of caution. For example, Koike and Hattori (1975a) reported a yield coefficient of 18 g-biomass/mole-NO_3^-, i.e., 0.290 g/g, a value which is very close to the Y_1 value found in this study. Nonetheless, although both studies utilized strains of *P. denitrificans*, they were not identical. The strain employed in the present study could not grow aerobically, at least with the medium tried. The strain utilized by Koike and Hattori (1975a), in contrast, could grow both aerobically and anaerobically. Furthermore, Koike and Hattori used a different carbon source, namely glutamate (which also served as nitrogen source for growth), as opposed to methanol used in the study reported here. In another study, Koike and Hattori (1975b), using the same culture as before, and glutamate as the carbon source, reported true yield coefficients on nitrate and nitrite as 0.46 and 0.367, respectively (in g/g). These values appear to compare favorably with the results reported here for nitrite, and much less favorably for nitrate. In the same study, Koike and Hattori (1975b), reported specific rates for maintenance, which -when converted to the units used in this study- are 0.0371 h^{-1} for nitrate, and 0.0279 h^{-1} for nitrite. A direct comparison between these values, and those found in the present study is not possible since Koike and Hattori used the model of Pirt (1965), which assumes direct utilization of the substrate for maintenance purposes. Possibly, a comparison between the two sets of values could be made based on the following rationale.

According to Pirt (1965), the rate of substrate consumption for maintenance purposes is given by

$$-r_s = m_s b \qquad (5.18)$$

Reproduced with permission of the copyright owner. Further reproduction prohibited without permission.

where m_s is the specific maintenance rate, and assumes values as those reported by Koike and Hattori (1975b).

According to Herbert (1958), the rate of biomass consumption for maintenance is given by

$$-r_b = \mu_c b \tag{5.19}$$

where μ_c is the specific maintenance rate, and assumes values as those found in the present study.

One could argue that the two models are equivalent only if

$$Y = \frac{\mu_c}{m_s} \tag{5.20}$$

The physical significance of equation (5.20) would be that a certain amount of the substrate instead of being directly utilized for maintenance, it is first converted to biomass and subsequently, this same amount of biomass is self oxidized for maintenance purposes.

If the foregoing arguments are true, the values of m_s which would be valid for the present study are

$$\text{for nitrate:} \quad m_{s1} = \frac{\mu_{c1}}{Y_1} = \frac{0.0586}{0.3093}\ h^{-1} = 0.1895\ h^{-1} \tag{5.21}$$

$$\text{for nitrite:} \quad m_{s2} = \frac{\mu_{c2}}{Y_2} = \frac{0.0457}{0.3090}\ h^{-1} = 0.1480\ h^{-1} \tag{5.22}$$

The values from (5.21) and (5.22), are an order of magnitude higher than those of Koike and Hattori. This unfavorable comparison should not be very surprising, as the conditions in the two studies are significantly different.

At a qualitative level, it is worth noticing that both the present study, and that of Koike and Hattori (1975b), have found that maintenance requirements associated with nitrate reduction are different from those for nitrite reduction. In addition, both studies have found that maintenance requirements associated with nitrite are lower than those regarding nitrate.

Reproduced with permission of the copyright owner. Further reproduction prohibited without permission.

One more thing needs to be mentioned regarding maintenance. It was observed experimentally that after depletion of nitrate and/or nitrite there was a slight increase in the biomass concentration before it stabilized at a constant value. The slight increases may be attributed to reduction of other intermediates such as nitrous oxide, something which will be discussed again later. Never was it observed that biomass decreased at the end of a run; yet, equations (5.2) and (5.13) predict a biomass decay to zero when nitrate and/or nitrite are depleted. For this reason, the maintenance terms in equations (5.2) and (5.13) were modified through multiplication by a Delta function implying that a specific maintenance term has a constant value as long as the substrate associated with it, is present in the medium, while it becomes zero as soon as that substrate is depleted.

After the maintenance terms were determined, the net specific growth rate data (Tables B-3 and B-4) were plotted versus the corresponding substrate concentration data as shown in Figures 5 and 6. It is clear from these plots that after an initial increase, the net specific growth rates drop with increasing concentrations of both nitrate, and nitrite. The data were regressed to the expressions μ_j - μ_{cj} (j = 1: nitrate; j = 2: nitrite), with μ_{cj} known, and μ_j having the form of expression (5.9). Regression was performed with the aid of a statistical software package (SAS) which is a non-linear algorithm based on the Marquart method, and performs optimal parameter search in a VAX/VMS platform. The computer program for such a search is given in Appendix E-4. The values obtained for the three constants appearing in expression (5.9) are shown in Table 1, along with the values for μ_c and Y which have been already discussed.

Table 1. Kinetic model parameters for bio-denitrification at 30 °C and pH = 7.1 ± 0.1.

Substrate (mg/L)	$\hat{\mu}_j$ (h^{-1})	K_j (mg/L)	K_{Ij} (mg/L)	μ_{cj} (h^{-1})	Y_j (g/g)
Nitrate (j = 1)	0.496	31.97	69.40	0.059	0.03093
Nitrite (j = 2)	0.699	52.72	35.62	0.046	0.03090

Reproduced with permission of the copyright owner. Further reproduction prohibited without permission.

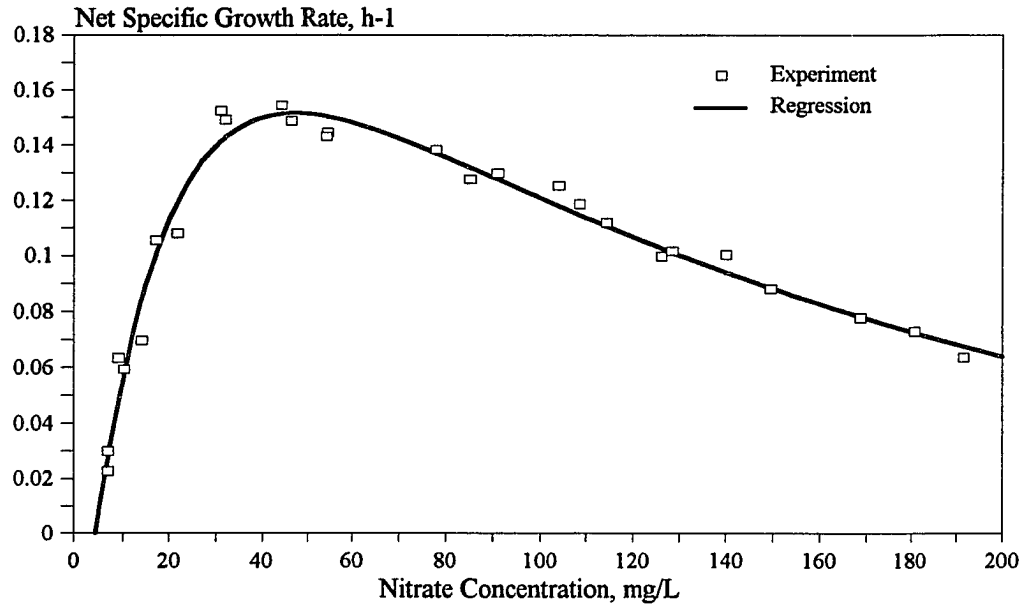

Figure 5 Net specific growth rate data on nitrate. Data have been fitted to an Andrews inhibitory expression modified according to Herbert for maintenance consideration. (T = 30 °C ; pH = 7.1 ± 0.1)

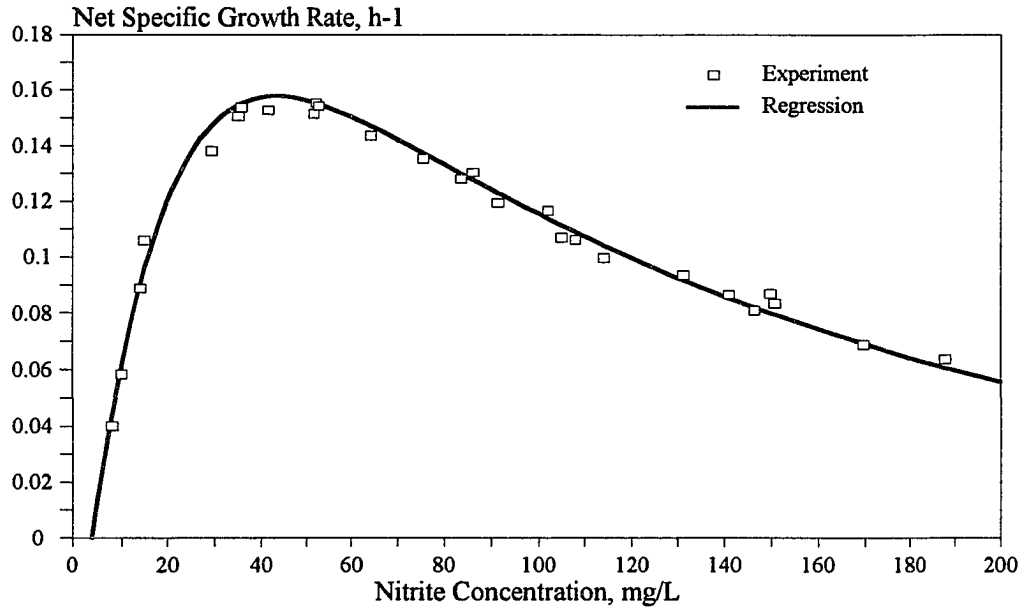

Figure 6 Net specific growth rate data on nitrite. Data have been fitted to an Andrews inhibitory expression modified according to Herbert for maintenance consideration. (T = 30 °C ; pH = 7.1 ± 0.1)

Reproduced with permission of the copyright owner. Further reproduction prohibited without permission.

Regarding the non-linear regression, it should be mentioned that when the μ_c values were given, the program converged to the values for the three parameters of expression (5.9), [reported in Table 1], regardless of the initial values (guesses) for the unknown parameters. When μ_c was allowed to be a fourth unknown parameter to be determined through regression, the program again converged regardless of initial guesses, but the parameter values were different from those reported in Table 1. Since μ_c could be determined independently as described previously, it was decided to keep the regression values for the constants in (5.9) when the value of μ_c was fixed in the regression algorithm. The solid curves shown in Figures 5 and 6 were generated based on the parameter values reported in Table 1. Clearly, the agreement between the curves and the data is excellent.

Based on the results discussed to this point, one should be able to generate complete time concentration profiles for biomass and nitrite, for cases where the medium does not contain nitrate. This could be done by integrating equations (5.1) and (5.2), along with expression (5.9). For consistency, one should substitute symbol *s*, which has been retained to denote nitrate concentration, with *u* (nitrite concentration). A computed code, given in Appendix E-1, was used for the simulations. Figure B-1 shows results of theoretically predicted profiles versus experimental data from three of the runs reported in Table B-2. The agreement is excellent, and this was the case with all experimental sets. This perfect agreement implies two things; first, although the specific growth rate constants were determined based on the initial data of the runs, the values obtained can describe the entire course of each experiment; second, the assumption that (at least in the absence of nitrate) intermediates such as nitrous and/or nitric oxide do not interfere with the kinetics of nitrite elimination, is a valid one.

To be able to generate time concentration profiles (for batch systems) for nitrate biological elimination, one should integrate equations (5.11) - (5.13). For this to be done, the value of parameter α is needed. Since the value of Y_1 was determined as discussed

Reproduced with permission of the copyright owner. Further reproduction prohibited without permission.

above, α could be determined via equation (5.15) provided that the "molecular formula" for the biomass were known. Determination of biomass composition was not attempted in the course of the present study. The value of parameter α was obtained by using biomass "molecular formulae" as shown in Table 2.

Table 2. Values for parameter α (gNO_2^- produced / gNO_3^- consumed).

Biomass Molecular Formula	Biomass Molecular Weight	α [from eq. (5.15)]	Reference for Molecular Formulae
$C_5H_9O_{2.5}N$	123	0.626	Shuler and Kargi (1992)
$C_4H_7O_2N$	101	0.601	Nurse (1980)
$C_5H_7O_2N$	113	0.616	Evans et al. (1992)

As can be seen from Table 2, there is little variation in the α values with biomass composition. Since the value based on the formula used by Evans et al. (1992), is close to the average of all values in Table 2, it was decided to use $\alpha = 0.616$ in the present study.

When expressions (5.16) and (5.17), with parameter values as in Table 1 and $K_{12} = K_{21} = 0$, were used along with $\alpha = 0.616$, integration of equations (5.11) - (5.13) yielded profiles which agreed very nicely with the data of all runs reported in Table B-1. Comparisons between data and predicted curves are shown in Figure B-2 for three of the experimental runs. Integration was performed by the code given in Appendix E-1. It should be mentioned that the agreement between data and model predicted concentration profiles is very good even for data sets which were not analyzed for the determination of the model parameters. Such experiments were performed just for model validation, and data from them are reported in Table B-8. An example of the good agreement between data and model predictions is given in the top graph of Figure 7.

Since one of the objectives of this study was to investigate reduction of media containing nitrate, nitrite, and nitrate/nitrite mixtures, a series of batch experiments

Reproduced with permission of the copyright owner. Further reproduction prohibited without permission.

starting with both nitrite and nitrate presence in the medium was performed. These data are reported in detail in Table B-5, and are for various temperatures. Only the data from runs at 30 °C are discussed in this section. When data from these runs were compared with predicted concentration profiles from equations (5.11) - (5.13), and (5.16), (5.17) with $K_{12} = K_{21} = 0$, it was found that the agreement was very good as long as the nitrite concentration in the medium was less than 15 mg/L; for higher values, the agreement was poor. For this reason, expressions (5.16) and (5.17) with non-zero values for K_{12} and K_{21} were tried, and it was found that if $K_{12} = 0.15$ L/mg and $K_{21} = 0.003$ L/mg the agreement between predictions [based on equations (5.11) - (5.13)], and data was excellent for all runs at 30 °C. Two examples are shown in Figure 7. Constants K_{12} and K_{21} express the inhibitory effect of nitrate on nitrite, and nitrite on nitrate, respectively. The numerical values of K_{12} and K_{21} indicate that nitrate presence has a stronger effect on nitrite removal, than the presence of nitrite on nitrate removal. These findings seem to be in good agreement with the observations of Kodama et al. (1969), and Timmermans and Van Haute (1983), in their studies reviewed in Chapter 2. Keeping the analogy with enzyme kinetics, one could argue that expressions (5.16) and (5.17) imply that nitrate may bind with nitrite reductase, but not on the active site of the enzyme; this binding does not yield any product, but reduces the affinity of the enzyme for nitrite. Similarly, nitrite binds on the nitrate reductase, but not on its active sites. Hence, the interaction is non-competitive since it does not reduce the availability of active sites on the enzymes.

In order to have more confidence regarding the quality of the experimental data, a nitrogen atom balance was written. Since the experiments were performed in sealed bottles, the amount of nitrogen (in all forms) should be constant at all times. To be more exact, because of the amount of nitrogen (in various forms) lost in the samples taken for analysis, the amount of nitrogen (in all forms) in the bottle changes. The balance is valid only if a correction is made for the amount lost in the samples. It is known that nitrate and nitrite are finally reduced to nitrogen, but this happens in the form of a series reaction

Reproduced with permission of the copyright owner. Further reproduction prohibited without permission.

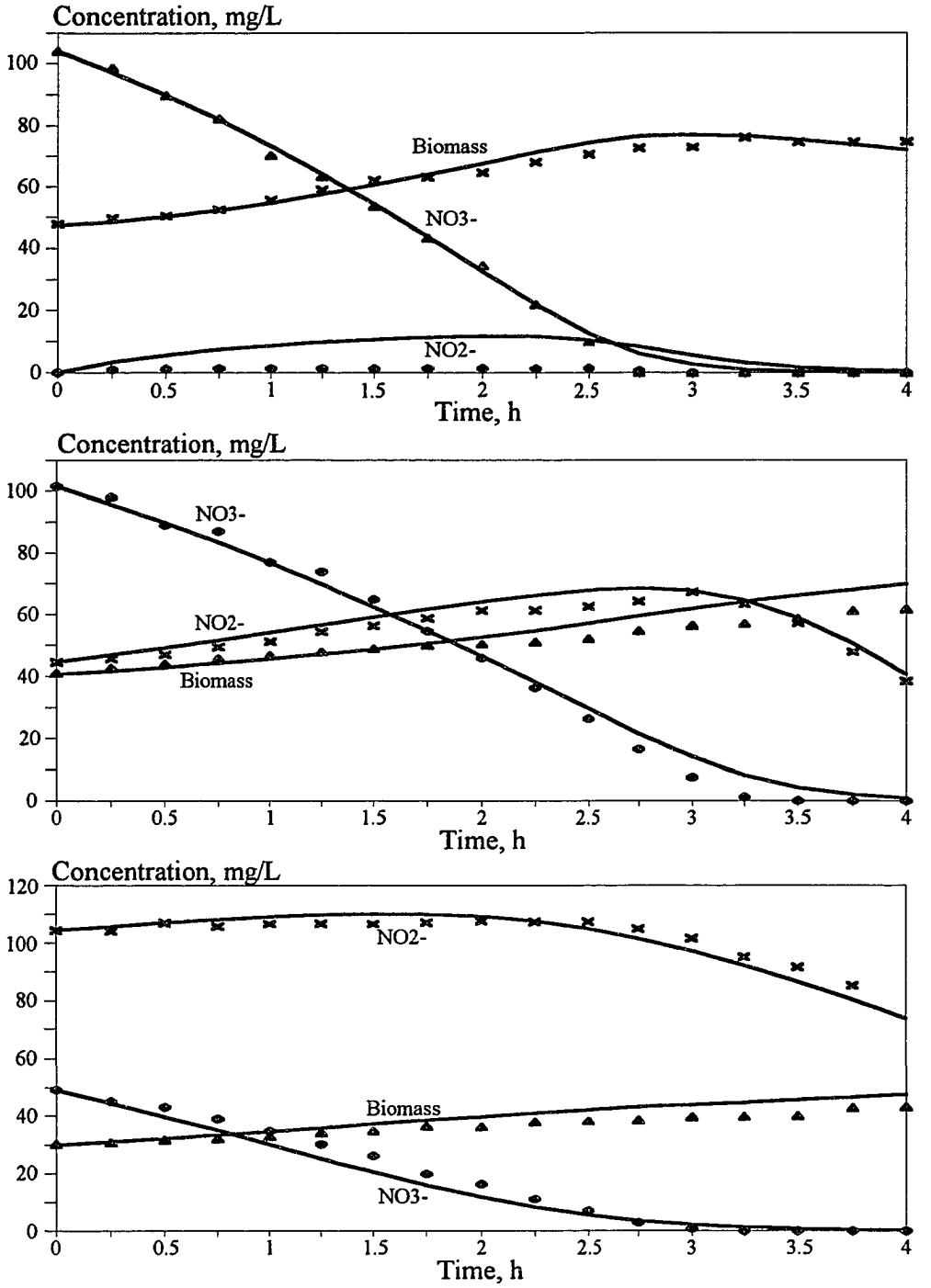

Figure 7 Comparison of experimental data (from runs 1H, 2G and 1G) and model predictions (curves) for reduction of nitrate (top), and nitrate/nitrite mixtures at 30 °C and pH = 7.1 ± 0.1.

Reproduced with permission of the copyright owner. Further reproduction prohibited without permission.

which involves possibly nitric and nitrous oxide formation (as intermediates). The GC analysis indicated that nitric oxide was not formed, as opposed to nitrous oxide. Hence, it was concluded that the organism used in the present study reduced nitrate/nitrite to nitrogen, through the following scheme:

$$\text{Nitrate } (NO_3^-) \longrightarrow \text{Nitrite } (NO_2^-) \longrightarrow \text{Nitrous Oxide } (N_2O) \longrightarrow \text{Nitrogen } (N_2)$$

This mechanism agrees with what has been reported by a number of researchers as has been discussed in Chapter 2.

A nitrogen atomic balance is based on measurements of NO_3^-, NO_2^-, and biomass in the liquid phase, and of nitrogen gas and nitrous oxide in the gas phase. Since the presence of gaseous components in the liquid phase was not directly measured, an exact nitrogen balance cannot be made. Two extreme cases were considered. In the first, it was assumed that nitrous oxide presence in the liquid can be neglected. In the second, it was assumed that the amount of nitrous oxide in the liquid is the one which can be determined from the amount present in the gas phase, assuming equilibrium conditions. This determination is shown in detail in Appendix C of the dissertation. Table B-6 (explanation of its entries given in Table B-6A), shows an example of how the nitrogen balances were determined. Column f of this table, indicates a low oxygen presence in the headspace of the bottle, as detected by GC analysis. Probably, some air was coming into the bottle during sampling. Since a nitrogen amount, contained in the air, was also introduced, a correction in the mass balance was made in order to account for this effect. Also, column e of Table B-6 indicates a considerable nitrogen gas presence in the beginning of the run. This is due to the fact that actual measurements were made after the bottle had been already spiked once with the same medium, and nitrate/nitrite were depleted, thus nitrogen had been produced. Similarly, this explains the presence of nitrous oxide (column d), in the beginning of the run. As the table indicates, nitrous oxide tended to accumulate in the headspace during the kinetic run. Experimentally, it was observed that eventually, nitrous

Reproduced with permission of the copyright owner. Further reproduction prohibited without permission.

oxide was depleted, but its depletion required a considerable amount of time. Column y of Table B-6 shows the total amount of process associated nitrogen in its various forms, assuming nitrous oxide presence in the liquid phase is considered. As can be seen from column z of the same table, the balance is correct within a 10 % error. If one assumes that no nitrous oxide is present in the liquid, the total nitrogen balance is shown as column y1 in Table B-6. Again, this balance is accurate within a 10 % error (column z1). These results are shown graphically in Figure B-3. Nitrogen balances were performed for a number of experimental runs, and the results are shown in Table B-7. Two more examples are shown in a graphical form in Figures 8, and B-4. The results indicate that, within experimental errors, the nitrogen balance is satisfied regardless of nitrous oxide presence or absence in the liquid phase. The assumption of no nitrous oxide presence in the liquid phase implies that the biological reduction of N_2O to nitrogen is mass transfer limited. On the other hand, the assumption of N_2O being in equilibrium between the gas and the water phase, implies that biological reduction of N_2O to nitrogen is limited by the reaction kinetics. The data are not enough in order to safely conclude which mechanism is really into effect. However, the fact that N_2O was depleted after long times in bottles which were relatively well shaken, seems to point towards kinetic limitation of the process.

Regarding the oxygen presence in the headspace of the bottles, it needs to be emphasized that it was low, and thus, oxygen presence in the liquid was negligible; this was confirmed by the dissolved oxygen indicator (resazurin). It should be also mentioned that when, occasionally, dissolved oxygen presence was detected, the data from those bottles were not used, and the experiments were repeated. This was done because DO presence caused the reaction to stop.

As already mentioned earlier, depletion of nitrate and nitrite is not an indication that their nitrogen content has been converted to nitrogen gas (and biomass). Hence, if one is interested in completely converting (reducing) nitrate/nitrite to nitrogen, equations

Reproduced with permission of the copyright owner. Further reproduction prohibited without permission.

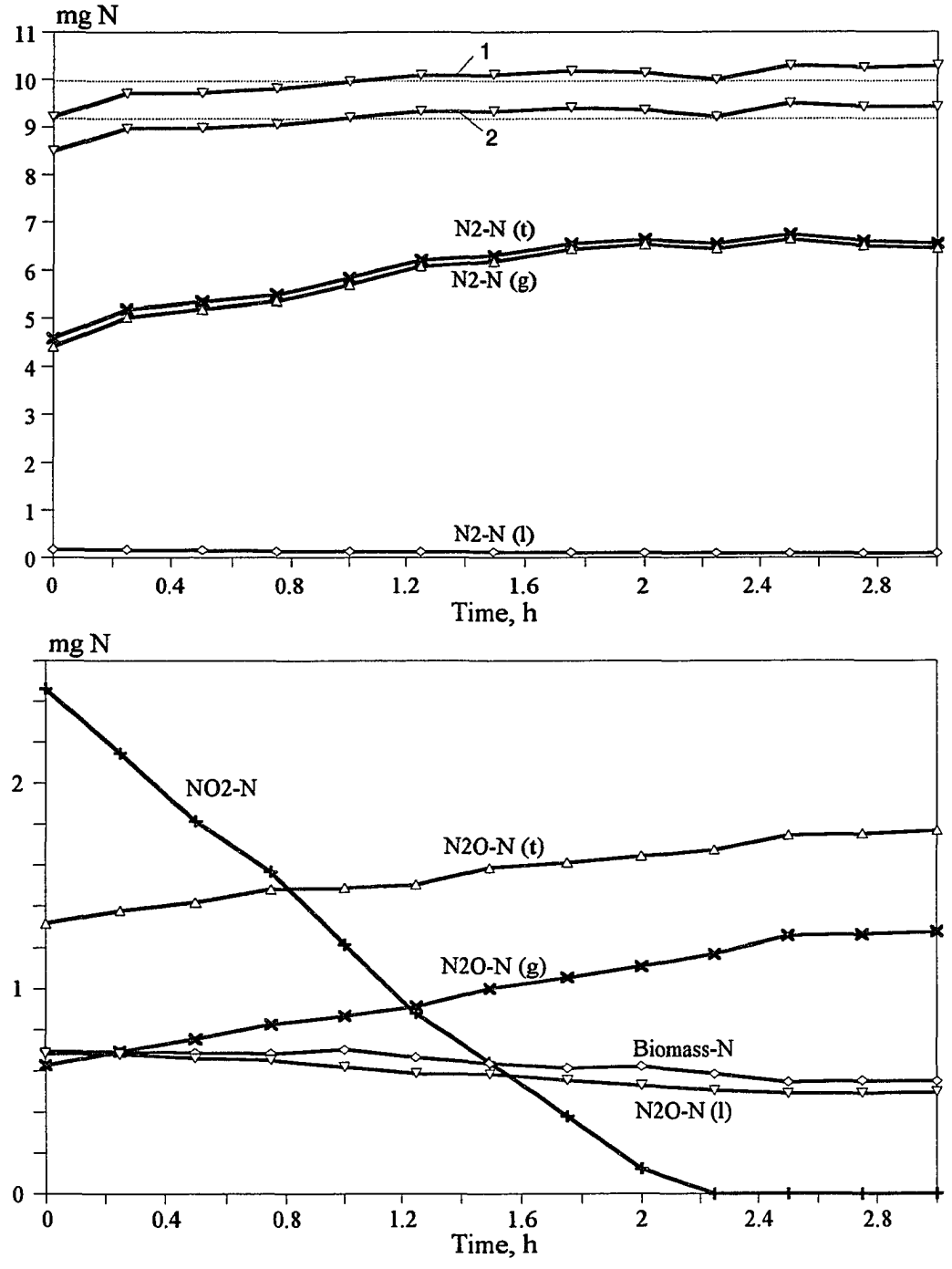

Figure 8 Nitrogen mass balance as a function of time during experimental run 20B. Curves 1 and 2 in the top diagram indicate total nitrogen when N_2O presence in the liquid is considered and neglected, respectively.

Reproduced with permission of the copyright owner. Further reproduction prohibited without permission.

(5.11) through (5.13) cannot predict the time needed to achieve this task, in a batch reactor. Further studies will be needed for examining N_2O reduction to nitrogen.

5.3.2 Investigation of the Effects of Temperature on the Kinetics

In order to study the effects of temperature on the kinetics, experiments were performed at 32.5, 35, and 38 °C, in addition to those at 30 °C which were discussed in the preceding section. These experiments were performed with either nitrate, or nitrite at initial concentrations of about 10, 20, 50, 80, and 150 mg/L.

The data from the experiments with nitrate are reported in Table B-9. The data at 30 °C reported in Table B-9 are the same as those reported in Table B-1, and are repeated for showing the complete set on which the analysis was based. Similarly, data from the experiments with nitrite are reported in Table B-10. The initial data from each run reported in Tables B-9, and B-10 were used in determining the values of the net specific growth rate, and apparent yield coefficient following the methodology discussed in the preceding section of this chapter. These values are summarized in Table B-11 for nitrate, and Table B-12 for nitrite. Some experiments (data not reported in detail), were also performed at 39 °C, and it was observed that the net specific growth rate was lower than that at 30 °C. When experiments were tried at 40 °C, it was observed that no reaction occurred. Figures 9 and 10, show the change of the net specific growth rate on nitrate and nitrite, respectively, as a function of temperature. One can easily see that in the range from 30 to 38 °C, there is an almost perfectly linear relationship between net specific growth rate and temperature, and the rates increase with temperature. Above 38 °C, the rates decrease with temperature. This diagram suggests that the optimum temperature is about 38 °C, and this implies that the organism used in this study is a mesophile.

The data from the experiments in the 30 - 38 °C range were subjected to further detailed analysis from different perspectives, as discussed below.

Reproduced with permission of the copyright owner. Further reproduction prohibited without permission.

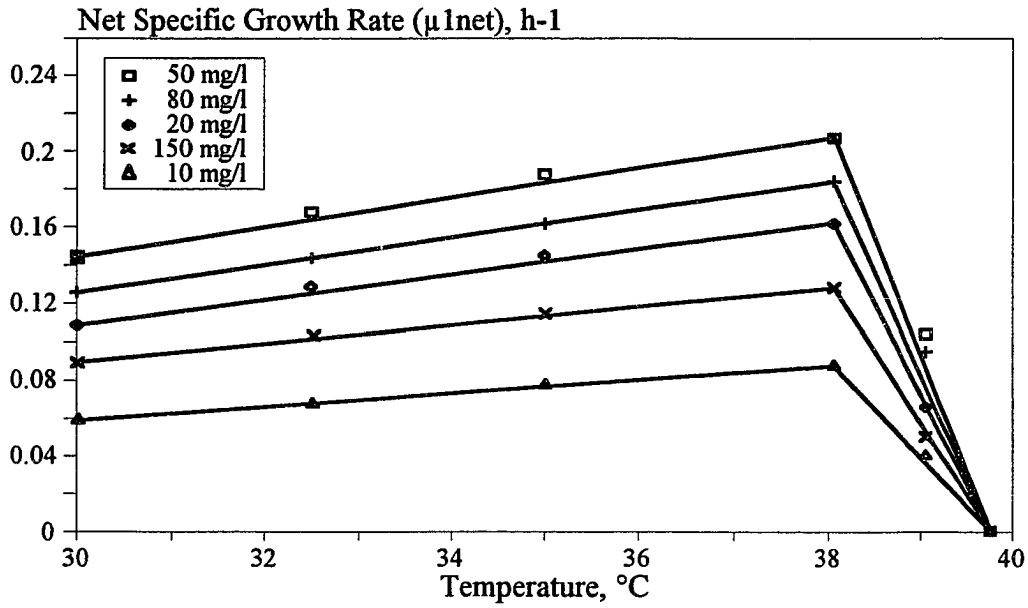

Figure 9 Temperature dependence of net specific growth rate on nitrate at pH = 7.1 ± 0.1.

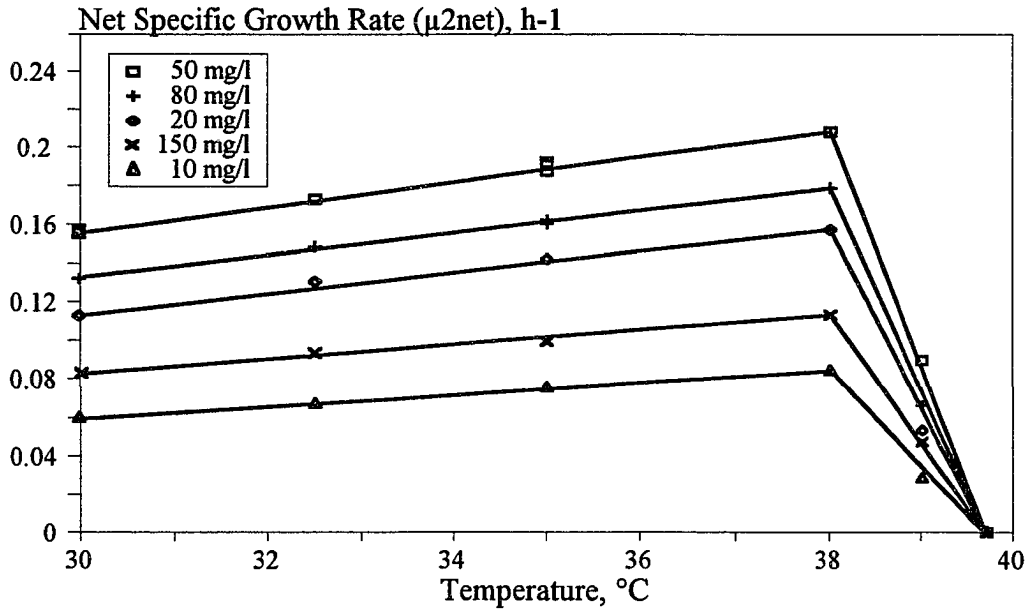

Figure 10 Temperature dependence of net specific growth rate on nitrite at pH = 7.1 ± 0.1.

Reproduced with permission of the copyright owner. Further reproduction prohibited without permission.

Initially, it was investigated whether the net specific growth rate has an Arrhenius dependence on temperature, in which case the following equation should be valid,

$$\ln(\mu_{jnet}) = A_j - \left(\frac{E_j}{R}\right)\frac{1}{T},\ j = 1, 2 \qquad (5.23)$$

where A_j is the frequency factor, E_j is the activation energy, R is the universal gas constant, T is the absolute temperature (K), j = 1 implies nitrate, and j = 2 implies nitrite.

If equation (5.23) is indeed valid, values of the specific growth rate at a given concentration, when plotted semilogarithmically versus inverse absolute temperature, should fall on a straight line. It should be also true that data from different concentrations should fall on parallel lines. In fact, this was the case for both nitrate and nitrite, as can be seen from Figures 11 and 12. From the slopes of these lines it was determined that the activation energies for nitrate and nitrite reduction are 8.586 and 7.206 Kcal/mole, respectively. Nakajima and coworkers have reported activation energies for denitrification in two different studies, with glucose as the carbon source. Using denitrifiers found in sediments of an eutrophic lake, they reported values of 9.32 and 8.13 Kcal/mole for nitrate and nitrite, respectively (Nakajima et al., 1984a). These values compare relatively well with those found in the present study. Using sludge samples from an oxidation ditch, the same researchers reported values of 14.10 and 12.67 Kcal/mole for nitrate and nitrite reduction, respectively (Nakajima et al., 1984b). It is interesting to observe that in all cases, the activation energy for nitrate reduction is found to be slightly higher than that for nitrite reduction.

Equation (5.23) allows prediction of the net specific growth rate at any temperature if its value is known at a single temperature. Clearly, predictions should be made for temperatures falling in the range of values used in determining the activation energy. Since the expressions for the specific growth rate at 30 °C were known, data were generated through experiments at 37 °C (see Table B-8), and the concentration profiles were predicted, based on two different approaches, through the model equations

Reproduced with permission of the copyright owner. Further reproduction prohibited without permission.

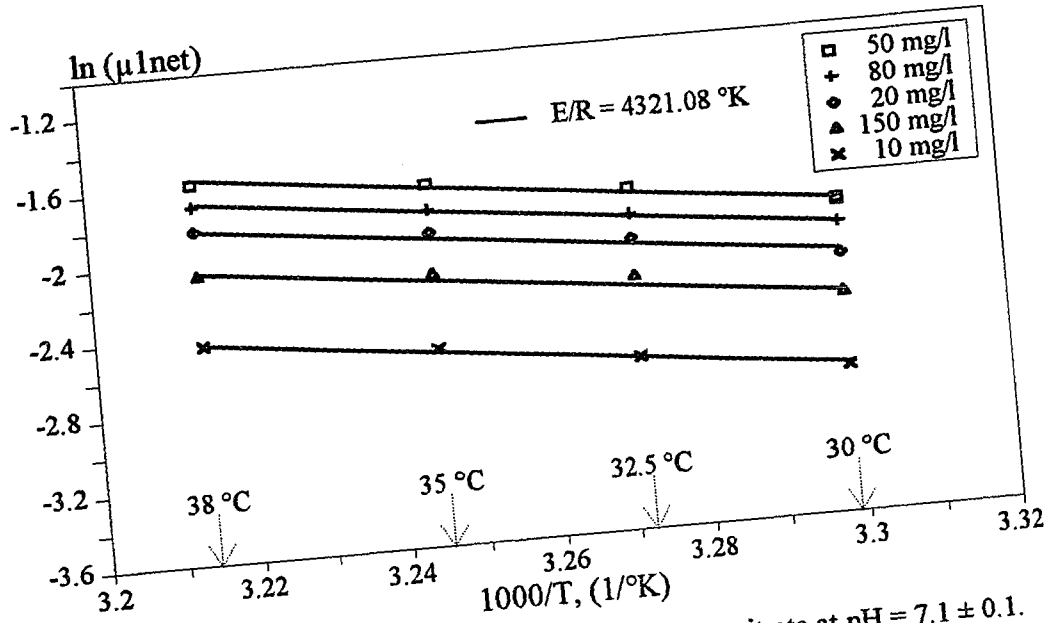

Figure 11 Arrhenius' plot for the net specific growth rate on nitrate at pH = 7.1 ± 0.1.

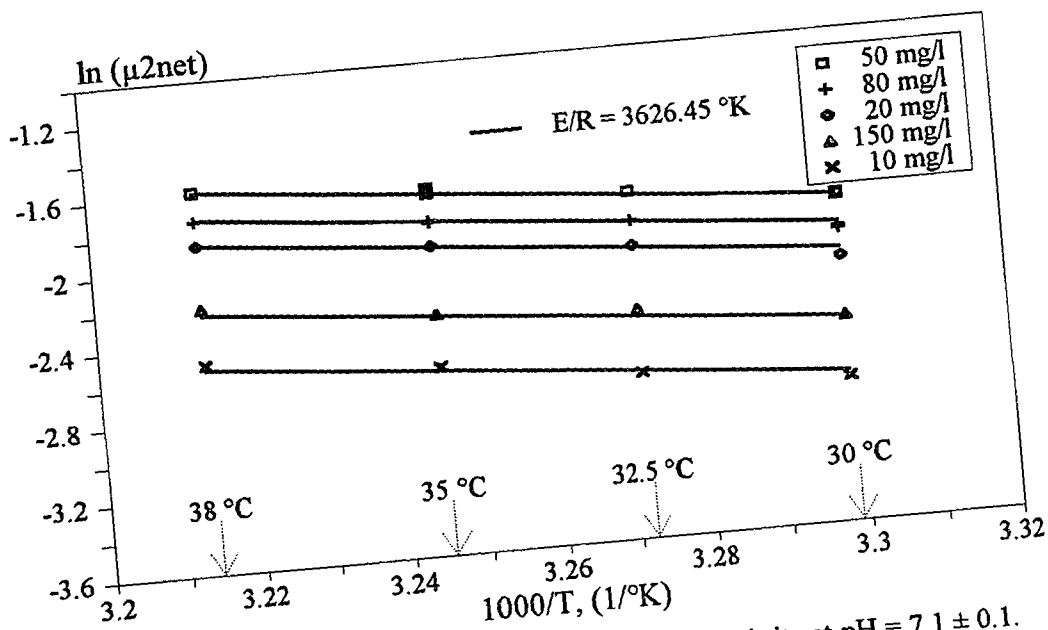

Figure 12 Arrhenius' plot for the net specific growth rate on nitrite at pH = 7.1 ± 0.1.

Reproduced with permission of the copyright owner. Further reproduction prohibited without permission.

discussed in the preceding section. In the first approach, no correction was made for the effect of temperature, while in the second, the net specific growth rate values were corrected for temperature via equation (5.23). It was found that if the correction for temperature is not made, predicted substrate concentration profiles deviate drastically from the data. Two examples are shown graphically is Figures B-5 and B-6. From these two figures one can see that temperature corrected profiles have a problem only with biomass concentrations at relatively large times after the initiation of the experimental runs. These deviations may be due to experimental error. Measurements of optical density were converted to biomass concentrations based on a calibration curve prepared at 30 °C.

Using the net specific growth rate values at 30 °C, and equation (5.23) one can generate the entire specific growth rate curves at different temperatures. This was done, and the curves are shown (as solid curves), in Figure B-7 for nitrate, and Figure B-8 for nitrite. The same curves could be derived by using the data of Tables B-11 and B-12. Data referring to a certain temperature were fitted to the Andrews expressions, as was done with the data at 30°C in section 5.2. It should be noted though that at temperatures other than 30 °C, data were available at only five initial concentrations. This approach led to determination of kinetic, and maintenance parameter values at various temperatures. These values are reported in Table 3 for nitrate, and Table 4 for nitrite. Using these constants, the net specific growth rate curves were generated, and are shown (as dashed curves), in Figures B-7 and B-8. As can be seen from these diagrams, the two approaches lead to practically identical results.

Regarding biological reduction of nitrate/nitrite mixtures, it was found (based on data reported in Table B-5), that the interaction constants, discussed in section 5.2, are also functions of temperature. Values of these constants at three temperatures, are shown in Table 5. An example of temperature corrected concentration profiles for NO_3^-/NO_2^-

Reproduced with permission of the copyright owner. Further reproduction prohibited without permission.

mixtures, and their comparison to experimental data, is shown in Figure B-9. Here, the agreement is very good.

Table 3 Kinetic constants for nitrate reduction at different temperatures (From regression of data to the Andrews-Herbert model). (pH = 7.1 ± 0.1)

	$\hat{\mu}_1$ (1/h)	K_1 (mg/L)	K_{I1} (mg/L)	μ_{c1} (1/h)
30 °C	0.496	31.973	69.403	0.0586
32.5 °C	0.509	26.277	80.539	0.0696
35 °C	0.522	21.936	99.859	0.0825
38 °C	0.535	17.608	123.251	0.1008

Table 4 Kinetic constants for nitrite reduction at different temperatures (From regression of data to the Andrews-Herbert model). (pH = 7.1 ± 0.1)

	$\hat{\mu}_2$ (1/h)	K_2 (mg/L)	K_{I2} (mg/L)	μ_{c2} (1/h)
30 °C	0.699	52.718	35.623	0.0457
32.5 °C	0.703	47.476	41.388	0.0529
35 °C	0.708	41.156	47.283	0.0611
38 °C	0.713	34.902	56.541	0.0725

Table 5 Temperature dependence of cross-inhibition parameters (pH = 7.1 ± 0.1).

Units: L/mg	30 °C	37 °C	38 °C
K_{12}	0.150	0.035	0.110
K_{21}	0.003	0.030	0.070

Reproduced with permission of the copyright owner. Further reproduction prohibited without permission.

It should be mentioned that concentration profiles for nitrate, nitrite, and nitrate/nitrite mixtures were generated through a code which is given in Appendix E-1.

It is not easy to compare the values for the activation energies obtained in this study, through equation (5.23), with those reported in other studies. The difficulty arises from the reasons discussed in the preceding section with regard to kinetic constants; namely, the organisms used in various studies are different, and so are the growth media. For example, activation energies for three psychrophilic strains of *Pseudomonas fluorescens* have been reported to be in the range of 8.7 to 9.4 Kcal/mole, while for *E. coli* which is a mesophile, a value of 14 Kcal/mole has been reported (Ingraham, 1958). In that study, a trypticase-soy medium was used. For *E. coli*, values of 14.5 Kcal/mole (Monod, 1942) and 15 Kcal/mole (Johnson and Lewin, 1946), have been also reported from experiments with synthetic media. It should be mentioned that in all three aforementioned studies, maintenance effects were not considered; hence, the reported values refer to the true specific growth rate, and not to the net specific growth rate, which is the case in the present study.

In a detailed study with *Aerobacter aerogenes* growing aerobically on glucose, Topiwala (1971) described growth with Monod's model, and maintenance requirements according to Herbert's model. He suggested that instead of an overall activation energy determined through equation (5.23), one should try to determine the temperature dependence of each kinetic constant separately. His results suggested the following. The yield coefficient is temperature independent; the inverse of the saturation constant, and the specific rate of biomass consumption follow Arrhenius' law; the maximum specific growth rate -in the temperature range tried- exhibited a maximum, and its temperature dependence could be explained via a difference of two Arrhenius expressions. A similar approach was used in the present study, regarding the constants reported in Tables 3 and 4. Since $\hat{\mu}_j$ did not exhibit a maximum in the temperature range of the experiments, it was fitted to an Arrhenius expression; the same was done for μ_{cj}, K_{lj}, and the inverse of K_j (j =

Reproduced with permission of the copyright owner. Further reproduction prohibited without permission.

1, 2). Equation (5.23) was used after substituting the parameter of interest for μ_{jnet}. The results are shown in Figure B-10 for the kinetic constants in the specific growth rate related to nitrate reduction, and Figure B-11 for those associated with nitrite reduction. As can be seen from these figures, all data fall perfectly on lines in the semilogarithmic plots. From the slopes of these lines, the activation energies were determined, while the intercept of the lines produced the frequency factors for the Arrhenius expressions. The values are reported in Tables 6 and 7, for nitrate and nitrite, respectively.

Table 6 Arrhenius constants for each kinetic parameter in the expression for nitrate reduction (pH = 7.1 ± 0.1).

	$\hat{\mu}_1$ (1/h)	$1/K_1$ (L/mg)	K_{I1} (mg/L)	μ_{c1} (1/h)
Frequency Factor*	9.84	3.48×10^8	5.23×10^{11}	8.40×10^7
E (cal/gmole)	1,800	13,900	13,700	12,700

* Units are the same as in the corresponding kinetic parameter.

Table 7 Arrhenius constants for each kinetic parameter in the expression for nitrite reduction (pH = 7.1 ± 0.1).

	$\hat{\mu}_2$ (1/h)	$1/K_2$ (L/mg)	K_{I2} (mg/L)	μ_{c2} (1/h)
Frequency Factor*	1.58	2.09×10^5	2.01×10^9	2.80×10^6
E (cal/gmole)	490	9,800	10,750	10,800

* Units are the same as in the corresponding kinetic parameter.

The values of activation energies for the various constants determined in this study, except μ_{cj}, are impossible to compare with those of Topiwala because the kinetic expression in his study is that of Monod, while in the present study the specific growth

Reproduced with permission of the copyright owner. Further reproduction prohibited without permission.

rate follows Andrews kinetics. If μ_m and $\hat{\mu}_j$ can be viewed as comparable, then the activation energies found here are one and two orders of magnitude less (for nitrate and nitrite, respectively), than the value reported by Topiwala. If the saturation constant in the Monod expression can be viewed as similar to K_j, then the activation energies found here, compare very favorably with that of 11.8 Kcal/mole reported by Topiwala. Finally, for μ_{cj} where comparisons can be made relatively safely, the values found here, and the 9 Kcal/mole reported by Topiwala, compare very nicely. Based on a study with *Pseudomonas fluorescens*, growing aerobically on glucose, Palumbo and Witter (1969), reported an activation energy of 8,430 cal/mole for the specific maintenance rate. This value compares nicely with those found here, and that reported by Topiwala. On the other hand, Palumbo and Witter reported that using the data of Marr et al. (1963), they calculated an activation energy of 20.2 Kcal/mole for the specific maintenance of a strain of *E. coli*. This last comparison seems to be incorrect because Marr et al., assume direct consumption of substrate for maintenance, rather than consumption of biomass through self oxidation, as is the case in all other studies mentioned previously. Perhaps it should be stated here that no study on the temperature effects under anaerobic conditions was found in the literature; thus, the present study is the first one in which such a detailed investigation was undertaken.

5.3.3 Investigation of the Effects of pH on the Kinetics

In order to investigate the effects of pH on the kinetics of nitrate and nitrite biological reduction, experiments were performed at 30 °C, various pH values, and initial concentrations of nitrate or nitrite at about 50 mg/L. Data from the experimental runs with nitrate are shown in Table B-13, and for nitrite reduction in Table B-14. These are the data sets used in the analysis presented in this section, and some of them are the same as in Tables B-1 and B-2.

Reproduced with permission of the copyright owner. Further reproduction prohibited without permission.

Enzyme kinetics depend on pH following various expressions, the most common of which involves a two-step ionization of the enzyme (Dixon and Webb, 1979; Bailey and Ollis, 1986), and can be expressed by the so called Michaelis pH-function (Michaelis, 1922). Using an analogy between enzyme kinetics, and kinetics of microbial growth, Antoniou et al. (1990), proposed the following expression for the pH-dependence of the net specific growth rate at a given substrate concentration,

$$\mu_{jnet} = \frac{\delta_j}{1 + \frac{[H^+]}{K_{H1j}} + \frac{K_{H2j}}{[H^+]}} \qquad (5.24)$$

where δ_j, K_{H1j}, and K_{H2j} are parameters having units of inverse time the first, and concentration the other two.

Equation (5.24) was used in analyzing the data obtained in the present study, both for nitrate (j = 1), and nitrite (j = 2).

The data from each run reported in Tables B-13 and B-14 were analyzed as explained in section 5.2 in order to obtain values of the net specific growth rate. These values are reported in Table B-15 for nitrate, and Table B-16 for nitrite. Fitting these values to equation (5.24), through the aid of SAS (a statistics application computer software package), the model parameter values were found, and are reported in Table 8.

Table 8 Parameters for the Michaelis functions expressing the dependence of the net specific growth rate on pH (data from Tables B-13 and B-14, obtained at 50 mg/L and T = 30 °C).

	pH_{opt}	δ (1/h)	K_{H1} (M)	K_{H2} (M)	pK_{H1}	pK_{H2}
Nitrate, NO_3^-	7.45	0.42	4.30×10^{-8}	2.93×10^{-8}	7.37	7.53
Nitrite, NO_2^-	7.20	1.35	1.47×10^{-8}	2.72×10^{-7}	7.83	6.57

Reproduced with permission of the copyright owner. Further reproduction prohibited without permission.

One can easily see from equation (5.24), that μ_{jnet} becomes maximum when,

$$[H^+] = \sqrt{K_{H1j} \cdot K_{H2j}} \tag{5.25}$$

From expression (5.25), it follows that the optimum pH is given by

$$pH_{jopt} = \frac{1}{2}(pK_{H1j} + pK_{H2j}) \tag{5.26}$$

The optimum pH values for net specific growth rate maximization are given in Table 8. Figure 13 shows the data fit to equation (5.24) using the parameter values reported in Table 8.

Data reported in the literature regarding the effect of pH, refer to the denitrification rate, rather than the specific growth rate. For this reason, based on the experimental data, average rates of nitrate and nitrite removal rates, expressed as g-nitrate (or nitrite)/g-biomass/h were calculated, and are reported in Tables B-15 and B-16. It was then assumed that these rates (RD_{jnet}), follow expressions analogous to (5.24), i.e.,

$$RD_{jnet} = \frac{\varepsilon_j}{1 + \frac{[H^+]}{K'_{jH1}} + \frac{K'_{jH2}}{[H^+]}} \tag{5.27}$$

where ε_j is a model parameter having units of g-NO_3^- (or NO_2^-)/g-biomass/h, and K'_{jH1}, and K'_{jH2} are model parameters having units of concentration.

As in the case of equation (5.24), it is easy to show that the denitrification rate (RD_{jnet}), becomes maximum at a pH-value given by

$$pH_{jopt} = \frac{1}{2}(pK'_{jH1} + pK'_{jH2}) \tag{5.28}$$

After fitting the data to equation (5.27), the model parameters were determined, and are given in Table 9, along with the optimal pH values. The results are also shown graphically in Figure 13. It is interesting to observe from Tables 8 and 9, that the optimal pH values are practically the same regardless of the approach used in determining them [i.e., either equation (5.26) or (5.28)]. It is also interesting to observe that the optimal pH for nitrite biological reduction is slightly lower than that for nitrate.

Reproduced with permission of the copyright owner. Further reproduction prohibited without permission.

Reproduced with permission of the copyright owner. Further reproduction prohibited without permission.

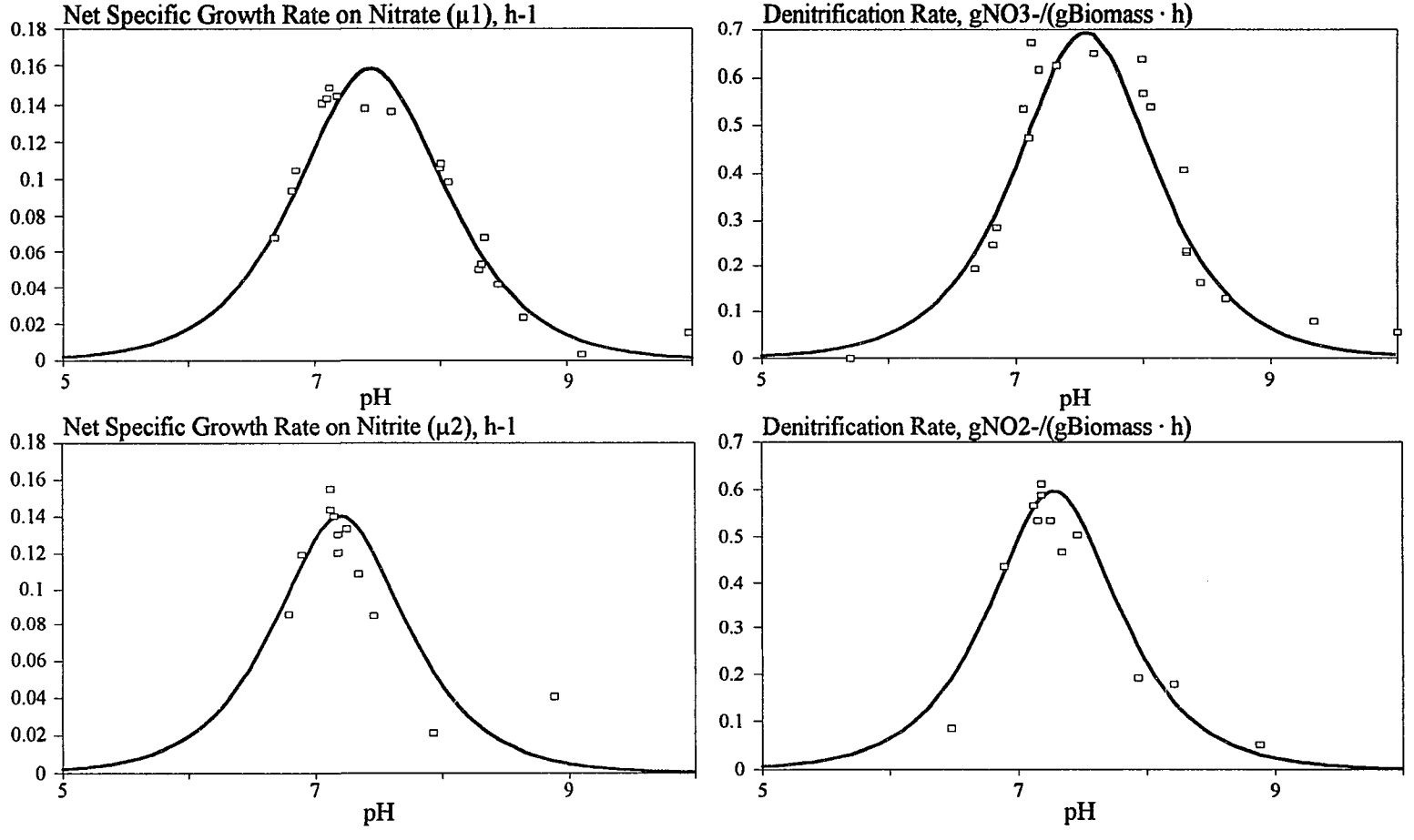

Figure 13 Dependence of net specific growth rates and denitrification rates on pH. Curves from fitting the data to the Michaelis pH-functions (data also shown in Tables B-12 and B-13; in all runs initial concentration of NO_3^- or NO_2^- = 50 mg/L, T = 30 °C).

Dawson and Murphy (1972), quote earlier findings of Delwiche according to which, *Pseudomonas aerugenosa* denitrifiers could grow in a pH range of 5.8 - 9.2, with the optimum being "somewhere between 7.0 and 8.2". Knowles (1982), in an extensive review of studies on denitrification concluded that denitrification can occur in a pH range of 5 - 11, with the optimum being in the range of 7.0 to 8.0. As can be seen from Tables 8 and 9, regarding pH_{opt}, and Figure 13, regarding the pH range over which denitrification is possible, the results of the present study, agree very nicely with those reported earlier in the literature.

Table 9 Parameters for the Michaelis functions expressing the dependence of NO_3^-/NO_2^- removal rates on pH (data from Tables B-13 and B-14, obtained at 50 mg/L and T = 30 °C).

	pH_{opt}	ε (g/gbiomass/h)	K'_{H1} (M)	K'_{H2} (M)	pK'_{H1}	pK'_{H2}
Nitrate, NO_3^-	7.55	2.7	1.95×10^{-8}	4.08×10^{-8}	7.71	7.39
Nitrite, NO_2^-	7.28	19.0	3.41×10^{-9}	8.00×10^{-7}	8.47	6.10

Hartman and Laubenberger (1968), proposed the idea that a deviation from the optimal pH value reduces the bacterial activity according to the mechanism of non-competitive inhibition. Using this notion, Timmermans and Van Haute (1983), in a study of denitrification with *Hyphomicrobium sp.*, proposed the following expressions in lieu of equations (5.24), and (5.27),

$$\mu_{jnet} = \frac{\mu_{jmax}}{1 + k_H\left(10^{|pH_{opt} - pH|} - 1\right)} \tag{5.29}$$

$$RD_{jnet} = \frac{RD_{jmax}}{1 + k'_H\left(10^{|pH_{opt} - pH|} - 1\right)} \tag{5.30}$$

where μ_{jnet} and μ_{jmax} have units of inverse time, RD_{jnet} and RD_{jmax} have units of g-nitrate (or nitrite)/g-biomass/h, and constants k_H, k'_H are dimensionless.

Reproduced with permission of the copyright owner. Further reproduction prohibited without permission.

When the data reported in Tables B-15 and B-16 were fitted to equations (5.29) and (5.30), model parameter values were obtained, and are shown in Table 10 for nitrate, and Table 11 for nitrite. To fit the data, a SAS algorithm was again used (see Appendix E-5). It is worth noticing that the optimum pH values determined via equations (5.29) and (5.30), are practically the same with those found via equations (5.24) and (5.27). Timmermans and Van Haute (1983), in their study, found that the optimum pH was 8.3 for both nitrate and nitrite. This value is higher than what was found in the present study, and a little away from the optimal range of 7.0 to 8.0 mentioned by Knowles (1982). A graphical representation of the data, along with the fitted curves [using equations (5.29) and (5.30)], is shown in Figure B-12. When the diagrams of this figure are compared to those of Figure 13, one could say that both approaches represent equally well the data, except for the nitrate reduction rate; in the last case, the approach through equation (5.27) represents the data much better than the one through equation (5.30).

Table 10 Parameters for the non-competitive inhibition functions expressing the dependence of the net specific growth rate on pH (data from Tables B-13 and B-14, obtained at 50 mg/L and T = 30 °C).

	pH_{opt}	μ_{max} (1/h)	k_H
Nitrate, NO_3^-	7.35	0.158	0.206
Nitrite, NO_2^-	7.12	0.148	0.679

Table 11 Parameters for the non-competitive inhibition functions expressing the dependence of the NO_3^-/NO_2^- removal rate on pH (data from Tables B-13 and B-14, obtained at 50 mg/L and T = 30 °C).

	pH_{max}	RD_{max} (g/gbiomass/h)	k_H'
Nitrate, NO_3^-	7.6	0.95	0.438
Nitrite, NO_2^-	7.2	0.75	0.927

Reproduced with permission of the copyright owner. Further reproduction prohibited without permission.

Although the experiments were performed at a single initial concentration value for nitrate and nitrite, it is reasonable to expect that the optimal pH values do not change with concentration. One should then expect that, for example, constants K_{H1j} and K_{H2j} in equation (5.24) are concentration independent. This leads to the following approach for determining variations of the net specific growth rate with pH at any concentration. Since detailed expressions for the net specific growth rate on nitrate or nitrite at pH = 7.1 were found in section 5.2, one could easily find the net specific growth rate at any concentration at pH = 7.1. Using this value as the left hand side of equation (5.24), and the values of constants K_{H1j} and K_{H2j} from Table 8, the only unknown will be δ_j. Once this is determined, the value of μ_{jnet} at any pH value could be found through equation (5.24). This methodology should be repeated for any concentration of interest.

Reproduced with permission of the copyright owner. Further reproduction prohibited without permission.

CHAPTER 6

ANALYSIS OF THE PROCESS OF BIOLOGICAL NITRATE/NITRITE REDUCTION IN A CONTINUOUSLY OPERATED SBR

The main purpose of the study presented in Chapter 5 was to accurately determine the kinetic characteristics of biological NO_3^-/NO_2^- reduction with *P. denitrificans* (ATCC 13867), so that the process could be studied in a continuously operated Sequencing Batch Reactor (SBR). The reasons for selecting the SBR mode of operation were discussed in Chapter 1. In this chapter the results of the study on NO_3^-/NO_2^- reduction in SBRs is presented. The general equations governing the process are first derived, the methodology for numerically solving the model equations is discussed, and data from SBR experiments are compared to the theoretical predictions.

6.1 Theory

Biological removal of nitrate and/or nitrite in a continuously operated SBR can be, in general, described with the following mass balances.

Total mass balance (assuming constant density):

$$\frac{dV}{dt} = Q_f - Q \tag{6.1}$$

Balance on nitrate:

$$\frac{ds}{dt} = \frac{Q_f}{V}(s_f - s) - \frac{b}{Y_1}\mu_1(s, u) \tag{6.2}$$

Balance on nitrite:

$$\frac{du}{dt} = \frac{Q_f}{V}(u_f - u) + \left[\frac{\alpha}{Y_1}\mu_1(s, u) - \frac{1}{Y_2}\mu_2(u, s)\right]b \tag{6.3}$$

Balance on biomass:

$$\frac{db}{dt} = -\frac{Q_f}{V}b + [\mu_1(s, u) + \mu_2(u, s)]\, b - [\mu_{c1}\cdot\Delta(s) + \mu_{c2}\cdot\Delta(u)]\, b \tag{6.4}$$

Reproduced with permission of the copyright owner. Further reproduction prohibited without permission.

where,

$$\mu_1(s, u) = \frac{\hat{\mu}_1 \; s}{K_1 + s + \frac{s^2}{K_{I1}} + K_{21}\, u \cdot s} \tag{6.5}$$

$$\mu_2(u, s) = \frac{\hat{\mu}_2 \; u}{K_2 + u + \frac{u^2}{K_{I2}} + K_{12}\, s \cdot u} \tag{6.6}$$

$$\Delta(s) \begin{cases} = 1, & \text{if } s > 0 \\ = 0, & \text{if } s = 0 \end{cases} \tag{6.7}$$

$$\Delta(u) \begin{cases} = 1, & \text{if } u > 0 \\ = 0, & \text{if } u = 0 \end{cases} \tag{6.8}$$

The values of the model parameters are those determined in Chapter 5. It should be restated that K_{12} , and K_{21} assume the non-zero values reported in the preceding Chapter, only if $u > 15$ mg/L; otherwise, they are both equal to zero.

Depending on the phase of the SBR cycle, Q_f and Q assume different values. For example, during the fill-phase Q = 0, while Q_f has a constant value, if the reactor is fed at a constant flowrate.

Equations (6.1) through (6.8), can be brought in a dimensionless form, when the following quantities are introduced.

$$y = \frac{s}{K_1} \qquad y_f = \frac{s_f}{K_1} \qquad \varepsilon_1 = K_{21} K_1 \qquad \gamma_1 = \frac{K_1}{K_{I1}} \qquad \lambda_1 = \frac{\mu_{c1}}{\hat{\mu}_2}$$

$$z = \frac{u}{K_1} \qquad z_f = \frac{u_f}{K_1} \qquad \varepsilon_2 = K_{12} K_1 \qquad \gamma_2 = \frac{K_1}{K_{I2}} \qquad \lambda_2 = \frac{\mu_{c2}}{\hat{\mu}_2}$$

$$x = \frac{b}{Y_1 K_1} \qquad \varphi = \frac{\hat{\mu}_1}{\hat{\mu}_2} \qquad \omega = \frac{K_2}{K_1} \qquad \eta = \frac{Y_1}{Y_2}$$

Reproduced with permission of the copyright owner. Further reproduction prohibited without permission.

$$\delta = \frac{V_o}{V_{max}} \qquad V' = \frac{V}{V_{max}} \qquad Q'_f = \frac{Q_f}{Q^*_f \sigma_1} \qquad Q' = \frac{Q}{Q^*_f \sigma_1}$$

$$\beta = \frac{\hat{\mu}_2 V_{max}}{Q^*_f \sigma_1} \qquad \theta = \frac{t Q^*_f \sigma_1}{V_{max}} \qquad \sigma_1 = \frac{t_1}{t_3} \qquad \sigma_2 = \frac{t_2 - t_1}{t_3} \qquad \sigma_3 = \frac{t_3 - t_2}{t_3}$$

The dimensionless form of the model equations is as follows.

$$\frac{dV'}{d\theta} = Q'_f - Q' \tag{6.9}$$

$$\frac{dy}{d\theta} = \frac{Q'_f}{V'}(y_f - y) - \beta \mu'_1(y, z)x \tag{6.10}$$

$$\frac{dz}{d\theta} = \frac{Q'_f}{V'}(z_f - z) + \left[\alpha \mu'_1(y, z) - \eta \mu'_2(z, y)\right]\beta x \tag{6.11}$$

$$\frac{dx}{d\theta} = -\frac{Q'_f}{V'}x + \left[\mu'_1(y, z) + \mu'_2(z, y)\right]\beta x - \left[\lambda_1 \Delta(y) + \lambda_2 \Delta(z)\right]\beta x \tag{6.12}$$

where,

$$\mu'_1(y, z) = \frac{\varphi y}{1 + y + \gamma_1 y^2 + \varepsilon_1 y z} \tag{6.13}$$

$$\mu'_2(z, y) = \frac{z}{\omega + z + \gamma_2 z^2 + \varepsilon_2 z y} \tag{6.14}$$

$$\Delta(y) \begin{cases} = 1, & \text{if } y > 0 \\ = 0, & \text{if } y = 0 \end{cases} \tag{6.15}$$

$$\Delta(z) \begin{cases} = 1, & \text{if } z > 0 \\ = 0, & \text{if } z = 0 \end{cases} \tag{6.16}$$

It is easier to follow the remaining part of the analysis, when the schematic of the SBR operation, shown in Figure A-3, is kept in mind.

At $t = 0$, or $\theta = 0$, the following equalities are valid.

$$Q_f = Q = 0; \quad Q'_f = Q' = 0; \quad V = V_o; \quad V' = \delta \tag{6.17}$$

Reproduced with permission of the copyright owner. Further reproduction prohibited without permission.

During the fill-phase, i.e., for $0 < \theta < \theta_1$, the following equalities hold.

$$Q_f = Q_f^*;\ Q = 0;\ Q_f' = \frac{1}{\sigma_1};\ Q' = 0 \tag{6.18}$$

Using equalities (6.18) in equation (6.9), and integrating the resulting equation under the initial condition given by (6.17), one can easily show that,

$$V' = \delta + \frac{1}{\sigma_1}\theta \tag{6.19}$$

At the end of the fill-phase, i.e., at $\theta = \theta_1$ the volume has reached its maximum value, hence, $V' = 1$. Taking this into account, equation (6.19) yields,

$$\theta_1 = \sigma_1(1 - \delta) \tag{6.20}$$

If the continuous cyclic mode of operation is to eventually reach a steady periodic orbit, the amount of mass fed to the reactor during the fill-phase, must be equal to the amount of mass discharged from the reactor during the draw-down phase. This leads to the following equalities.

$$Q_f \cdot t_1 = Q_f^* \cdot t_1 = Q(t_3 - t_2),\ \text{and}\ Q' = \frac{1}{\sigma_3} \tag{6.21}$$

During the second phase of the cycle, there is no input to, or output from the reactor, while the volume of the reactor contents is maintained at its maximum value. Thus, for $\theta_1 \le \theta \le \theta_2$,

$$Q_f' = Q' = 0;\ V' = 1 \tag{6.22}$$

During the final phase of the cycle, $Q_f = 0$ while Q' is given by equation (6.21). Taking this into account, and integrating equation (6.9) from $\theta = \theta_2$ to $\theta = \theta_3$, under the initial condition (6.22), one gets for $\theta_2 \le \theta \le \theta_3$,

$$V' = 1 - \frac{1}{\sigma_3}(\theta - \theta_2) \tag{6.23}$$

At the end of a cycle, i.e., at $\theta = \theta_3$ the volume of the reactor contents returns to the value it had at $\theta = 0$, i.e., $V' = \delta$. Taking this into account, equation (6.23) yields,

$$\sigma_3(1 - \delta) = \theta_3 - \theta_2 \tag{6.24}$$

Reproduced with permission of the copyright owner. Further reproduction prohibited without permission.

Since $\theta_3 - \theta_2 = \sigma_3\theta_3$, equation (6.24) implies that

$$\theta_3 = 1 - \delta \tag{6.25}$$

Using the results of the foregoing analysis -the lines of which have been also used by others (Dikshitulu, 1993; Sanyal, 1990; Chang, 1987)- one can easily show that instead of equations (6.9) through (6.12), the following ones can be equivalently used for describing the system.

$$\frac{dy}{d\theta} = \frac{(y_f - y)M}{\delta\sigma_1 + \theta} - \beta\mu_1'(y, z)\,x \tag{6.26}$$

$$\frac{dz}{d\theta} = \frac{(z_f - z)M}{\delta\sigma_1 + \theta} + \left[\alpha\mu_1'(y, z) - \eta\mu_2'(z, y)\right]\beta x \tag{6.27}$$

$$\frac{dx}{d\theta} = \frac{-xM}{\delta\sigma_1 + \theta} + \left[\mu_1'(y, z) + \mu_2'(z, y)\right]\beta x - \left[\lambda_1\Delta(y) + \lambda_2\Delta(z)\right]\beta x \tag{6.28}$$

with

$$M \begin{cases} = 1, & \text{for } 0 \le \theta \le \sigma_1(1 - \delta) \\ = 0, & \text{for } \sigma_1(1 - \delta) \le \theta \le 1 - \delta \end{cases} \tag{6.29}$$

Equations (6.26) through (6.28), along with relations (6.13) through (6.16), and (6.29), constitute a three-dimensional non-autonomous dynamical system. The system is non-autonomous, due to external forcing through equation (6.29), or in physical terms, due to the variation of the inlet flowrate from a constant non-zero value during the fill-phase, to a zero value for the remaining part of the cycle.

Due to the fact that the system is forced, it cannot reach steady state solutions. Instead, when transients decay, variables y, z, and x enter an oscillatory pattern which repeats itself. This repeated pattern is called an orbit or a cycle.

Reproduced with permission of the copyright owner. Further reproduction prohibited without permission.

The system can have two qualitatively different solutions (outcomes). The first, is the washout solution, and is possible due to the fact that biomass is not fed to the reactor and no biomass settling occurs; hence, unless the biomass lost during the draw-down phase is made-up for during the first two phases of the cycle, the culture eventually washes out of the reactor. Clearly, this outcome is totally undesirable from the design view point. The second type of solution is one in which the culture establishes itself in the reactor, and denitrification proceeds.

As the kinetics are quite complex, the solution of interest may exhibit multiplicity. That is, under a given set of operating conditions, the system may reach different final cycles each one of which implies a different degree of denitrification of the inlet stream. In such cases, one needs to find conditions for reaching the cycle which performs the highest conversion of the pollutants (reactants). It may also be possible, that both types of cycles (washout and survival) can arise under a given set of operating conditions. This is a case of multiplicity of qualitatively different solutions.

In order to investigate what types of solutions the system has, one needs to analyze equations (6.26) through (6.29). These equations, when the kinetic parameters are known, has five design, or operating, parameters; namely, β, δ, σ_1, z_f, and y_f. Hence, the complete picture of the possible system outcomes comprises of regions in the 5-dimensional space of the operating parameters. Since an analysis in the 5-dimensional space is too complicated, one can examine the dynamic behavior of the system when one, or two of the operating parameters vary. In cases where the system can theoretically reach multiple outcomes, not all of them are physically realizable. Only stable periodic solutions can be reached by a physical system which is not controlled. Application of process control can force a system to attain states which are inherently unstable. Stability of periodic solutions can be examined by determining their characteristic, or Floquet, multipliers. This can only be done numerically, as explained in the following section.

Reproduced with permission of the copyright owner. Further reproduction prohibited without permission.

6.2 Numerical Methodology and Studies

The real interest in studying this system is to find the dynamical behavior of continuous SBR operation when wastes containing both nitrate and nitrite are to be treated. Since this system is quite complex, originally, the case where the inlet streams contain nitrite only, was considered. Cases where the inlet contains nitrate only, were not considered since nitrite is produced in such cases and thus, they fall in the category of nitrate/nitrite mixtures. From the results of the kinetic study presented in Chapter 5, the following model parameter values were used: $\alpha = 0.616$, $\varphi = 0.71$, $\varepsilon_1 = 0.0959$ when $z > 0.439$ and $\varepsilon_1 = 0$ when $z < 0.439$, $\gamma_1 = 0.461$, $\lambda_1 = 0.0839$, $\omega = 1.649$, $\eta = 1.001$, $\gamma_2 = 0.898$, $\lambda_2 = 0.0654$, $\varepsilon_2 = 4.796$ when $z > 0.439$ and $\varepsilon_2 = 0$ when $z < 0.439$. Of the remaining five operating parameters two were fixed, namely, $\delta = 0.5$ and $\sigma_1 = 0.1$, while the other three (β, y_f, z_f) were allowed to vary. This choice was made because in applications one expects to have frequent variations in the inlet flowrate (thus, β), and inlet composition (thus, y_f and z_f).

The methodology which was followed for analyzing the dynamics of the system, is that of Dikshitulu et al. (1993). It is based on the computation of the periodic solutions as fixed points of the Poincaré map, and determination of their stability via the character of the Floquet multipliers which are the eigenvalues of the Jacobian matrix of the map. This Jacobian matrix of the map (evaluated at the fixed point), is equal to the matrix which consists of the solutions to the variational equations of the original system, when this matrix is evaluated at time equal to the period of the cycle. This leads to the preparation of bifurcation diagrams, and operating diagrams. A special software package AUTO (Doedel, 1986), was used for the calculations. This package has also continuation algorithms for tracing the curves which separate regimes in the operating parameter space where the system has different solutions.

Figures 14 and 15 show the two types of bifurcation diagrams which arise in cases where the reactor is fed with medium containing nitrite only. In such cases, since there is

Reproduced with permission of the copyright owner. Further reproduction prohibited without permission.

no nitrate, equation (6.26) is not needed, and the system is two-dimensional from the dynamical point of view. As a result, the stability of the solutions is determined by the magnitude of two Floquet multipliers. The vertical axis of diagrams of Figures 14 and 15, shows the value of the nitrite concentration (in dimensionless form) at the end of a periodic cycle. This concentration is valid for the reactor contents, and the exit stream, and is physically realizable when the solution is stable. Stable solutions are shown as thick solid lines/curves, while unstable solutions are shown as dotted lines/curves. The horizontal axis in these diagrams shows the value of β, which is a measure of the hydraulic residence time. Vertical lines in the diagrams simply separate regimes of β-values in which the behavior is different. Points on the horizontal thick lines, imply that the concentration of nitrite at the end of the cycle is equal to that in the inlet stream; i.e., the culture has washed-out and no denitrification occurs. Points on the solid curves imply that the concentration of nitrite at the end of a cycle is less than that in the inlet stream hence, the culture has survived and denitrification occurs. As expected, the larger the residence time, the higher the conversion of nitrite and thus, the lower is the nitrite concentration at the end of the cycle. All points on the solid curves represent solutions the two Floquet multipliers of which are less than one in magnitude, i.e., they both lie inside the unit circle in the complex plane. The value of β which separates regions I and II in Figure 14, and regions II and III in Figure 15, is a value where a transcritical bifurcation occurs. The physical significance of this particular β-value is the following. For the case of Figure 14, it indicates the minimum hydraulic residence time which one needs to use so that the culture does not wash-out; for the case of Figure 15, it indicates the minimum hydraulic residence time which one needs to use in order to avoid potential chances of washing out the culture. The value of βwhich separates regions I and III in Figure 15, is a point where a turning point or limit point bifurcation occurs. At this point, which is also known as saddle-node bifurcation, a stable and an unstable branch of the survival solution meet. This point indicates the minimum hydraulic residence time which needs to be used

Reproduced with permission of the copyright owner. Further reproduction prohibited without permission.

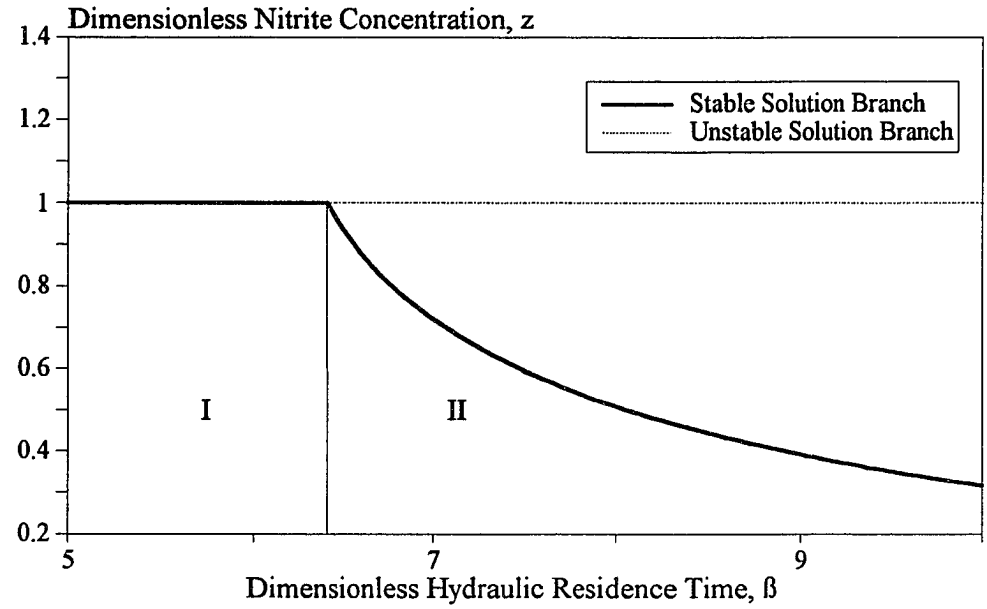

Figure 14 Bifurcation diagram (type I) of periodic states. This plot indicates the nitrite concentration at the end of a steady cycle as a function of β. It corresponds to Figure 16 when $z_f = 1$. The vertical line separates different solution regimes.

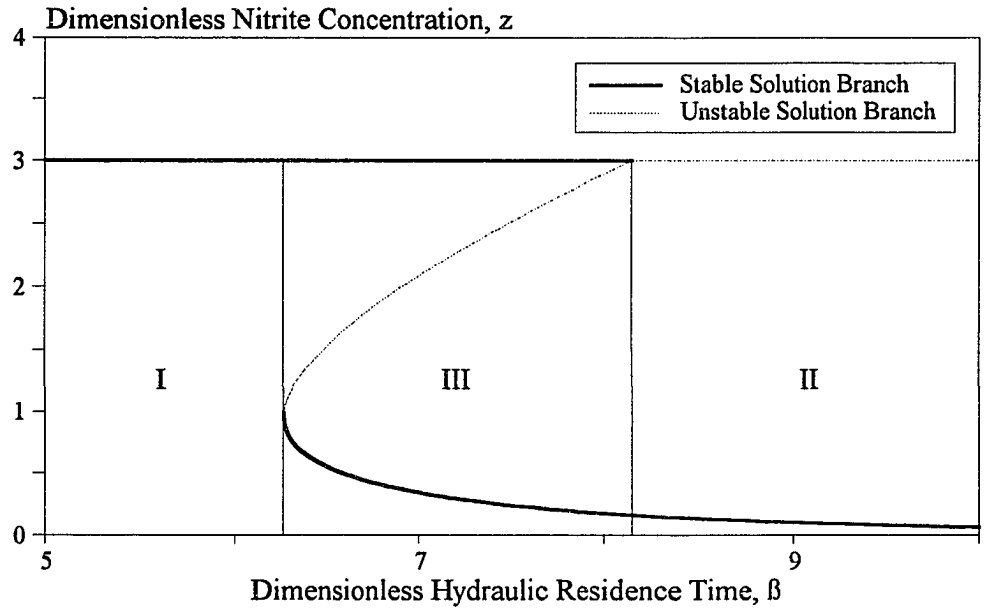

Figure 15 Bifurcation diagram (type II) of periodic states. This plot indicates the nitrite concentration at the end of a steady cycle as a function of β. It corresponds to Figure 16 when $z_f = 3$. Vertical lines separate different solution regimes.

Reproduced with permission of the copyright owner. Further reproduction prohibited without permission.

in order for the culture to have a chance to establish itself in the reactor. The existence of region III in Figure 15, implies that there are β-values which when selected, lead to multiple steady outcomes. In this case the culture will either survive or be washed-out. Which one of two outcomes is really reached, depends on the conditions used during process start-up. If the desired state of survival is reached, it is not globally stable; that is, smaller or larger perturbations during operation may cause the system to reach its other stable solution, i.e., washout. This can be avoided by applying process control in a way which does not allow the system to deviate much from its survival state.

Bifurcation diagrams such as those shown in Figures 14 and 15 can be prepared for various values of inlet nitrite concentration (z_f). The results can then be presented in the β- z_f plane, as shown in Figure 16. Such diagrams are called operating diagrams, and can be used as follows. For a given waste stream containing nitrite (z_f fixed), one can see what cycle the reactor will enter for different β-values. Clearly, values falling in region I (washout) should be avoided. It is also interesting to observe that if the stream contains nitrite at very high levels, region III, where the possibility of washing out the culture exists, seems unavoidable, at least with reasonable β-values. This suggests that one should either apply control as discussed earlier, or dilute the stream with water so that z_f drops, and then reasonable β-values lead to region II which is the safest for operation. The outcomes for each region are given in Table 12. It should be mentioned that the boundaries of the different regions in the diagram of Figure 16, are not constructed by preparing the bifurcation diagrams at various z_f-values. This would require a tremendous amount of computer time. Construction of these boundaries is done by the code discussed earlier, as follows. Since the bifurcation points are points at which one of the Floquet multipliers is equal to 1 in magnitude, the code makes one bifurcation diagram and then, does a two parameter continuation in the β- z_f plane by solving an equation which has a solution implying that one of the Floquet multipliers is equal to 1 in magnitude. This way, the loci of the bifurcation points are generated, and represent boundaries of regions in the

Reproduced with permission of the copyright owner. Further reproduction prohibited without permission.

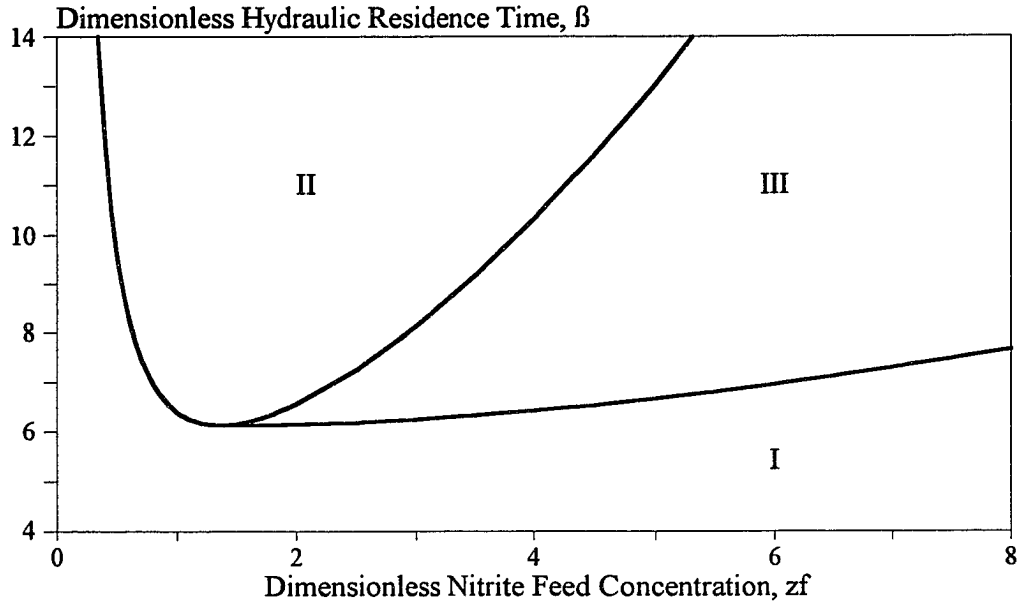

Figure 16 Operating diagram for a Sequencing Batch Reactor (SBR) when the feed stream contains nitrite only. For this diagram, T = 30 °C, pH = 7.1 ± 0.1, and the dimensionless parameters are $\delta = 0.5$, $\sigma_1 = 0.1$, ($y_f = 0$). The outcomes for each region are given in Table 12.

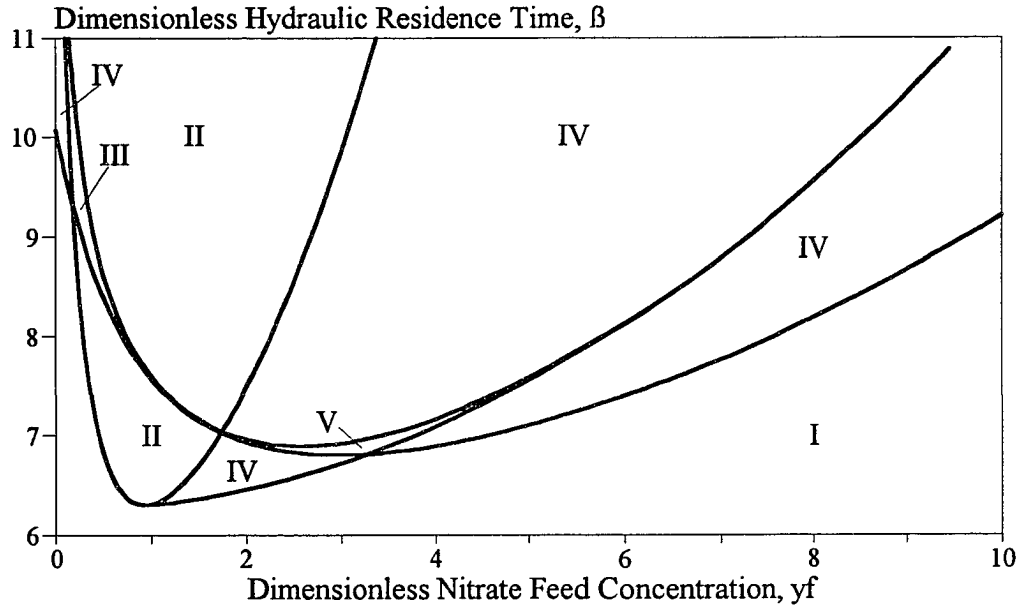

Figure 17 Operating diagram for a Sequencing Batch Reactor (SBR) when the feed stream contains a mixture of nitrate and nitrite. For this diagram, the inlet nitrite concentration is always taken as 96 mg/L ($z_f = 3$). Other parameters are $\delta = 0.5$, $\sigma_1 = 0.1$, T = 30 °C, pH = 7.1 ± 0.1. The outcomes for each region are given in Table 12.

Reproduced with permission of the copyright owner. Further reproduction prohibited without permission.

operating diagram. It should be also mentioned that in some cases the code fails to complete the continuation in the parameter space, and this problem can be corrected by starting with other bifurcation diagrams (i.e., values of z_f other than the one used in initiating the code).

Table 12 Stability characteristics of periodic states in each region of the operating diagrams (Figures 16 and 17); **S** = stable, **U** = unstable periodic state.

Region in Figure 16	Washout State	Survival State
I	**S**	-
II	**U**	**S**
III	**S**	**U, S**
Region in Figure 17	**Washout State**	**Survival State**
I	**S**	-
II	**U**	**S**
III	**U**	**S, U, S**
IV	**S**	**U, S**
V	**S**	**U, S, U, S**

The dynamics of reduction of nitrate/nitrite mixtures under SBR operation are much more complex than what has been already discussed. The sequential reaction nitrate to nitrite to final products, the inhibitory kinetics, the cross-inhibitory kinetic interference between nitrate and nitrite, lead to regions in the operating parameter space where up to three stable cycles are possible. Figures D-8 and D-11 show two examples of the most complex bifurcation diagrams which were found. Figure 17 shows an operating diagram in the β- y_f plane. This diagram was prepared under a constant nitrite concentration in the feed stream, namely 96 mg/L (i.e., $z_f = 3$); this was the value used in the experiments

Reproduced with permission of the copyright owner. Further reproduction prohibited without permission.

which are discussed in the following section. The outcomes (solutions), and their stability or instability characteristics for all regions appearing in Figure 17, are given in Table 12. It should be mentioned that the case of nitrate/nitrite mixtures is a three-dimensional system. In this case, the code tracks three instead of two Floquet multipliers for generating the bifurcation or operating diagrams.

6.3 SBR Experiments and Validation of the Theory

In order to verify the theoretically predicted types of behavior of the denitrification process during continuous SBR operation, experiments were performed with the unit shown in Figure A-2. The procedures for these experiments are discussed in Chapter 4.

Table D-1 shows the conditions used in two experiments with medium containing nitrite only. It was decided to keep all but one operating parameters the same in both experiments, and vary the remaining parameter in a way which, according to theory, would lead to different outcomes. It was decided to run experiments with streams containing nitrite at 50 mg/L (i.e., $z_f = 1.564$). A bifurcation diagram was prepared, and in shown in Figure D-1. For the first experiment, a value for the feed flowrate was selected in a way that the resulting β value would fall in region I of Figure D-1. Theory predicts that the culture will eventually washout. Figure D-3 shows the experimental data from 4 cycles; each cycle lasted for 4 hours. There is a clear indication that the nitrite concentration in the reactor tends to reach the value of 50 mg/L which was the value at the inlet stream. Conversely, the biomass concentration drops continuously, with a tendency to washout. The curves shown in Figure D-3 are theoretically predicted transient concentration profiles. These profiles are generated by integrating equations (6.26) through (6.28) subject to the initial conditions shown in Table D-1. Integration was performed through the use of a computer code based on the 4th-order Runge-Kutta method. This code is given in Appendix E-2. From the biomass concentration profile, one can see that after 12 hours of operation it looks like the reaction stopped. It should

Reproduced with permission of the copyright owner. Further reproduction prohibited without permission.

be mentioned that the biomass concentration is low already, but it may be that the reaction stopped due to an oxygen leak in the reactor.

The second experiment with nitrite differed from the first only in the value of the medium flowrate during the fill-phase of the cycle. This value was selected in a way which resulted in a β-value falling in region II of Figure D-1. The prediction was that the culture would establish itself in the reactor. Also, as shown by the arrows in Figure D-1, the prediction is that at the end of the steady cycle, the nitrite concentration in the reactor would be z = 0.58, i.e., about 18 mg/L. Using this value as the initial condition for integrating equations (6.26) through (6.28), one can easily get (after 1 or 2 cycles) the predicted nitrite and biomass concentration profiles during the steady cycle of the system. These profiles are shown in Figure D-2. The importance of these profiles is the following. If a steady cycle of survival is to be experimentally seen, the experiment should not be started with random values for the biomass and nitrite concentration in the reactor. This would lead to very lengthy transients, and the experiment should run over a long period before the steady cycle is reached. On the other hand, if one selects start-up conditions (i.e., b_o and u_o) in such a way that they fall on, or close to the expected steady cycle, then a relatively short experiment would be enough in order to test (see) if the predicted cycle is reached. This was the procedure followed. Figure D-2 was used in selecting a pair of b_o and u_o values to start-up the experiments. The results are shown in Figure D-4. Within experimental error, data and predicted concentration profiles show a cyclic pattern which repeats itself, as theory predicted. This experiment lasted for 4 cycles, which in this case imply 20 hours of continuous operation. The frequency of sampling, indicates how tedious the experiments are to perform.

One more thing needs to be mentioned regarding these two experiments. Since the value of nitrite concentration in the feed stream was the same, going to Figure 16, the implication is that the two experiments were performed under operating conditions which

Reproduced with permission of the copyright owner. Further reproduction prohibited without permission.

fall on a line parallel to the β-axis of the operating diagram. On point falls in region I and leads to washout, while the other falls in region II and leads to culture survival.

Experiments were also performed with feed-streams containing mixtures of nitrate and nitrite. In all experiments, 10% of the cycle time was devoted to filling the reactor (σ_1 = 0.1), the minimum to maximum volume of the reactor contents was 0.5, (δ = 0.5), and - within experimental error- the nitrite concentration in the feed stream was about 96 mg/L. Hence, the operating diagram is that shown in Figure 17. The conditions for the various experimental runs are shown in Table D-2. The experiments were performed under different nitrate concentrations in the inlet stream, y_f and/or different flowrate, hence different β, so that the predicted complex behavior shown in Figure 17 could be verified.

Experiments SBR-3 and SBR-4, are in a sense the analogue of what was observed in experiments SBR-1 and SBR-2. Both experiments were performed under essentially the same nitrate concentration in the feed, but different flowrate (β). For SBR-3 the operating conditions fall in region I of the diagram shown in Figure 17, while for SBR-4, conditions fall in region II. As predicted, SBR-3 leads to washout, and SBR-4 in stable cycle where the culture survives, and denitrification occurs. These results are shown in Figures D-5 for SBR-3, and D-6 for SBR-4. Regarding SBR-4, one can easily see that the agreement between data and model predicted concentration profiles is very good for nitrite and biomass, but not so great for nitrate. On the other hand, one should realize that nitrate concentration values fall so low that the likelihood of experimental error is high. It is also interesting to observe that although nitrate gets depleted at the end of the cycle (complete treatment), almost nothing happens to the nitrite which essentially remains at its value at the inlet stream. Since this is also predicted by the theory, it means that the model can be used not only for determining where the culture will survive, but also for selecting operating conditions under which both nitrate and nitrite would get depleted.

The remaining three experiments, SBR-5, SBR-6, and SBR-7 were performed under operating conditions which fall in region(s) IV of operating diagram (Figure 17).

Reproduced with permission of the copyright owner. Further reproduction prohibited without permission.

This region was of particular concern for two reasons. First, it dominates most of the operating diagram, something which implies that in most cases one would have to operate in such a region. Second, it is a region in which theory predicts that both the washout and one of the culture survival states are stable. For these reasons, the objectives of the experiments were to demonstrate that both outcomes are in fact possible in this region, and to show that when survival is reached, conditions of operation can be selected in a way which leads to complete denitrification of the feed stream.

Figure D-7 shows the results of experiment SBR-5. Under the operating conditions of this experiment, theory predicts that depending on how the system is started-up it would go either to washout, or to survival. Furthermore, it predicts that the transients may be very long. The start-up conditions were selected in such a way that, it would take many cycles but, eventually the culture would be washed-out. The data show in fact a tendency towards washout, but this experiment was not very successful because the data suggest that the biomass lost its activity relatively quickly, probably due to air (oxygen) leaks in the reactor.

Experiments SBR-6 and SBR-7 were carefully designed in order to see the steady cycles of survival. As in the case of SBR-2, the bifurcation diagrams were prepared (Figures D-8 and D-11), and the survival steady cycle concentration profiles were prepared (Figures D-9 and D-12), for proper selection of the start-up conditions for the experiments. The case of SBR-6 resembles that of SBR-4. Theory predicts that if the system is properly started-up, denitrification will be taking place in a stable steady cycle, but nitrite will not really be treated. This means that some amount of the nitrite fed to the reactor is reduced, but this amount is balanced by the nitrite produced during the nitrate reduction. Figure D-10 shows the experimental data, along with predicted concentration profiles. The agreement is very good, and the data show that nitrite is in fact, essentially, not treated. Experiment SBR-7 was selected in order to demonstrate that complete nitrate and nitrite removal can in fact be achieved in SBRs, in a stable steady cycle. The results

Reproduced with permission of the copyright owner. Further reproduction prohibited without permission.

shown in Figure D-13 are a demonstration of self repeating cycles, at the end of which the effluent has neither nitrate, nor nitrite while both were present in the feed stream at concentrations of about 100 mg/L. The length of each cycle for experiment SBR-7 is 7 hours. After frequent sampling during the first three cycles, a break was taken by the experimenter while the unit kept operating. This is why no data are shown for the fourth cycle. Measurements were repeated during the fifth cycle, and clearly the pattern keeps repeating itself.

Despite the complexity, and length of the experiments, an excellent agreement was found between theory and experimental data. It is believed that these experiments fully validated the theoretical model which could be now used with confidence in design calculations.

Reproduced with permission of the copyright owner. Further reproduction prohibited without permission.

CHAPTER 7

CONCLUSIONS AND RECOMMENDATIONS

Fundamental kinetic studies on the reduction of nitrate, nitrite, and their mixtures were performed with a strain of *Pseudomonas denitrificans* (ATCC 13867). Methanol served as the carbon source and was supplied in excess (2 : 1 mole ratio relative to nitrate and/or nitrite). Nitrate and nitrite served as terminal electron acceptors, as well as sources of nitrogen for biomass synthesis. The results were explained under the assumption that respiration is a growth associated process. It was found that the sequence of complete reduction of nitrate and/or nitrite to nitrogen is,

$$\text{Nitrate } (NO_3^-) \longrightarrow \text{Nitrite } (NO_2^-) \longrightarrow \text{Nitrous Oxide } (N_2O) \longrightarrow \text{Nitrogen } (N_2)$$

It was found that the specific growth rate of the biomass on either nitrate, or nitrite follows Andrews inhibitory kinetics. Nitrite is more inhibitory than nitrate, as can be judged from the values of the inhibition constants in the Andrews expression. It was also found that the culture has severe maintenance requirements which can be described by Herbert's model, i.e., by self oxidation of portions of the biomass. The specific rates of biomass consumption for maintenance purposes were found to be unusually high; at 30 °C and pH = 7.1, these rates were equal to about 28% of the maximum specific growth rate on nitrate, and 22% of the maximum specific growth rate on nitrite.

It was also found that nitrate and nitrite are involved in a cross-inhibitory non-competitive kinetic interaction. The extent of this interaction is negligible when the presence of nitrite is low, but considerable when nitrite is present at levels above 15 mg/L. Interestingly, it was found that nitrate inhibits the rate of nitrite removal much more than nitrite inhibits the rate of nitrate conversion. In fact, the values of the constants expressing this cross-inhibition were found to differ by two orders of magnitude. These results seem to suggest that the culture exhibits a preference towards nitrate.

Reproduced with permission of the copyright owner. Further reproduction prohibited without permission.

Studies on the effects of temperature have shown that the culture cannot grow at temperatures above 40 °C. The optimal temperature for nitrate or nitrite reduction was found to be about 38 °C. Experiments in the temperature range of 30 to 38 °C have shown that one could possibly use an Arrhenius expression to describe the effect of temperature on the net specific growth rates. The activation energy for use of nitrate by the culture was found to be 8.6 Kcal/mole, while for use of nitrite, 7.21 Kcal/mole. A more detailed analysis of the results has shown that instead of using an overall Arrhenius expression to describe the temperature effects, one can use -as proposed by Topiwala- expressions describing the variation, with temperature, of each one of the four kinetic constants involved in the Andrews/Herbert expression for the net specific growth rate. The results have shown that three of the four constants can be described by Arrhenius expressions, while the fourth one follows an inverse Arrhenius expression.

Studies on the effects of pH, have shown that a value of about 7.5 is optimal. More specifically, it was found that the culture uses nitrate optimally at pH values between 7.4 and 7.6, while nitrite is used optimally at slightly lower pH values in the range of 7.2 to 7.3. These studies were performed at a temperature of 30 °C.

The data indicate that the presence of nitrous oxide in the gas phase is substantial at the time of nitrate and/or nitrite depletion. Nitrous oxide seems to be reduced to nitrogen long after nitrate and nitrite have been consumed, as some measurements have indicated. Although the nitrous oxide presence in the liquid phase was not measured, calculations for the period up to the complete disappearance of nitrate/nitrite have shown that the nitrogen balance closes reasonably well whether one assumes no N_2O presence in the liquid phase (i.e., fast reaction, or mass transfer limitation), or N_2O presence at levels dictated by thermodynamic equilibrium (i.e., kinetic limitation). It is suspected that nitrous oxide reduction to nitrogen is a kinetic-limited process, but further studies are needed for verifying this idea. Such experiments will lead to determination of rates of N_2O reduction,

Reproduced with permission of the copyright owner. Further reproduction prohibited without permission.

and will help estimating the time of reaction (or volume of reactor), needed for complete reduction of nitrate and nitrite to the final product, i.e., to nitrogen gas.

The detailed kinetic model derived from the small scale batch experiments was used as the basis for describing nitrate/nitrite reduction in a continuously operated periodic reactor which operates in the SBR mode. The model was subjected to a detailed analysis based on the bifurcation theory of forced systems. Two cases were considered; one in which the feed stream contains nitrite only, and one in which a mixture of nitrate and nitrite is present in the inlet stream to the reactor. In both cases it was found that the system has two qualitatively different solutions. One is the unwanted washout state, while the second is a periodic state of culture survival. It was also found that these outcomes can happen either in separate domains of the operating parameter space, or in the same domain. Furthermore, in the case of nitrate/nitrite mixtures, it was found that the survival state can exhibit multiplicity. This means that under the same operating conditions, the reactor can achieve a high or low conversion of the nitrate/nitrite mixture, depending on the conditions under which the process is started-up. The results of this analysis have been presented in the form of bifurcation diagrams, and two-dimensional operating diagrams.

Experiments were performed with a 2 liter reactor operated continuously in the SBR mode, in order to experimentally test whether the complex behavior predicted by theory is in fact realizable. Various experiments with either nitrite only, or with nitrate/nitrite mixtures in the feed stream, were performed under operating conditions falling in different regions of the operating diagrams. The operating conditions which were varied, were the flowrate and composition of the inlet stream. In all cases, the experimental data confirmed the model predictions both at the qualitative, and quantitative level. Furthermore, it was experimentally shown that proper operating conditions can be selected so that at the end of the steady SBR cycle the concentrations of both nitrate and

Reproduced with permission of the copyright owner. Further reproduction prohibited without permission.

nitrite are zero in the effluent. It was also shown that improper selection of operating conditions may lead to complete nitrate conversion, but nitrite accumulation.

The model of SBR operation has been experimentally validated, and can now be used in further studies. In this work, for all experiments, 10 % of the total cycle time was allocated for filling the reactor and the ratio of minimum to maximum volume of reactor contents was always kept at 0.5. However, the model can now be used to optimize these parameters for any given case. Numerical studies should be performed in order to see whether the 0.5 value is really the best one to use. The overall objective of these suggested studies, should be to find the best operating parameters in order to maximize the productivity of a reactor of a given size, or to for a given productivity to minimize the required reactor volume.

Future SBR studies should also take into account the kinetics of nitrous oxide reduction to nitrogen, if one is interested in sizing and scheduling SBRs for complete reduction of nitrate and nitrite to nitrogen.

Finally, in this study with SBRs it was assumed that no settling of biomass occurs at the end of a cycle. This was done in order to facilitate the study of the dynamics without interference from physical phenomena, such as settling. In reality, biomass settling should occur in real applications. This reduces the potential for biomass washout, and leads to higher biomass concentrations -thus higher denitrification rates- in the reactor. Future studies should consider settling, and investigate its impact on the dynamics and reactor design.

Reproduced with permission of the copyright owner. Further reproduction prohibited without permission.

APPENDIX A

CALIBRATION CURVES AND EXPERIMENTAL APPARATUS

Reproduced with permission of the copyright owner. Further reproduction prohibited without permission.

Table A-1 Weights of biomass condensate from a 1 L suspension having an absorbance of 0.254 UOD

	Tube 1	Tube 2
Empty tube weight, g	8.9002	8.8052
Wet weight, g	9.2439	9.2340
Dry weight, g	8.9292	8.8413
Biomass dry weight, g	0.0290	0.0361
Total biomass, g in 1L	0.0651	

0.0651 g/L / 0.254 UOD = 256.3 g/L/UOD

Table A-2 Areas of Peaks for N_2 GC Calibration

	Area for injection volume (mL) of		
Sample No.	0.025	0.1	0.2
1	216850	867158	1768989
2		868654	1791855
3		884456	1781959
4		852580	1753915
Average Area	216850	868212	1774180

The response factor for nitrogen was 3.681×10^{-12} mole/unit area.

Table A-3 Areas of Peaks for O_2 GC Calibration

	Area for injection volume (mL) of		
Sample No.	0.025	0.1	0.2
1	46557	192669	374892
2		184824	361385
3		189554	369809
4		187707	372818
Average Area	46557	188689	369726

The response factor for oxygen was 4.656×10^{-12} mole/unit area.

Reproduced with permission of the copyright owner. Further reproduction prohibited without permission.

Table A-4 Areas of Peaks for N_2O GC Calibration

	Area for injection volume (mL) of		
Sample No.	0.025	0.050	0.075
1	362619	807357	1131162
2	366363	781748	1119846
3	403001	780011	1182958
4	399874	765942	1129876
5	381379	768642	1119462
6		772766	
Average Area	382647	779411	1136660

The response factor for nitrous oxide was 3.607×10^{-12} mole/unit area.

Reproduced with permission of the copyright owner. Further reproduction prohibited without permission.

Reproduced with permission of the copyright owner. Further reproduction prohibited without permission.

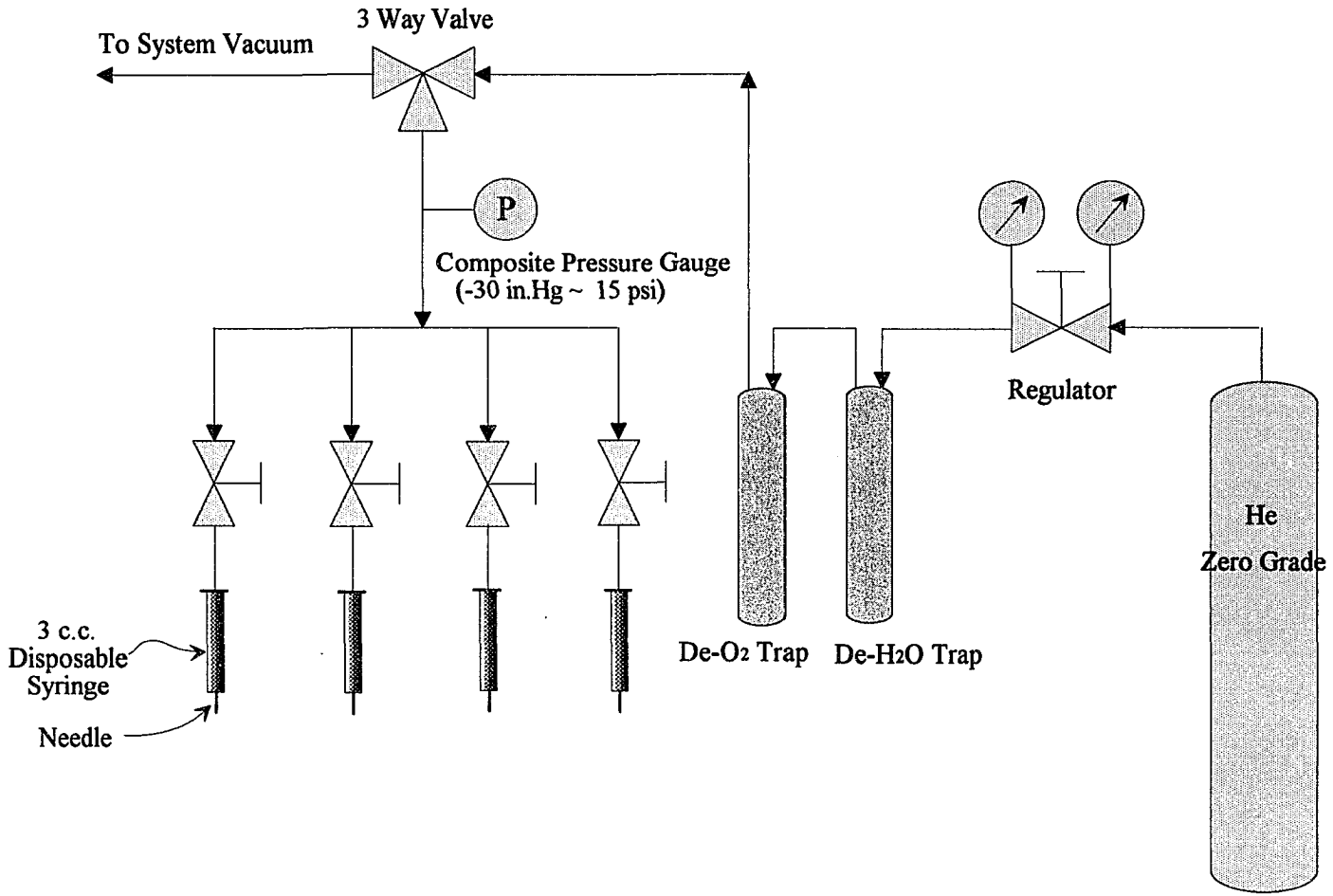

Figure A-1 Helium Purge System used in Denitrification Kinetic Studies

Reproduced with permission of the copyright owner. Further reproduction prohibited without permission.

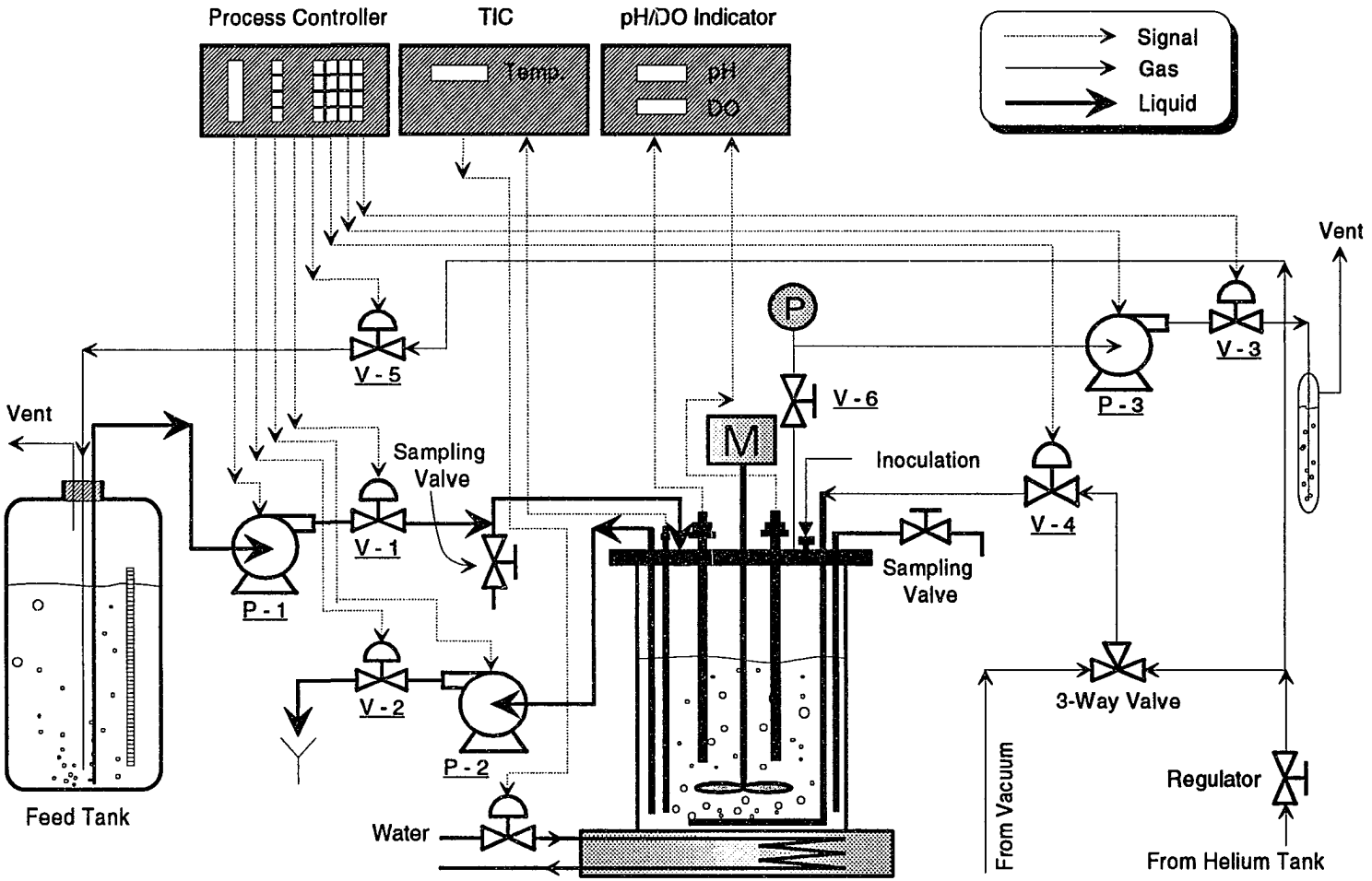

Figure A-2 Schematic diagram of the Sequencing-Batch-Reactor (SBR) used in the experiments

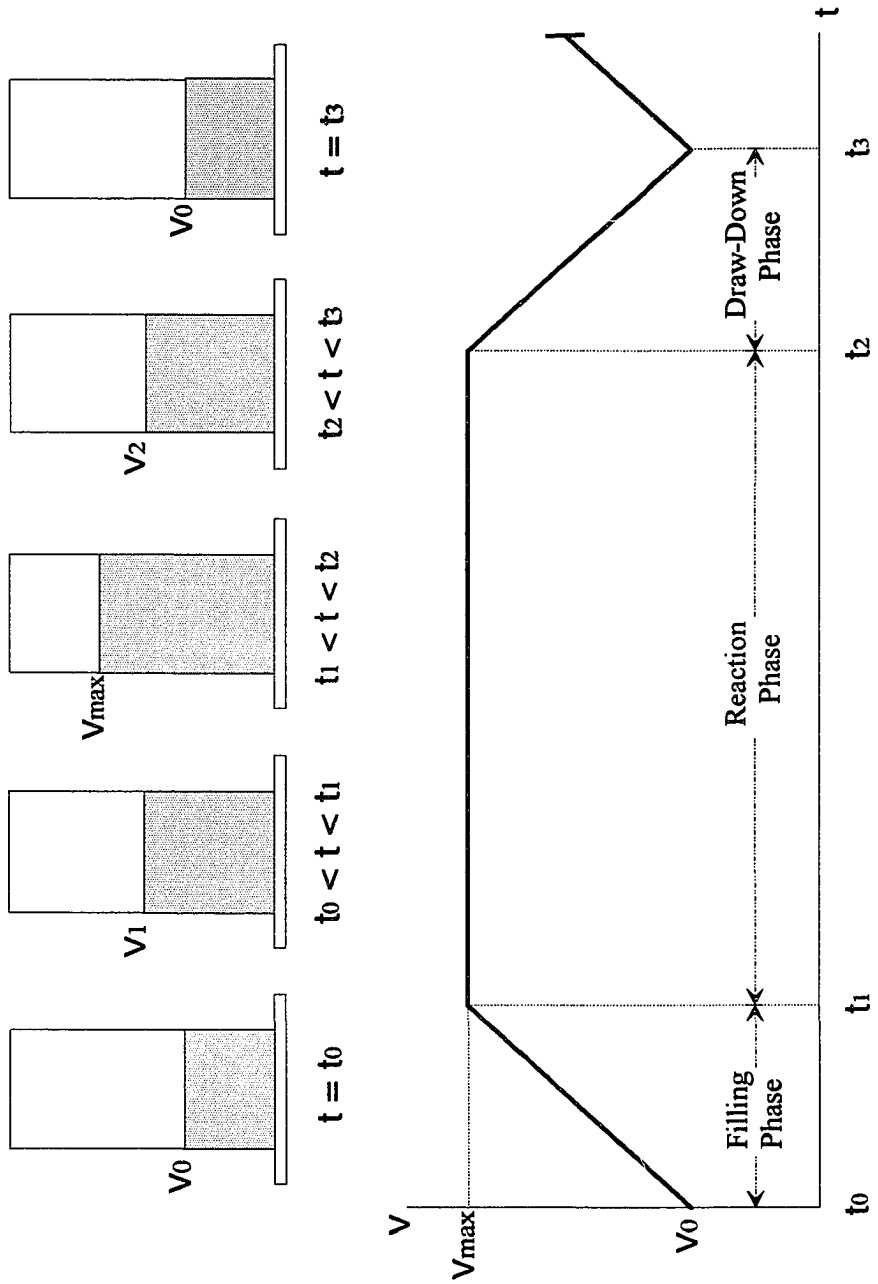

Figure A-3 Reactor Contents Volume Variation during a SBR Cycle

Reproduced with permission of the copyright owner. Further reproduction prohibited without permission.

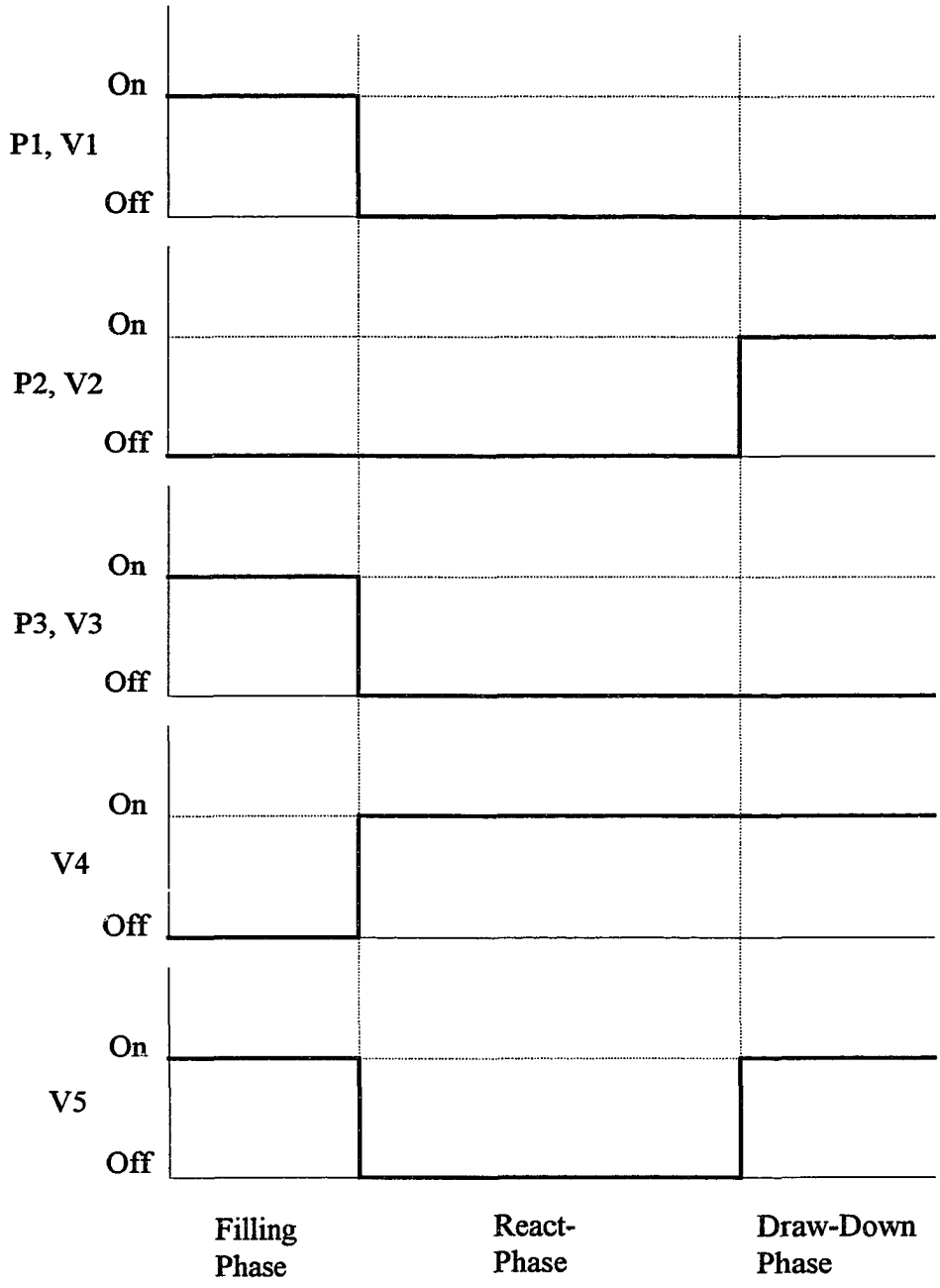

Figure A-4 Valve and pump position (on/off) during SBR operation.
(P: Pump, V: Solenoid Valve)

Reproduced with permission of the copyright owner. Further reproduction prohibited without permission.

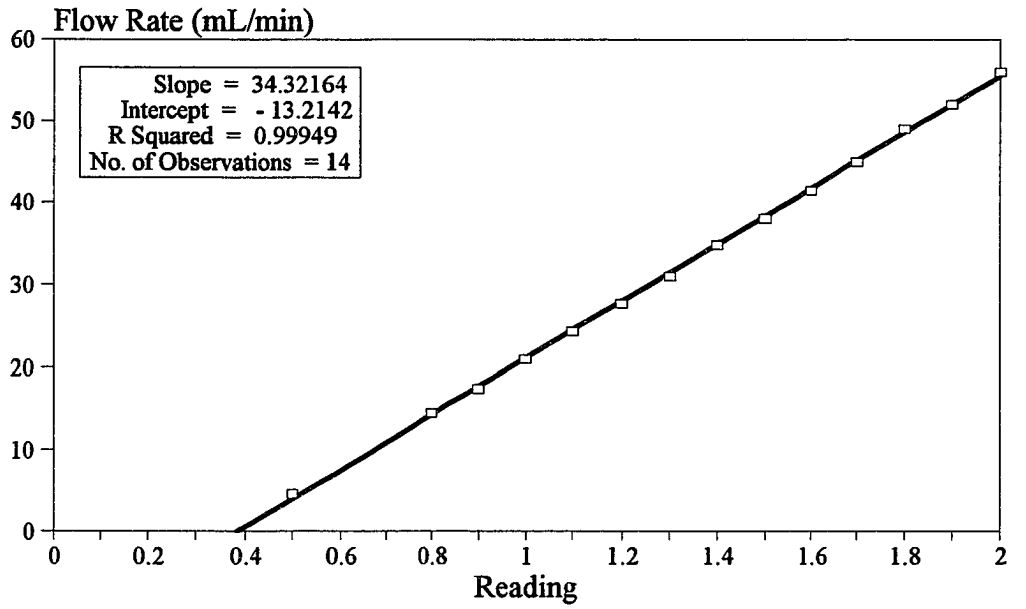

Figure A-5 Calibration curve for the pumps used in SBR experiments. The reactor was pressurized with helium at 3 psig.

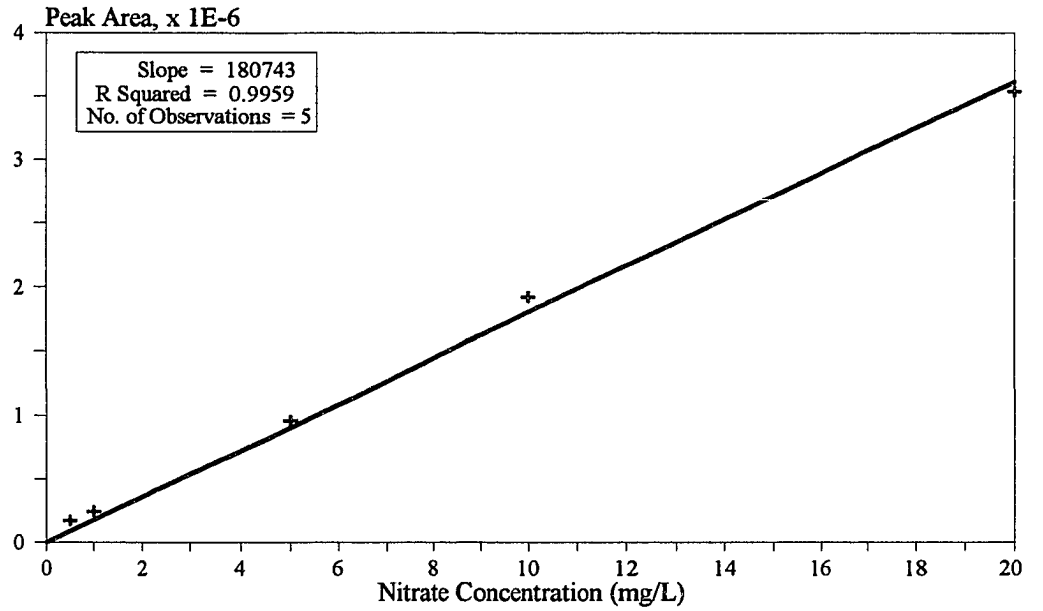

Figure A-6 Ion Chromatography (IC) calibration curve for nitrate.

Reproduced with permission of the copyright owner. Further reproduction prohibited without permission.

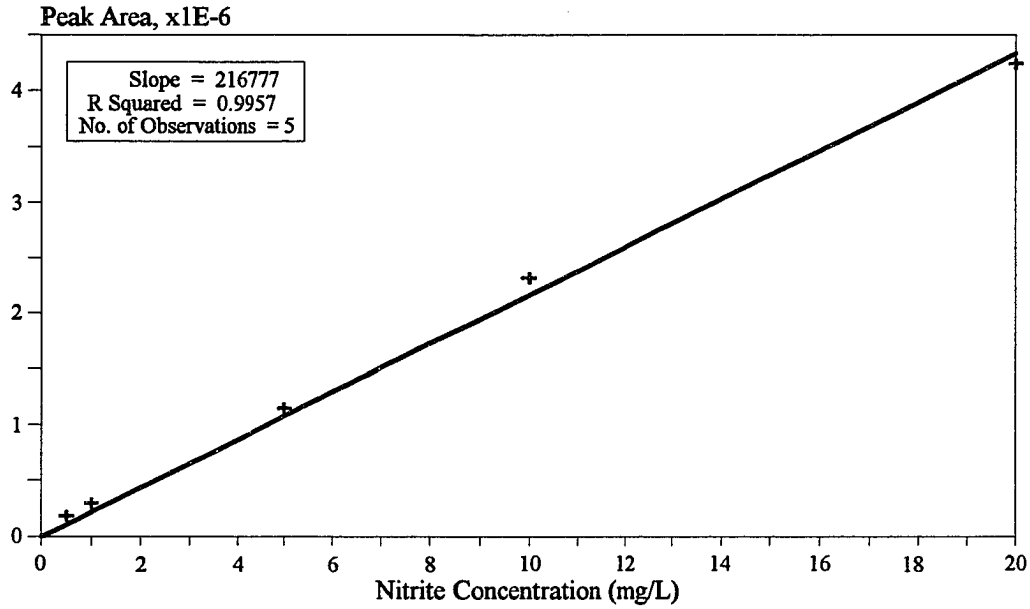

Figure A-7 Ion Chromatography (IC) calibration curve for nitrite.

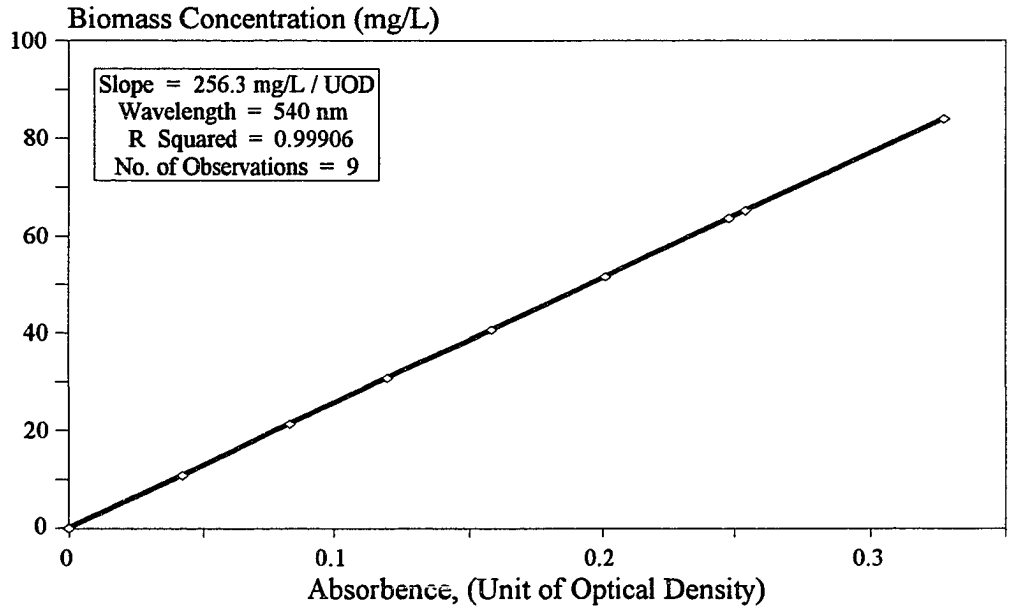

Figure A-8 Calibration curve for biomass concentration measurement by optical density. Measurements were made at a wavelength of 540 nm and room temperature.

Reproduced with permission of the copyright owner. Further reproduction prohibited without permission.

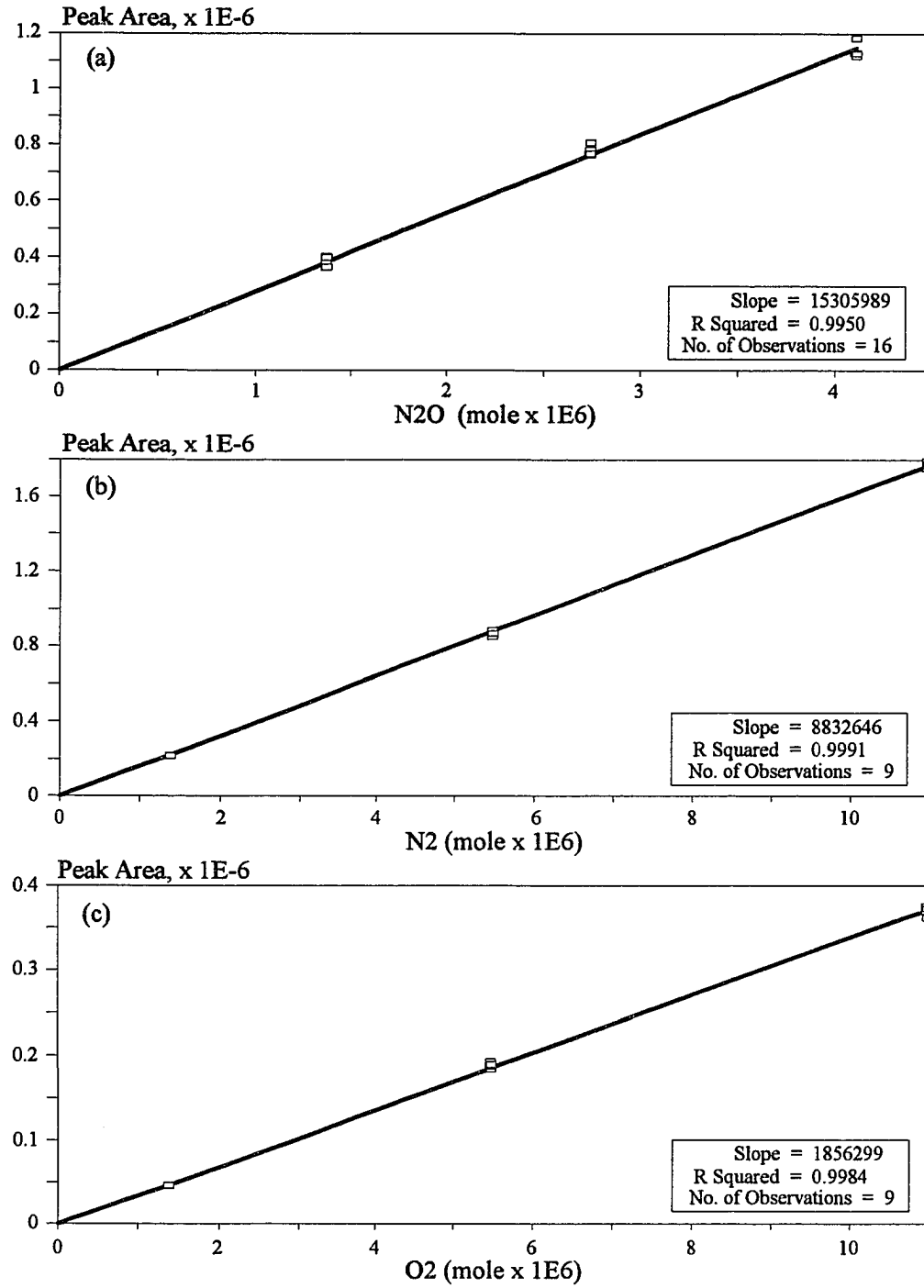

Figure A-9 Gas Chromatography (GC) calibration curves for nitrous oxide (a), nitrogen (b), and oxygen (c).

Reproduced with permission of the copyright owner. Further reproduction prohibited without permission.

Reproduced with permission of the copyright owner. Further reproduction prohibited without permission.

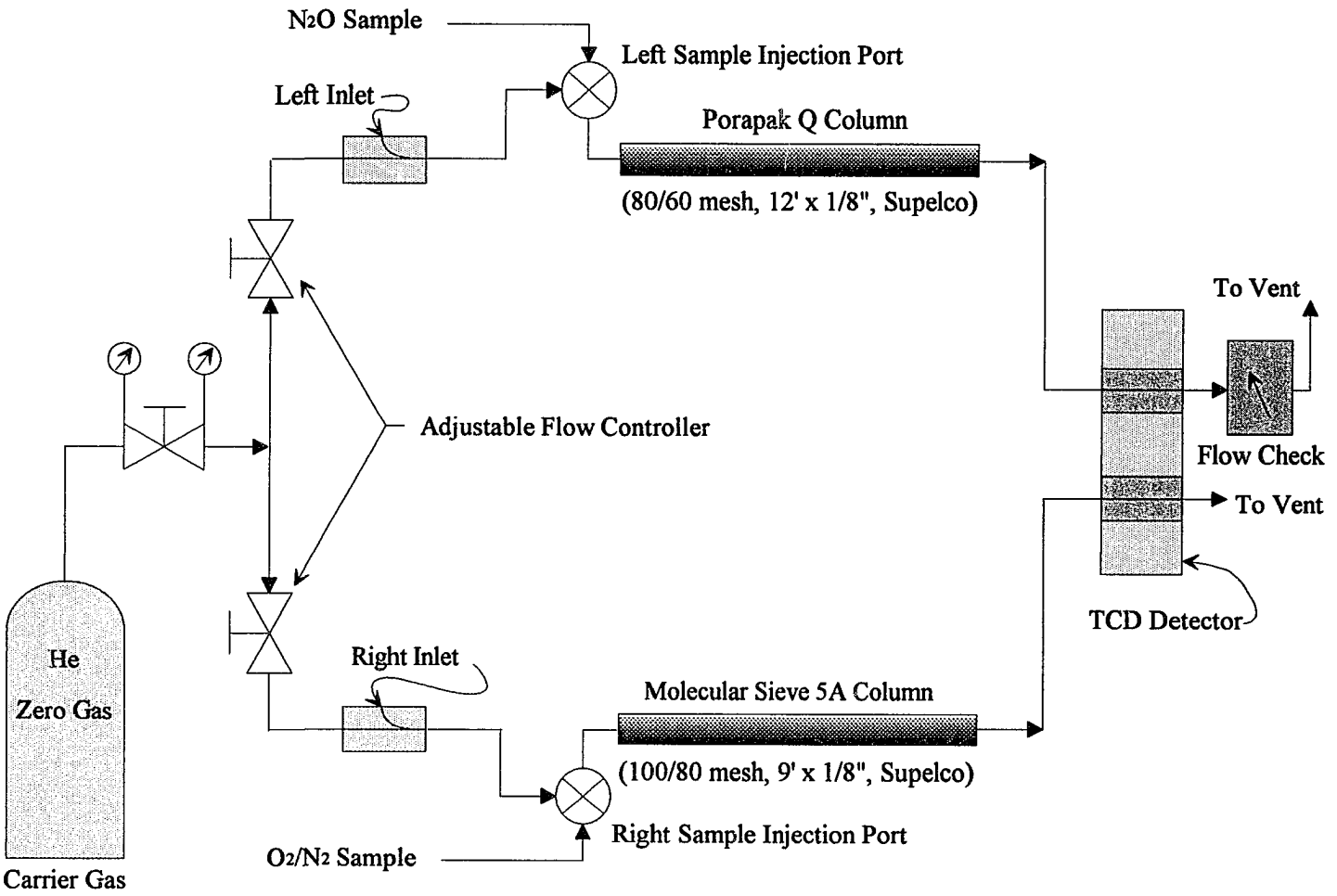

Figure A-10 Carle Gas Chromatograph AGC 111H Flow System

APPENDIX B

KINETIC DATA, RAW AND PROCESSED CONCENTRATION PROFILES, AND OTHER CURVES BASED ON KINETIC RUNS

Reproduced with permission of the copyright owner. Further reproduction prohibited without permission.

Table B-1 Experimental data for determining the kinetics of nitrate reduction at 30 °C and pH 7.1 ± 0.1. (All concentrations are in mg/L)

Time	Run 1A (V_o = 131 mL) (pH = 7.18 ~ 7.19)					Run 2A (V_o = 131 mL) (pH = 7.08 ~ 7.07)				
(min.)	NO_3^-	NO_2^-	*b*	N_2O	N_2	NO_3^-	NO_2^-	*b*	N_2O	N_2
0	6.9	0	33.32	45.20	590.7	16.49	1.00	43.83	36.59	1562
15	0	2.44	33.70	30.30	530.9	13.47	2.91	44.34	70.79	1400
30	0	1.27	34.09	26.74	510.6	6.96	2.13	45.11	32.27	1243
45	0	0	34.86	36.78	512.8	0	0	45.37	29.91	1098
60	0	0	36.65	29.82	457.0	0	0	45.62	39.10	1270
75	0	0	35.11	27.14	407.2	0	0	45.88	37.90	1132
90	0	0	35.37	26.32	386.2	0	0	46.13	50.80	997
105										
120										
135										
150										
165										
180										

Time	Run 3A (V_o = 104 mL) (pH = 7.11 ± 0.00)					Run 4A (V_o = 131 mL) (pH = 7.17 ~ 7.18)				
(min.)	NO_3^-	NO_2^-	*b*	N_2O	N_2	NO_3^-	NO_2^-	*b*	N_2O	N_2
0	9.16	0	55.62	19.40	128.0	10.28	2.32	34.09	49.59	577.0
15	1.02	1.69	56.64	19.61	124.9	4.89	0.42	34.47	31.30	498.1
30	0	0	57.67	19.64	124.9	0	0.45	34.86	29.23	468.3
45	0	0	57.92	19.65	125.0	0	0	35.50	30.89	432.0
60						0	0	36.65	30.39	397.7
75										
90										
105										
120										
135										
150										
165										
180										

Reproduced with permission of the copyright owner. Further reproduction prohibited without permission.

Table B-1 (Continued) Experimental data for determining the kinetics of nitrate reduction at 30 °C and pH 7.1 ± 0.1. (All concentrations are in mg/L)

Time	Run 5A (V_o = 131 mL) (pH = 7.14 ~ 7.17)					Run 6A (V_o = 133 mL) (pH = 7.11 ~ 7.15)				
(min.)	NO_3^-	NO_2^-	*b*	N_2O	N_2	NO_3^-	NO_2^-	*b*	N_2O	N_2
0	14.09	1.82	34.09	37.18	1165	29.26	2.19	53.57	7.70	214.1
15	8.36	0.25	34.60	35.11	1001	28.20	3.30	50.23	77.57	993.1
30	5.74	0	35.58	33.94	875.4	17.20	1.75	52.03	59.45	890.6
45	0	0	36.91	29.69	776.8	2.27	1.71	53.57	88.87	850.8
60	0	0	36.91	32.21	770.3	0	1.45	53.31	94.87	832.6
75										
90										
105										
120										
135										
150										
165										
180										

Time	Run 7A (V_o = 104 mL) (pH = 6.93 ~ 6.96)					Run 8A (V_o = 132 mL) (pH = 7.12 ~ 7.15)				
(min.)	NO_3^-	NO_2^-	*b*	N_2O	N_2	NO_3^-	NO_2^-	*b*	N_2O	N_2
0	21.76	0	50.75	19.98	185.0	31.11	1.22	31.01	-	-
15	10.45	2.18	51.52	20.40	180.3	29.15	2.01	32.55	22.72	329.1
30	2.56	3.28	53.57	20.81	179.5	24.78	2.39	33.58	22.95	316.9
45	0	0	55.87	21.89	170.7	17.09	2.07	34.86	42.53	335.2
60	0	0	56.13	23.79	156.3	9.95	2.30	36.91	22.98	285.1
75						4.30	1.24	39.47	28.06	278.0
90						0	0.50	41.52	28.55	271.1
105						0	0	43.06	28.20	235.5
120						0	0	42.80	27.83	246.5
135										
150										
165										
180										

Reproduced with permission of the copyright owner. Further reproduction prohibited without permission.

Table B-1 (Continued) Experimental data for determining the kinetics of nitrate reduction at 30 °C and pH 7.1 ± 0.1. (All concentrations are in mg/L)

Time	Run 9A (V_o = 132 mL) (pH = 7.18 ~ 7.20)					Run 10A (V_o = 132 mL) (pH = 7.10 ~ 7.12)				
(min.)	NO_3^-	NO_2^-	*b*	N_2O	N_2	NO_3^-	NO_2^-	*b*	N_2O	N_2
0	32.07	3.56	33.06	35.10	1726	44.13	2.61	35.37	34.34	464.8
15	15.07	3.06	34.34	44.95	1553	32.16	3.04	35.37	27.77	487.4
30	9.19	2.69	35.63	47.27	1466	16.54	2.69	36.39	34.69	413.2
45	3.52	2.14	38.70	52.30	1405	6.54	2.96	39.21	32.97	481.1
60	0.86	3.17	36.91	51.17	1188	1.15	2.42	40.75	38.50	487.8
75	0	2.00	38.45	54.20	1065	0	0	42.03	33.52	473.2
90	0	1.97	40.50	52.73	1050	0	0	42.03	38.45	447.0
105	0	0	40.11	48.34	1030	0	0	42.03	31.93	439.3
120	0	0	39.98	49.90	944.4	0	0	42.54	38.10	414.1
135										
150										
165										
180										

Time	Run 11A (V_o = 104 mL) (pH = 7.12 ~ 7.13)					Run 12A (V_o = 131 mL) (pH = 7.02 ~ 7.10)				
(min.)	NO_3^-	NO_2^-	*b*	N_2O	N_2	NO_3^-	NO_2^-	*b*	N_2O	N_2
0	46.34	0	39.47	16.79	96.77	52.57	4.16	34.86	30.02	274.3
15	37.17	1.20	42.42	17.68	95.71	46.78	3.55	36.14	43.26	266.8
30	30.37	1.51	42.78	17.89	91.02	44.84	2.22	37.42	46.22	264.5
45	22.64	1.72	44.08	17.74	87.54	40.81	1.75	39.21	45.70	270.8
60						37.04	1.55	40.50	46.38	269.3
75						29.30	1.54	42.54	33.16	252.6
90						24.06	1.47	42.80	33.65	244.4
105						17.61	1.66	45.62	40.39	274.8
120						11.42	1.59	45.11	34.66	265.8
135						4.32	1.76	46.39	46.32	267.6
150						0	1.46	48.95	37.29	262.5
165						0	0	51.77	41.41	265.2
180						0	0	52.03	35.18	274.3

Reproduced with permission of the copyright owner. Further reproduction prohibited without permission.

Table B-1 (Continued) Experimental data for determining the kinetics of nitrate reduction at 30 °C and pH 7.1 ± 0.1. (All concentrations are in mg/L)

Time	Run 13A (V_o = 132 mL) (pH = 7.10 ~ 7.14)					Run 14A (V_o = 132 mL) (pH = 7.17 ~ 7.20)				
(min.)	NO_3^-	NO_2^-	*b*	N_2O	N_2	NO_3^-	NO_2^-	*b*	N_2O	N_2
0	55.50	0	28.45	23.94	369.9	56.62	1.41	36.65	31.91	482.9
15	54.29	0.31	28.45	26.54	377.1	54.55	2.51	36.14	33.80	459.3
30	49.96	0.26	28.96	26.86	477.6	51.71	3.92	37.93	33.76	444.3
45	46.69	0.80	32.04	25.72	346.3	37.56	3.51	38.70	38.58	406.2
60	43.42	1.01	32.55	26.56	291.0	34.22	1.52	40.50	37.70	378.5
75	24.30	1.41	33.32	36.54	325.6	30.65	2.46	41.52	37.86	374.4
90	14.60	1.40	35.11	29.44	387.2	10.26	0	43.83	39.26	361.5
105	0	0	35.63	41.54	361.4	0.55	0	45.37	38.43	344.1
120	0	0	37.68	31.24	381.4	0	0	46.39	34.77	331.1
135										
150										
165										
180										

Time	Run 15A (V_o = 131 mL) (pH = 7.01 ~ 7.08)					Run 16A (V_o = 125 mL) (pH = 7.12 ~ 7.14)				
(min.)	NO_3^-	NO_2^-	*b*	N_2O	N_2	NO_3^-	NO_2^-	*b*	N_2O	N_2
0	58.78	0.96	36.39	29.53	368.3	77.05	1.37	72.28	17.02	559.0
15	55.48	2.55	38.70	34.52	348.6	63.42	3.58	57.15	13.12	515.0
30	47.18	2.71	40.24	48.80	327.0	52.27	2.38	58.95	16.92	486.5
45	41.57	2.92	41.78	55.70	316.1	42.70	2.53	66.38	14.00	460.3
60	33.66	3.45	43.57	51.14	300.4	33.80	2.55	69.20	14.56	446.0
75	24.89	4.12	44.60	56.74	280.6	25.34	0.91	71.76	13.37	433.0
90	14.14	5.36	46.90	47.95	272.4	24.87	1.18	70.23	13.10	397.7
105	10.10	6.71	47.42	54.84	262.1	22.29	0	67.15	11.50	405.7
120	0.91	8.48	49.21	53.72	262.8	21.87	0	72.28	11.06	384.7
135	0	9.89	48.44	49.62	262.5					
150	0	6.59	48.70	55.90	248.5					
165	0	1.58	49.47	42.26	244.8					
180	0	0	49.21	39.40	244.3					

Reproduced with permission of the copyright owner. Further reproduction prohibited without permission.

Table B-1 (Continued) Experimental data for determining the kinetics of nitrate reduction at 30 °C and pH 7.1 ± 0.1. (All concentrations are in mg/L)

Time	Run 17A (V_o = 105 mL) (pH = 7.11 ± 0.00)					Run 18A (V_o = 105 mL) (pH = 7.13 ± 0.00)				
(min.)	NO_3^-	NO_2^-	*b*	N_2O	N_2	NO_3^-	NO_2^-	*b*	N_2O	N_2
0	77.89	0.	46.39	17.51	118.3	85.22	0	46.65	15.67	137.4
15	68.92	2.92	48.44	17.90	112.1	73.44	1.49	48.44	16.51	130.1
30	57.11	5.36	50.75	18.56	107.2	61.72	2.58	49.72	17.00	122.4
45	48.06	7.14	51.52	19.44	110.0	53.13	3.83	51.52	18.73	120.0
60						40.80	4.27	53.05	23.87	119.2
75										
90										
105										
120										
135										
150										
165										
180										

Time	Run 19A (V_o = 105 mL) (pH = 7.12 ± 0.00)					Run 20A (V_o = 134 mL) (pH = 7.14 ~ 7.20)				
(min.)	NO_3^-	NO_2^-	*b*	N_2O	N_2	NO_3^-	NO_2^-	*b*	N_2O	N_2
0	90.91	0	32.81	18.08	121.0	98.83	0.20	46.65	41.76	484.8
15	83.33	2.95	33.83	18.96	121.1	92.03	3.86	47.67	53.08	483.4
30	72.30	5.19	34.60	17.83	121.1	85.59	2.82	49.47	57.72	475.8
45	62.84	7.13	36.91	18.93	108.0	74.78	3.35	50.75	57.81	418.6
60						58.84	3.31	52.54	55.25	476.8
75						37.84	3.54	55.10	46.28	385.9
90						27.45	3.28	55.87	50.01	360.2
105						7.64	1.65	56.13	47.95	353.7
120						2.31	3.45	58.44	65.64	350.1
135						0	0	60.23	50.82	338.7
150						0	0	58.95	50.50	322.9
165						0	0	59.46	48.16	294.8
180						0	0	58.95	49.42	304.7

Reproduced with permission of the copyright owner. Further reproduction prohibited without permission.

Table B-1 (Continued) Experimental data for determining the kinetics of nitrate reduction at 30 °C and pH 7.1 ± 0.1. (All concentrations are in mg/L)

Time	Run 21A (V_o = 105 mL) (pH = 7.11 ~ 7.12)					Run 22A (V_o = 130 mL) (pH = 7.22 ~ 7.25)				
(min.)	NO_3^-	NO_2^-	*b*	N_2O	N_2	NO_3^-	NO_2^-	*b*	N_2O	N_2
0	104.07	0	40.11	16.83	95.51	105.64	0.35	28.45	19.99	145.2
15	93.85	2.22	41.52	17.21	94.29	102.81	0.78	29.47	20.66	143.0
30	85.48	3.86	44.08	18.61	94.30	98.48	1.15	30.24	21.30	136.5
45	75.41	4.93	44.08	18.31	94.30	94.43	1.65	31.27	21.72	126.5
60						89.11	2.16	32.04	21.21	131.3
75						84.79	2.74	32.55	19.40	130.6
90						77.77	3.40	34.34	21.14	122.5
105						71.26	3.75	35.62	22.22	127.3
120						65.86	4.30	36.14	21.88	116.1
135						57.57	5.03	37.16	21.50	126.3
150						53.24	5.94	37.93	21.73	124.1
165						46.28	6.82	38.70	22.81	122.1
180						37.82	7.45	39.98	22.51	127.7

Time	Run 23A (V_o = 105 mL) (pH = 7.10 ~ 7.12)					Run 24A (V_o = 105 mL) (pH = 7.12 ~ 7.13)				
(min.)	NO_3^-	NO_2^-	*b*	N_2O	N_2	NO_3^-	NO_2^-	*b*	N_2O	N_2
0	114.35	0	45.11	19.15	174.7	126.23	0	35.37	17.08	84.77
15	104.88	2.03	46.39	19.64	163.2	112.55	1.61	36.39	16.49	84.77
30	95.36	3.41	49.21	20.26	156.5	105.91	2.75	39.47	17.47	86.33
45	90.11	4.88	48.18	20.99	154.1	97.62	3.30	41.78	19.51	80.98
60										
75										
90										
105										
120										
135										
150										
165										
180										

Reproduced with permission of the copyright owner. Further reproduction prohibited without permission.

Table B-1 (Continued) Experimental data for determining the kinetics of nitrate reduction at 30 °C and pH 7.1 ± 0.1. (All concentrations are in mg/L)

Time	Run 25A (V_o = 125 mL) (pH = 7.17 ~ 7.22)					Run 26A (V_o = 129 mL) (pH = 7.10 ~ 7.14)				
(min.)	NO_3^-	NO_2^-	*b*	N_2O	N_2	NO_3^-	NO_2^-	*b*	N_2O	N_2
0	153.71	0.74	68.69	19.92	425.6	138.48	0	51.26	49.23	520.6
15	128.51	0.40	69.46	54.59	411.4	127.27	2.91	54.85	74.47	493.3
30	120.14	0.49	71.76	60.72	428.7	113.72	2.63	55.10	55.05	468.8
45	111.08	0	74.84	57.46	364.0	102.03	2.20	58.18	56.28	423.2
60	105.39	0	69.20	55.26	319.4	84.73	1.79	58.44	66.20	414.8
75	-	0	72.02	59.62	322.7	71.21	1.72	62.79	73.70	422.4
90	96.82	0	71.76	59.79	305.6	50.30	1.37	67.66	66.84	417.8
105	93.61	0	72.02	54.81	304.1	30.62	1.04	69.71	66.13	381.4
120	93.24	0	72.28	49.80	258.3	15.70	0	73.30	66.66	376.2
135	92.31	0	71.76	58.52	275.9	10.71	0	72.79	66.89	359.9
150	91.79	0	71.25	-	-	6.18	0	72.79	70.11	348.9
165	90.81	0	69.97	57.88	257.4	1.89	0	74.07	69.04	353.1
180	86.75	0	70.23	-	-	0	0	73.30	70.42	326.6

Time	Run 27A (V_o = 133 mL) (pH = 7.18 ~ 7.23)					Run 28A (V_o = 106 mL) (pH = 7.01 ~ 7.03)				
(min.)	NO_3^-	NO_2^-	*b*	N_2O	N_2	NO_3^-	NO_2^-	*b*	N_2O	N_2
0	140.08	0	34.86	44.00	586.6	149.59	0	48.18	16.63	128.0
15	137.97	1.79	35.63	30.72	493.7	147.49	1.01	48.18	17.30	129.9
30	129.59	2.14	36.65	30.74	470.6	142.54	1.33	49.21	17.16	129.9
45	106.87	1.91	38.44	31.43	430.8	134.57	1.35	50.23	18.32	119.6
60	94.34	1.29	39.21	34.02	419.2	128.71	1.24	52.03	17.84	115.8
75	78.79	2.40	40.24	34.09	384.0					
90	63.51	1.24	42.80	36.79	367.4					
105	56.75	1.44	43.31	36.87	345.5					
120	50.09	3.61	43.83	33.46	395.4					
135	27.82	3.34	46.65	42.82	323.7					
150	17.76	3.94	46.65	40.59	312.8					
165										
180										

Reproduced with permission of the copyright owner. Further reproduction prohibited without permission.

Table B-1 (Continued) Experimental data for determining the kinetics of nitrate reduction at 30 °C and pH 7.1 ± 0.1. (All concentrations are in mg/L)

Time	Run 29A (V_o = 135 mL) (pH = 7.06 ~ 7.19)					Run 30A (V_o = 106 mL) (pH = 7.11 ~ 7.12)				
(min.)	NO_3^-	NO_2^-	*b*	N_2O	N_2	NO_3^-	NO_2^-	*b*	N_2O	N_2
0	168.70	0	44.85	54.71	589.8	180.85	0	41.78	19.16	166.3
15	164.82	0	44.08	50.36	553.6	176.43	2.13	42.55	19.85	160.9
30	158.11	0	46.39	50.52	527.2	168.20	3.41	44.08	21.05	164.8
45	143.33	0	47.16	50.52	572.0	163.03	5.42	46.65	21.47	154.6
60	130.16	0	49.47	50.61	575.6					
75	115.51	0	49.47	55.04	543.1					
90	95.63	0	53.05	56.03	520.8					
105	72.89	0	52.54	57.77	519.5					
120	50.80	0	56.13	82.61	524.5					
135	41.50	0	56.90	83.92	500.2					
150	19.08	0	60.74	76.59	491.3					
165	2.40	0	60.49	63.45	443.0					
180	0	0	62.79	66.37	451.8					

Time	Run 31A (V_o = 106 mL) (pH = 7.13 ~ 7.14)					Run 32A (V_o = 106 mL) (pH = 7.10 ~ 7.14)				
(min.)	NO_3^-	NO_2^-	*b*	N_2O	N_2	NO_3^-	NO_2^-	*b*	N_2O	N_2
0	191.63	0	47.93	23.86	360.6	231.46	3.89	21.79	12.20	114.0
15	181.17	2.85	48.70	25.28	342.9	229.92	4.11	22.04	13.15	114.9
30	175.12	4.40	49.47	25.46	325.6	219.91	4.18	22.81	13.08	111.3
45	162.29	5.80	50.23	26.91	304.6	216.60	4.63	23.07	13.37	107.0
60	156.26	7.30	51.52	29.40	284.8	214.90	4.99	23.58	13.41	99.66
75						210.17	5.23	24.60	13.48	100.7
90						206.25	5.65	24.60	13.68	103.2
105						204.47	6.48	24.60	13.17	101.4
120						202.19	6.89	25.37	13.00	93.81
135						201.04	7.39	26.14	13.33	94.89
150						197.39	8.24	26.66	13.82	96.44
165						193.02	8.76	27.17	13.42	93.42
180						188.55	9.51	27.42	13.55	90.34

Reproduced with permission of the copyright owner. Further reproduction prohibited without permission.

Table B-2 Experimental data for determining the kinetics of nitrite reduction at 30 °C and pH 7.1 ± 0.1. (All concentrations are in mg/L)

Time	Run 1B (V_o = 129 mL) (pH = 7.12 ~ 7.15)					Run 2B (V_o = 129 mL) (pH = 7.11 ~ 7.13)				
(min.)	NO_3^-	NO_2^-	*b*	N_2O	N_2	NO_3^-	NO_2^-	*b*	N_2O	N_2
0	0	8.61	34.34	26.26	159.0	0	9.66	38.44	30.20	304.8
15	0	6.47	34.86	28.08	151.1	0	5.11	37.93	30.62	279.7
30	0	1.14	35.63	22.37	142.0	0	3.12	38.44	27.54	269.6
45	0	0.34	35.88	18.33	137.0	0	0	38.70	26.01	241.0
60	0	0	35.88	16.83	135.8	0	0	39.21	28.91	235.7
75	0	0	35.11	19.17	126.8	0	0	39.21	21.37	195.2
90	0	0	35.88	18.16	121.8	0	0	38.96	23.53	187.0
105						0	0	39.21	18.88	205.7
120						0	0	39.21	19.29	200.0
135										
150										
165										
180										

Time	Run 3B (V_o = 104 mL) (pH = 7.12 ~ 7.13)					Run 4B (V_o = 129 mL) (pH = 7.21 ~ 7.23)				
(min.)	NO_3^-	NO_2^-	*b*	N_2O	N_2	NO_3^-	NO_2^-	*b*	N_2O	N_2
0	0	10.09	47.67	19.16	123.1	0	18.58	40.75	24.59	389.7
15	0	4.48	48.18	19.27	111.0	0	15.03	41.26	38.42	386.3
30	0	0	49.47	18.94	98.33	0	9.21	42.80	41.50	382.6
45	0	0	48.95	20.11	132.7	0	5.02	42.55	50.80	356.6
60						0	2.69	45.62	54.87	340.9
75						0	2.52	45.62	40.16	348.8
90						0	1.96	44.85	40.16	331.1
105						0	0	46.65	51.76	291.6
120										
135										
150										
165										
180										

Reproduced with permission of the copyright owner. Further reproduction prohibited without permission.

Table B-2 (Continued) Experimental data for determining the kinetics of nitrite reduction at 30 °C and pH 7.1 ± 0.1. (All concentrations are in mg/L)

Time	Run 5B (V_o = 132 mL) (pH = 7.11 ~ 7.15)					Run 6B (V_o = 132 mL) (pH = 7.17 ~ 7.19)				
(min.)	NO_3^-	NO_2^-	*b*	N_2O	N_2	NO_3^-	NO_2^-	*b*	N_2O	N_2
0	0	19.93	36.39	30.86	476.7	0	37.89	35.11	44.37	721.7
15	0	16.84	33.83	34.92	462.9	0	30.26	35.37	29.89	670.8
30	0	14.13	33.83	42.32	521.1	0	19.53	36.39	33.28	682.2
45	0	6.69	34.60	26.59	522.5	0	8.50	37.68	31.57	678.6
60	0	2.70	36.39	34.16	410.4	0	0	38.70	29.98	523.6
75	0	0	37.42	27.92	466.9	0	0	38.70	36.15	562.3
90	0	0	37.42	30.75	371.0	0	0	39.21	30.43	445.2
105	0	0	37.42	27.87	433.9	0	0	38.70	29.34	415.2
120	0	0	37.93	32.12	407.5	0	0	38.70	28.91	393.8
135	0	0	37.93	37.43	425.6					
150	0	0	37.42	30.73	379.5					
165	0	0	37.42	31.07	302.2					
180	0	0	37.42	27.17	363.8					

Time	Run 7B (V_o = 132 mL) (pH = 7.18 ~ 7.23)					Run 8B (V_o = 132 mL) (pH = 7.18 ~ 7.24)				
(min.)	NO_3^-	NO_2^-	*b*	N_2O	N_2	NO_3^-	NO_2^-	*b*	N_2O	N_2
0	0	29.85	48.44	31.94	447.0	0	32.56	30.76	18.54	1613
15	0	29.27	46.65	27.21	365.5	0	21.65	31.27	20.51	1619
30	0	27.32	47.93	42.33	348.9	0	16.70	32.81	44.69	1541
45	0	19.49	49.98	43.12	347.2	0	10.97	33.32	53.54	1417
60	0	7.06	50.23	36.70	350.3	0	11.01	34.34	22.48	1306
75	0	2.18	51.52	40.77	334.6	0	0	35.88	20.39	1108
90	0	0	55.10	27.98	307.2	0	0	36.39	21.45	1155
105	0	0	54.08	34.65	295.9	0	0	36.91	24.75	1034
120	0	0	54.59	43.75	284.2	0	0	36.39	26.09	991.9
135						0	0	36.39	25.39	951.7
150						0	0	36.14	34.97	948.1
165						0	0	36.39	28.86	838.7
180						0	0	37.42	28.82	886.8

Reproduced with permission of the copyright owner. Further reproduction prohibited without permission.

Table B-2 (Continued) Experimental data for determining the kinetics of nitrite reduction at 30 °C and pH 7.1 ± 0.1. (All concentrations are in mg/L)

Time	Run 9B (V_o = 133 mL) (pH = 7.14 ~ 7.18)					Run 10B (V_o = 130 mL) (pH = 6.98 ~ 7.02)				
(min.)	NO_3^-	NO_2^-	*b*	N_2O	N_2	NO_3^-	NO_2^-	*b*	N_2O	N_2
0	0	35.71	55.36	20.85	139.0	0	-	41.52	18.41	350.7
15	0	30.52	57.92	26.24	135.8	0	35.11	40.24	17.95	280.5
30	0	19.73	59.46	26.45	130.2	0	26.06	42.55	22.96	280.0
45	0	13.41	62.28	25.32	125.0	0	19.04	43.57	19.08	260.3
60	0	8.90	63.05	25.26	120.9	0	11.97	45.62	18.48	248.2
75	0	1.92	64.33	24.98	-	0	5.22	46.90	19.58	235.1
90	0	0	65.61	23.76	117.3	0	0	46.90	29.69	229.2
105	0	0	66.38	24.52	112.7	0	0	48.18	20.24	224.3
120	0	0	64.84	24.82	106.9	0	0	49.21	20.04	260.0
135										
150										
165										
180										

Time	Run 11B (V_o = 132 mL) (pH = 7.17 ~ 7.21)					Run 12B (V_o = 132 mL) (pH = 7.17 ~ 7.22)				
(min.)	NO_3^-	NO_2^-	*b*	N_2O	N_2	NO_3^-	NO_2^-	*b*	N_2O	N_2
0	0	39.90	46.65	27.36	351.3	0	40.29	48.18	34.20	501.5
15	0	36.80	47.42	29.21	359.0	0	40.25	45.62	27.21	384.8
30	0	29.05	49.47	39.00	416.6	0	29.89	47.16	32.69	393.3
45	0	19.36	51.77	37.38	329.9	0	24.70	49.98	46.43	355.8
60	0	11.54	53.82	30.43	323.4	0	9.52	52.80	39.55	369.9
75	0	5.70	55.36	28.34	294.8	0	2.16	49.98	30.29	352.2
90	0	1.05	58.18	33.15	296.2	0	2.13	52.03	30.29	339.3
105	0	0	57.67	39.61	279.4	0	0	52.80	32.14	325.0
120	0	0	56.90	29.82	262.2	0	0	53.82	35.58	306.2
135										
150										
165										
180										

Reproduced with permission of the copyright owner. Further reproduction prohibited without permission.

Table B-2 (Continued) Experimental data for determining the kinetics of nitrite reduction at 30 °C and pH 7.1 ± 0.1. (All concentrations are in mg/L)

Time	Run **13B** (V_o = 131 mL) (pH = 7.15 ~ 7.20)					Run **14B** (V_o = 105 mL) (pH = 7.13 ~ 7.15)				
(min.)	NO_3^-	NO_2^-	*b*	N_2O	N_2	NO_3^-	NO_2^-	*b*	N_2O	N_2
0	0	41.56	31.01	13.05	135.3	0	51.78	40.50	15.48	67.96
15	0	36.25	32.29	14.55	143.3	0	43.88	52.54	16.08	67.57
30	0	30.97	33.32	15.04	130.3	0	35.44	44.08	16.85	71.16
45	0	25.76	34.86	14.25	122.9	0	24.72	44.60	16.62	71.49
60	0	20.53	35.62	14.08	120.4					
75	0	15.50	36.91	15.58	114.4					
90	0	9.13	38.19	16.29	119.5					
105	0	3.12	38.70	16.96	118.1					
120	0	0	37.68	15.62	117.3					
135										
150										
165										
180										

Time	Run **15B** (V_o = 105 mL) (pH = 7.12 ~ 7.14)					Run **16B** (V_o = 107 mL) (pH = 7.14 ~ 7.19)				
(min.)	NO_3^-	NO_2^-	*b*	N_2O	N_2	NO_3^-	NO_2^-	*b*	N_2O	N_2
0	0	52.26	46.65	18.00	107.2	0	52.88	51.52	17.95	116.0
15	0	42.62	46.65	17.77	99.42	0	46.02	51.52	17.50	110.6
30	0	33.60	48.95	16.84	100.5	0	38.64	51.77	18.81	111.3
45	0	21.68	49.47	18.65	100.2	0	32.20	54.08	21.61	106.5
60	0	12.35	49.21	18.84	100.8	0	23.44	55.36	20.43	106.0
75						0	16.60	55.87	20.87	-
90						0	8.32	56.39	20.72	-
105						0	0	56.90	20.49	117.3
120						0	0	56.90	19.88	98.24
135						0	0	57.67	20.21	97.85
150										
165										
180										

Reproduced with permission of the copyright owner. Further reproduction prohibited without permission.

Table B-2 (Continued) Experimental data for determining the kinetics of nitrite reduction at 30 °C and pH 7.1 ± 0.1. (All concentrations are in mg/L)

Time	Run **17B** (V_o = 131 mL) (pH = 7.15 ~ 7.19)					Run **18B** (V_o = 132 mL) (pH = 7.18 ~ 7.24)				
(min.)	NO_3^-	NO_2^-	*b*	N_2O	N_2	NO_3^-	NO_2^-	*b*	N_2O	N_2
0	0	64.22	31.01	13.84	136.2	0	69.79	48.70	33.25	345.2
15	0	58.92	33.58	14.65	139.8	0	62.94	48.95	30.21	336.0
30	0	52.40	33.32	14.41	124.7	0	54.59	51.52	35.94	334.8
45	0	49.50	34.60	15.45	128.3	0	46.77	52.54	28.24	314.2
60	0	43.34	36.65	14.90	131.3	0	33.36	54.08	28.15	301.0
75	0	39.91	37.42	16.29	120.7	0	26.32	55.62	46.35	273.7
90	0	29.67	38.19	15.49	124.9	0	18.68	59.97	285.4	280.9
105	0	24.33	38.19	15.46	131.7	0	3.70	59.20	39.16	264.7
120	0	12.14	40.50	15.66	120.3	0	2.05	62.79	30.73	264.4
135						0	0	62.79	39.67	273.7
150						0	0	61.51	42.50	261.4
165						0	0	61.77	30.21	240.8
180						0	0	60.74	39.45	231.1

Time	Run **19B** (V_o = 131 mL) (pH = 7.18 ~ 7.25)					Run **20B** (V_o = 107 mL) (pH = 7.15 ~ 7.23)				
(min.)	NO_3^-	NO_2^-	*b*	N_2O	N_2	NO_3^-	NO_2^-	*b*	N_2O	N_2
0	0	75.00	43.57	24.04	311.4	0	75.56	52.54	18.62	107.6
15	0	73.23	44.60	24.46	307.1	0	68.48	54.34	19.18	110.6
30	0	60.03	43.57	24.46	308.0	0	60.26	56.13	21.44	108.3
45	0	49.34	45.88	35.42	306.6	0	54.28	58.18	19.96	93.64
60	0	30.53	47.42	43.05	291.9	0	48.87	62.28	18.16	101.8
75	0	26.59	49.47	24.94	281.9	0	36.21	61.77	19.65	95.73
90	0	17.20	51.00	31.57	291.9	0	25.40	62.02	20.45	99.18
105	0	-	-	-	-	0	15.82	62.79	19.60	97.63
120	0	0	55.62	28.07	274.4	0	5.37	67.15	20.53	94.86
135	0	0	55.62	40.56	299.5	0	0	66.64	20.62	100.6
150	0	0	56.39	28.05	256.7	0	0	65.87	21.21	95.90
165	0	0	56.39	34.94	247.9	0	0	66.64	20.00	96.29
180	0	0	56.13	34.94	236.9	0	0	66.12	21.50	97.25

Reproduced with permission of the copyright owner. Further reproduction prohibited without permission.

Table B-2 (Continued) Experimental data for determining the kinetics of nitrite reduction at 30 °C and pH 7.1 ± 0.1. (All concentrations are in mg/L)

Time	Run **21B** (V_o = 105 mL) (pH = 7.11 ~ 7.13)					Run **22B** (V_o = 105 mL) (pH = 7.12 ~ 7.14)				
(min.)	NO_3^-	NO_2^-	*b*	N_2O	N_2	NO_3^-	NO_2^-	*b*	N_2O	N_2
0	0	91.49	39.73	16.75	132.3	0	86.04	42.29	16.52	220.6
15	0	87.70	40.50	18.03	127.4	0	79.74	43.83	16.56	225.9
30	0	82.96	42.03	15.93	130.0	0	74.58	45.62	16.47	211.2
45	0	70.87	41.52	15.90	109.5	0	68.69	45.36	16.55	233.9
60	0	65.45	43.83	15.96	107.5	0	61.12	77.93	17.66	210.0
75										
90										
105										
120										
135										
150										
165										
180										

Time	Run **23B** (V_o = 135 mL) (pH = 7.09 ~ 7.13)					Run **24B** (V_o = 133 mL) (pH = 7.11 ~ 7.14)				
(min.)	NO_3^-	NO_2^-	*b*	N_2O	N_2	NO_3^-	NO_2^-	*b*	N_2O	N_2
0	0	91.41	42.80	16.05	100.8	0	102.25	42.03	9.30	67.56
15	0	88.17	42.80	17.53	-	0	94.44	43.57	11.30	84.94
30	0	85.29	44.60	-	81.51	0	87.49	44.85	12.16	-
45	0	78.65	45.88	15.97	74.86	0	80.69	45.88	13.00	-
60	0	74.29	47.16	15.58	84.04	0	75.19	46.13	13.09	106.9
75	0	72.10	47.93	15.94	95.65	0	67.83	47.42	15.66	102.8
90	0	61.78	49.47	17.37	77.60	0	62.70	47.67	16.45	106.0
105	0	56.44	50.23	17.83	83.70	0	58.00	47.93	19.33	108.1
120	0	46.96	52.29	16.99	82.68	0	52.88	49.21	15.93	143.1
135						0	48.22	50.23	19.73	121.7
150						0	38.67	52.03	19.15	116.7
165						0	26.70	52.80	23.92	120.6
180						0	22.42	53.57	24.02	117.2

Reproduced with permission of the copyright owner. Further reproduction prohibited without permission.

Table B-2 (Continued) Experimental data for determining the kinetics of nitrite reduction at 30 °C and pH 7.1 ± 0.1. (All concentrations are in mg/L)

Time	Run 25B (V_o = 105 mL) (pH = 7.14 ~ 7.25)					Run 26B (V_o = 131 mL) (pH = 6.97 ~ 7.06)				
(min.)	NO_3^-	NO_2^-	*b*	N_2O	N_2	NO_3^-	NO_2^-	*b*	N_2O	N_2
0	0	102.49	47.42	-	121.6	0	104.96	36.39	25.64	370.1
15	0	97.51	47.16	13.73	100.9	0	101.32	37.42	24.83	363.3
30	0	92.38	47.16	14.12	101.3	0	98.52	38.70	23.46	373.3
45	0	83.22	48.44	15.10	102.5	0	92.72	39.98	21.38	338.7
60	0	75.75	48.18	15.19	98.55	0	87.92	40.24	-	306.2
75	0	67.18	48.44	16.26	100.6	0	82.43	41.01	30.46	314.1
90	0	61.87	48.44	18.13	95.89	0	76.73	42.03	23.40	272.6
105	0	52.74	48.95	17.25	94.85	0	65.58	43.31	24.40	278.4
120	0	42.64	49.98	16.59	94.66	0	58.10	44.34	24.00	264.9
135	0	33.95	53.57	17.42	96.61	0	52.98	46.39	37.76	284.0
150	0	26.28	51.77	17.54	97.13	0	47.43	46.90	36.23	278.3
165	0	17.69	52.80	17.48	94.58	0	33.57	47.67	26.81	254.5
180	0	7.78	52.29	18.07	97.51	0	28.19	48.70	36.19	254.2

Time	Run 27B (V_o = 106 mL) (pH = 7.12 ~ 7.13)					Run 28B (V_o = 131 mL) (pH = 7.15 ~ 7.18)				
(min.)	NO_3^-	NO_2^-	*b*	N_2O	N_2	NO_3^-	NO_2^-	*b*	N_2O	N_2
0	0	114.06	50.49	17.11	140.1	0	115.21	29.73	21.72	349.4
15	0	111.74	51.77	17.37	139.8	0	112.34	30.76	22.53	264.4
30	0	104.82	51.77	18.48	137.8	0	108.46	30.50	22.12	230.3
45	0	95.21	54.59	19.22	131.3	0	105.69	30.76	23.15	276.2
60						0	95.05	32.29	-	267.0
75						0	92.71	32.55	23.43	257.3
90						0	87.62	32.81	-	241.6
105						0	84.92	33.06	22.48	228.2
120						0	74.76	34.60	-	237.8
135										
150										
165										
180										

Reproduced with permission of the copyright owner. Further reproduction prohibited without permission.

Table B-2 (Continued) Experimental data for determining the kinetics of nitrite reduction at 30 °C and pH 7.1 ± 0.1. (All concentrations are in mg/L)

Time	Run **29B** (V_o = 106 mL) (pH = 7.09 ~ 7.12)					Run **30B** (V_o = 134 mL) (pH = 7.11 ~ 7.15)				
(min.)	NO_3^-	NO_2^-	*b*	N_2O	N_2	NO_3^-	NO_2^-	*b*	N_2O	N_2
0	0	131.12	53.82	20.90	227.6	0	141.63	38.44	-	-
15	0	123.11	53.57	21.14	214.1	0	138.95	39.21	-	-
30	0	112.85	55.10	21.81	209.0	0	133.12	40.50	-	-
45	0	104.90	56.13	22.76	201.7	0	131.37	41.01	-	-
60						0	128.50	42.03	-	-
75						0	126.00	42.03	-	-
90						0	121.33	42.80	-	-
105						0	106.61	44.34	-	-
120						0	96.49	45.88	-	-
135										
150						* N_2O, N_2 measurements were not				
165						made for this run.				
180										

Time	Run **31B** (V_o = 106 mL) (pH = 7.14 ~ 7.22)					Run **32B** (V_o = 132 mL) (pH = 6.99 ~ 7.05)				
(min.)	NO_3^-	NO_2^-	*b*	N_2O	N_2	NO_3^-	NO_2^-	*b*	N_2O	N_2
0	0	145.43	44.34	17.89	129.9	0	146.49	41.26	20.29	331.1
15	0	141.76	45.37	19.30	126.8	0	140.22	42.03	20.64	332.4
30	0	130.70	46.65	19.63	119.3	0	130.67	42.03	19.51	343.6
45	0	129.77	48.18	-	125.2	0	120.19	43.83	20.93	316.4
60	0	116.15	49.47	20.69	119.8	0	110.83	44.85	19.77	296.1
75	0	106.86	51.26	19.98	-	0	102.27	45.62	32.56	295.7
90	0	96.51	51.77	19.87	116.0	0	93.62	46.65	31.79	306.6
105	0	86.30	53.82	19.58	107.7	0	82.14	49.47	30.03	292.7
120	0	76.26	54.59	20.52	-	0	78.50	47.93	25.68	270.1
135	0	65.51	57.41	20.49	85.85	0	62.33	51.00	24.59	259.5
150	0	54.19	57.92	20.51	108.2	0	59.39	51.26	25.41	251.2
165	0	44.17	58.69	21.98	111.4	0	57.01	52.54	26.38	249.7
180	0	32.63	60.23	21.75	111.8	0	48.01	52.29	26.66	238.5

Reproduced with permission of the copyright owner. Further reproduction prohibited without permission.

Table B-2 (Continued) Experimental data for determining the kinetics of nitrite reduction at 30 °C and pH 7.1 ± 0.1. (All concentrations are in mg/L)

Time	Run 33B (V_o = 106 mL) (pH = 7.12 ~ 7.14)					Run 34B (V_o = 107 mL) (pH = 7.13 ~ 7.15)				
(min.)	NO_3^-	NO_2^-	*b*	N_2O	N_2	NO_3^-	NO_2^-	*b*	N_2O	N_2
0	0	156.52	45.11	16.26	94.16	0	169.76	33.83	15.50	68.96
15	0	150.74	45.88	16.18	97.26	0	160.93	34.34	15.87	67.50
30	0	144.22	47.16	17.14	90.96	0	153.57	34.86	16.64	79.98
45	0	131.37	50.75	17.60	103.7	0	148.57	35.88	16.69	70.51
60										
75										
90										
105										
120										
135										
150										
165										
180										

Time	Run 35B (V_o = 131 mL) (pH = 7.13 ~ 7.15)					Run 36B (V_o = 107 mL) (pH = 7.09 ~ 7.11)				
(min.)	NO_3^-	NO_2^-	*b*	N_2O	N_2	NO_3^-	NO_2^-	*b*	N_2O	N_2
0	0	187.92	36.65	15.79	101.5	0	230.19	26.91	8.01	87.54
15	0	182.84	37.42	16.26	109.5	0	226.37	27.17	7.80	82.45
30	0	181.31	37.68	16.55	110.3	0	226.13	28.19	7.62	86.19
45	0	169.21	38.44	16.42	104.2	0	223.97	28.19	7.38	82.08
60	0	152.26	40.75	15.24	105.2	0	223.62	27.94	7.50	79.01
75	0	135.85	41.26	16.30	103.6	0	223.06	27.68	7.60	74.33
90	0	119.36	42.55	16.31	98.22	0	221.65	27.94	-	88.92
105	0	108.00	43.57	16.21	100.5	0	220.80	27.42	7.27	72.89
120	0	98.25	44.34	15.39	96.60	0	220.71	27.42	6.53	82.94
135										
150										
165										
180										

Reproduced with permission of the copyright owner. Further reproduction prohibited without permission.

Table B-3 Net specific growth rates and apparent yield coefficients of biomass on nitrate at T = 30 °C and pH = 7.1 ± 0.1. Data used in Figures 3 and 5.

Experimental Run	Initial nitrate concentration (mg/L)	Net specific growth rate, μ_{1net} (h^{-1})	Apparent yield coefficient, $Y_{1app.}$ (g biomass/g nitrate)
1A	6.90	0.037587	0.12006
2A	6.96	0.025992	0.09365
3A	9.16	0.063497	0.15567
4A	10.28	0.059426	0.16972
5A	14.09	0.069754	0.16595
6A	17.20	0.105700	0.19490
7A	21.76	0.108134	0.21300
8A	31.11	0.152641	0.20894
9A	32.07	0.149323	0.18604
10A	44.13	0.154594	0.21488
11A	46.34	0.148988	0.21429
12A	52.57	0.146239	0.22566
13A	54.29	0.143144	0.24815
14A	54.55	0.144629	0.21676
15A	55.48	0.149886	0.22849
16A	77.05	0.122112	0.20037
17A	77.89	0.138392	0.21057
18A	89.94	0.129602	0.21800
19A	90.91	0.129882	0.20415
20A	98.83	0.109623	0.21481
21A	104.07	0.125402	0.21974
22A	108.64	0.118662	0.21568
23A	114.35	0.112052	0.21770
24A	126.23	0.099853	0.18427
25A	128.51	0.101797	0.19940
26A	138.48	0.109695	0.19512
27A	140.08	0.086344	0.18522
28A	149.59	0.088163	0.20808
29A	168.70	0.078012	0.18380
30A	180.85	0.072950	0.17602
31A	191.63	0.063662	0.17025
32A	231.46	0.046784	0.13418

Reproduced with permission of the copyright owner. Further reproduction prohibited without permission.

Table B-4 Net specific growth rates and apparent yield coefficients of biomass on nitrite at T = 30 °C and pH = 7.1 ± 0.1. Data used in Figures 4 and 6.

Experimental Run	Initial nitrite concentration (mg/L)	Net specific growth rate, μ_{2net} (h^{-1})	Apparent yield coefficient, $Y_{2app.}$ (g biomass/g nitrite)
1B	8.61	0.061290	0.17563
2B	5.11	0.040135	0.14588
3B	10.09	0.058334	0.17560
4B	15.03	0.105819	0.22555
5B	16.84	0.088903	0.22019
6B	30.26	0.089554	0.18905
7B	29.27	0.107559	0.21452
8B	32.56	0.122024	0.23543
9B	35.71	0.153594	0.24175
10B	35.11	0.169798	0.24343
11B	36.80	0.175823	0.24935
12B	40.25	0.182432	0.24239
13B	41.56	0.176821	0.24879
14B	51.78	0.169408	0.26157
15B	52.26	0.155217	0.22909
16B	38.64	0.174614	0.24865
17B	64.22	0.143488	0.23783
18B	69.79	0.112561	0.22512
19B	60.03	0.154150	0.21969
20B	75.56	0.135322	0.23592
21B	91.49	0.088551	0.19531
22B	86.04	0.130294	0.23012
23B	88.17	0.138783	0.23288
24B	102.25	0.116618	0.20711
25B	102.49	0.154150	0.21969
26B	104.96	0.126304	0.23622
27B	114.06	0.099603	0.22030
28B	108.46	0.061895	0.16870
29B	131.12	0.093475	0.20140
30B	141.63	0.090309	0.19840
31B	145.43	0.086910	0.19842
32B	146.49	0.080810	0.18249
33B	150.74	0.083461	0.19808
34B	169.76	0.068818	0.09067
35B	187.92	0.055175	0.17039
36B	230.19	0.043455	0.15892

Reproduced with permission of the copyright owner. Further reproduction prohibited without permission.

Table B-5 Data from small scale experiments involving reduction of nitrate/nitrite mixtures at pH = 7.1 ± 0.1. (All concentrations are in mg/L)

	Run 1G (V_o = 131 mL) (pH = 7.20 - 7.26) T = 30 °C					Run 2G (V_o = 106 mL) (pH = 7.14 - 7.25) T = 30 °C				
Time (min.)	NO_3^-	NO_2^-	*b*	N_2O	N_2	NO_3^-	NO_2^-	*b*	N_2O	N_2
0	49.24	104.51	29.99	17.94	149.5	101.6	44.71	40.75	17.49	123.3
15	44.66	104.32	30.50	18.61	147.1	98.16	45.73	42.55	18.14	116.6
30	39.94	107.02	31.52	18.86	141.7	89.05	47.22	43.83	18.11	113.0
45	35.10	105.91	31.78	19.17	136.5	87.05	49.47	45.37	18.11	104.9
60	30.18	106.70	32.55	19.58	129.2	77.02	51.16	46.39	17.82	101.2
75	25.27	106.79	33.83	21.06	129.8	73.96	54.48	47.42	19.04	95.44
90	20.47	106.72	34.60	20.61	125.6	64.86	56.35	48.44	19.32	93.39
105	15.94	107.27	36.14	20.68	120.6	54.67	58.73	49.47	19.37	90.56
120	11.84	107.78	35.88	21.34	117.3	45.93	61.33	49.98	19.35	85.85
135	8.36	107.47	37.68	22.46	123.0	36.39	61.38	50.49	20.12	85.85
150	5.60	107.35	37.93	21.08	117.2	26.35	62.45	51.52	20.53	84.23
165	3.58	104.87	38.19	20.55	117.6	16.52	64.16	54.08	21.30	82.86
180	2.20	101.66	39.21	22.76	117.1	7.53	67.27	55.87	22.47	77.50
195	1.30	95.23	39.47	23.19	116.4	1.15	63.38	56.39	21.99	77.50
210	0.75	91.72	39.72	23.74	117.5	0	57.25	57.92	22.55	81.17
225	0.43	85.21	42.55	23.06	117.4	0	47.94	60.49	23.21	86.41
240	0.24	75.00	42.80	24.06	121.5	0	38.47	61.00	23.21	86.84

Reproduced with permission of the copyright owner. Further reproduction prohibited without permission.

Table B-5 (Continued) Data from small scale experiments involving reduction of nitrate/nitrite mixtures at pH = 7.1 ± 0.1. (All concentrations are in mg/L)

Time	Run 3G (V_o = 105 mL) (pH = 7.17 - 7.26) T = 30 °C					Run 4G (V_o = 105 mL) (pH = 7.18 - 7.25) T = 30 °C				
(min.)	NO_3^-	NO_2^-	*b*	N_2O	N_2	NO_3^-	NO_2^-	*b*	N_2O	N_2
0	107.2	11.12	42.54	18.18	114.9	108.7	4.85	43.31	19.70	142.3
15	99.58	10.24	44.34	18.39	109.6	101.4	3.76	44.08	18.93	130.6
30	92.72	8.69	47.16	18.56	111.8	92.39	2.29	46.65	19.79	126.2
45	85.73	6.79	47.67	19.37	109.5	88.76	1.18	47.42	20.97	124.8
60	78.68	5.34	48.44	20.02	107.6	80.38	0.92	49.98	20.38	117.2
75	72.74	4.12	50.23	20.68	94.13	79.15	1.17	51.52	21.19	117.7
90	66.38	3.36	53.31	21.11	94.13	66.16	0.95	53.05	21.69	116.0
105	57.92	2.63	54.08	22.07	100.0	58.96	1.16	54.59	22.78	113.1
120	48.28	2.32	56.39	22.45	100.0	46.22	1.05	55.36	24.02	113.1
135	39.22	2.29	59.72	22.34	100.2	35.82	1.31	56.64	23.97	112.5
150	28.60	2.25	60.49	24.41	96.89	29.64	1.49	58.18	25.59	112.1
165	17.71	2.35	61.26	24.21	96.89	19.19	1.43	59.20	27.47	109.1
180	6.92	2.20	64.08	24.67	93.55	8.35	1.44	60.23	26.37	109.7
195	0	0.26	64.33	24.32	95.67	0	0.79	63.05	27.75	111.2
210	0	0	66.12	24.77	96.34	0	0	65.10	28.10	105.6
225	0	0	67.41	25.74	92.53	0	0	64.59	28.99	107.8
240	0	0	70.23	24.81	90.95	0	0	64.84	27.83	108.4

Reproduced with permission of the copyright owner. Further reproduction prohibited without permission.

Table B-5 (Continued) Data from small scale experiments involving reduction of nitrate/nitrite mixtures at pH = 7.1 ± 0.1. (All concentrations are in mg/L)

Time	Run 5G (V_o = 108 mL) (pH = 7.03 - 7.13) T = 37 °C					Run 6G (V_o = 108 mL) (pH = 7.04 - 7.17) T = 38 °C				
(min.)	NO_3^-	NO_2^-	*b*	N_2O	N_2	NO_3^-	NO_2^-	*b*	N_2O	N_2
0	105.5	53.49	62.02	18.78	258.8	105.1	41.76	70.74	28.10	256.4
15	96.37	51.91	65.87	13.36	246.5	95.34	42.25	73.04	29.63	234.6
30	88.85	49.31	67.66	23.81	239.5	89.12	40.44	74.58	28.45	231.0
45	79.42	46.92	70.23	28.35	223.4	82.78	36.09	74.84	29.56	225.8
60	67.97	43.94	71.76	26.98	211.9	77.41	38.22	73.56	29.17	201.4
75	54.76	40.12	75.61	27.70	204.1	70.50	37.98	75.61	29.88	201.6
90	43.06	36.90	79.20	30.42	199.9	61.30	36.43	77.92	30.59	190.5
105	29.25	33.77	82.53	31.04	192.4	52.30	35.95	78.43	30.98	187.6
120	16.78	29.50	87.89	34.03	194.6	41.90	34.57	80.99	32.02	181.9
135	4.98	22.61	95.55	34.69	182.1	32.28	32.41	83.30	37.80	181.9
150	0	11.97	98.62	33.20	180.6	12.88	29.17	85.09	37.10	182.4
165	0	0	102.0	35.25	180.9	10.35	25.90	88.42	36.45	185.1
180	0	0	101.4	35.67	179.7	2.07	22.56	88.42	37.82	191.8
195						0	14.50	89.96	35.48	194.2
210						0	2.93	91.24	38.87	194.2
225						0	0	95.09	36.06	194.2
240						0	0	95.34	34.13	194.2

Reproduced with permission of the copyright owner. Further reproduction prohibited without permission.

Table B-5 (Continued) Data from small scale experiments involving reduction of nitrate/nitrite mixtures at pH = 7.1 ± 0.1. (All concentrations are in mg/L)

	Run 7G (V_o = 131 mL) (pH = 7.20 - 7.26) T = 30 °C				
Time (min.)	NO_3^-	NO_2^-	*b*	N_2O	N_2
0	101.06	54.38	31.27	17.25	158.82
15	97.51	54.36	32.04	17.92	155.11
30	93.55	54.76	32.81	18.82	149.47
45	89.07	54.76	33.58	18.63	150.78
60	82.53	54.63	34.09	18.24	143.63
75	77.83	55.96	35.37	19.04	141.02
90	72.69	57.18	36.39	20.16	147.66
105	65.96	57.69	37.16	20.27	140.09
120	59.53	59.25	37.93	20.60	140.71
135	53.35	61.99	38.96	21.76	143.84
150	44.21	62.03	40.24	20.71	139.47
165	36.85	64.47	41.01	22.63	143.64
180	28.18	64.24	42.03	23.21	145.67
195	19.87	65.83	43.31	22.70	145.22
210	13.18	65.53	43.06	23.59	137.69
225	5.87	66.10	44.34	25.46	145.65
240	1.86	64.19	45.88	25.57	151.32

Reproduced with permission of the copyright owner. Further reproduction prohibited without permission.

Reproduced with permission of the copyright owner. Further reproduction prohibited without permission.

Table B-6 Detailed determination of the atomic nitrogen balance for run 22A.

column	a	b	c	d	d1	e	e1	f	g	h	i	j	k	ℓ	ℓ1	m	m1	n
Time (min.)	NO_3^- (mg/L)	NO_2^- (mg/L)	*b* (mg/L)	N_2O,g (mg/L)	N_2O,ℓ (mg/L)	N_2,g (mg/L)	N_2,ℓ (mg/L)	O_2,g (mg/L)	V_ℓ (L)	V_g (L)	NO_3^- (mg)	NO_2^- (mg)	*b* (mg)	N_2O,g (mg)	N_2O,ℓ (mg)	N_2,g (mg)	N_2,ℓ (mg)	O_2 (mg)
0	105.64	0.35	28.45	19.99	10.833	145.2	2.171	14.22	0.130	0.030	13.733	0.046	3.698	0.600	1.408	4.356	0.282	0.427
15	102.81	0.78	29.47	20.66	11.196	143.0	2.139	15.08	0.126	0.034	12.954	0.098	3.714	0.702	1.411	4.862	0.269	0.513
30	98.48	1.15	30.24	21.30	11.543	136.5	2.041	13.94	0.122	0.038	12.014	0.140	3.690	0.809	1.408	5.187	0.249	0.530
45	94.43	1.65	31.27	21.72	11.770	126.5	1.892	12.99	0.118	0.042	11.143	0.192	3.690	0.912	1.389	5.313	0.223	0.546
60	89.11	2.16	32.04	21.21	11.494	131.3	1.964	15.37	0.114	0.046	10.159	0.246	3.652	0.976	1.310	6.040	0.224	0.707
75	84.79	2.74	32.55	21.18	11.478	130.6	1.953	17.00	0.110	0.050	9.327	0.301	3.581	1.059	1.263	6.530	0.215	0.850
90	77.77	3.40	34.34	21.14	11.456	122.5	1.832	14.58	0.106	0.054	8.244	0.360	3.640	1.142	1.214	6.615	0.194	0.787
105	71.26	3.75	35.62	22.22	12.041	127.3	1.904	17.42	0.102	0.058	7.269	0.382	3.634	1.289	1.228	7.383	0.194	1.010
120	65.86	4.30	36.14	21.88	11.857	116.1	1.886	17.42	0.098	0.062	6.454	0.421	3.542	1.357	1.162	7.818	0.185	1.080
135	57.57	5.03	37.16	21.50	11.651	126.3	1.889	17.97	0.094	0.066	5.412	0.473	3.493	1.419	1.095	8.336	0.176	1.186
150	53.24	5.94	37.93	21.73	11.776	124.1	1.856	18.20	0.090	0.070	4.792	0.535	3.414	1.521	1.060	8.687	0.167	1.274
165	46.28	6.82	38.70	22.81	12.361	122.1	1.826	18.57	0.086	0.074	3.980	0.587	3.328	1.688	1.063	9.035	0.157	1.374
180	37.82	7.45	39.98	22.51	12.198	122.1	1.827	19.01	0.082	0.078	3.101	0.611	3.279	1.756	1.000	9.527	0.150	1.483
195	29.51	7.87	40.75	23.29	12.621	123.7	1.850	19.15	0.078	0.082	2.302	0.614	3.179	1.910	0.984	10.143	0.144	1.570
210	23.14	8.61	42.29	23.68	12.832	124.9	1.868	20.13	0.074	0.086	1.712	0.637	3.129	2.036	0.950	10.741	0.138	1.731
225	16.51	9.34	42.80	23.43	12.697	126.7	1.895	21.01	0.070	0.090	1.156	0.654	2.996	2.109	0.889	11.403	0.133	1.891
240	9.68	9.82	43.57	24.64	13.353	127.0	1.899	21.61	0.066	0.094	0.639	0.648	2.876	2.316	0.881	11.938	0.125	2.031

Reproduced with permission of the copyright owner. Further reproduction prohibited without permission.

Table B-6 (Continued) Detailed determination of the atomic nitrogen balance for run 22A.

column	o	p	q	r	r1	r2	t	u	w	x	y	z	w1	x1	y1	z1
Time (min.)	NO_3-N (mg)	NO_2-N (mg)	*bio*-N (mg)	N_2O-N,g (mg)	N_2O-N,ℓ (mg)	N_2O-N,t (mg)	O_2-N (mg)	N_2-N,t (mg)	δN (mg)	∑δN (mg)	total-N (mg)	relative error,%	δN (mg)	∑δN (mg)	total-N (mg)	relative error,%
0	3.101	0.014	0.458	0.382	0.896	1.278	1.404	3.234	0.153	0.153	8.238	-11.49	0.126	0.126	7.315	-11.906
15	2.925	0.030	0.460	0.447	0.898	1.345	1.688	3.444	0.153	0.306	8.510	-8.57	0.124	0.250	7.556	-9.308
30	2.713	0.043	0.457	0.515	0.896	1.411	1.744	3.692	0.150	0.456	8.772	-5.75	0.120	0.371	7.791	-6.172
45	2.516	0.059	0.457	0.581	0.884	1.464	1.796	3.740	0.147	0.603	8.839	-5.03	0.117	0.487	7.840	-5.578
60	2.294	0.075	0.452	0.621	0.834	1.455	2.327	3.936	0.143	0.746	8.958	-3.76	0.114	0.601	7.977	-3.897
75	2.106	0.092	0.444	0.674	0.803	1.477	2.798	3.947	0.140	0.886	8.951	-3.83	0.111	0.712	7.974	-3.965
90	1.861	0.110	0.451	0.726	0.773	1.499	2.592	4.218	0.134	1.020	9.159	-1.60	0.105	0.817	8.183	-1.446
105	1.641	0.116	0.450	0.820	0.782	1.602	3.326	4.252	0.132	1.152	9.213	-1.02	0.101	0.918	8.198	-1.270
120	1.457	0.128	0.439	0.863	0.739	1.603	3.555	4.448	0.127	1.279	9.354	0.49	0.097	1.015	8.350	0.568
135	1.222	0.144	0.433	0.903	0.697	1.600	3.904	4.609	0.120	1.399	9.407	1.07	0.091	1.106	8.417	1.366
150	1.082	0.163	0.423	0.968	0.674	1.642	4.194	4.660	0.118	1.517	9.488	1.93	0.088	1.194	8.490	2.248
165	0.899	0.179	0.412	1.074	0.676	1.751	4.523	4.669	0.115	1.632	9.541	2.51	0.083	1.277	8.510	2.489
180	0.700	0.186	0.406	1.117	0.637	1.754	4.881	4.796	0.108	1.740	9.582	2.95	0.077	1.354	8.560	3.088
195	0.520	0.187	0.394	1.215	0.626	1.842	5.169	5.119	0.103	1.843	9.904	6.40	0.071	1.425	8.859	6.695
210	0.387	0.194	0.388	1.296	0.604	1.900	5.698	5.181	0.099	1.942	9.992	7.35	0.067	1.491	8.937	7.629
225	0.261	0.199	0.371	1.342	0.566	1.907	6.224	5.311	0.094	2.037	10.087	8.37	0.062	1.553	9.038	8.847
240	0.144	0.197	0.356	1.474	0.561	2.035	6.686	5.377	0.091	2.127	10.237	9.98	0.057	1.610	9.159	10.304

Reproduced with permission of the copyright owner. Further reproduction prohibited without permission.

Table B-6A Description of quantities and symbols appearing in the columns of Table B-6

a : concentration of nitrate in the liquid phase determined by Ion Chromatography (IC).

b : concentration of nitrite in the liquid phase determined by IC analysis.

c : biomass concentration measured spectrophotometrically; concentration = 256.3 × OD; OD = optical density of sample.

d : concentration of nitrous oxide in the headspace of the vial (gas phase), determined by Gas Chromatography (GC).

d1 : concentration of nitrous oxide in the liquid phase, estimated as explained in Appendix C.

e : concentration of nitrogen in the gas phase, determined by GC analysis.

e1 : concentration of nitrogen in the liquid phase, estimated as explained in Appendix C.

f : concentration of oxygen in the gas phase, determined by GC analysis.

g : volume of the liquid phase in the closed bottle.

h : volume of the head space of the closed bottle; each entry of this column is equal to 0.16 – g* (in L), where g* is the corresponding entry in column g.

i, j, k, ℓ1, m1 : mass of various components of the liquid phase. These values are determined by multipling concentrations (columns a, b, c, d1, e1 by the corresponding volume (column g).

ℓ, m, n : mass of various components of the gas phase, determined by multipling the values of columns d, e, f with the corresponding entry of column h.

o : nitrogen content of nitrate (NO_3^-); entries of column i multiplied by 14/62.

p : nitrogen content of nitrite (NO_2^-); entries of column j multiplied by 14/46.

q : nitrogen content of biomass ($C_5H_7O_2N$); entries of column k multiplied by 14/113.

r : nitrogen content of nitrous oxide (N_2O) present in the gas phase; entries of column ℓ multiplied by 28/44.

r1 : nitrogen content of nitrous oxide (N_2O) present in the liquid phase; entries of column ℓ1 multiplied by 28/44.

r2 : total nitrogen content of nitrous oxide (N_2O); sum of entries of columns r and r1.

t : nitrogen content of air corresponding to oxygen (O_2) measurements appearing in column n; entries of column n multiplied by 79/21 × 1/32 × 28.

u : total nitrogen gas (N_2) associated with the denitrification process; sum of entries of columns m and m1, minus corresponding entries of column t.

w : nitrogen content of the gas and liquid samples when N_2O is considered in the liquid phase; entries determined through the formula: 0.004R + 0.0001S; where R is the sum of the entries of columns o, p, q, r1, and m1 divided by the entry of column g; S is the sum of entries of columns r and m, minus the entry of column t, divided by the entry of column h, 0.004 is the volume of the liquid sample (4 mL), and 0.0001 is the volume of the gas sample (0.1 mL).

x : total amount of process associated nitrogen lost in the samples since the beginning of the experiment (sum of all previous entries of column w).

y : total process associated nitrogen content of the bottle (reactor) if no samples were taken; sum of entries of columns o, p, q, r, r1, and u, minus the entry of column w.

z : relative error: 100 × (M – N) / M; M = average value of entries of column y; N = entry of column y.

w1, x1, y1, z1 : same as w, x, y, z, respectively except that column r1 is not considered (i.e., no N_2O present in the liquid phase).

Reproduced with permission of the copyright owner. Further reproduction prohibited without permission.

Reproduced with permission of the copyright owner. Further reproduction prohibited without permission.

Table B-7 Nitrogen balance during biological denitrification: Data from various kinetic runs. Columns I and II indicate balances when N_2O presence in the liquid is neglected and considered, respectively.

	Total N (mg)									
Time	Run **22A**		Run **20B**		Run **25B**		Run **1G**		Run **2G**	
(h)	I	II	I	II	I	II	I	II	I	II
0	7.315	8.238	8.512	9.225	8.893	8.912	10.007	10.842	10.406	11.069
0.25	7.556	8.510	8.988	9.722	9.152	9.190	10.155	11.021	10.498	11.185
0.50	7.791	8.772	8.993	9.736	9.371	9.428	10.715	11.592	10.390	11.076
0.75	7.840	8.839	9.063	9.824	9.433	9.511	10.842	11.731	10.372	11.059
1	7.980	8.958	9.212	9.966	9.573	9.672	10.689	11.595	10.426	11.103
1.25	7.974	8.951	9.346	10.096	9.725	9.846	11.037	12.002	10.566	11.281
1.50	8.183	9.159	9.336	10.110	9.789	9.936	10.850	11.798	10.714	11.437
1.75	8.198	9.213	9.418	10.192	9.790	9.960	11.341	12.291	10.565	11.289
2	8.350	9.354	9.368	10.144	9.869	10.061	11.053	12.027	10.485	11.209
2.25	8.417	9.407	9.226	10.005	10.099	10.316	11.255	12.267	10.673	11.417
2.50	8.490	9.488	9.508	10.301	10.249	10.491	11.492	12.458	10.704	11.458
2.75	8.510	9.541	9.435	10.260	10.072	10.337	11.389	12.340	10.800	11.571
3	8.560	9.582	9.439	10.298	10.107	10.398	11.821	12.837	11.134	11.930
3.25	8.859	9.904			10.151	10.467	11.685	12.714	11.247	12.033
3.50	8.937	9.992			10.224	10.565	11.968	13.012	11.163	11.960
3.75	9.038	10.087			10.517	10.883	12.154	13.180	11.425	12.233
4	9.159	10.237			10.366	10.755	12.127	13.178	11.632	12.440
Average	8.303	9.308	9.219	9.991	9.846	10.043	11.211	12.170	10.776	11.515
± error	± 0.99	± 1.07	± 0.71	± 0.77	± 0.69	± 0.85	± 1.06	± 1.15	± 0.65	± 0.72

Reproduced with permission of the copyright owner. Further reproduction prohibited without permission.

Table B-7 (Continued) Nitrogen balance during biological denitrification: Data from various kinetic runs. Columns I and II indicate balances when N_2O presence in the liquid is neglected and considered, respectively.

	Total N (mg)											
Time	Run **3G**		Run **4G**		Run **5G**		Run **6G**		Run **1H**		Run **2H**	
(h)	I	II	I	II	I	II	I	II	I	II	I	II
0	9.324	10.005	10.440	11.153	18.004	18.730	19.068	20.153	7.607	8.321	11.137	11.763
0.25	9.510	10.175	10.159	10.819	18.264	19.048	18.696	19.838	7.675	8.375	11.275	11.916
0.50	9.484	10.155	10.153	10.815	18.644	19.552	19.177	20.277	7.738	8.500	11.374	12.008
0.75	9.466	10.163	10.406	11.079	18.637	19.701	19.293	20.432	7.930	8.679	11.352	12.022
1	9.682	10.399	10.516	11.142	18.608	19.627	19.334	20.459	7.978	8.709	11.497	12.173
1.25	9.983	10.720	10.617	11.239	18.251	19.293	19.773	20.921	8.213	9.016	11.642	12.319
1.50	9.905	10.654	10.752	11.358	18.780	19.904	19.560	20.729	8.270	9.036	11..770	12.477
1.75	9.827	10.601	10.848	11.453	18.584	19.727	19.927	21.108	8.148	8.930	11.825	12.532
2	10.061	10.845	11.100	11.704	18.864	20.089	20.100	21.309	8.317	9.139	12.271	12.980
2.25	10.320	11.101	11.293	11.863	18.691	19.933	20.319	21.680	8.503	9.354	12.249	12.960
2.50	10.344	11.172	11.156	11.730	19.045	20.251	20..216	21.560	8.627	9.472	12.403	13.114
2.75	10.267	11.090	11.211	11.789	19.787	21.040	20.609	21.937	8.754	9.628	12.583	13.273
3	10.274	11.106	11.431	11.950	19.777	21.040	20.752	22.111	8.694	9.553	12.476	13.186
3.25	10.571	11.396	11.523	12.030			20.750	22.060	8.860	9.715	12.542	13.253
3.50	10.781	11.615	11.440	11.954			20.891	22.321	8.879	9.704	12.562	13.303
3.75	10.782	11.631	11.413	11.943			20.657	22.081	8.897	9.732	12.772	13.521
4	10.659	11.494	11.474	11.983			20.642	22.076	8.808	9.657	12.922	13.644
Average ± error	10.073 ± 0.75	10.842 ± 0.84	10.937 ± 0.78	11.529 ± 0.71	18.764 ± 1.02	19.841 ± 1.12	19.986 ± 1.29	21.238 ± 1.40	8.347 ± 0.74	9.148 ± 0.83	12.038 ± 0.90	12.732 ± 0.97

Table B-8 Data from small scale experiments involving reduction of nitrate or nitrite at pH = 7.1 ± 0.1. (All concentrations are in mg/L)

Time	Run 1H (V_o = 107 mL) (pH = 7.16 ~ 7.21) T = 30 °C					Run 2H (V_o = 106 mL) (pH = 7.16 ~ 7.28) T = 37 °C				
(min.)	NO_3^-	NO_2^-	*b*	N_2O	N_2	NO_3^-	NO_2^-	*b*	N_2O	N_2
0	104.1	0	47.42	18.63	87.10	0	154.99	42.55	16.50	106.55
15	98.70	1.02	49.21	18.28	86.04	0	147.35	44.08	16.90	105.12
30	89.79	1.23	49.98	20.03	84.03	0	146.06	44.60	16.71	100.77
45	82.31	1.29	52.03	19.63	84.59	0	134.62	45.11	17.79	102.34
60	70.41	1.29	55.10	19.10	85.51	0	123.44	46.39	17.96	98.09
75	63.41	1.32	58.44	21.39	86.99	0	120.84	47.16	18.03	98.09
90	53.60	1.24	61.51	20.13	86.93	0	112.02	49.21	19.12	98.09
105	43.34	1.32	62.54	20.70	82.87	0	101.89	51.77	19.36	98.09
120	34.63	1.39	64.08	22.18	82.71	0	91.00	54.59	19.06	96.16
135	21.95	1.32	67.41	23.27	82.03	0	81.66	57.41	19.16	99.77
150	9.89	1.34	69.97	23.05	82.54	0	70.54	60.23	19.16	99.77
165	0	0.60	72.02	24.32	84.45	0	62.64	58.18	18.26	90.61
180	0	0	72.28	23.62	79.36	0	49.96	60.49	19.20	90.61
195	0	0	75.35	23.46	80.02	0	37.59	59.97	19.24	93.35
210	0	0	73.81	21.83	78.81	0	24.95	63.05	20.83	92.43
225	0	0	73.81	22.38	76.81	0	13.90	64.08	21.30	88.29
240	0	0	74.07	21.46	77.81	0	2.70	64.08	19.62	88.93

Reproduced with permission of the copyright owner. Further reproduction prohibited without permission.

Table B-8 (Continued) Data from small scale experiments involving reduction of nitrate or nitrite at pH = 7.1 ± 0.1. (All concentrations are in mg/L)

Time	Run 3H (V_o = 106 mL) (pH = 7.19 ~ 7.30) T = 37 °C					Run 4H (V_o = 108 mL) (pH = 6.98 ~ 7.07) T = 38 °C				
(min.)	NO_3^-	NO_2^-	*b*	N_2O	N_2	NO_3^-	NO_2^-	*b*	N_2O	N_2
0	147.48	0	36.39	17.16	119.17	156.24	0	72.02	25.40	254.97
15	141.97	1.71	37.68	18.14	125.51	149.87	1.17	74.07	29.85	248.34
30	130.86	2.39	38.19	17.46	114.51	131.89	1.03	76.12	31.55	227.56
45	121.26	2.70	39.98	17.36	115.94	125.99	1.19	75.61	33.29	227.56
60	116.32	3.09	41.52	18.45	112.72	113.19	1.36	77.40	33.11	189.91
75	104.58	3.26	42.80	20.59	117.06	102.23	1.61	79.97	28.06	181.96
90	97.07	3.55	46.65	18.71	117.97	88.18	1.87	81.50	33.02	181.96
105	91.13	3.83	48.44	21.18	120.61	73.99	2.15	82.02	36.03	214.96
120	81.60	4.28	52.80	22.15	119.78	60.73	2.39	85.60	35.75	188.87
135	71.94	4.69	55.10	23.85	115.32	43.96	2.50	88.42	37.77	172.97
150	61.83	5.08	56.64	23.85	113.08	30.24	2.68	91.24	37.82	187.13
165	53.46	6.04	57.67	27.19	110.83	18.05	1.43	93.55	38.76	164.32
180	35.65	6.30	61.26	27.89	117.09	6.97	0.82	94.83	36.05	165.63
195	25.46	6.83	62.28	28.30	123.35	0	0	96.88	41.28	167.48
210	13.64	5.81	65.61	30.71	124.49	0	0	97.39	39.95	166.15
225	4.16	3.75	66.64	31.97	127.75					
240	0	0	71.25	31.73	129.08					

Reproduced with permission of the copyright owner. Further reproduction prohibited without permission.

Table B-8 (Continued) Data from small scale experiments involving reduction of nitrate or nitrite at pH = 7.1 ± 0.1. (All concentrations are in mg/L)

	Run 5H (V_o = 108 mL) (pH = 7.00 ~ 7.12) T = 38 °C				
Time (min.)	NO_3^-	NO_2^-	*b*	N_2O	N_2
0	0	160.20	76.12	41.48	246.70
15	0	151.04	74.84	34.40	240.44
30	0	139.89	75.10	35.36	222.37
45	0	128.35	75.86	34.14	210.26
60	0	117.82	76.38	35.46	200.14
75	0	106.57	78.68	33.91	262.61
90	0	91.02	78.94	35.30	177.15
105	0	81.79	80.22	36.57	168.65
120	0	64.98	81.76	43.57	168.65
135	0	53.49	83.81	37.72	181.70
150	0	37.93	85.86	36.92	173.54
165	0	25.65	86.63	35.35	177.71
180	0	10.44	89.71	35.78	190.75
195	0	0	91.50	37.01	176.70
210	0	0	90.99	34.24	176.54
225					
240					

Reproduced with permission of the copyright owner. Further reproduction prohibited without permission.

Reproduced with permission of the copyright owner. Further reproduction prohibited without permission.

Table B-9 Kinetic data for studying the temperature effects on nitrate reduction at pH = 7.1 ± 0.1. (All concentrations are in mg/L)

Time	Run 1C (T = 30 °C) (pH = 7.10 ~ 7.14, V_o = 132 mL)					Run 2C (T = 30 °C) (pH = 7.17 ~ 7.20, V_o = 132 mL)					Run 3C (T = 32.5 °C) (pH = 7.12 ~ 7.16, V_o =131 mL)				
(min.)	NO_3^-	NO_2^-	*b*	N_2O	N_2	NO_3^-	NO_2^-	*b*	N_2O	N_2	NO_3^-	NO_2^-	*b*	N_2O	N_2
0	55.50	0	28.45	23.94	369.9	56.62	1.41	36.65	31.91	482.9	49.02	0	26.40	194.8	8.75
15	54.29	0.31	28.45	26.54	377.1	54.55	2.51	36.14	33.80	459.3	40.88	0.98	27.42	187.2	9.04
30	49.96	0.26	28.96	22.10	447.6	51.71	3.95	37.93	-	444.3	35.65	1.43	28.71	186.0	10.13
45	46.69	0.80	32.04	25.72	346.3	37.56	3.51	38.70	38.58	406.2	27.36	1.69	29.99	183.5	9.34
60	43.42	0	32.55	26.56	291.0	34.22	1.52	40.50	37.70	378.5	16.51	2.14	32.29	185.6	10.71
75	24.30	1.47	33.32	36.54	325.6	30.65	2.46	41.52	-	374.4	8.84	2.34	33.32	168.2	9.49
90	14.60	1.40	35.11	29.44	387.2	10.26	0	43.83	39.26	361.5	1.23	2.34	35.63	181.9	-
105	0	0	35.62	41.54	361.4	0	0	45.37	-	344.1	0	0	36.65	180.3	12.45
120	0	0	37.68	31.24	381.4	0	0	46.39	34.77	331.1	0	0	36.65	169.7	10.40

Time	Run 4C (T = 35 °C) (pH = 7.13 ~ 7.14, V_o = 105 mL)					Run 5C (T = 38 °C) (pH = 7.10 ~ 7.13, V_o = 105 mL)					Run 6C (T = 30 °C) (pH = 7.17 ~ 7.18, V_o = 131 mL)				
(min.)	NO_3^-	NO_2^-	*b*	N_2O	N_2	NO_3^-	NO_2^-	*b*	N_2O	N_2	NO_3^-	NO_2^-	*b*	N_2O	N_2
0	55.69	0	38.19	17.65	130.8	55.52	0	50.49	20.86	147.7	10.28	2.32	34.09	49.59	577.0
15	47.39	2.24	40.50	16.60	129.8	40.45	3.46	54.85	22.83	149.0	4.89	0.42	33.83	31.30	498.1
30	37.90	3.09	40.75	16.80	124.0	28.22	5.03	56.39	23.04	155.2	0	0.45	35.11	-	-
45	25.36	2.63	40.24	16.39	122.4	16.93	4.56	58.69	26.14	148.5	0	0	34.86	29.23	468.4
60						3.40	3.24	61.51	25.53	143.9	0	0	35.37	31.06	448.1
75															
90															
105															
120															

Reproduced with permission of the copyright owner. Further reproduction prohibited without permission.

Table B-9 (Continued) Kinetic data for studying the temperature effects on nitrate reduction at pH = 7.1 ± 0.1(Concentrations in mg/L)

Time	Run 7C (T = 32.5 °C) (pH = 7.01 ~ 7.03, V_o = 104 mL)					Run 8C (T = 35 °C) (pH = 7.08 ~ 7.13, V_o = 104 mL)					Run 9C (T = 38 °C) (pH = 7.19 ~ 7.19, V_o = 104 mL)				
(min.)	NO_3^-	NO_2^-	*b*	N_2O	N_2	NO_3^-	NO_2^-	*b*	N_2O	N_2	NO_3^-	NO_2^-	*b*	N_2O	N_2
0	11.09	0	51.26	16.80	158.5	8.61	0	45.11	19.24	152.0	11.44	0	37.68	22.78	172.2
15	4.77	0.66	52.29	18.21	150.9	1.75	0	46.13	18.62	151.0	7.58	0	37.11	22.68	172.6
30	1.10	0.66	53.57	17.89	144.8	0	0	46.90	18.80	146.4	2.55	0	37.93	23.15	165.5
45	0	0	54.08	17.50	136.2	0	0	46.90	18.27	134.0	0	0	38.96	24.34	167.7
60	0	0	54.08	17.10	130.4										
75															
90															
105															
120															

Time	Run 10C (T = 30 °C) (pH = 6.93 ~ 6.96, V_o = 104 mL)					Run 11C (T = 32.5 °C) (pH = 7.12 ~ 7.13, V_o = 104 mL)					Run 12C (T = 35 °C) (pH = 7.04 ~ 7.06, V_o = 104 mL)				
(min.)	NO_3^-	NO_2^-	*b*	N_2O	N_2	NO_3^-	NO_2^-	*b*	N_2O	N_2	NO_3^-	NO_2^-	*b*	N_2O	N_2
0	21.76	0	50.75	19.98	185.0	20.55	0	49.47	19.62	147.6	18.81	0	43.57	19.79	125.6
15	10.45	2.18	51.52	20.40	180.3	15.51	0.74	49.47	19.15	150.2	6.19	3.02	45.62	19.76	127.9
30	2.56	3.28	53.57	20.81	179.5	9.82	0.66	51.52	18.90	138.0	0	1.62	47.16	21.24	139.8
45	0	0	55.87	21.89	170.7	4.39	0.53	51.77	20.38	136.4	0	0	48.95	19.96	130.7
60	0	0	56.13	23.79	156.3	0	0	49.72	19.45	130.9	0	0	48.44	20.27	126.2
75															
90															
105															
120															

Reproduced with permission of the copyright owner. Further reproduction prohibited without permission.

Table B-9 (Continued) Kinetic data for studying the temperature effects on nitrate reduction at pH = 7.1 ± 0.1(Concentrations in mg/L)

Time	Run **13C** (T = 38 °C) (pH = 6.95 ~ 7.13, V_o = 104 mL)					Run **14C** (T = 30 °C) (pH = 7.13 ~ 7.13, V_o = 105 mL)					Run **15C** (T = 30 °C) (pH = 7.15 ~ 7.16, V_o = 125 mL)				
(min.)	NO_3^-	NO_2^-	*b*	N_2O	N_2	NO_3^-	NO_2^-	*b*	N_2O	N_2	NO_3^-	NO_2^-	*b*	N_2O	N_2
0	21.37	0	46.65	23.65	154.1	85.22	0	46.65	15.67	137.4	90.90	0	57.67	61.32	431.4
15	6.94	2.77	49.21	22.90	164.9	73.14	1.49	48.44	16.51	130.1	77.05	0.47	58.69	68.64	432.4
30	0	0.32	52.29	21.98	143.9	61.72	2.58	49.72	17.00	122.4	58.87	0.45	60.74	66.35	466.6
45	0	0	51.77	23.44	140.3	53.13	3.83	51.52	18.73	120.0	45.66	0.54	63.82	64.73	521.1
60	0	0	51.26	22.05	136.9	40.80	4.27	53.05	23.87	119.2	33.80	0	66.12	66.07	514.7
75											26.45	0	66.64	67.73	498.0
90											23.29	0	69.20	66.86	467.0
105											21.87	0	68.43	63.51	465.4
120											21.52	0	69.20	70.16	436.5

Time	Run **16C** (T = 32.5 °C) (pH = 7.11 ~ 7.11, V_o = 105 mL)					Run **17C** (T = 35 °C) (pH = 7.13 ~ 7.15, V_o = 105 mL)					Run **18C** (T = 38 °C) (pH = 7.12 ~ 7.13, V_o = 105 mL)				
(min.)	NO_3^-	NO_2^-	*b*	N_2O	N_2	NO_3^-	NO_2^-	*b*	N_2O	N_2	NO_3^-	NO_2^-	*b*	N_2O	N_2
0	81.30	0	46.47	16.96	129.8	84.67	0	43.83	17.79	133.9	83.38	0	39.21	16.82	100.0
15	75.89	1.17	48.44	16.70	136.2	71.75	3.06	45.88	17.62	124.1	74.27	1.84	41.26	17.69	100.8
30	73.78	2.07	49.47	15.90	124.7	59.49	4.61	49.47	17.49	123.4	60.28	2.47	42.58	19.41	95.22
45	66.70	2.55	49.47	16.14	115.0	48.69	4.56	49.98	17.54	125.1	-	-	43.83	19.49	94.72
60						35.52	3.97	51.52	18.31	120.8					
75															
90															
105															
120															

Reproduced with permission of the copyright owner. Further reproduction prohibited without permission.

Table B-9 (Continued) Kinetic data for studying the temperature effects on nitrate reduction at pH = 7.1 ± 0.1(Concentrations in mg/L)

Time	Run **19C** (T = 30 °C) (pH = 7.01 ~ 7.03, V_o = 106 mL)					Run **20C** (T = 32.5 °C) (pH = 7.03 ± 0.00, V_o = 106 mL)					Run **21C** (T = 35 °C) (pH = 7.03 ~ 7.09, V_o = 106 mL)				
(min.)	NO_3^-	NO_2^-	*b*	N_2O	N_2	NO_3^-	NO_2^-	*b*	N_2O	N_2	NO_3^-	NO_2^-	*b*	N_2O	N_2
0	149.59	0	48.18	16.63	127.98	152.51	0	48.70	20.30	107.30	150.65	0	41.01	19.31	163.45
15	147.49	1.01	48.18	17.30	129.93	146.40	1.10	48.44	20.21	-	145.51	0.74	41.26	21.64	163.65
30	142.54	1.33	49.21	17.16	-	143.56	1.01	49.47	20.31	163.23	143.80	0.70	42.55	19.92	163.53
45	134.57	1.35	50.23	18.32	119.63	135.73	1.39	51.26	19.22	150.38	132.55	0.85	43.31	19.53	150.55
60	128.71	1.24	52.03	17.84	115.82	126.10	1.33	52.54	19.16	142.18	125.61	1.14	44.08	-	142.65
75															
90															
105															
120															

Time	Run **22C** (T = 38 °C) (pH = 7.12 ~ 7.14, V_o = 106 mL)				
(min.)	NO_3^-	NO_2^-	*b*	N_2O	N_2
0	148.82	0	42.03	19.89	123.60
15	135.19	1.75	43.31	20.44	121.99
30	124.94	2.24	45.11	21.60	120.17
45	112.51	2.79	47.42	22.45	121.13
60	97.76	3.43	47.67	23.44	110.37
75					
90					
105					
120					

Reproduced with permission of the copyright owner. Further reproduction prohibited without permission.

Table B-10 Kinetic data for studying the temperature effects on nitrite reduction at pH = 7.1 ± 0.1. (All concentrations are in mg/L)

Time	Run **1D** (T = 30 °C) (pH = 7.12 ~ 7.14, V_o = 105 mL)					Run **2D** (T = 30 °C) (pH = 7.13 ~ 7.15, V_o = 105 mL)					Run **3D** (T = 32.5 °C) (pH = 7.14 ~ 7.17, V_o = 131 mL)				
(min.)	NO_3^-	NO_2^-	*b*	N_2O	N_2	NO_3^-	NO_2^-	*b*	N_2O	N_2	NO_3^-	NO_2^-	*b*	N_2O	N_2
0	1.16	52.26	46.65	18.00	107.3	1.13	51.78	41.01	15.48	67.96	1.04	49.65	29.22	15.28	139.3
15	0	42.62	46.65	17.77	99.42	0	43.88	42.55	16.08	67.57	0	51.60	30.76	16.94	127.8
30	0	33.60	48.95	16.84	100.5	0	35.44	44.08	16.85	71.16	0	48.16	29.99	14.64	125.6
45	0	21.68	49.47	18.65	100.2	0	24.72	44.60	16.63	71.49	0	43.77	30.24	16.39	122.6
60	0	12.35	26.14	18.84	100.8						0	39.27	30.76	14.72	115.2
75											0	32.78	32.81	16.47	120.1
90											0	26.88	32.04	15.06	114.3
105											0	19.96	34.86	14.83	115.1
120											0	11.08	35.88	15.36	114.1

Time	Run **4D** (T = 35 °C) (pH = 7.15 ~ 7.19, V_o = 131 mL)					Run **5D** (T = 35 °C) (pH = 7.15 ~ 7.19, V_o = 131 mL)					Run **6D** (T = 35 °C) (pH = 7.12 ~ 7.13, V_o = 131 mL)				
(min.)	NO_3^-	NO_2^-	*b*	N_2O	N_2	NO_3^-	NO_2^-	*b*	N_2O	N_2	NO_3^-	NO_2^-	*b*	N_2O	N_2
0	0	48.55	24.35	14.83	118.7	0.75	54.07	25.37	15.66	107.0	1.10	49.87	34.60	17.89	133.0
15	0	47.87	25.63	15.25	107.3	0	47.15	26.66	16.07	114.6	0.68	46.38	36.39	17.56	125.8
30	0	44.28	25.12	14.78	114.8	0	39.15	26.91	18.25	110.7	0	45.20	36.91	17.18	118.6
45	0	34.34	26.14	15.05	95.42	0	33.21	27.94	15.35	100.0	0	37.99	37.93	18.23	116.6
60	0	32.38	26.66	15.43	107.6	0	30.95	28.70	15.60	105.1	0	35.20	38.70	17.95	117.0
75	0	22.97	28.45	15.88	96.97	0	27.53	29.99	15.99	92.78	0	31.11	38.44	18.02	109.7
90	0	14.81	28.19	16.13	103.2	0	24.48	30.24	17.21	97.44	0	26.55	39.47	20.29	116.7
105	0	11.55	30.24	16.88	102.1	0	18.66	31.52	16.22	98.39	0	24.65	40.50	18.17	114.1
120	0	7.46	29.99	15.92	107.0	0	14.98	31.01	16.86	105.2	0	20.83	38.44	17.72	112.1

Reproduced with permission of the copyright owner. Further reproduction prohibited without permission.

Table B-10(Continued) Kinetic data for studying the temperature effects on nitrite reduction at pH = 7.1±0.1 (Concentrations in mg/L)

Time	Run **7D** (T = 38 °C) (pH = 7.11 ~ 7.17, V_o = 131 mL)					Run **8D** (T = 30 °C) (pH = 7.12 ~ 7.13, V_o = 104 mL)					Run **9D** (T = 32.5 °C) (pH = 7.11 ~ 7.12, V_o = 104 mL)				
(min.)	NO_3^-	NO_2^-	*b*	N_2O	N_2	NO_3^-	NO_2^-	*b*	N_2O	N_2	NO_3^-	NO_2^-	*b*	N_2O	N_2
0	0.93	51.51	25.89	12.26	120.8	0	10.09	47.67	19.16	123.1	0	10.72	46.13	18.33	132.9
15	0	46.96	27.17	16.29	120.0	0	4.48	48.18	19.27	111.0	0	4.87	46.65	18.59	130.5
30	0	41.53	27.94	16.72	120.5	0	0	49.47	18.94	98.33	0	0	47.42	20.19	130.5
45	0	33.84	29.47	17.67	123.0	0	0	48.95	20.11	132.7	0	0	48.70	18.19	145.5
60	0	28.09	29.99	18.27	123.1										
75	0	19.95	31.52	18.79	131.9										
90	0	12.46	32.81	18.47	136.3										
105	0	4.35	34.09	19.57	134.2										
120	0	0	34.86	20.27	143.5										

Time	Run **10D** (T = 35 °C) (pH = 7.06 ~ 7.07, V_o = 104 mL)					Run **11D** (T = 38 °C) (pH = 7.14 ~ 7.15, V_o = 104 mL)					Run **12D** (T = 30 °C) (pH = 7.20 ~ 7.23, V_o = 129 mL)				
(min.)	NO_3^-	NO_2^-	*b*	N_2O	N_2	NO_3^-	NO_2^-	*b*	N_2O	N_2	NO_3^-	NO_2^-	*b*	N_2O	N_2
0	0	9.97	31.01	17.95	115.2	0	10.83	38.06	15.76	184.6	0	21.42	33.58	17.59	327.4
15	0	5.84	31.27	-	-	0	5.51	38.70	15.48	156.8	0	17.35	37.42	24.63	324.0
30	0	1.01	31.91	17.58	112.9	0	0	39.73	14.99	157.5	0	14.74	36.65	24.91	336.7
45	0	0	33.58	17.23	114.8	0	0	39.47	15.26	155.0	0	13.28	36.65	22.56	316.4
60											0	13.41	40.24	21.26	298.9
75											0	11.14	36.91	23.19	290.6
90											0	7.46	39.98	23.29	276.3
105											0	6.07	42.55	24.83	273.2
120											0	3.87	45.37	24.44	262.4

Reproduced with permission of the copyright owner. Further reproduction prohibited without permission.

Table B-10(Continued) Kinetic data for studying the temperature effects on nitrite reduction at pH = 7.1±0.1 (Concentrations in mg/L)

Time	Run **13D** (T = 32.5 °C) (pH = 7.11 ~ 7.13, V_o = 104 mL)					Run **14D** (T = 35 °C) (pH = 7.03 ~ 7.06, V_o = 104 mL)					Run **15D** (T = 38 °C) (pH = 7.15 ~ 7.17, V_o = 104 mL)				
(min.)	NO_3^-	NO_2^-	*b*	N_2O	N_2	NO_3^-	NO_2^-	*b*	N_2O	N_2	NO_3^-	NO_2^-	*b*	N_2O	N_2
0	0	21.98	41.78	16.59	146.8	1.26	20.98	41.01	18.22	149.48	0	21.83	36.14	16.48	105.46
15	0	16.78	41.01	17.46	142.2	0	14.46	41.01	19.12	138.72	0	14.88	37.68	17.47	100.25
30	0	11.91	42.55	18.62	136.5	0	8.22	42.55	19.13	145.78	0	6.72	38.70	17.11	100.00
45	0	7.05	43.31	17.97	150.2	0	2.06	43.83	18.99	147.08	0	0	39.21	17.67	97.26
60	0	1.69	43.31	-	130.6	0	0	43.83	19.25	147.08	0	0	39.73	16.65	96.98
75															
90															
105															
120															

Time	Run **16D** (T = 30 °C) (pH = 7.11 ~ 7.13, V_o = 105 mL)					Run **17D** (T = 30 °C) (pH = 7.12 ~ 7.14, V_o = 105 mL)					Run **18D** (T = 32.5 °C) (pH = 7.10 ~ 7.13, V_o = 105 mL)				
(min.)	NO_3^-	NO_2^-	*b*	N_2O	N_2	NO_3^-	NO_2^-	*b*	N_2O	N_2	NO_3^-	NO_2^-	*b*	N_2O	N_2
0	2.19	91.49	40.50	16.75	132.31	2.55	86.04	42.29	16.52	143.26	2.01	89.78	44.08	19.26	125.84
15	1.11	83.70	40.50	18.03	127.43	1.18	79.74	43.83	16.56	146.73	0.78	81.57	45.88	16.01	122.02
30	0	82.96	42.03	15.93	130.04	0	74.58	45.62	16.47	137.17	0	74.58	46.90	17.90	117.60
45	0	70.87	41.52	15.90	109.51	0	68.69	45.37	16.55	151.94	0	66.86	47.67	16.47	116.34
60	0	65.45	43.83	15.96	107.49	0	61.12	47.93	17.66	136.42	0	61.35	48.18	16.62	108.49
75															
90															
105															
120															

Reproduced with permission of the copyright owner. Further reproduction prohibited without permission.

Table B-10(Continued) Kinetic data for studying the temperature effects on nitrite reduction at pH = 7.1±0.1 (Concentrations in mg/L)

Time	Run **19D** (T = 32.5 °C) (pH = 7.11 ~ 7.13, V_o = 105 mL)					Run **20D** (T = 35 °C) (pH = 7.09 ~ 7.13, V_o = 105 mL)					Run **21D** (T = 35 °C) (pH = 7.10 ~ 7.18, V_o = 105 mL)				
(min.)	NO_3^-	NO_2^-	*b*	N_2O	N_2	NO_3^-	NO_2^-	*b*	N_2O	N_2	NO_3^-	NO_2^-	*b*	N_2O	N_2
0	2.84	85.19	47.93	17.39	158.32	2.56	83.82	47.16	14.81	136.06	2.08	86.95	42.80	15.13	138.95
15	1.59	80.32	49.98	17.86	159.53	1.37	78.68	48.95	17.37	148.11	0.96	77.21	42.80	16.05	129.62
30	0	74.64	52.03	17.85	159.68	0	71.98	50.23	18.58	131.44	0	69.48	44.85	16.51	122.55
45	0	66.89	52.29	18.59	154.43	0	62.38	52.03	19.15	130.43	0	59.02	47.67	16.71	126.97
60	0	59.07	53.31	18.33	155.59	0	56.67	52.80	18.48	129.42	0	47.89	47.93	16.71	124.94
75											0	36.32	48.44	17.44	127.32
90											0	25.35	49.72	18.05	125.22
105											0	12.13	51.26	19.01	125.20
120											0	0.70	52.54	19.04	119.24

Time	Run **22D** (T = 38 °C) (pH = 7.11 ~ 7.14, V_o = 105 mL)					Run **23D** (T = 30 °C) (pH = 6.99 ~ 7.03, V_o = 132 mL)					Run **24D** (T = 32.5 °C) (pH = 7.10 ~ 7.13, V_o = 106 mL)				
(min.)	NO_3^-	NO_2^-	*b*	N_2O	N_2	NO_3^-	NO_2^-	*b*	N_2O	N_2	NO_3^-	NO_2^-	*b*	N_2O	N_2
0	3.03	82.92	47.16	16.33	160.65	0	146.49	41.26	20.29	331.12	4.32	159.84	51.52	19.45	160.82
15	2.06	79.93	47.16	18.64	155.62	0	140.22	42.03	20.64	332.35	2.70	149.65	51.52	19.55	157.79
30	0	74.20	49.21	20.89	145.72	0	130.67	42.03	19.51	343.64	1.33	148.20	52.80	19.27	155.46
45	0	64.71	48.95	19.99	142.95	0	120.19	43.83	20.93	316.38	0	140.24	52.80	19.24	146.47
60	0	59.77	50.75	19.44	145.58	0	118.83	44.85	19.77	296.12	0	135.01	54.08	19.61	153.90
75						0	102.27	45.62	32.56	295.72					
90						0	93.62	46.65	31.79	306.59					
105						0	82.14	49.47	30.03	292.70					
120						0	78.50	47.93	25.68	270.07					

Reproduced with permission of the copyright owner. Further reproduction prohibited without permission.

Table B-10(Continued) Kinetic data for studying the temperature effects on nitrite reduction at pH = 7.1±0.1 (Concentrations in mg/L)

Time	Run **25D** (T = 35 °C) (pH = 7.02 ~ 7.04, V_o = 106 mL)					Run **26D** (T = 38 °C) (pH = 7.13 ~ 7.16, V_o = 106 mL)				
(min.)	NO_3^-	NO_2^-	*b*	N_2O	N_2	NO_3^-	NO_2^-	*b*	N_2O	N_2
0	4.24	160.15	43.31	19.53	175.54	4.03	155.56	42.80	17.83	132.74
15	2.30	154.86	44.34	20.54	156.43	2.92	150.63	42.80	18.70	138.23
30	1.73	152.05	45.11	20.74	171.73	1.94	145.07	44.85	18.77	131.49
45	1.16	145.30	47.16	20.76	170.05	1.32	135.87	47.16	19.13	135.16
60	0	136.40	47.67	-	154.16	0.81	131.89	46.90	19.06	183.21
75										
90										
105										
120										

Table B-11 Net specific growth rates and apparent yield coefficients of biomass on nitrate at pH = 7.1 ± 0.1 and various temperatures. Data used in Figures 9 and 11.

Experimental Run	Initial nitrate concentration (mg/L)	Temperature (°C)	Net specific growth rate, μ_{1net} (h^{-1})	Apparent yield coefficient, $Y_{1app.}$ (g biomass/g nitrate)
1C, 13A	54.29	30	0.143144	0.24815
2C, 14A	54.55	30	0.144629	0.21676
3C	49.02	32.5	0.167540	0.18329
4C	55.69	35	0.187293	0.17554
5C	55.52	38	0.206265	0.16275
6C, 4A	10.28	30	0.059426	0.16972
7C	11.09	32.5	0.068119	0.16297
8C	8.61	35	0.078004	0.16513
9C	11.44	38	0.087435	0.16302
10C, 7A	21.76	30	0.108134	0.21300
11C	20.55	32.5	0.128228	0.20806
12C	18.81	35	0.144675	0.18667
13C	21.37	38	0.161186	0.17741
14C,18A	89.94	30	0.129602	0.21800
15C, 16A	77.05	30	0.122112	0.20037
16C	81.30	32.5	0.145725	0.20241
17C	94.67	35	0.163559	0.18445
18C	83.38	38	0.183483	0.14156
19C, 28A	149.59	30	0.088163	0.20808
20C	152.51	32.5	0.104993	0.19759
21C	150.65	35	0.116305	0.18409
22C	148.82	38	0.127453	0.14994

Reproduced with permission of the copyright owner. Further reproduction prohibited without permission.

Table B-12 Net specific growth rates and apparent yield coefficients of biomass on nitrite at pH = 7.1 ± 0.1 and various temperatures. Data used in Figures 10 and 12.

Experimental Run	Initial nitrite concentration (mg/L)	Temperature (°C)	Net specific growth rate, μ_{2net} (h^{-1})	Apparent yield coefficient, $Y_{2app.}$ (g biomass/g nitrite)
1D, 15B	52.26	30	0.155217	0.22909
2D, 14B	51.78	30	0.153315	0.26157
3D	51.60	32.5	0.170831	0.18888
4D	48.55	35	0.185379	0.16583
5D	48.07	35	0.188412	0.18642
6D	49.87	35	0.190005	0.18725
7D	51.51	38	0.205977	0.17002
8D, 3B	10.09	30	0.058334	0.17560
9D	10.72	32.5	0.065397	0.17268
10D	9.97	35	0.073628	0.16957
11D	10.83	38	0.082389	0.15440
12D	21.42	30	0.110795	0.23757
13D	21.98	32.5	0.128353	0.23641
14D	20.98	35	0.140118	0.22746
15D	21.83	38	0.155136	0.22158
16D, 21B	83.70	30	0.088551	0.19531
17D, 22B	86.04	30	0.130294	0.23012
18D	81.57	32.5	0.146314	0.21924
19D	85.19	32.5	0.146228	0.19124
20D	83.82	35	0.158268	0.20163
21D	77.21	35	0.130122	0.18143
22D	79.93	38	0.176738	0.15922
23D, 32B	146.49	30	0.080810	0.18249
24D	149.65	32.5	0.091334	0.17407
25D	154.86	35	0.097185	0.18405
26D	150.63	38	0.111047	0.18633

Reproduced with permission of the copyright owner. Further reproduction prohibited without permission.

Reproduced with permission of the copyright owner. Further reproduction prohibited without permission.

Table B-13 Kinetic data for studying the effect of pH on nitrate reduction at 30 °C. (All concentrations are in mg/L)

Time	Run 1E (pH = 6.68 ± 0.00, V_o = 114 mL)					Run 2E (pH = 6.82 ± 0.00, V_o = 107 mL)					Run 3E (pH = 6.85 ± 0.00, V_o = 110 mL)				
(min.)	NO_3^-	NO_2^-	*b*	N_2O	N_2	NO_3^-	NO_2^-	*b*	N_2O	N_2	NO_3^-	NO_2^-	*b*	N_2O	N_2
0	42.10	0	55.62	23.98	277.1	46.38	0	58.69	24.33	511.0	48.95	0	48.95	23.90	97.18
15	41.22	0	55.62	42.61	237.8	44.65	0	60.49	36.72	482.9	48.11	0	47.67	27.52	89.35
30	38.40	0	56.39	40.45	234.9	41.66	0	60.23	38.51	465.2	44.43	0	49.21	28.34	88.20
45	34.47	0	56.90	46.48	-	39.48	0	61.51	41.75	428.3	41.20	0	49.47	29.95	86.32
60	31.07	0	58.69	43.30	218.6	31.41	0	62.54	-	397.2	-	0	50.23	28.50	83.08
75															
90															
105															
120															

Time	Run 4E (pH = 7.06 ~ 7.10, V_o = 106 mL)					Run 5E (Same as Run 13A) (pH = 7.10 ~ 7.14, V_o = 132 mL)					Run 6E (Same as Run 11A) (pH = 7.12 ~ 7.13, V_o = 104 mL)				
(min.)	NO_3^-	NO_2^-	*b*	N_2O	N_2	NO_3^-	NO_2^-	*b*	N_2O	N_2	NO_3^-	NO_2^-	*b*	N_2O	N_2
0	48.62	0	70.74	25.92	284.2	55.50	0	28.45	23.94	369.9	46.34	0	39.21	16.79	96.78
15	38.31	0.67	70.74	25.92	283.6	54.29	0.31	28.45	26.54	377.1	37.17	1.20	42.29	17.68	95.70
30	28.19	0.75	74.07	29.16	264.4	49.96	0.26	28.96	22.10	447.6	30.37	1.51	41.78	17.89	91.02
45	19.37	0.97	76.38	33.47	259.3	46.69	0.80	32.04	25.72	346.3	22.64	1.72	44.08	17.74	87.54
60	8.72	0.66	77.92	31.37	253.7	43.42	0	32.55	26.56	291.1					
75						24.30	1.47	33.32	36.54	325.6					
90						14.60	1.40	35.11	29.44	387.2					
105						0	0	35.62	41.54	361.4					
120						0	0	37.68	31.24	381.4					

Reproduced with permission of the copyright owner. Further reproduction prohibited without permission.

Table B-13 (Continued) Kinetic data for studying the effect of pH on nitrate reduction at 30 °C. (All concentrations are in mg/L)

Time	Run 7E (Same as 14A) (pH = 7.17 ~ 7.20, V_o = 132 mL)					Run 8E (pH = 7.32 ~ 7.42, V_o = 112 mL)					Run 9E (pH = 7.99 ~ 8.04, V_o = 110 mL)				
(min.)	NO_3^-	NO_2^-	*b*	N_2O	N_2	NO_3^-	NO_2^-	*b*	N_2O	N_2	NO_3^-	NO_2^-	*b*	N_2O	N_2
0	56.62	1.41	36.65	31.91	482.9	48.14	0	71.51	18.86	336.1	47.99	0	52.29	-	-
15	54.55	2.51	36.14	33.80	459.2	41.72	4.91	73.81	19.87	310.9	38.95	4.44	51.77	2.46	118.5
30	51.71	3.92	37.93	33.80	444.3	21.76	6.88	77.66	19.94	308.5	30.91	8.52	52.29	2.61	114.3
45	37.56	3.51	38.70	38.59	406.2	10.96	7.99	77.15	21.62	280.7	22.45	12.07	54.59	2.66	101.0
60	34.22	1.52	40.50	37.70	378.5	0.89	7.87	79.97	21.31	289.4					
75	30.65	2.46	41.52	37.70	374.4										
90	10.26	0	43.83	39.26	361.5										
105	0	0	45.37	39.10	344.1										
120	0	0	46.39	34.77	331.1										

Time	Run 10E (pH = 8.00 ± 0.00, V_o = 112 mL)					Run 11E (pH = 8.06 ~ 8.08, V_o = 113 mL)					Run 12E (pH = 8.30 ~ 8.20, V_o = 109 mL)				
(min.)	NO_3^-	NO_2^-	*b*	N_2O	N_2	NO_3^-	NO_2^-	*b*	N_2O	N_2	NO_3^-	NO_2^-	*b*	N_2O	N_2
0	47.67	0	55.87	3.08	133.0	47.01	0	49.47	3.73	98.18	49.70	0	64.33	3.49	256.6
15	41.55	5.00	55.62	2.28	115.9	40.87	3.79	49.47	2.54	59.32	44.25	1.72	62.28	0	239.0
30	31.15	9.27	55.87	2.74	108.8	34.25	7.56	50.49	2.59	-	44.23	2.53	61.26	0	394.4
45	24.48	13.23	58.44	2.62	108.1	26.20	11.43	53.05	2.31	-	42.73	3.31	62.02	1.72	-
60	14.78	15.98	59.97	2.64	103.1						38.60	3.64	61.77	0	260.4
75															
90															
105															
120															

Reproduced with permission of the copyright owner. Further reproduction prohibited without permission.

Table B-13 (Continued) Kinetic data for studying the effect of pH on nitrate reduction at 30 °C. (All concentrations are in mg/L)

Time	Run 13E (pH = 8.32 ~ 8.12, V_o = 114 mL)					Run 14E (pH = 8.34 ~ 8.28, V_o = 114 mL)					Run 15E (pH = 8.45 ~ 8.43, V_o = 113 mL)				
(min.)	NO_3^-	NO_2^-	*b*	N_2O	N_2	NO_3^-	NO_2^-	*b*	N_2O	N_2	NO_3^-	NO_2^-	*b*	N_2O	N_2
0	49.28	0	47.93	0	111.9	49.05	0	58.95	1.67	292.4	54.70	0.78	61.26	452.9	294.2
15	45.39	2.38	47.93	1.89	107.0	43.61	2.09	58.95	1.67	292.4	51.17	2.58	60.23	422.7	274.5
30	38.24	4.85	48.70	0	98.18	41.56	3.79	59.97	0	247.2	49.02	3.40	61.51	386.3	250.9
45	34.41	7.91	49.21	0	96.45	38.62	4.88	62.30	0	269.8	47.19	4.18	61.77	270.0	175.4
60															
75															
90															
105															
120															

Time	Run 16E (pH = 8.65 ~ 8.63, V_o = 109 mL)					Run 17E (pH = 9.34 ~ 9.25, V_o = 110 mL)					Run 18E (pH = 10.01 ~ 10.03, V_o = 110 mL)				
(min.)	NO_3^-	NO_2^-	*b*	N_2O	N_2	NO_3^-	NO_2^-	*b*	N_2O	N_2	NO_3^-	NO_2^-	*b*	N_2O	N_2
0	50.81	0	64.33	4.67	452.6	51.59	0	64.08	9.50	344.0	51.36	0	61.26	0	-
15	49.17	1.89	65.36	0	356.6	49.63	1.82	64.33	0	346.6	50.08	0.65	58.95	-	-
30	45.74	3.01	65.87	0	335.3	48.46	2.31	62.54	0	333.8	49.54	0.68	56.39	-	-
45	44.13	3.66	65.61	0	335.4	47.84	2.61	61.77	0	268.8	48.93	0.82	55.62	0	31.02
60	42.46	4.26	66.12	0	294.5										
75															
90															
105															
120															

Reproduced with permission of the copyright owner. Further reproduction prohibited without permission.

Table B-13 (Continued) Kinetic data for studying the effect of pH on nitrate reduction at 30 °C. (All concentrations are in mg/L)

Time	Run 19E (pH = 11.60 ± 0.00, V_o = 109 mL)					Run 20E (pH = 11.92 ~ 11.90, V_o = 110 mL)					Run 21E (pH = 12.19 ~ 12.18, V_o = 110 mL)				
(min.)	NO_3^-	NO_2^-	*b*	N_2O	N_2	NO_3^-	NO_2^-	*b*	N_2O	N_2	NO_3^-	NO_2^-	*b*	N_2O	N_2
0	46.64	0	25.37	0	804.0	50.03	0	23.58	0	186.2	50.84	0	24.09	0	249.9
15	46.02	0	26.14	0	805.8	48.65	0	23.58	0	199.5	50.14	0	24.35	0	250.1
30	46.61	0	22.55	0	802.8	48.74	0	23.84	0	224.6	-	0	24.09	0	261.0
45	46.39	0	24.09	0	710.8	49.07	0	23.58	0	176.6	49.49	0	24.35	0	230.7
60															
75															
90															
105															
120															

Time	Run 22E (pH = 12.58 ~ 12.55, V_o = 115 mL)					Run 23E (pH = 12.64 ± 0.00, V_o = 116 mL)					Run 24E (pH = 12.86 ~ 12.84, V_o = 117 mL)				
(min.)	NO_3^-	NO_2^-	*b*	N_2O	N_2	NO_3^-	NO_2^-	*b*	N_2O	N_2	NO_3^-	NO_2^-	*b*	N_2O	N_2
0	48.03	0	23.32	0	900.0	50.01	0	23.07	0	325.0	52.67	0	18.45	0	901.3
15	48.11	0	22.30	0	822.8	51.14	0	23.32	0	307.4	52.13	0	18.45	0	838.2
30	50.19	0	21.27	0	668.3	49.71	0	22.55	0	285.5	52.14	0	18.45	0	788.3
45	49.33	0	21.53	0	651.7	49.70	0	21.79	0	273.2	52.30	0	18.45	0	736.2
60											52.30	0	18.20	0	701.0
75															
90															
105															
120															

Reproduced with permission of the copyright owner. Further reproduction prohibited without permission.

Table B-14 Kinetic data for studying the effect of pH on nitrite reduction at 30 °C. (All concentrations are in mg/L)

Time	Run 1F (pH = 6.48 ± 0.00, V_o = 115 mL)					Run 2F (pH = 6.89 ~ 6.85, V_o = 107 mL)					Run 3F (Same as Run 15B) (pH = 7.12 ~ 7.14, V_o = 105 mL)				
(min.)	NO_3^-	NO_2^-	*b*	N_2O	N_2	NO_3^-	NO_2^-	*b*	N_2O	N_2	NO_3^-	NO_2^-	*b*	N_2O	N_2
0	0	56.25	55.87	20.27	361.0	0	54.40	52.29	18.20	150.7	1.16	52.26	46.65	18.00	107.3
15	0	54.86	55.36	79.06	377.0	0	49.25	54.59	32.62	148.9	0	42.62	46.65	17.77	99.4
30	0	49.18	55.10	81.59	362.7	0	42.43	56.39	36.06	138.5	0	33.60	48.95	16.84	100.5
45	0	52.70	55.10	90.55	353.4	0	36.44	57.41	35.53	139.5	0	21.68	49.47	18.65	100.2
60						0	30.08	59.21	39.36	146.6	0	12.35	49.21	18.84	100.8
75															
90															
105															
120															

Time	Run 4F (pH = 7.15 ~ 7.19, V_o = 106 mL)					Run 5F (pH = 7.18 ~ 7.26, V_o = 131 mL)					Run 6F (pH = 7.18 ~ 7.24, V_o = 131 mL)				
(min.)	NO_3^-	NO_2^-	*b*	N_2O	N_2	NO_3^-	NO_2^-	*b*	N_2O	N_2	NO_3^-	NO_2^-	*b*	N_2O	N_2
0	0	56.41	56.39	14.58	105.3	0	64.80	46.65	24.93	324.7	2.74	59.86	43.06	21.66	297.5
15	0	49.04	61.51	13.70	104.4	0	61.57	45.37	27.22	315.9	1.47	55.64	46.65	22.79	293.3
30	0	41.34	60.49	14.57	105.7	0	63.06	45.37	37.62	334.4	0	50.16	45.62	23.58	294.4
45	0	32.63	61.77	14.73	103.8	0	52.06	46.39	22.53	330.0	0	41.12	46.65	24.81	298.6
60	0	24.52	63.05	14.81	101.4	0	37.58	48.44	26.00	301.8	0	31.52	48.18	25.31	295.4
75						0	18.67	48.95	28.01	300.2	0	27.16	50.23	25.91	273.0
90						0	18.26	49.98	33.74	294.0	0	18.00	53.57	-	272.5
105						0	8.58	51.77	28.37	286.9	0	15.61	55.87	36.88	271.9
120						0	4.22	52.29	28.37	276.6	0	7.95	54.59	40.54	255.6

Reproduced with permission of the copyright owner. Further reproduction prohibited without permission.

Table B-14 (Continued) Kinetic data for studying the effect of pH on nitrite reduction at 30 °C. (All concentrations are in mg/L)

Time	Run 7F (pH = 7.25 ~ 7.30, V_o = 107 mL)					Run 8F (pH = 7.34 ~ 7.36, V_o = 108 mL)					Run 9F (pH = 7.46 ~ 7.47, V_o = 109 mL)				
(min.)	NO_3^-	NO_2^-	*b*	N_2O	N_2	NO_3^-	NO_2^-	*b*	N_2O	N_2	NO_3^-	NO_2^-	*b*	N_2O	N_2
0	0	54.63	52.29	11.90	74.6	0	56.90	54.85	20.34	197.1	0	56.46	53.31	15.01	88.90
15	0	49.22	52.80	11.33	49.2	0	52.57	56.90	14.43	195.98	0	48.99	54.08	9.15	87.93
30	0	41.76	54.59	10.97	79.3	0	45.35	57.92	12.38	-	0	43.17	55.36	8.48	-
45	0	28.41	5510	12.12	80.68	0	37.93	58.69	12.67	184.03	0	36.19	55.36	8.61	-
60	0	25.60	56.39	12.83	82.78	0	30.26	59.21	12.24	171.16	0	28.62	57.41	8.78	89.77
75															
90															
105															
120															

Time	Run 10F (pH = 7.93 ~ 7.95, V_o = 110 mL)					Run 11F (pH = 8.21 ~ 8.33, V_o = 115 mL)					Run 12F (pH = 8.88 ~ 9.09, V_o = 111 mL)				
(min.)	NO_3^-	NO_2^-	*b*	N_2O	N_2	NO_3^-	NO_2^-	*b*	N_2O	N_2	NO_3^-	NO_2^-	*b*	N_2O	N_2
0	0	55.32	67.15	4.81	531.7	0	58.57	32.81	-	195.7	0	53.11	56.39	9.48	374.2
15	0	52.81	68.94	5.04	-	0	58.28	30.24	2.24	172.6	0	52.38	58.18	2.01	337.4
30	0	49.92	67.92	-	546.0	0	56.30	31.27	0	131.0	0	52.15	59.46	1.39	321.4
45	0	45.55	68.69	4.72	521.3	0	54.32	30.76	0	125.4	0	52.10	59.46	0	292.8
60											0	50.18	58.69	0	282.4
75															
90															
105															
120															

Table B-15 Net specific growth rates of biomass on nitrate and average nitrate removal rates at T = 30 °C and various pH values. Data used in Figures 13 and B-12.

Experimental Run	Initial nitrate concentration (mg/L)	pH	Net specific growth rate, μ_{1net} (h^{-1})	Average denitrification rate, RD (g NO_3^-/h/g Biomass)
1E	42.10	6.68	0.06832	0.19298
2E	46.38	6.82	0.09383	0.24697
3E	48.95	6.85	0.10474	0.28454
4E	48.62	7.06	0.14080	0.53680
5E, 13A	54.29	7.10	0.14314	0.47519
6E, 11A	46.34	7.12	0.14899	0.67292
7E, 14A	54.55	7.17	0.14463	0.61550
8E	48.14	7.32	0.13821	0.62384
9E	47.99	7.99	0.10605	0.63723
10E	47.67	8.00	0.10845	0.56785
11E	47.01	8.06	0.09847	0.54129
12E	49.70	8.30	0.04990	-
13E	49.28	8.32	0.05277	0.40821
14E	49.05	8.34	0.04217	0.22939
15E	54.70	8.45	0.04167	0.16278
16E	50.81	8.65	0.02357	0.12802
17E	51.59	9.34	-0.05531	0.07946
18E	51.36	10.01	-0.13366	0.05544
19E	46.64	11.60	0.01941	0.01348
20E	50.03	11.92	0.0	0
21E	50.14	12.19	0.00847	0
22E	48.03	12.58	-0.18400	0
23E	50.01	12.64	0.0	0
24E	52.67	12.86	0.0	0

Reproduced with permission of the copyright owner. Further reproduction prohibited without permission.

Table B-16 Net specific growth rates of biomass on nitrite and average nitrite removal rates at T = 30 °C and various pH values. Data used in Figures 13 and B-12.

Experimental Run	Initial nitrite concentration (mg/L)	pH	Net specific growth rate, μ_{2net} (h^{-1})	Average denitrification rate, RD (g NO_2^-/h/g Biomass)
1F	56.25	6.48	-0.01848	0.08531
2F	54.40	6.89	0.11958	0.43623
3F, 15B	52.26	7.12	0.15522	0.83267
4F	56.41	7.15	0.14041	0.53399
5F	52.06	7.18	0.12058	0.61229
6F	59.86	7.18	0.13064	0.58794
7F	54.63	7.25	0.13366	0.53423
8F	56.90	7.34	0.10912	0.46712
9F	56.46	7.46	0.08512	0.50289
10F	55.32	7.93	0.02118	0.19179
11F	58.57	8.21	-0.06411	0.17828
12F	53.11	8.88	0.04079	0.05092

Reproduced with permission of the copyright owner. Further reproduction prohibited without permission.

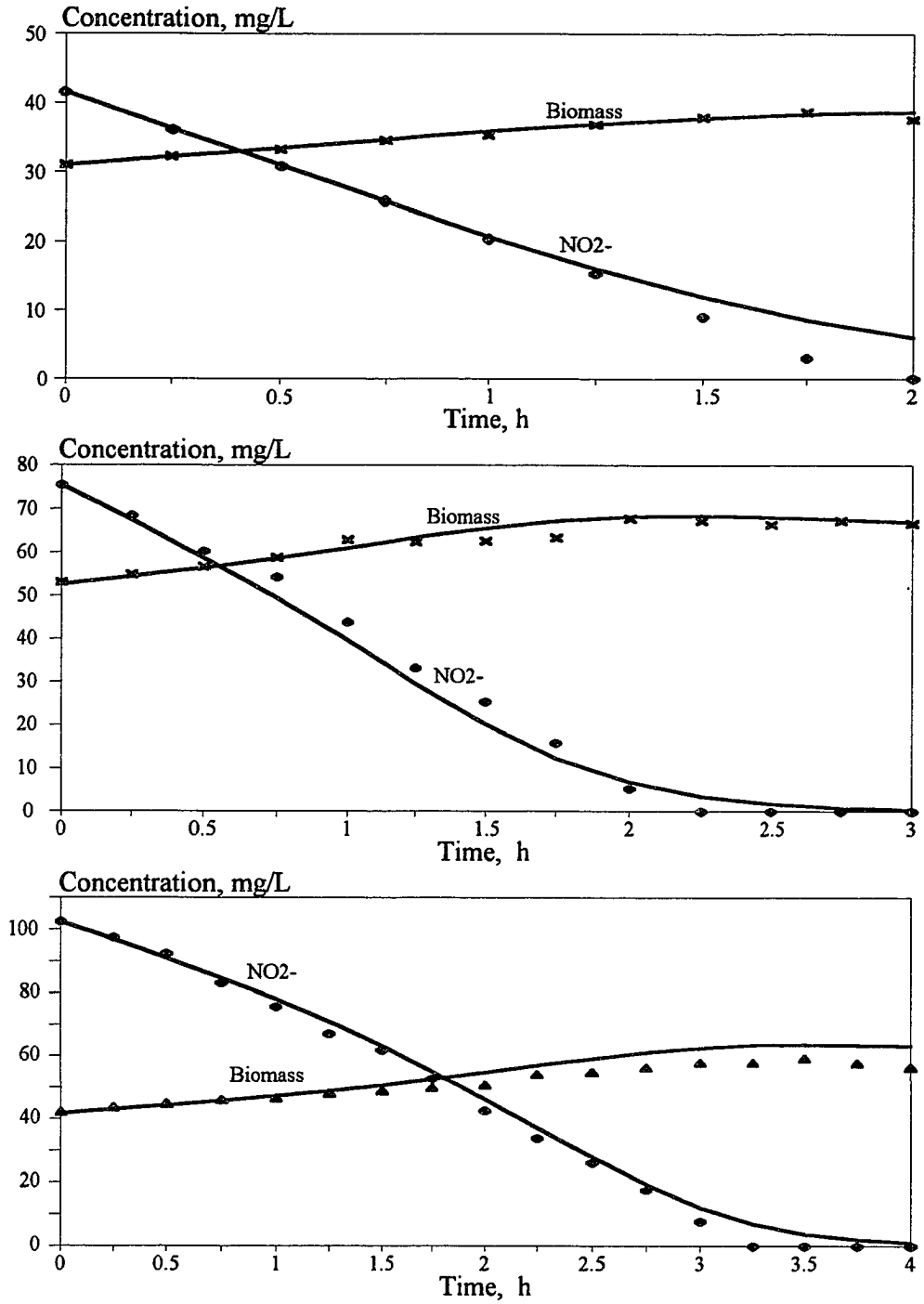

Figure B-1 Comparison of experimental data (from runs 13B, 20B, and 25B) and model predictions (curves) for nitrite consumption at 30 °C and pH = 7.1 ± 0.1.

Reproduced with permission of the copyright owner. Further reproduction prohibited without permission.

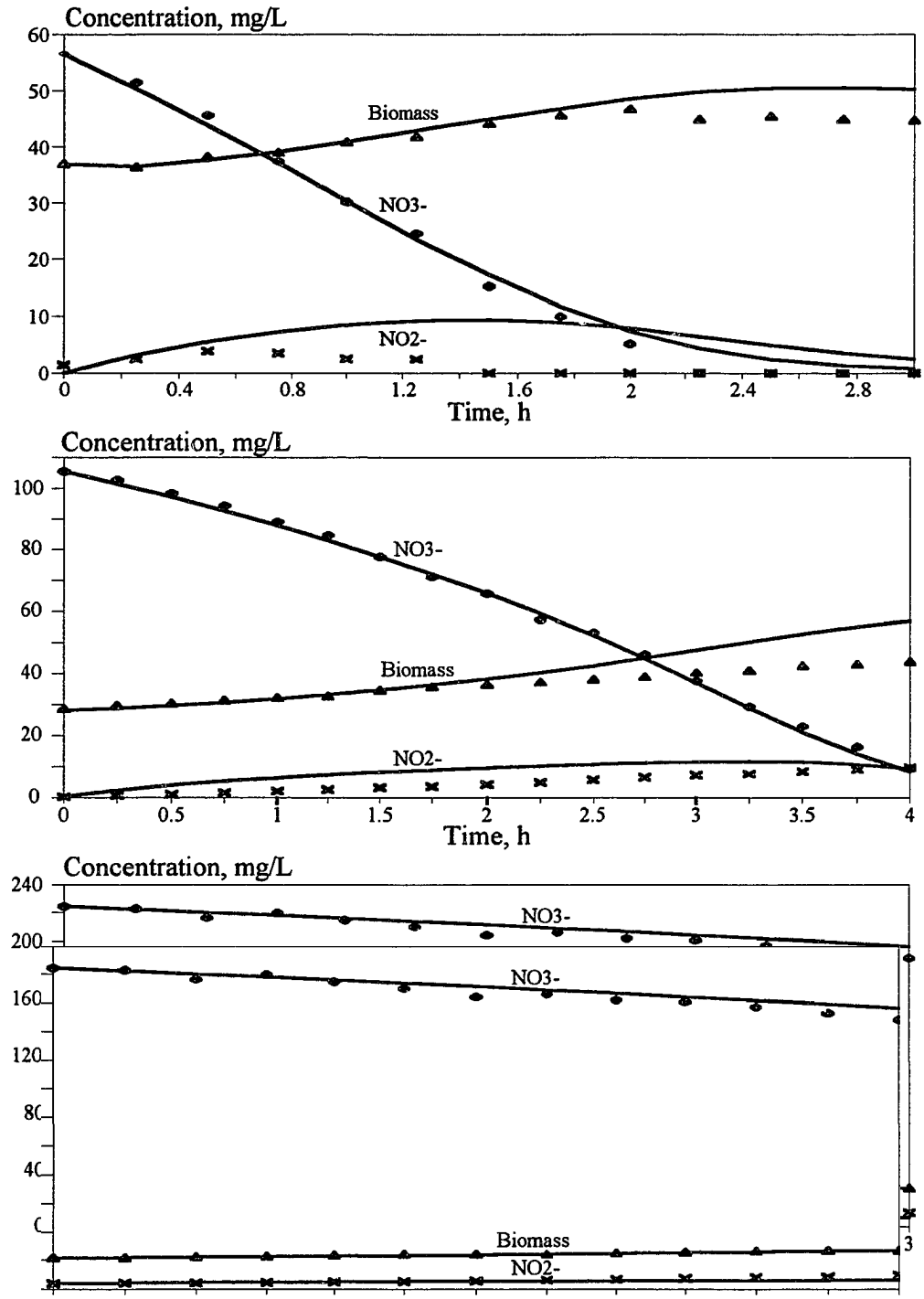

Figure B-2 Comparison of experimental data (from runs 14A, 22A, and 32A) and model predictions (curves) for nitrate consumption at 30 °C and pH = 7.1 ± 0.1.

Reproduced with permission of the copyright owner. Further reproduction prohibited without permission.

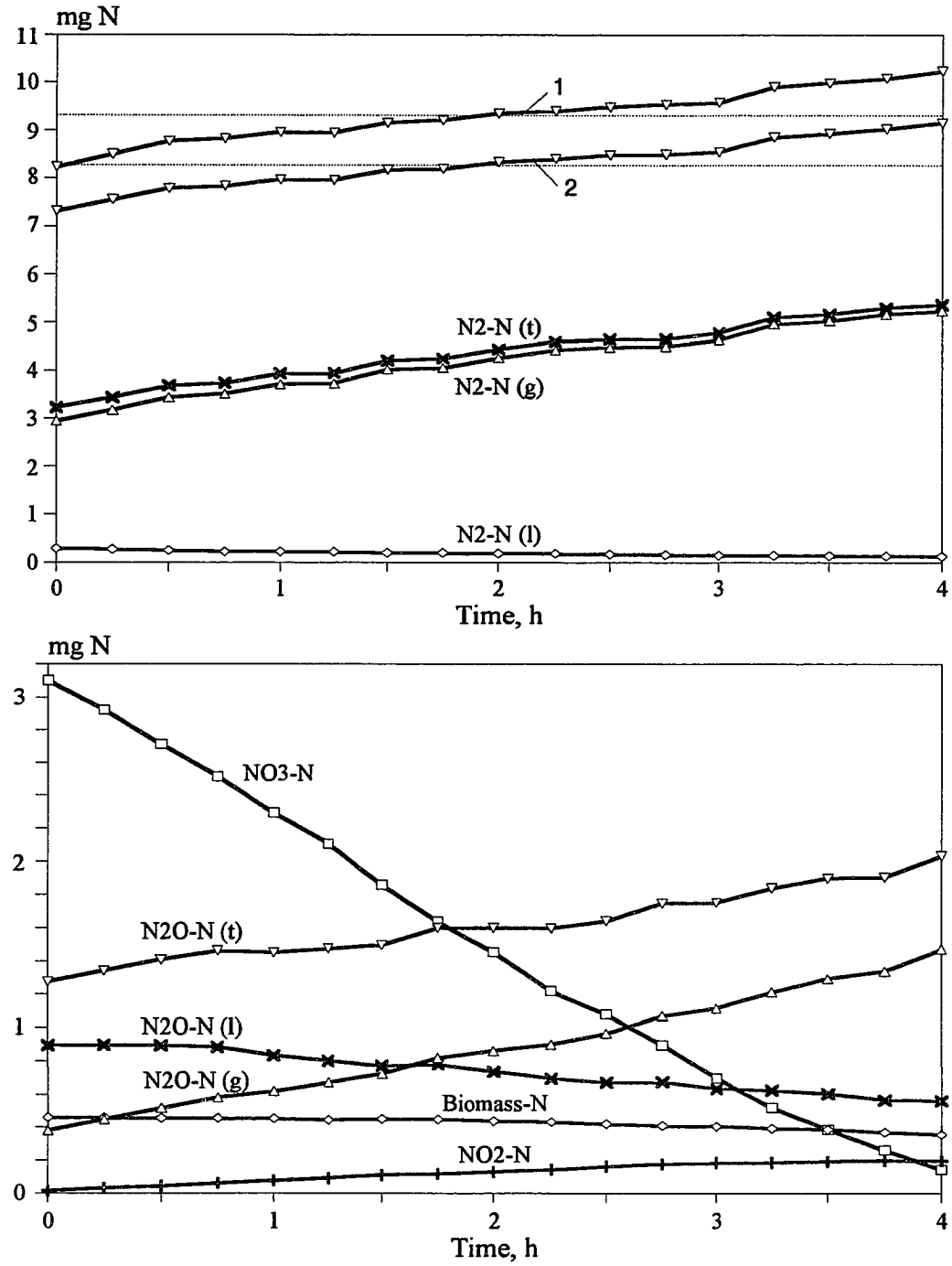

Figure B-3 Nitrogen mass balance as a function of time during experimental run 22A. Curves 1 and 2 in top diagram indicate total nitrogen when N_2O presence in the liquid is considered and neglected, respectively.

Reproduced with permission of the copyright owner. Further reproduction prohibited without permission.

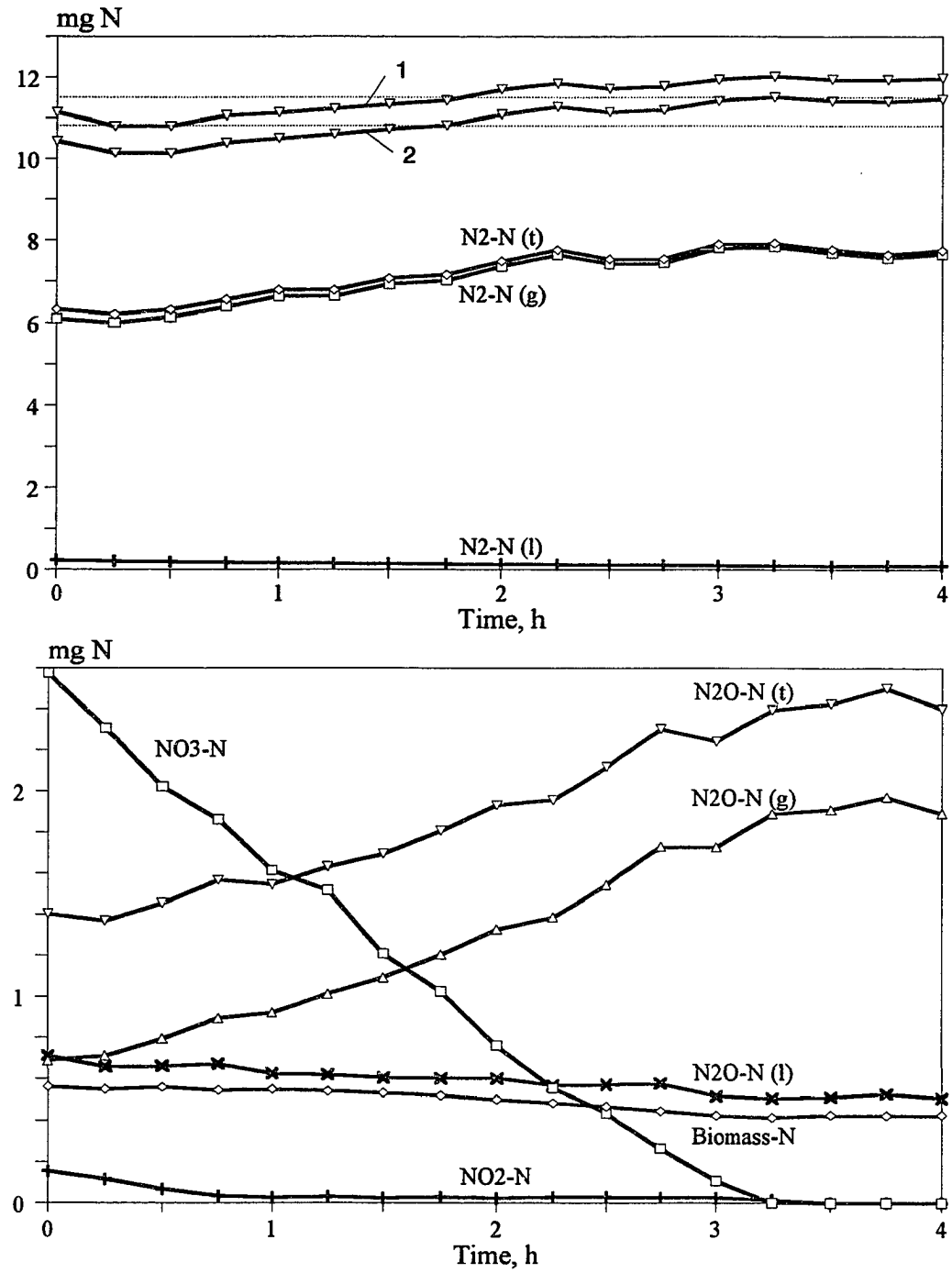

Figure B-4 Nitrogen mass balance as a function of time during experimental run 4G. Curves 1 and 2 in top diagram indicate total nitrogen when N_2O presence in the liquid is considered and neglected, respectively.

Reproduced with permission of the copyright owner. Further reproduction prohibited without permission.

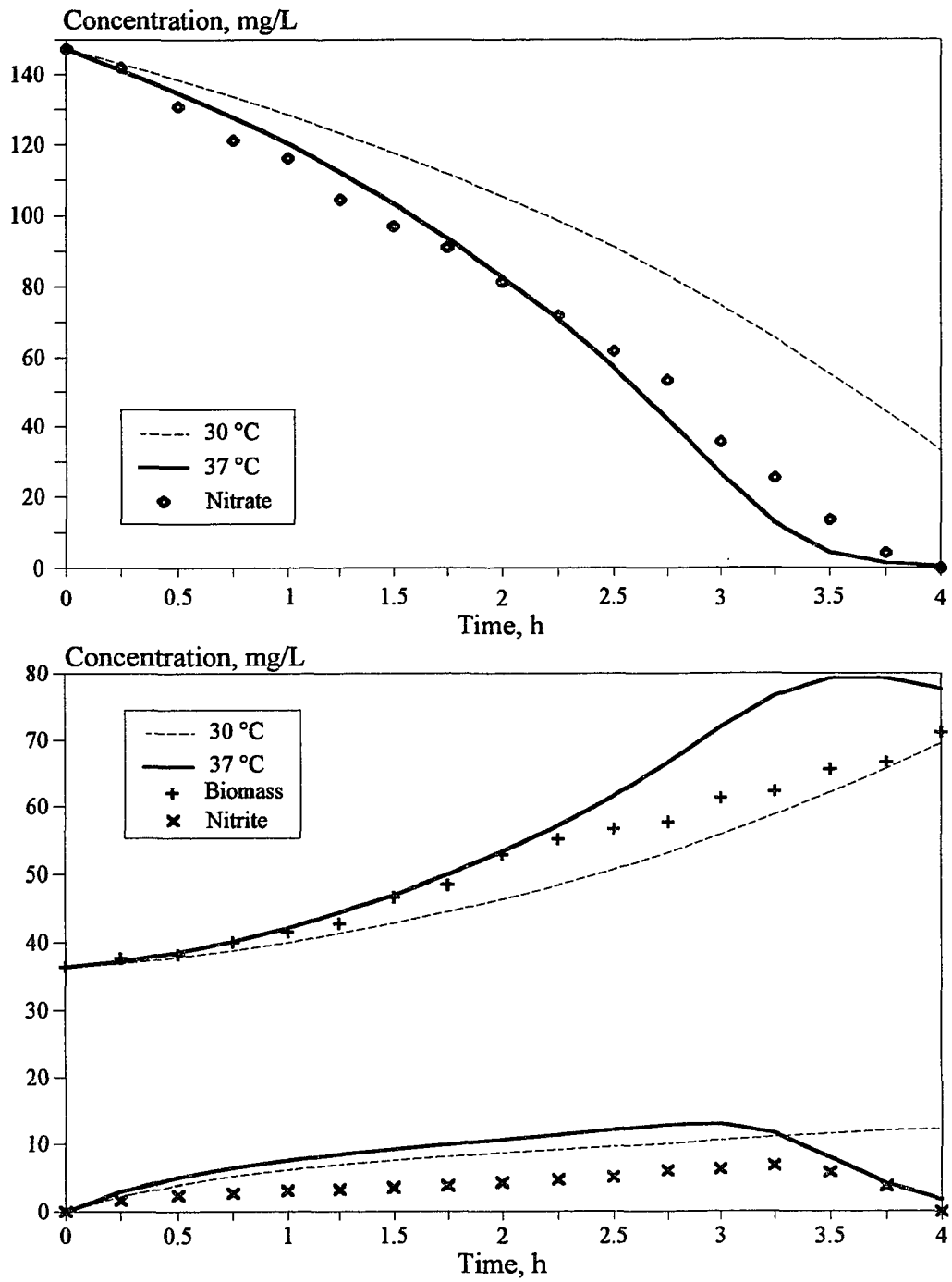

Figure B-5 Nitrate reduction at 37 °C (pH = 7.1 ± 0.1). Curves indicate model predictions with constants corrected for temperature (solid). Dashed curves are model predictions with values of constants at 30 °C. Data are from run 3H.

Reproduced with permission of the copyright owner. Further reproduction prohibited without permission.

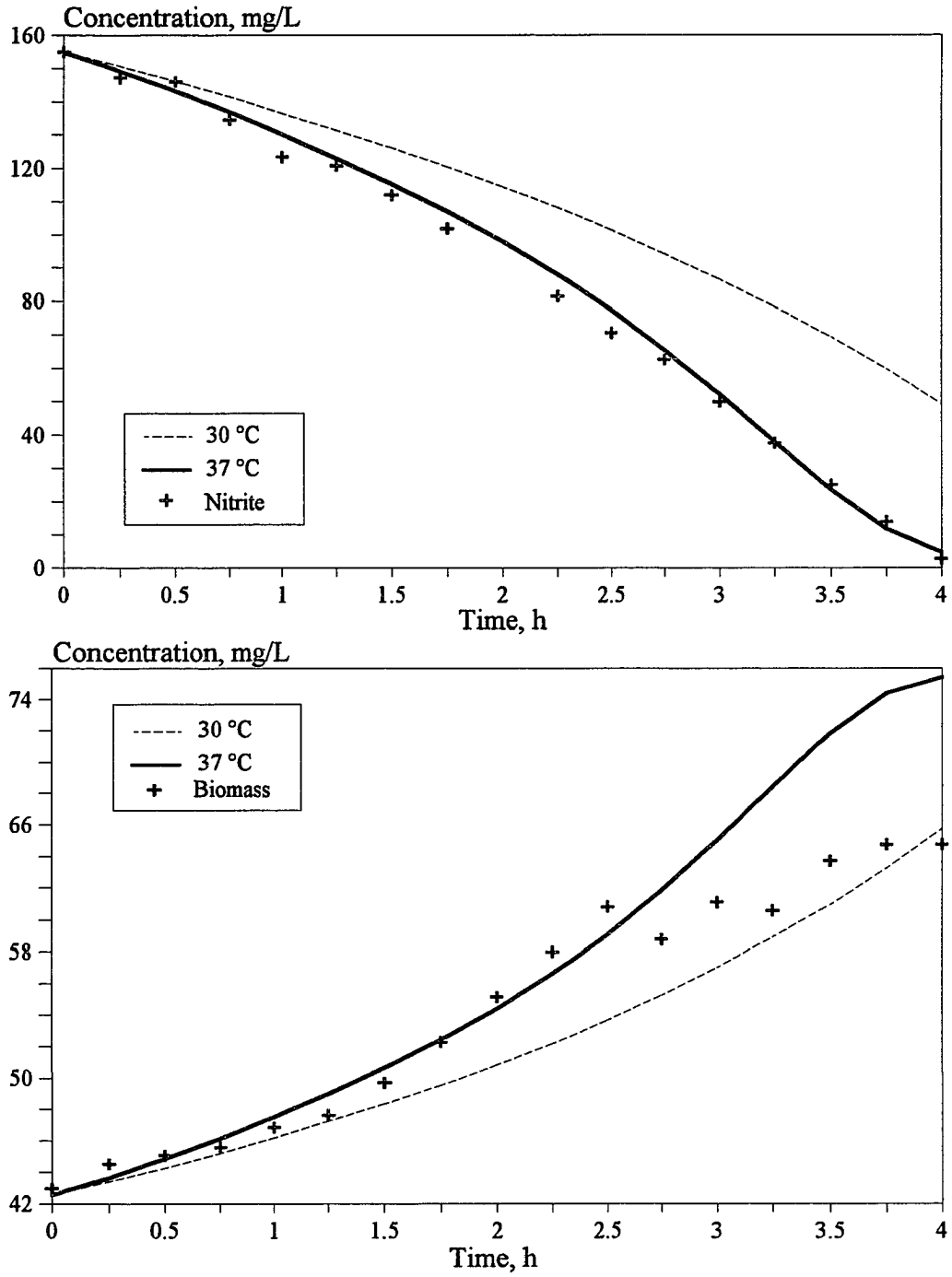

Figure B-6 Nitrite reduction at 37 °C (pH = 7.1 ± 0.1). Solid curves are model predictions; dashed curves are model predictions based on constants at 30 °C. This graph indicates the dependence of biokinetic constants on temperature. Data are from run 2H.

Reproduced with permission of the copyright owner. Further reproduction prohibited without permission.

Reproduced with permission of the copyright owner. Further reproduction prohibited without permission.

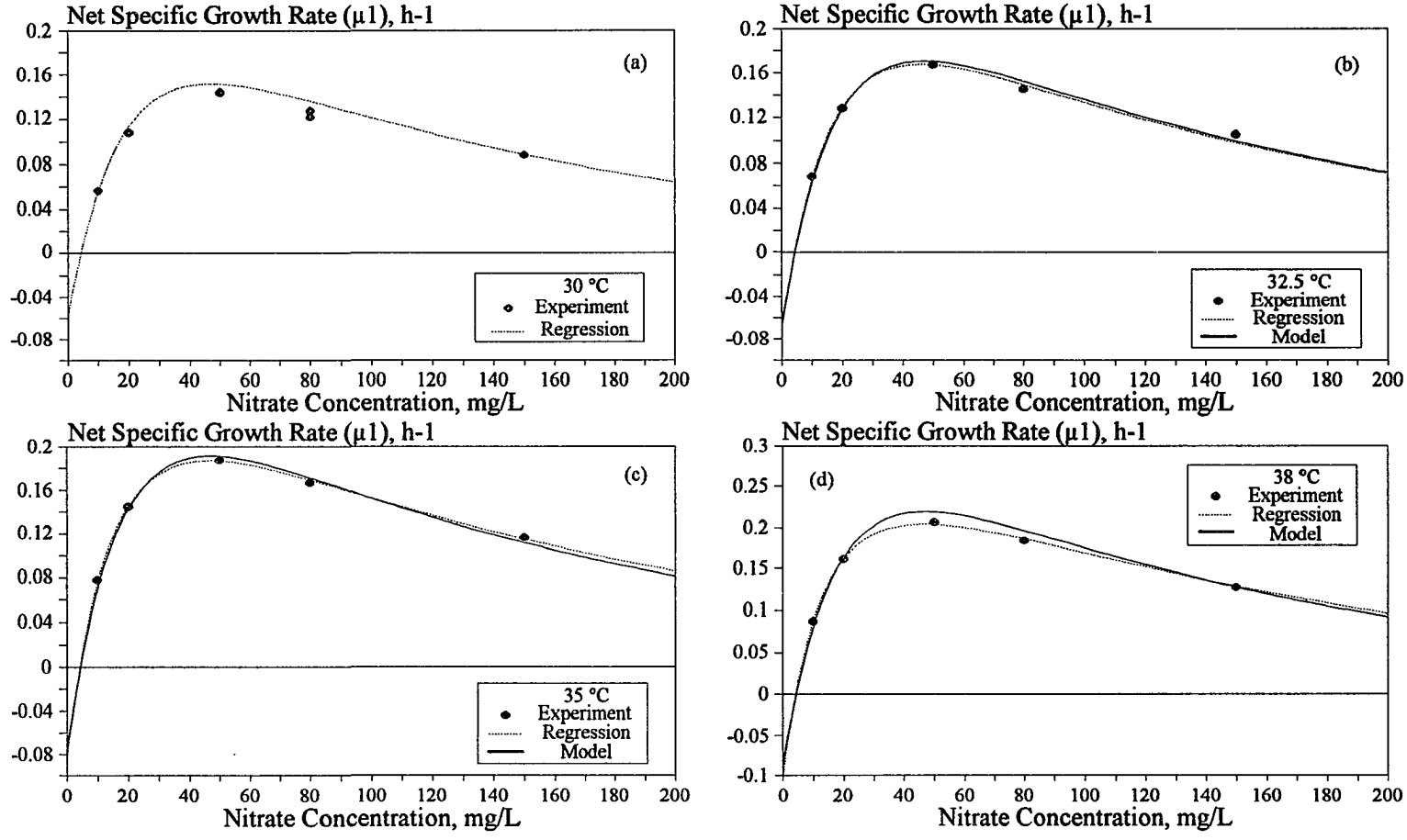

Figure B-7 Comparison of experimental data and model predictions for the net specific growth rate on nitrate at different temperatures. Solid curves indicate model predictions corrected for temperature based on an overall activation energy; dashed curves indicate the results of regression of the data to the Andrews/Herbert model (pH = 7.1 ± 0.1).

Reproduced with permission of the copyright owner. Further reproduction prohibited without permission.

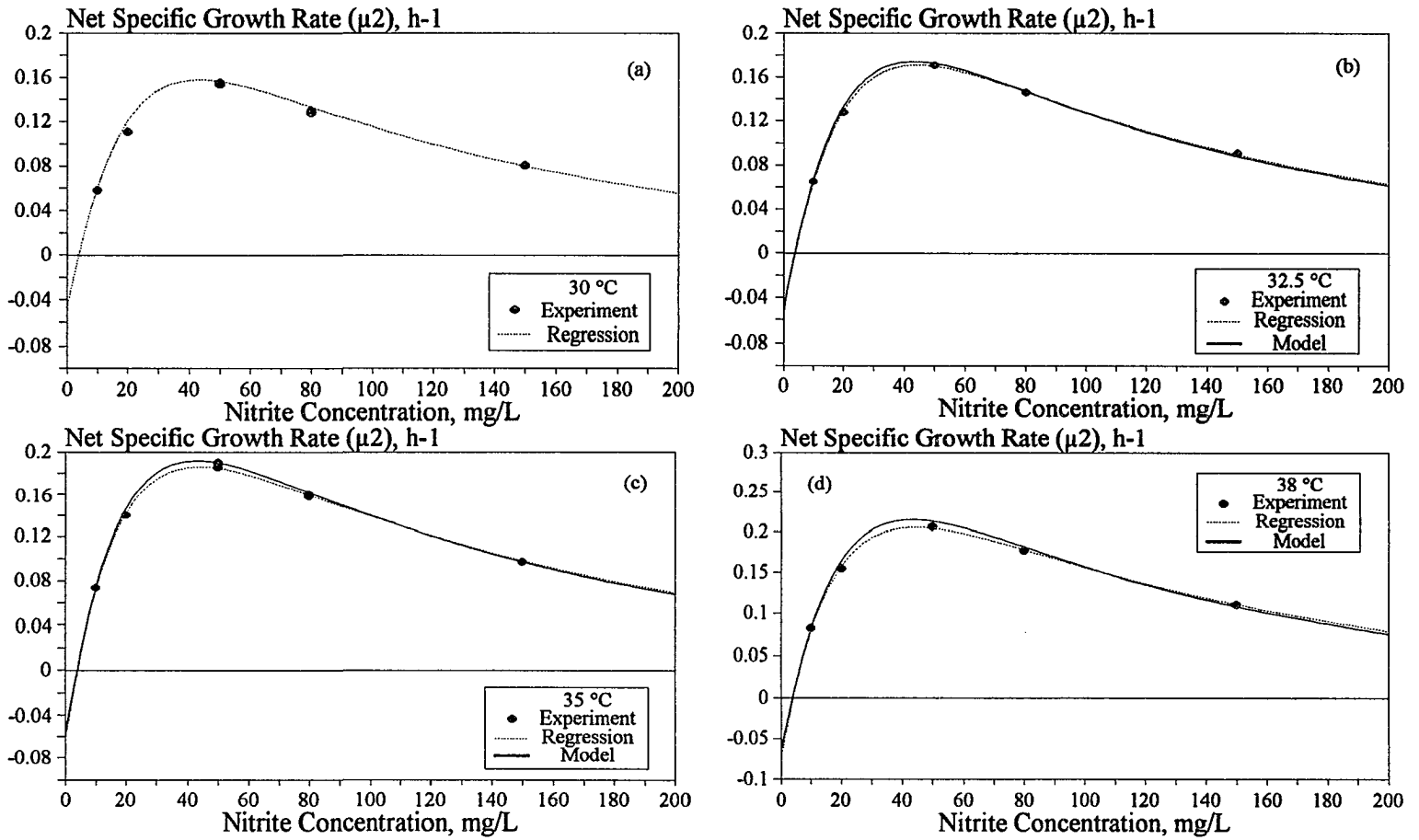

Figure B-8 Comparison of experimental data and model predictions for the net specific growth rate on nitrite at different temperatures. Solid curves indicate model predictions corrected for temperature based on an overall activation energy; dashed curves indicate the results of regression of the data to the Andrews/Herbert model (pH = 7.1 ± 0.1).

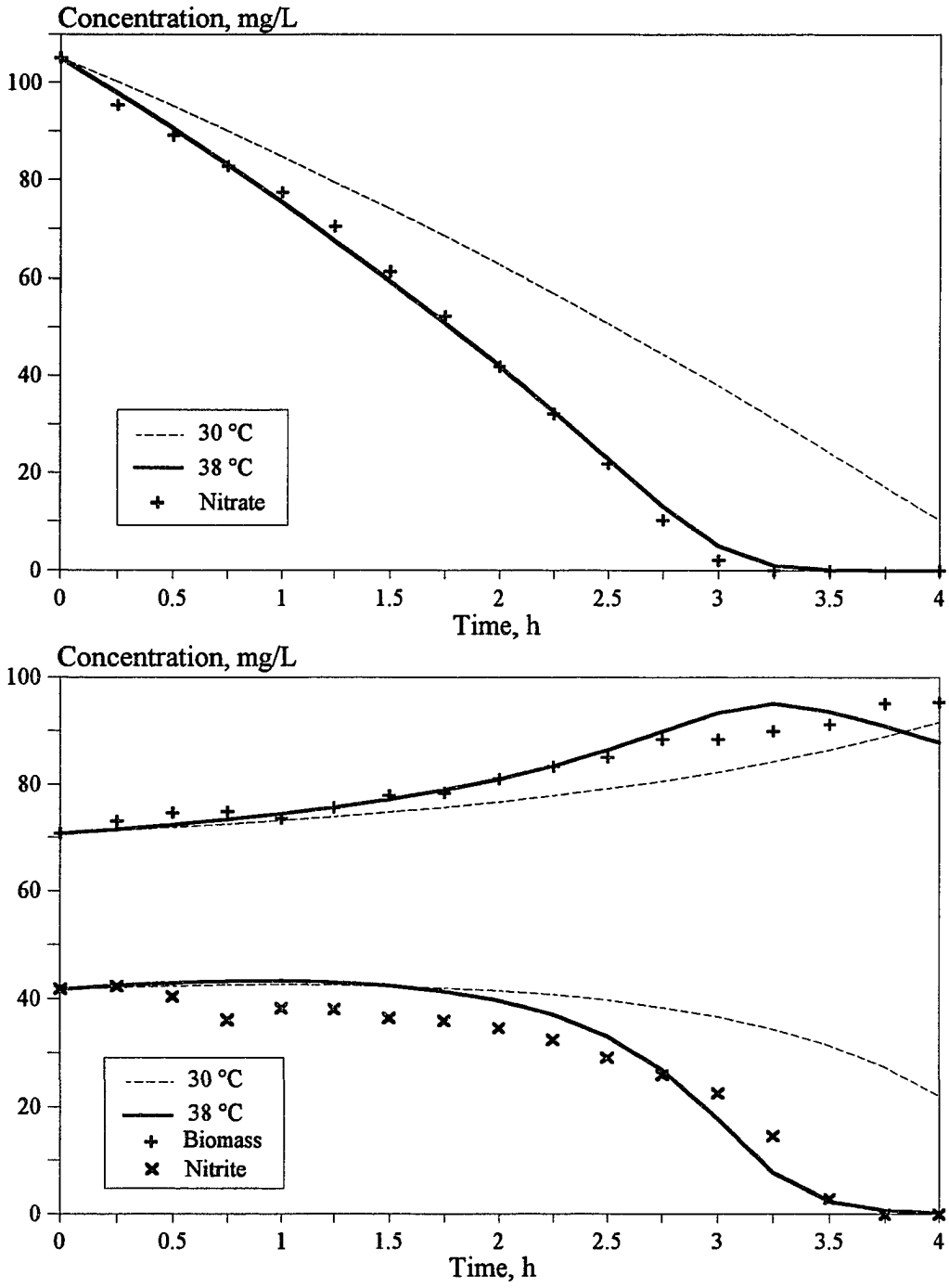

Figure B-9 Biological removal of a NO_3^-/NO_2^- mixture at 38°C (pH = 7.1 ± 0.1). Solid curves indicate model predictions with constants corrected for temperature; dashed curves are predictions based on constants at 30 °C. Data are from run 6G.

Reproduced with permission of the copyright owner. Further reproduction prohibited without permission.

Reproduced with permission of the copyright owner. Further reproduction prohibited without permission.

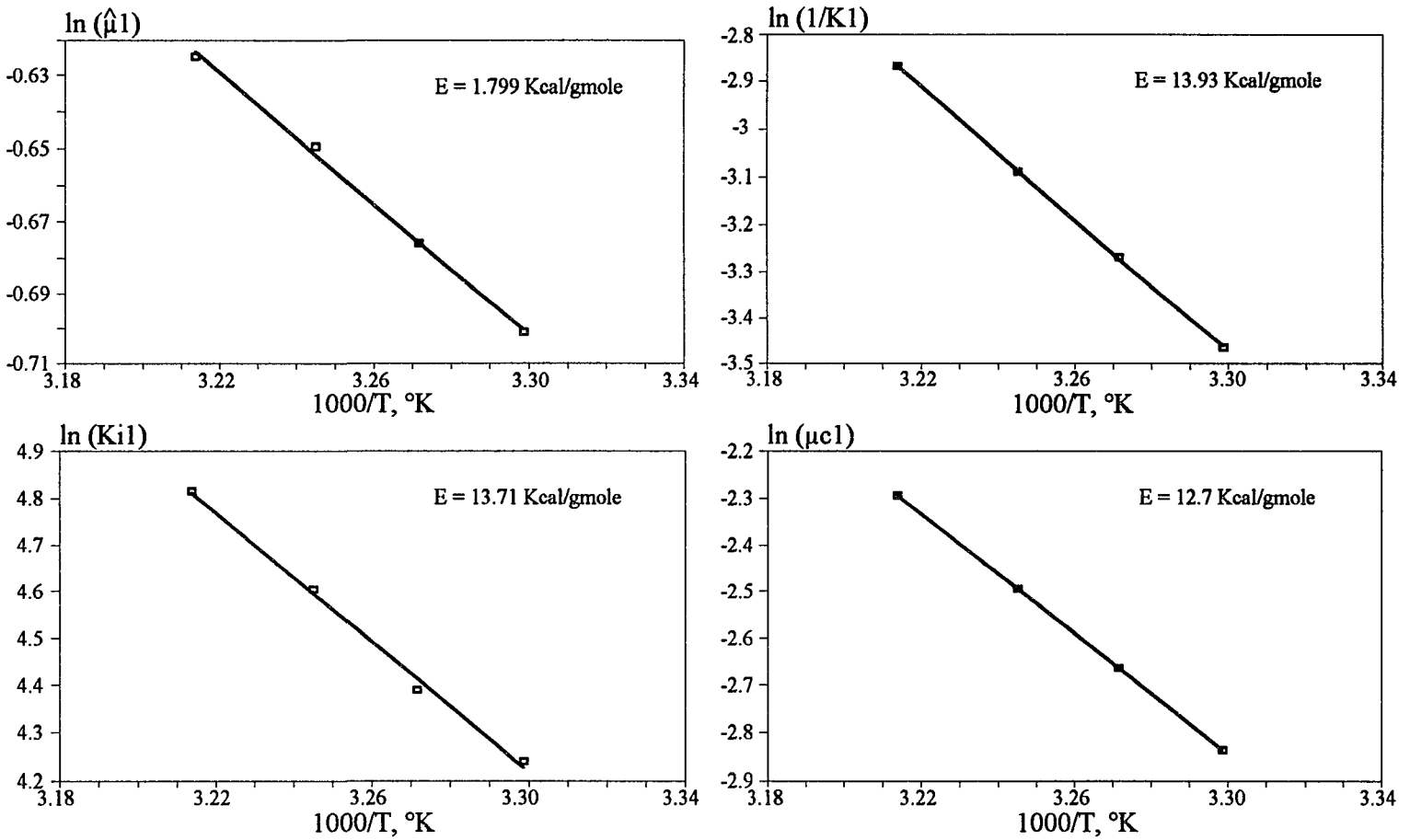

Figure B-10 Arrhenius plots for individual kinetic constants in the expression for nitrate reduction. Values of constants are from regressions of experimental data at different temperatures (pH = 7.1 ± 0.1).

Reproduced with permission of the copyright owner. Further reproduction prohibited without permission.

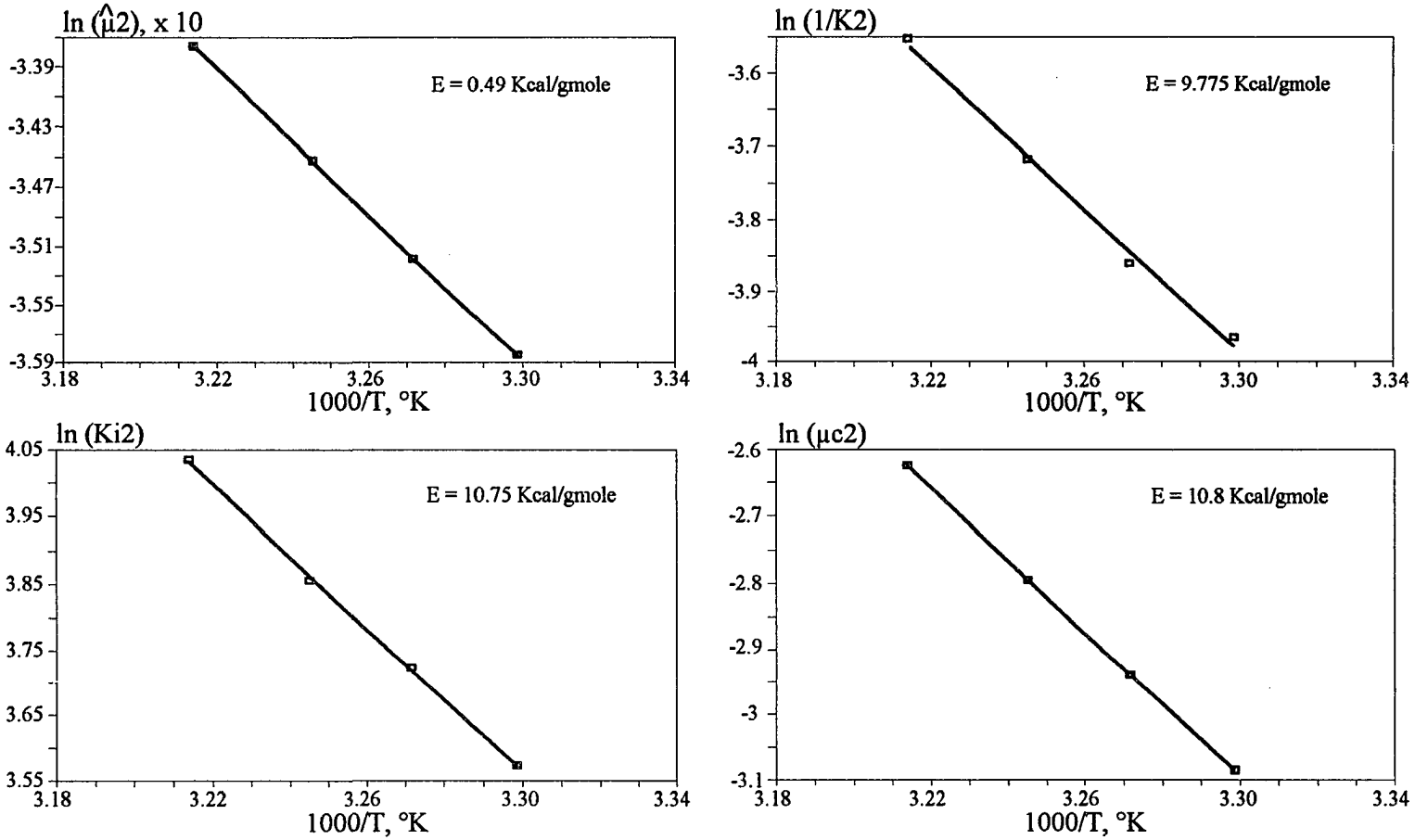

Figure B-11 Arrhenius plots for individual kinetic constants in the expression for nitrite reduction. Values of constants are from regressions of experimental data at different temperatures (pH = 7.1 ± 0.1).

Reproduced with permission of the copyright owner. Further reproduction prohibited without permission.

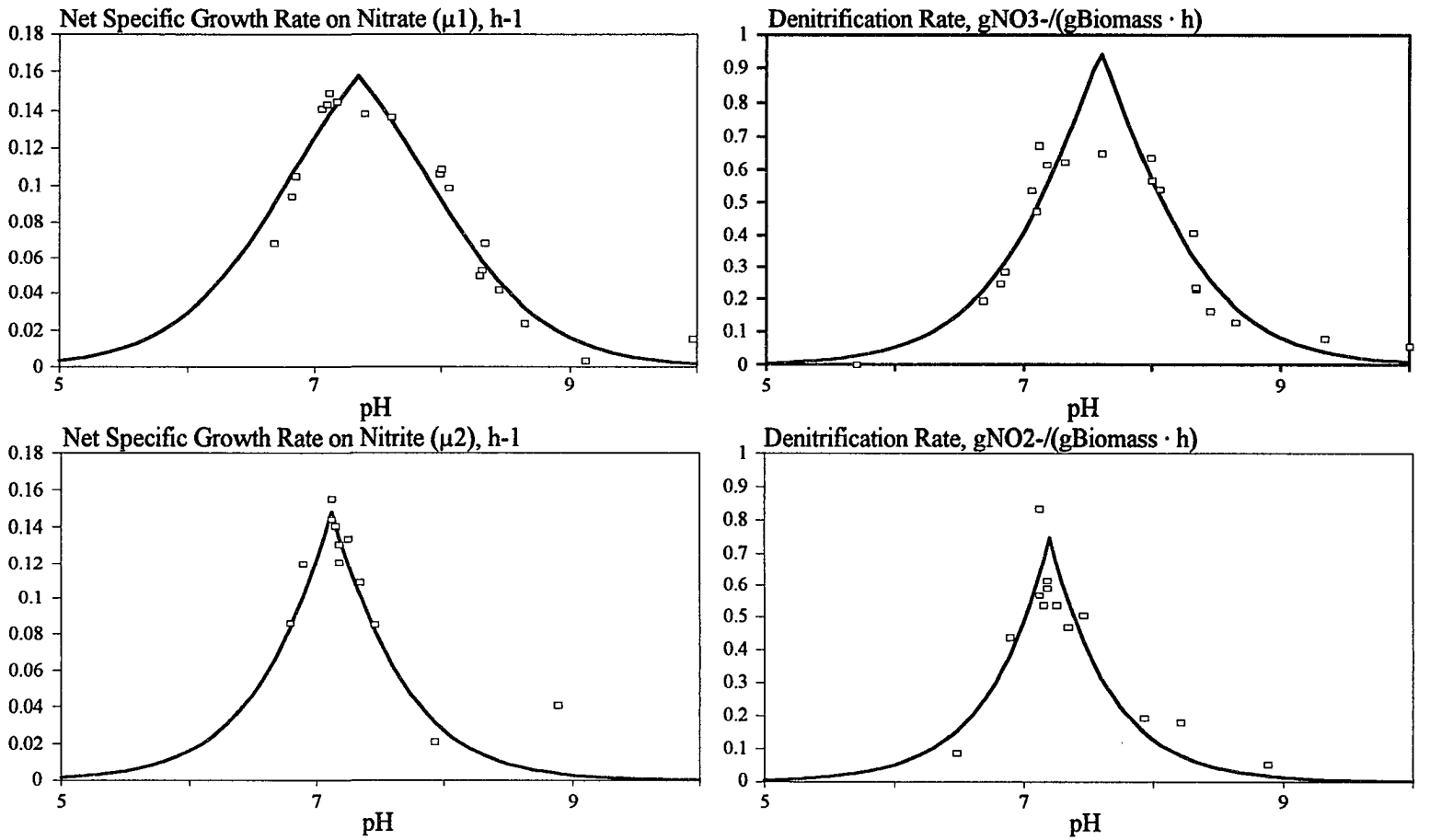

Figure B-12 Dependence of net specific growth rates and denitrification rates on pH. Curves from fitting the data to the non-competitive inhibition pH-functions (data also shown in Tables B-12 and B-13; in all runs the initial concentration of NO_3^- or NO_2^- is 50 mg/L, T = 30 °C).

APPENDIX C

ESTIMATION OF THE PRESENCE OF NITROGEN AND NITROUS OXIDE IN THE LIQUID PHASE

Reproduced with permission of the copyright owner. Further reproduction prohibited without permission.

Gas solutes are so dilute that Henry's law is applicable, and one needs to measure the mole fraction in the liquid phase at a single pressure[1].

Henry's law can be written as

$$p_j = y_j P = K_j x_j \qquad (C.1)$$

where p_j is the partial pressure of the solute; P is the total pressure; y_j and x_j are the mole fractions of the solute in the gas and liquid phase, respectively; K_j is a function of temperature, characteristic for a particular solute.

For nitrogen, the value of K_{N_2} at 30 °C is given[2] as 92400 atm/mole fraction. For nitrous oxide, the value of K_{N_2O} can be found as follows. Published data[3,4] indicate that there is a linear relationship between ln K and ln T, over specific temperature ranges. For nitrous oxide, one can find the following,

T (°C)	0	35
K_{N_2O} (atm/mole fraction)	987	2960

Using the data above, one can show that

$$K_{N_2O} = \left(\frac{T}{273.15}\right)^{9.11} \times 987 \qquad (C.2)$$

From equation (C.2), and for T = 30 °C (303.15 K), one gets K_{N_2O} = 2550 atm/mole fraction.

Assuming that the pressure in the headspace of the bottle (reactor), remains at 1 atm, from equation (C.1) and the values of K_j discussed above, one gets,

---

[1] Hildebrand, J. H. and R. L. Scott, *Regular Solutions*. Chapter 2, p.23, Printice-Hall, Englewood, New Jersey (1962)

[2] Thibodeaux, L. J. *Chemodynamics*. John Wiley & Sons, New York, NY (1979)

[3] Grayson, M. (ed.), *Kirk-Othmer Encyclopedia of Chemical Technology*. 3rd Edition, 9:99 John Wiley & Sons, New York, New York (1980)

[4] US National Research Council. *International Critical Tables of Numerical Data, Phisics, Chemistry and Technology*. First Edition, 3:259 McGraw-Hill, New York, New York (1928)

Reproduced with permission of the copyright owner. Further reproduction prohibited without permission.

$$x_{N_2} = \frac{y_{N_2}}{92,400} \tag{C.3}$$

$$x_{N_2O} = \frac{y_{N_2O}}{2,550} \tag{C.4}$$

Since the amount of N_2 and N_2O in the gas phase are known (columns m and ℓ of Table B-6), and if it is assumed that the gas behaves as an ideal one, one can calculate y_{N_2} and y_{N_2O} from the following equations,

$$y_{N_2} = \frac{m_{N_2}RT}{28,000V_g} \tag{C.5}$$

$$y_{N_2O} = \frac{m_{N_2O}RT}{44,000V_g} \tag{C.6}$$

where m_{N_2} and m_{N_2O} are the entries of columns m and ℓ, respectively, of Table B-6, and V_g is the corresponding entry of column h of Table B-6.

Combining equations (C.3) and (C.5) one gets

$$x_{N_2} = \frac{m_{N_2}RT}{28,000 \cdot V_g \cdot 92,400} \tag{C.7}$$

Similarly from (C.4) and (C.6) one gets

$$x_{N_2O} = \frac{m_{N_2O}RT}{44,000 \cdot V_g \cdot 2,550} \tag{C.8}$$

Now assuming that the liquid phase is practically only water, one can get

$$x_{N_2} = \frac{C_{N_2}}{28,000 \cdot \frac{1,000}{18}}$$

$$\text{or,} \quad C_{N_2} = \frac{28,000 \cdot 1000 \cdot x_{N_2}}{18} \tag{C.9}$$

where C_{N_2} is the concentration of N_2 in the liquid phase (in units of mg/L).

Similarly from (C.4) and (C.6) one gets

$$C_{N_2O} = \frac{44,000 \cdot 1000 \cdot x_{N_2O}}{18} \tag{C.10}$$

where C_{N_2O} is the concentration of N_2O in the liquid phase (in units of mg/L).

Reproduced with permission of the copyright owner. Further reproduction prohibited without permission.

From equations (C.7) and (C.9) it follows that

$$C_{N_2} = \frac{m_{N_2} RT \cdot 1,000}{18 \cdot V_g \cdot 92,400} \qquad (C.11)$$

Observe that m_{N_2}/V_g is actually the gas phase concentration of N_2, i.e., column e of Table B-6. Hence, from the measured values shown in column e one can calculate the values of column e1 (Table B-6), via equation (C.11). The value of T is 303.15 K and R = 0.082 L·atm/mole/K.

Similarly, from equations (C.8) and (C.10), one gets

$$C_{N_2O} = \frac{m_{N_2O} RT \cdot 1,000}{18 \cdot V_g \cdot 2,550} \qquad (C.12)$$

Again, the ratio m_{N_2O}/V_g is the measured value of N_2O gas phase concentration measured at a particular instant of time. These values are given as entries of column d in Table B-6. From these values, and using equation (C.12) the entries of column d1 in Table B-6 are calculated.

Since the value of K_{N_2O} plays an important role in calculating the N_2O presence in water, a further search of the literature was performed regarding K_{N_2O} values. The following data were found regarding saturation solubilities of N_2O in water for P = 1 atm.

	In 100 mL water		
V_{N_2O} dissolved (mL)	[5] 60.82	[6] 53.00	[5,7] 130.52
T	hot	30 °C	cold

Saturation concentrations are concentrations of N_2O in water when the water is in equilibrium with a N_2O gas atmosphere. Thus,

[5] Perry, J. H. and C. Chilton, *Chemical Engineer Handbook.* 5th Edition, McGraw-Hill, New York, New York (1973)

[6] Kunerth, W. "Solubility of CO_2 and N_2O in Certain Solvents." *Phys. Rev.*, 19:512-524 (1922)

[7] Streuli, C. A. and P. R. Averell, *The Analytical Chemistry of Nitrogen And Its Compounds.* Part I, John Wiley & Sons, New York, New York (1970)

Reproduced with permission of the copyright owner. Further reproduction prohibited without permission.

$$K_{N_2O} = \frac{1}{x_{N_2O,\,sat}} \qquad [y_{N_2O} = 1 \text{ in this case}]$$

If one assumes ideal gas behavior for N_2O, and if the liquid phase is considered as made up of water only,

$$x_{N_2O,\,sat} = \frac{V_{N_2O} \cdot 18}{RT \cdot 100} \tag{C.13}$$

where V_{N_2O} is the volume of N_2O gas dissolved in water at saturation. Thus, from the value of V_{N_2O} reported at 30 °C,

$$K_{N_2O} = \frac{1}{x_{N_2O,\,sat}} = \frac{RT \times 100}{18 \times 0.053} = 2606 \text{ atm/mole}$$

The value of 2606 atm/mole can be viewed as close to the value of 2550 atm/mole which, as discussed earlier, was obtained from correlation (C.2). If a value of 2606 atm/mole was to be used, the changes in the values of entries of column d1 in Table B-6 should be negligible.

It should be mentioned that the procedure discussed above regarding estimation of N_2O presence in the liquid phase, implicitely assumes that N_2O reacts so slowly in the liquid phase that equilibrium is always maintained.

Reproduced with permission of the copyright owner. Further reproduction prohibited without permission.

APPENDIX D

OPERATING CONDITIONS FOR SBR RUNS, SBR DATA, AND COMPARISONS BETWEEN EXPERIMENTAL AND THEORETICAL SBR CONCENTRATION PROFILES

Reproduced with permission of the copyright owner. Further reproduction prohibited without permission.

Table D-1 Conditions for experiments SBR-1 and SBR-2. Feed stream contains nitrite only.

Experiment	SBR-1	SBR-2
Region in Figure 16	I	II
β	5.59	6.99
u_f (mg/L)	51.07	50.88
z_f	1.60	1.59
u_o (mg/L)	30.87	26.90
z_o	0.965	0.841
b_o (mg/L)	2.05	8.77
x_o	0.207	0.886
V_{max} (L)	2.0	2.0
V_o (L)	1.0	1.0
δ	0.5	0.5
t_3 (h)	4.0	5.0
t_1 (h)	0.4	0.5
σ_1	0.1	0.1
Q_f^* (L/h)	2.5	2.0

Reproduced with permission of the copyright owner. Further reproduction prohibited without permission.

Table D-2 Conditions for experiments SBR-3 through SBR-7. Feed streams contain mixtures of nitrate and nitrite.

Experiment	SBR-3	SBR-4	SBR-5	SBR-6	SBR-7
Region in Figure 17	I	II	IV	IV	IV
β	5.59	6.99	7.54	6.65	9.78
s_f (mg/L)	37.25	34.43	75.45	63.75	96.33
y_f	1.165	1.077	2.36	1.994	3.013
u_f (mg/L)	95.21	106.10	99.37	98.51	93.14
z_f	2.978	3.318	3.108	3.081	2.913
s_o (mg/L)	12.46	23.02	64.17	5.36	0
y_o	0.39	0.72	2.007	0.168	0
u_o (mg/L)	89.51	97.13	73.87	122.37	0
z_o	2.80	3.04	2.31	3.83	0
b_o (mg/L)	6.41	8.48	4.61	17.68	44.34
x_o	0.648	0.857	0.466	1.788	4.484
V_{max} (L)	2.0	2.0	2.0	2.0	2.0
V_o (L)	1.0	1.0	1.0	1.0	1.0
δ	0.5	0.5	0.5	0.5	0.5
t_3 (h)	4.0	5.0	5.4	4.76	7.0
t_1 (h)	0.4	0.5	0.54	0.476	0.7
σ_1	0.1	0.1	0.1	0.1	0.1
Q_f^* (L/h)	2.5	2.0	1.866	2.1	1.428

Reproduced with permission of the copyright owner. Further reproduction prohibited without permission.

Table D-3 Data from Sequencing-Batch-Reactor (SBR) experiments at pH = 7.1 ± 0.1 and T = 30 °C. (All concentrations are in mg/L)

Run SBR-1 (pH = 7.03 - 7.26)							
Cycle 1				Cycle 2			
(h)	NO_3^-	NO_2^-	*b*	(h)	NO_3^-	NO_2^-	*b*
0	0	30.87	2.050	4	0	39.17	1.794
0.20	0	37.50	1.743	4.20	0	42.42	1.338
0.40	0	40.80	1.538	4.40	0	43.78	1.282
0.75	0	40.95	1.487	4.75	0	43.93	1.282
1	0	40.84	1.487	5	0	43.83	1.282
1.33	0	40.78	1.487	5.33	0	43.88	1.282
1.67	0	40.58	1.487	5.67	0	43.87	1.282
2	0	40.81	1.538	6	0	43.45	1.333
2.33	0	40.28	1.538	6.33	0	43.32	1.333
2.67	0	40.16	1.538	6.67	0	43.18	1.410
3	0	39.83	1.589	7	0	42.93	1.410
3.33	0	39.48	1.666	7.33	0	42.45	1.487
3.67	0	39.64	1.666	7.67	0	42.31	1.538
4	0	39.17	1.794	8	0	42.13	1.538
Cycle 3				Cycle 4			
8	0	42.13	1.538	12	0	44.65	1.282
8.20	0	43.97	1.082	12.20	0	45.78	0.875
8.40	0	46.28	1.025	12.40	0	47.07	0.769
8.75	0	46.17	1.025	12.75	0	47.37	0.769
9	0	45.79	1.025	13	0	47.30	0.769
9.33	0	45.43	1.077	13.33	0	47.46	0.769
9.67	0	45.24	1.077	13.67	0	47.21	0.769
10	0	45.36	1.155	14	0	47.27	0.769
10.33	0	45.37	1.155	14.33	0	47.48	0.769
10.67	0	45.01	1.230	14.67	0	47.28	0.769
11	0	44.85	1.256	15	0	47.32	0.769
11.33	0	44.81	1.256	15.33	0	47.43	0.769
11.67	0	44.58	1.256	15.67	0	47.19	0.769
12	0	44.65	1.282	16	0	47.14	0.769

Reproduced with permission of the copyright owner. Further reproduction prohibited without permission.

Table D-3 (Continued) Data from Sequencing-Batch-Reactor (SBR) experiments at pH = 7.1 ± 0.1 and T = 30 °C. (All concentrations are in mg/L)

Run SBR-2 (pH = 7.06 - 7.28)							
Cycle 1				Cycle 2			
(h)	NO_3^-	NO_2^-	*b*	(h)	NO_3^-	NO_2^-	*b*
0	0	26.90	8.765	5	0	22.79	9.227
0.25	0	33.97	6.758	5.25	0	29.82	6.651
0.50	0	37.47	6.408	5.50	0	33.78	5.107
0.75	0	37.22	6.664	5.75	0	33.41	5.363
1	0	36.89	6.664	6	0	32.52	5.513
1.33	0	35.94	6.920	6.33	0	31.67	5.613
1.67	0	34.42	7.176	6.67	0	30.99	5.870
2	0	33.32	7.176	7	0	29.87	6.126
2.33	0	32.53	7.433	7.33	0	28.78	6.382
2.67	0	32.03	7.689	7.67	0	28.33	6.639
3	0	31.23	7.689	8	0	26.85	6.901
3.33	0	30.16	7.945	8.33	0	25.54	7.164
3.67	0	28.70	8.202	8.67	0	24.61	7.676
4	0	27.65	8.458	9	0	23.60	7.933
4.33	0	25.66	8.714	9.33	0	22.52	8.189
4.67	0	24.15	8.971	9.67	0	20.99	8.445
5	0	22.79	9.227	10	0	19.90	8.702
Cycle 3				Cycle 4			
10	0	19.90	8.702	15	0	17.29	8.314
10.25	0	28.11	6.151	15.25	0	26.05	6.264
10.50	0	33.49	4.870	15.50	0	30.76	4.982
10.75	0	32.66	5.126	15.75	0	29.35	5.239
11	0	32.08	5.382	16	0	28.87	5.495
11.33	0	31.21	5.639	16.33	0	26.76	5.751
11.67	0	29.53	5.895	16.67	0	25.58	6.008
12	0	28.68	6.151	17	0	24.59	6.264
12.33	0	27.43	6.408	17.33	0	23.60	6.520
12.67	0	26.47	6.664	17.67	0	22.51	6.776
13	0	25.10	6.920	18	0	21.34	7.033
13.33	0	24.54	7.176	18.33	0	20.70	7.545
13.67	0	23.11	7.433	18.67	0	18.77	7.802
14	0	22.07	7.689	19	0	17.98	8.171
14.33	0	20.28	7.945	19.33	0	17.2	8.427
14.67	0	18.90	8.202	19.67	0	16.37	8.683
15	0	17.29	8.314	20	0	16.07	8.939

Reproduced with permission of the copyright owner. Further reproduction prohibited without permission.

Table D-3 (Continued) Data from Sequencing-Batch-Reactor (SBR) experiments at pH = 7.1 ± 0.1 and T = 30 °C. (All concentrations are in mg/L)

Run SBR-3
(pH = 7.05 - 7.18)

Cycle 1				Cycle 2			
(h)	NO_3^-	NO_2^-	*b*	(h)	NO_3^-	NO_2^-	*b*
0	12.46	89.51	6.408	4	15.46	96.45	5.382
0.40	23.98	93.26	3.588	4.40	25.45	96.55	2.307
1	21.66	92.18	3.973	5	25.00	96.54	2.307
1.5	19.98	92.55	4.101	5.5	24.55	96.25	2.307
2	18.81	93.86	4.357	6	24.12	95.86	2.050
2.5	17.51	94.70	4.613	6.5	24.02	95.85	2.050
3	16.27	95.19	4.870	7	24.61	95.76	2.563
3.5	15.69	96.18	5.126	7.5	23.09	95.56	2.255
4	15.46	96.45	5.382	8	23.20	95.11	2.512

Run SBR-4
(pH = 7.03 - 7.26)

Cycle 1				Cycle 2				Cycle 3			
(h)	NO_3^-	NO_2^-	*b*	(h)	NO_3^-	NO_2^-	*b*	(h)	NO_3^-	NO_2^-	*b*
0	23.02	97.13	8.483	5	13.37	99.29	7.945	10	0	100.14	8.714
0.25	25.87	98.41	7.433	5.25	14.65	103.33	5.639	10.25	6.34	102.44	6.920
0.5	27.36	104.62	5.382	5.5	21.09	104.14	4.613	10.5	10.49	104.09	5.895
0.75	26.71	103.95	5.639	5.75	17.77	104.00	4.870	10.75	11.72	104.50	5.895
1	25.64	102.32	5.639	6	17.21	106.08	4.998	11	7.95	104.82	6.151
1.33	25.58	102.00	5.895	6.33	14.53	106.50	5.126	11.33	5.94	104.53	6.664
1.67	24.53	101.07	5.895	6.67	9.86	106.23	5.382	11.67	3.81	104.44	6.664
2	24.04	101.32	5.895	7	9.49	106.24	5.895	12	3.08	104.15	7.176
2.33	23.79	101.98	5.895	7.33	5.94	105.68	6.408	12.33	2.60	104.64	7.176
2.67	22.88	101.00	6.151	7.67	5.13	106.52	6.664	12.67	1.68	104.94	7.433
3	22.67	101.89	6.408	8	3.11	106.30	6.920	13	0.64	104.01	7.433
3.33	20.68	101.65	6.664	8.33	1.24	106.55	7.176	13.33	0	104.28	7.689
3.67	20.02	101.40	6.920	8.67	0	106.48	7.561	13.67	0	104.35	7.689
4	17.72	100.65	7.176	9	0	104.08	7.945	14	0	103.80	7.945
4.33	15.18	100.44	7.433	9.33	0	104.99	8.202	14.33	0	103.37	8.202
4.67	13.59	100.67	7.689	9.67	0	102.75	8.458	14.67	0	102.19	8.458
5	13.37	99.29	7.945	10	0	100.14	8.714	15	0	101.99	8.714

Reproduced with permission of the copyright owner. Further reproduction prohibited without permission.

Table D-3 (Continued) Data from Sequencing-Batch-Reactor (SBR) experiments at pH = 7.1 ± 0.1 and T = 30 °C. (All concentrations are in mg/L)

Run SBR-5 (pH = 7.13 - 7.26)							
Cycle 1				Cycle 2			
(h)	NO_3^-	NO_2^-	*b*	(h)	NO_3^-	NO_2^-	*b*
0	64.17	73.87	4.613	5.4	59.60	83.85	3.332
0.267	67.74	80.71	3.486	5.667	62.56	88.62	2.819
0.55	69.20	87.33	2.948	5.95	66.11	91.37	2.307
1	68.71	88.42	3.076	6.4	65.90	93.21	2.307
1.5	67.75	87.81	3.076	6.9	65.28	92.45	2.435
2	67.29	87.61	3.076	7.4	64.77	91.62	2.563
2.5	66.61	86.82	3.076	7.9	64.01	91.56	2.435
3	64.64	85.56	3.076	8.4	63.21	91.71	2.435
3.5	63.39	84.73	3.204	8.9	63.20	91.45	2.435
4	61.94	83.86	3.204	9.4	62.48	91.29	2.435
4.5	61.34	83.88	3.204	9.9	61.87	90.30	2.435
5	60.60	83.80	3.332	10.4	61.29	90.18	2.307
5.4	59.60	83.85	3.332	10.8	60.53	89.84	2.307
Run SBR-6 (pH = 7.07 - 7.26)							
Cycle 1				Cycle 2			
(h)	NO_3^-	NO_2^-	*b*	(h)	NO_3^-	NO_2^-	*b*
0	5.36	122.37	17.685	4.767	0	101.38	17.941
0.233	21.20	115.52	13.584	5	29.39	95.12	13.021
0.483	23.43	113.62	10.508	5.25	36.47	95.89	9.971
1	29.08	112.05	10.765	5.767	35.77	94.69	10.227
1.5	25.49	111.20	11.277	6.267	33.28	97.54	10.483
2	21.52	113.04	12.431	6.767	28.65	96.74	10.739
2.5	15.56	108.71	13.456	7.267	24.36	97.48	11.508
3	8.53	108.96	14.225	7.767	22.20	96.01	12.534
3.5	4.17	107.62	15.634	8.267	18.74	96.20	13.687
4	0	106.03	17.044	8.767	15.62	95.87	14.071
4.767	0	101.38	17.941	9.533	11.03	95.36	15.584

Reproduced with permission of the copyright owner. Further reproduction prohibited without permission.

Table D-3 (Continued) Data from Sequencing-Batch-Reactor (SBR) experiments at pH = 7.1 ± 0.1 and T = 30 °C. (All concentrations are in mg/L)

Run SBR-7 (pH = 7.10 - 7.28)							
Cycle 1				Cycle 2			
(h)	NO_3^-	NO_2^-	*b*	(h)	NO_3^-	NO_2^-	*b*
0	0	0	44.340	7	0	0	30.300
0.35	15.71	31.88	33.063	7.35	20.05	32.20	24.605
0.70	24.36	51.43	25.630	7.70	31.68	51.28	19.223
1	19.86	54.31	26.399	8	26.09	52.52	19.735
1.5	12.03	56.25	28.706	8.5	21.22	55.40	20.248
2	7.05	45.19	30.756	9	16.73	55.04	21.273
2.5	3.12	35.35	31.269	9.5	11.54	55.20	23.067
3	0	24.03	32.550	10	8.37	53.01	25.630
3.5	0	11.45	33.319	10.5	3.50	49.79	28.193
4	0	5.23	34.600	11	0	40.87	30.756
4.5	0	0	34.344	11.5	0	34.34	31.525
5	0	0	33.832	12	0	21.51	32.038
5.5	0	0	33.300	12.5	0	13.35	32.374
6	0	0	32.500	13	0	8.53	33.706
6.5	0	0	31.000	13.5	0	5.73	31.475
7	0	0	30.300	14	0	1.36	29.731
Cycle 3				Cycle 5			
14	0	1.36	29.731	28	0	3.43	26.398
14.35	21.82	34.19	22.298	28.35	33.54	37.25	18.454
14.70	30.46	50.10	18.197	28.70	45.19	47.11	14.097
15	28.46	49.21	18.197	29	44.45	46.15	14.353
15.5	22.35	49.65	18.966	29.5	34.77	45.44	15.891
16	16.71	51.24	19.991	30	28.68	46.39	17.172
16.5	11.87	50.78	21.786	30.5	25.59	45.92	18.928
17	5.17	48.65	23.580	31	18.42	45.11	20.723
17.5	1.34	43.57	25.117	31.5	13.08	46.59	22.517
18	0	37.29	27.296	32	5.49	44.46	24.017
18.5	0	24.17	28.706	32.5	3.50	36.95	25.554
19	0	16.30	29.987	33	0	28.74	26.836
19.5	0	10.56	30.243	33.5	0	20.43	28.605
20	0	5.81	30.168	34	0	13.61	28.861
20.5	0	1.43	29.655	34.5	0	8.74	29.630
21	0	0	28.399	35	0	4.57	29.130

Reproduced with permission of the copyright owner. Further reproduction prohibited without permission.

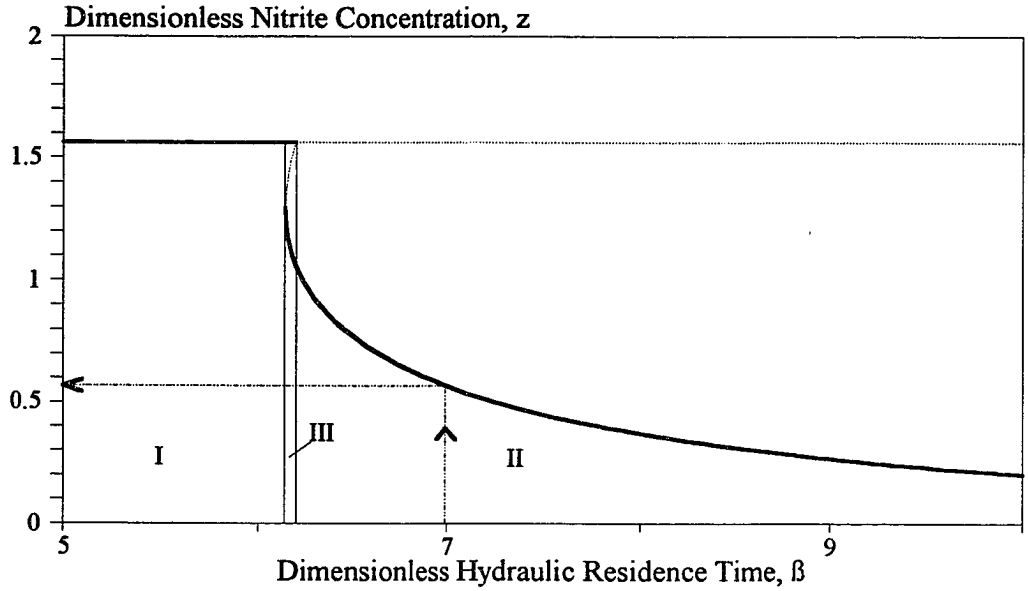

Figure D-1 Bifurcation diagram for $z_f = 1.564$ and $y_f = 0$; other parameters as in Figure 16. This diagram was used in designing experiments SBR-1 and SBR-2.

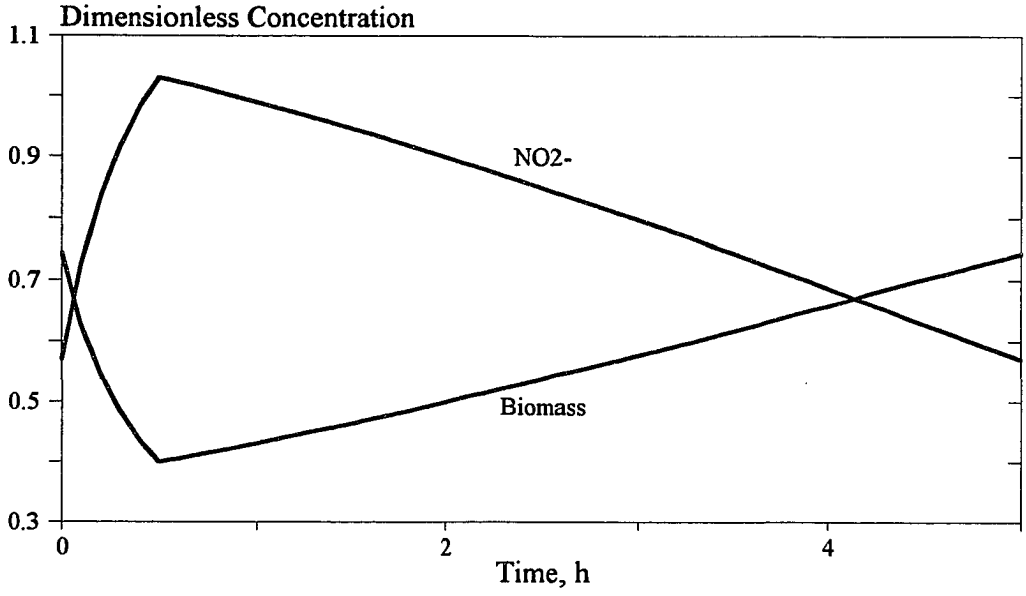

Figure D-2 Predicted steady cycle concentration pofiles corresponding to Figure D-1 when $\beta = 6.987$. These predictions were verified with experiment SBR-2 (see also Figure D-4).

Reproduced with permission of the copyright owner. Further reproduction prohibited without permission.

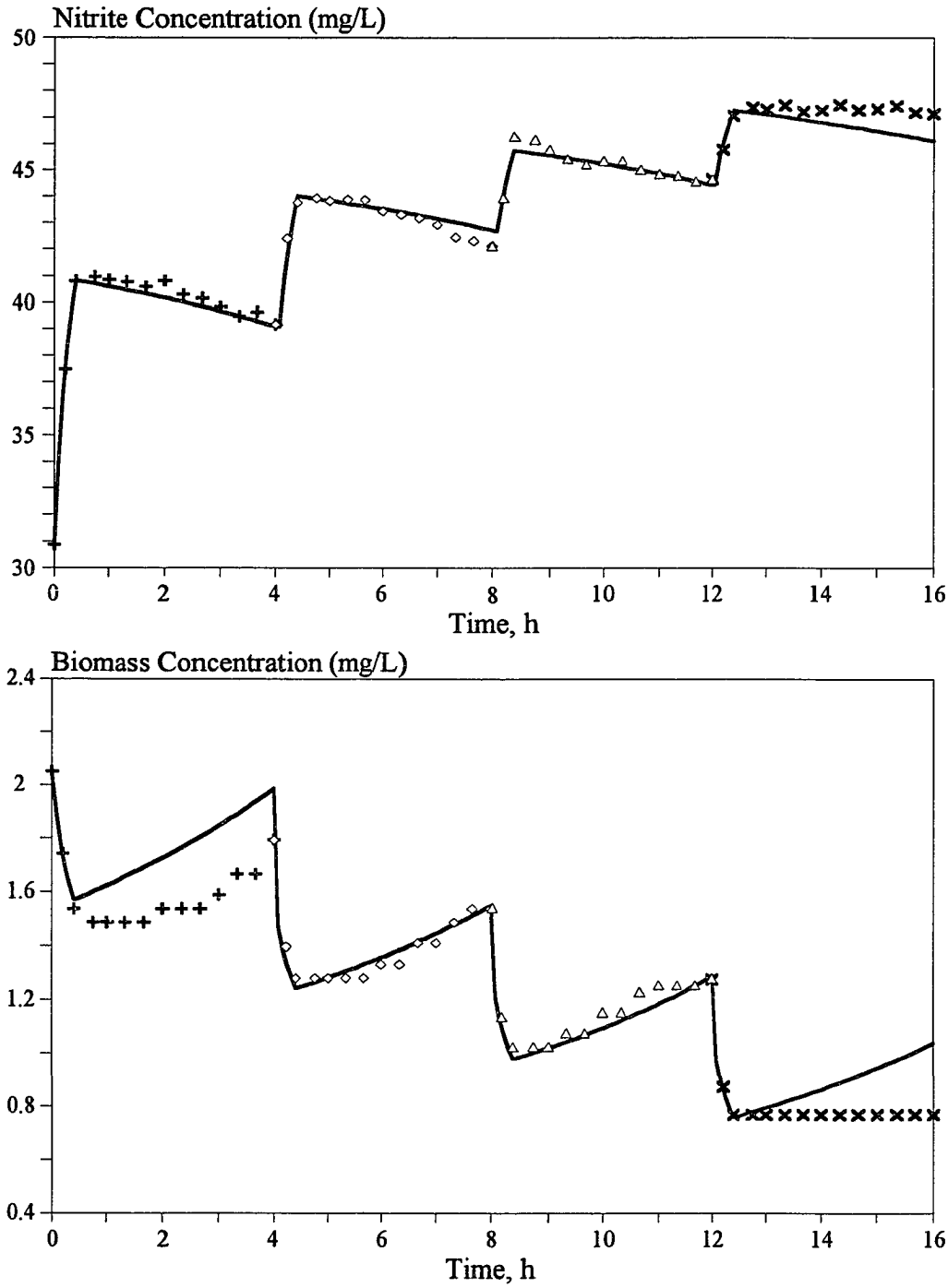

Figure D-3 Concentration profiles of nitrite (top) and biomass (bottom) for experiment SBR-1. Conditions for this experiment are given in Table D-1. This experiment corresponds to a point in region I of Figure 16. The system reaches a washout state.

Reproduced with permission of the copyright owner. Further reproduction prohibited without permission.

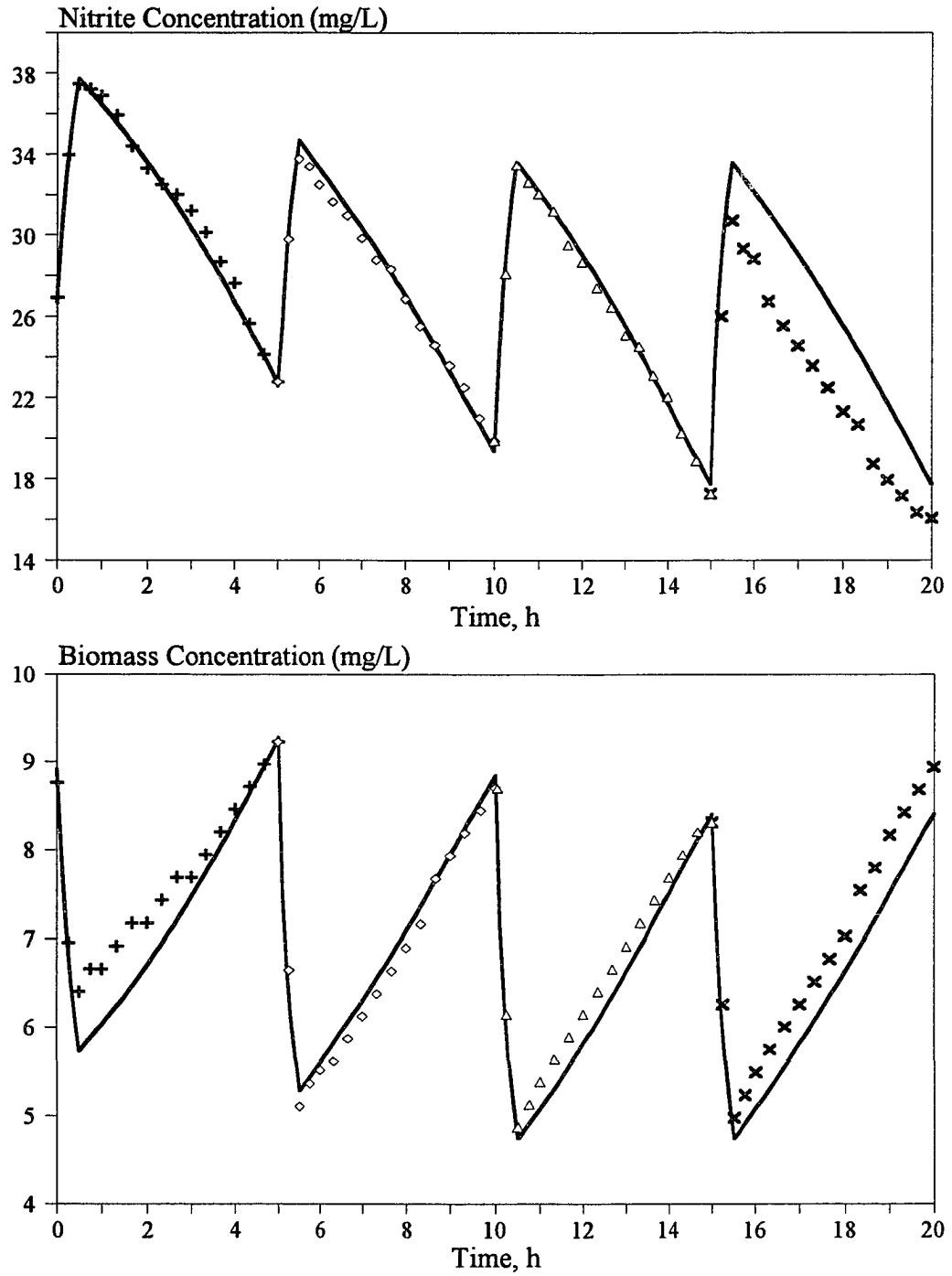

Figure D-4 Concentration profiles of nitrite (top) and biomass (bottom) for experiment SBR-2. Conditions for this experiment are given in Table D-1. This experiment corresponds to a point in region II of Figure 16. The system reaches a survival periodic state.

Reproduced with permission of the copyright owner. Further reproduction prohibited without permission.

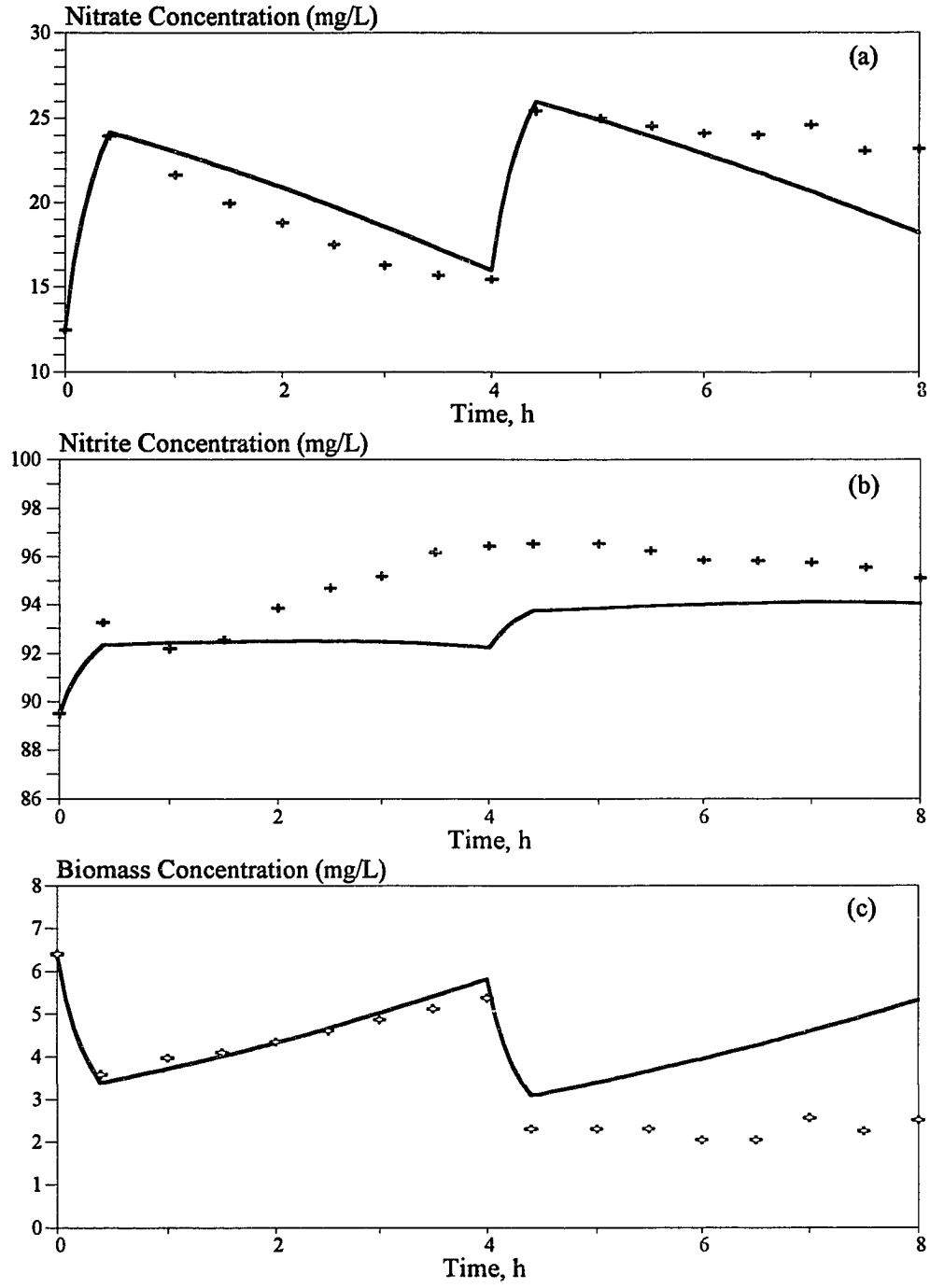

Figure D-5 Concentration profiles of nitrate (a), nitrite (b), and biomass (c) for experiment SBR-3 operating with a feed stream containing a mixture of nitrate and nitrite. Conditions for this experiment are given in Table D-2. This experiment corresponds to a point in region I of Figure 17. The system reaches a washout state.

Reproduced with permission of the copyright owner. Further reproduction prohibited without permission.

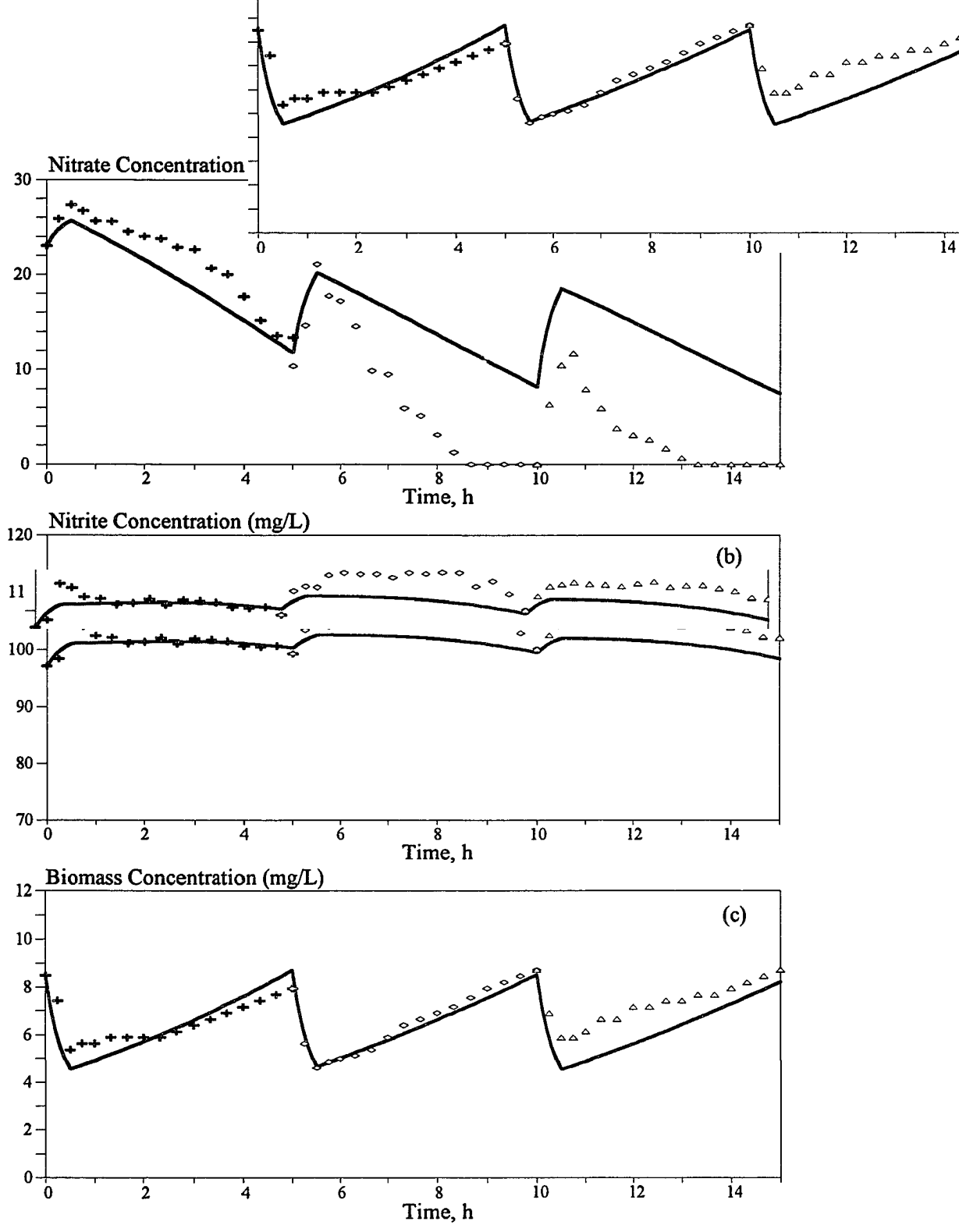

Figure D-6 Concentration profiles of nitrate (a), nitrite (b), and biomass (c) for experiment SBR-4 operating with a feed stream containing a mixture of nitrate and nitrite. Conditions for this experiment are given in Table D-2. This experiment corresponds to a point in region II of Figure 17. The system reaches a survival periodic state.

Reproduced with permission of the copyright owner. Further reproduction prohibited without permission.

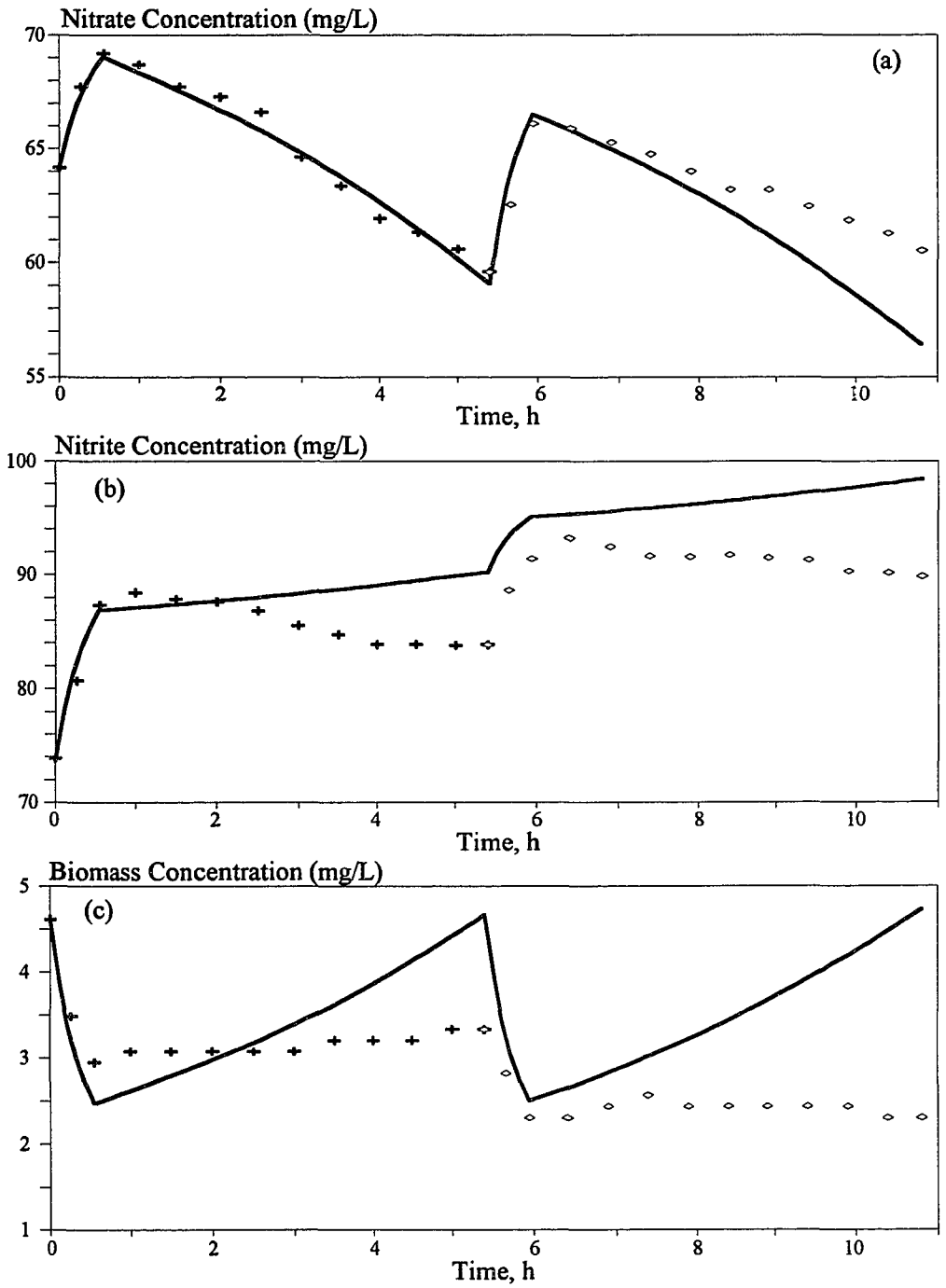

Figure D-7 Concentration profiles of nitrate (a), nitrite (b), and biomass (c) for experiment SBR-5 operating with a feed stream containing a mixture of nitrate and nitrite. Conditions for this experiment are given in Table D-2. This experiment corresponds to a point in region IV of Figure 17. The system reaches a washout state.

Reproduced with permission of the copyright owner. Further reproduction prohibited without permission.

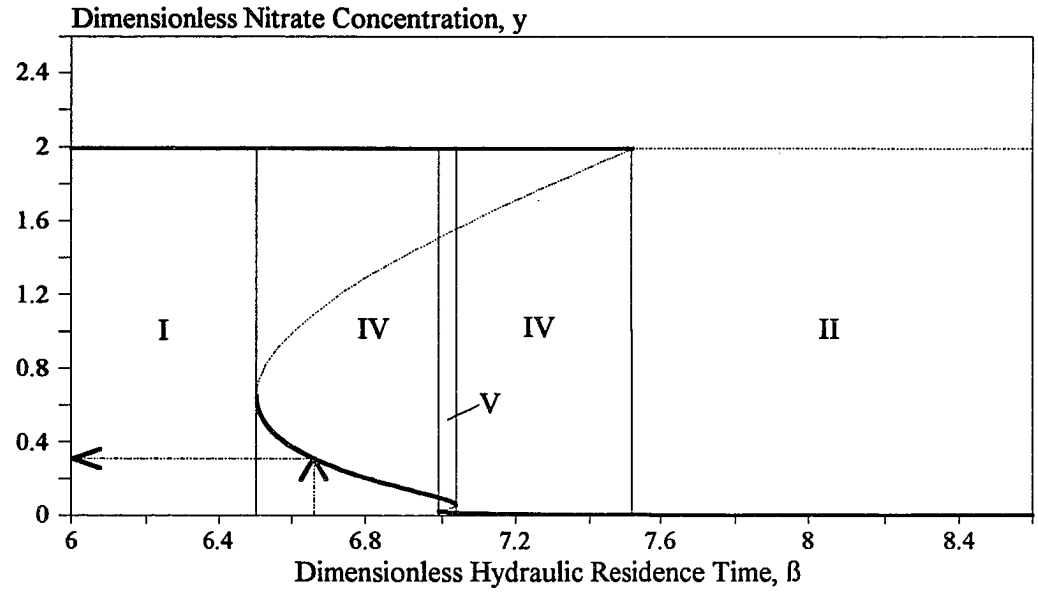

Figure D-8 Bifurcation diagram of periodic states for NO_3^-/NO_2^- mixtures. This diagram indicates the nitrate concentration at the end of a steady cycle as a function of β. For this case, $y_f = 1.994$, $z_f = 3.081$; other parameters as in Figure 17. This diagram was the basis for designing experiment SBR-6.

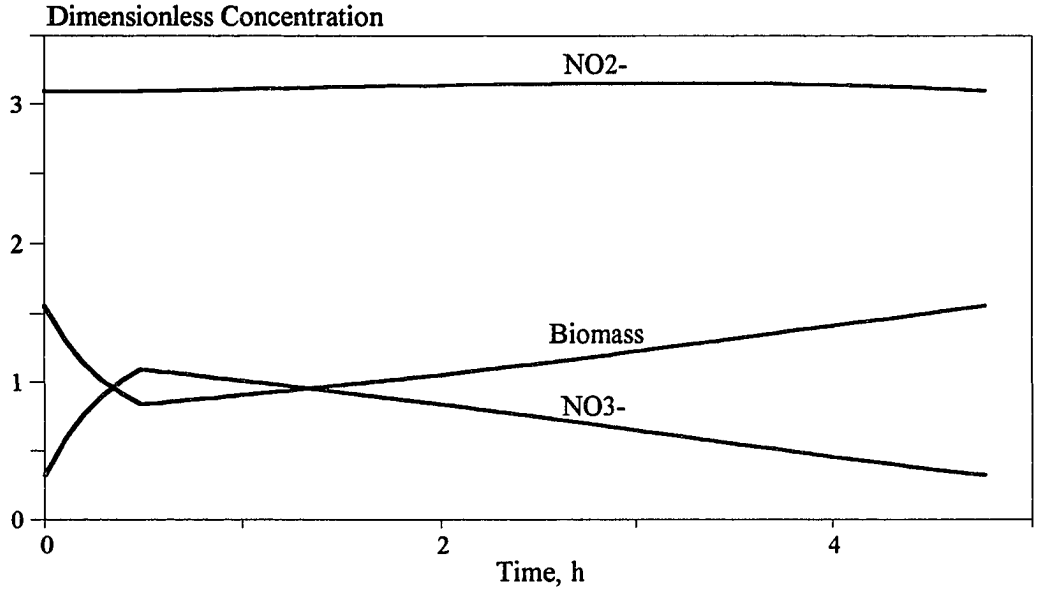

Figure D-9 Predicted steady cycle concentration pofiles corresponding to Figure D-8 when β = 6.65. These predictions were verified with experiment SBR-6 (see also Figure D-10).

Reproduced with permission of the copyright owner. Further reproduction prohibited without permission.

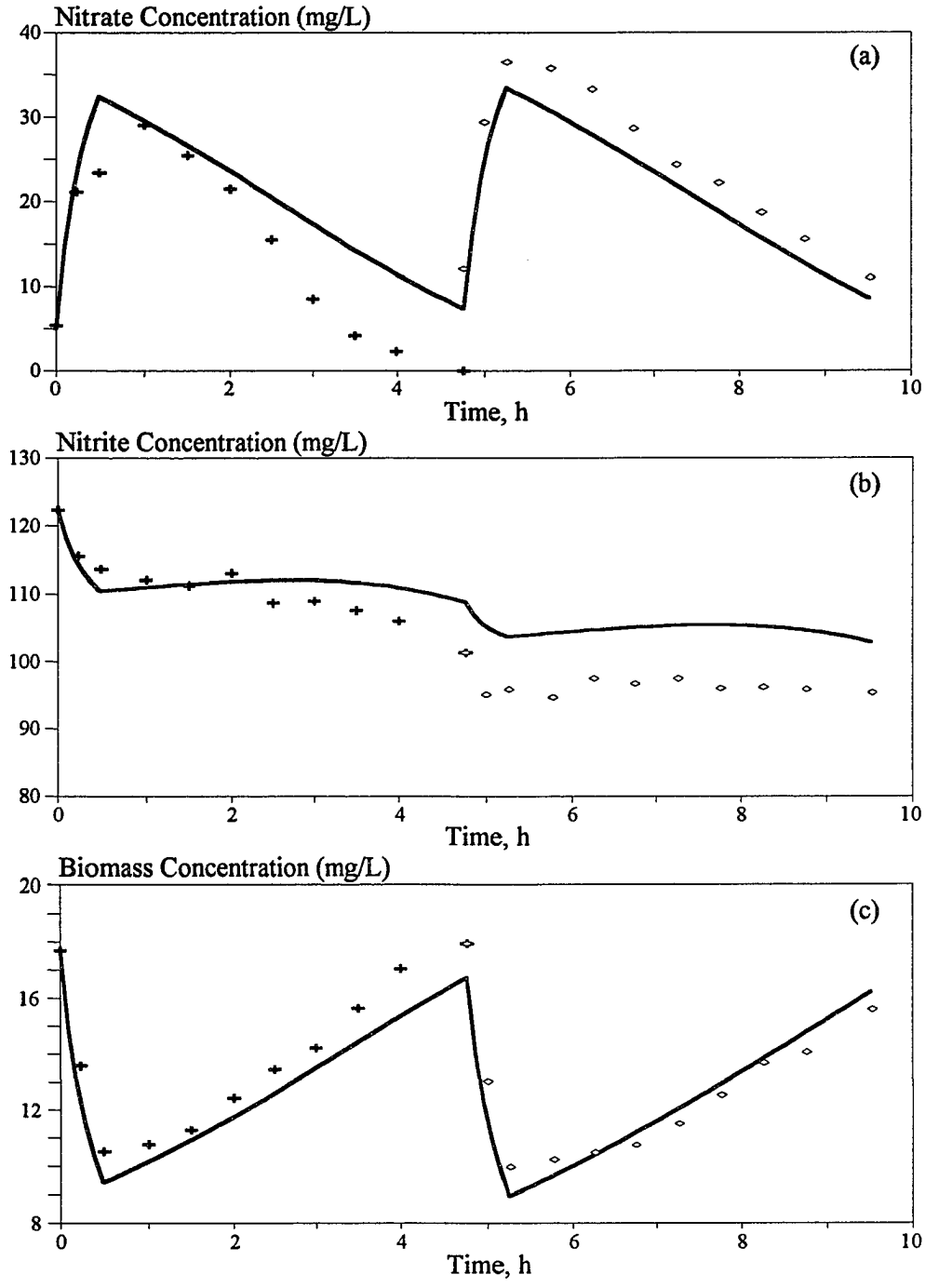

Figure D-10 Concentration profiles of nitrate (a), nitrite (b), and biomass (c) for experiment SBR-6 operating with a feed stream containing a mixture of nitrate and nitrite. Conditions for this experiment are given in Table D-2. This experiment corresponds to a point in region IV of Figure 17. The system reaches a survival periodic state.

Reproduced with permission of the copyright owner. Further reproduction prohibited without permission.

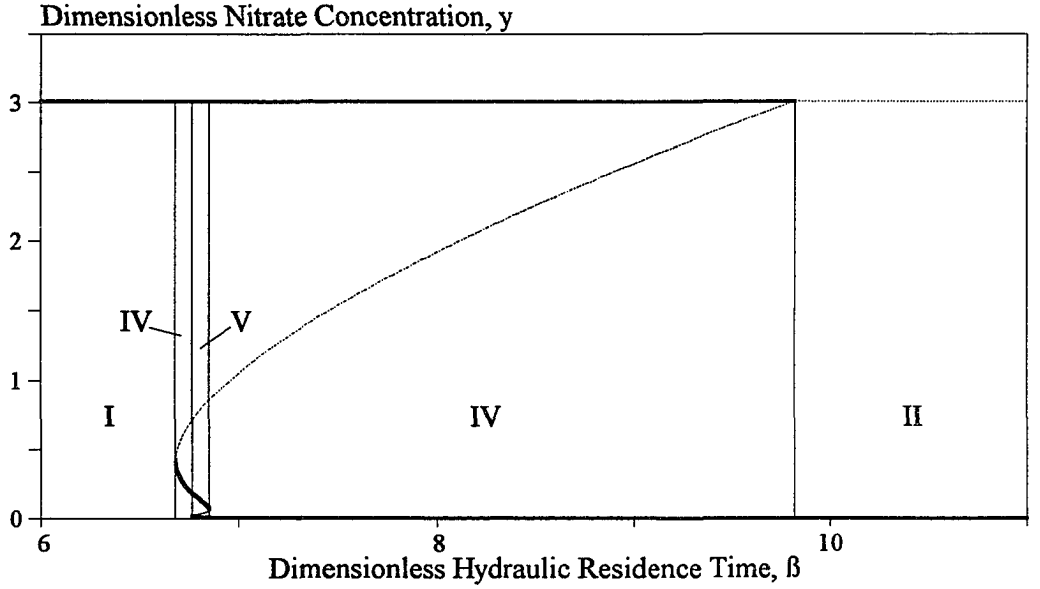

Figure D-11 Bifurcation diagram of periodic states for NO_3^-/NO_2^- mixtures. This diagram indicates the nitrate concentration at the end of a steady cycle as a function of β. For this case, $y_f = 3.013$, $z_f = 2.913$; other parameters as in Figure 17. This diagram was the basis for designing experiment SBR-7.

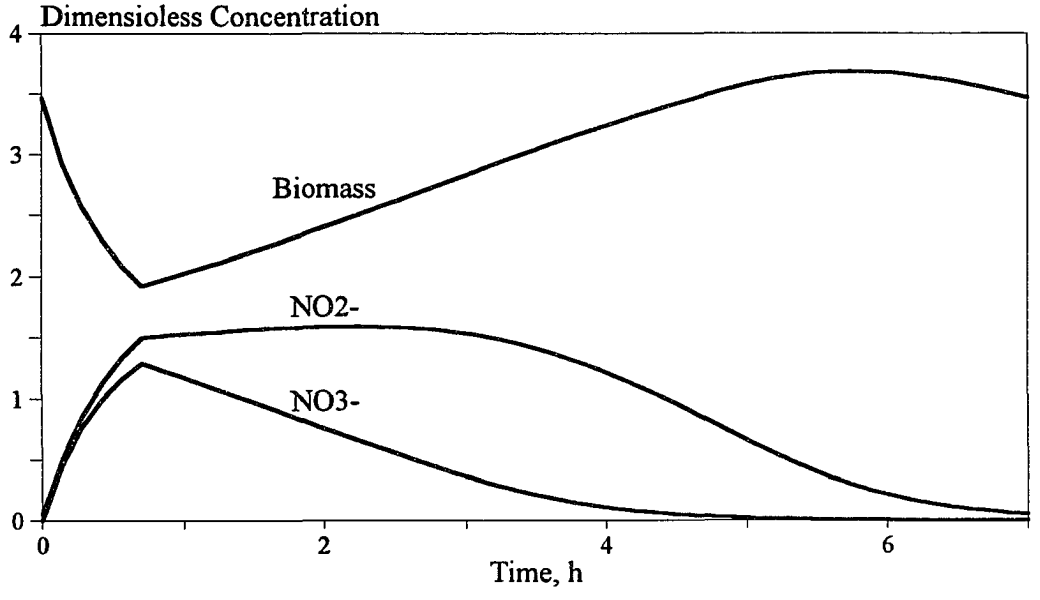

Figure D-12 Predicted steady cycle concentration pofiles corresponding to Figure D-11 when β = 9.78. These predictions were verified with experiment SBR-7 (see also Figure D-13).

Reproduced with permission of the copyright owner. Further reproduction prohibited without permission.

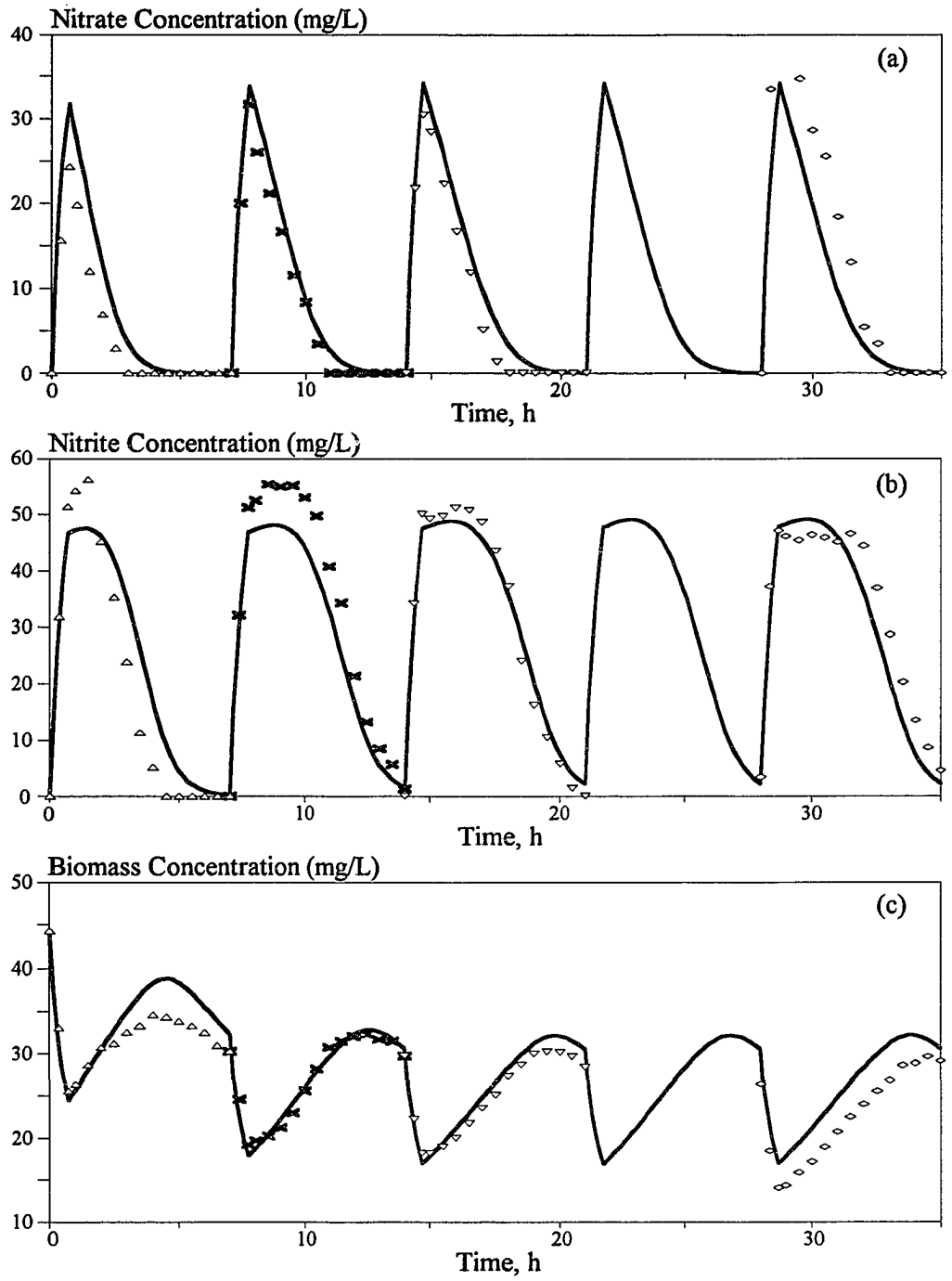

Figure D-13 Concentration profiles of nitrate (a), nitrite (b), and biomass (c) for experiment SBR-7 operating with a feed stream containing a mixture of nitrate and nitrite. Conditions for this experiment are given in Table D-2. This experiment corresponds to a point in region IV of Figure 17. The system reaches a survival periodic state.

Reproduced with permission of the copyright owner. Further reproduction prohibited without permission.

APPENDIX E

COMPUTER CODES

Reproduced with permission of the copyright owner. Further reproduction prohibited without permission.

APPENDIX E-1

Computer Code for Predicting NO_3^-, NO_2^-, and Biomass Concentration Profiles in Batch Reactors

Reproduced with permission of the copyright owner. Further reproduction prohibited without permission.

```
C
      PROGRAM Model
C
      IMPLICIT DOUBLE PRECISION (A-H,O-Z)
      DOUBLE PRECISION K1, KI1, MUHEAD1, MUC1, MUC10, K21, K210
      DOUBLE PRECISION K2, KI2, MUHEAD2, MUC2, MUC20, K12, K120
C
      OPEN (10,FILE = '[JXW7025.MODEL.3]OUT.', STATUS = 'NEW')
      OPEN (20,FILE = '[JXW7025.MODEL.3]IN.' ,    STATUS = 'OLD')
C
      MUHEAD1 =  0.49605855
      K1      = 31.97343690
      KI1     = 69.40299434
      MUC10   =  0.05860000
C
      MUHEAD2 =  0.69872418
      K2      = 52.71838499
      KI2     = 35.62271099
      MUC20   =  0.04570000
C
      Y1      =  0.3093
      Y2      =  0.3090
C
      ALPHA   =  (1.0 / 62.0049 - Y1 / 113.0) * 46.0055
C
      READ (20, *) S0, U0, B0, T, HOUR, K120, K210
C
      T0      =  273.15 + 30.
      T       =  273.15 + T
C
      STEP    =  1.
      TIMEUP  =  HOUR * 3600.
      B       =  B0   * 256.3
      S       =  S0
      U       =  U0
      MUC1    =  MUC10
      MUC2    =  MUC20
      K12     =  K120
      K21     =  K210
C
      WRITE (10,100) TIME, S, U, B/256.3
C
      I       = 1
C
      TIME    = 0.0
C
C     CALL PARA(T,MUHEAD1,K1,KI1,MUC10,MUHEAD2,K2,KI2,MUC20)
C
      DO 70 TIME  =  0.01, TIMEUP + 1., STEP
C
         IF (I.EQ.901) THEN
            WRITE (10,100) (TIME-1.) / 3600.,SNXT,UNXT,BNXT / 256.3
            I = 1
         ENDIF
C
         IF (S.EQ.0.) THEN
            MUC1 = 0.0
         ELSE
            MUC1 = MUC10
         ENDIF
C
         IF (U.EQ.0.) THEN
            MUC2 = 0.0
         ELSE
```

Reproduced with permission of the copyright owner. Further reproduction prohibited without permission.

```
            MUC2 = MUC20
         ENDIF
C
         IF (U.LT.15.0) THEN
            K12  = 0.0
            K21  = 0.0
         ELSE
            K12  = K120
            K21  = K210
         ENDIF
C
         CALL RUNKU(MUHEAD1,K1,KI1,MUC1,Y1,MUHEAD2,K2,KI2,MUC2,
     &           Y2,ALPHA,T,T0,STEP,S,U,B,SNXT,UNXT,BNXT,EPSLN1,EPSLN2,
     &           K12,K21)
C
         S  =  SNXT
         U  =  UNXT
         B  =  BNXT
C
         I  =  I + 1
C
   70 CONTINUE
C
  100 FORMAT(15X,F7.2,3(3X,F9.4))
C
  999 STOP
      END
C-----------------------------------------------------------------------
      SUBROUTINE PARA(T,MUHEAD1,K1,KI1,MUC10,MUHEAD2,K2,KI2,MUC20)
C
      IMPLICIT DOUBLE PRECISION (A-H,O-Z)
      DOUBLE PRECISION K1, KI1, MUHEAD1, MUC10, K2, KI2, MUHEAD2, MUC20
      DOUBLE PRECISION K12, K21
C
      MUHEAD1 =  9.8433 * EXP(-1799 / 1.9869 / T)
      K1      =  1. / 3.4777 E8 * EXP(13932 / 1.9869 / T)
      KI1     =  5.2300 E11 * EXP(-13707 / 1.9869 / T)
      MUC10   =  8.4035 E7  * EXP(-12700 / 1.9869 / T)
C
      MUHEAD2 =  1.5767 * EXP(- 490 / 1.9869 / T)
      K2      =  1./ 2.0922 E5  * EXP( 9775 / 1.9869 / T)
      KI2     =  2.0070 E9  * EXP(-10750 / 1.9869 / T)
      MUC20   =  2.7964 E6  * EXP(-10800 / 1.9869 / T)
C
      RETURN
      END
C-----------------------------------------------------------------------
      SUBROUTINE RUNKU(MUHEAD1,K1,KI1,MUC1,Y1,MUHEAD2,K2,KI2,
     &             MUC2,Y2,ALPHA,T,T0,STEP,S,U,B,SNXT,UNXT,BNXT,EPSLN1,
     &             EPSLN2,K12,K21)
C
      IMPLICIT DOUBLE PRECISION (A-H,O-Z)
      DOUBLE PRECISION K1, KI1, MUHEAD1, MUC1, K2, KI2, MUHEAD2, MUC2
      DOUBLE PRECISION K12, K21
C
      FUN1(S1,U1,B1) = - (MUHEAD1 * S1 / (K1 + S1 + S1 ** 2. / KI1 +
     &                    K21 * U1 * S1)) / Y1 * B1 / 3600.
     &                 * EXP(- 4321.08 * (1./T - 1./T0))
C
      FUN2(S1,U1,B1) = + (MUHEAD1 * S1 / (K1 + S1 + S1 ** 2. / KI1 +
     &                    K21 * U1 * S1)) / Y1 * B1 / 3600. * ALPHA
     &                 * EXP(- 4321.08 * (1./T - 1./T0))
     &                - (MUHEAD2 * U1 / (K2 + U1 + U1 ** 2. / KI2 +
     &                    K12 * S1 * U1)) / Y2 * B1 / 3600.
```

Reproduced with permission of the copyright owner. Further reproduction prohibited without permission.

```
     &                  * EXP(- 3626.45 * (1./T - 1./T0))
C
      FUN3(S1,U1,B1) =    (MUHEAD1 * S1 / (K1 + S1 + S1 ** 2. / KI1 +
     &                     K21 * U1 * S1) - MUC1) * B1 / 3600.
     &                  * EXP(- 4321.08 * (1./T - 1./T0))
     &                 + (MUHEAD2 * U1 / (K2 + U1 + U1 ** 2. / KI2 +
     &                    K12 * S1 * U1) - MUC2) * B1 / 3600.
     &                  * EXP(- 3626.45 * (1./T - 1./T0))
C
      SK1 = STEP * FUN1(S,U,B)
      UK1 = STEP * FUN2(S,U,B)
      BK1 = STEP * FUN3(S,U,B)
C
      SK2 = STEP * FUN1((S + SK1/2.),(U + UK1/2.),(B + BK1/2.))
      UK2 = STEP * FUN2((S + SK1/2.),(U + UK1/2.),(B + BK1/2.))
      BK2 = STEP * FUN3((S + SK1/2.),(U + UK1/2.),(B + BK1/2.))
C
      SK3 = STEP * FUN1((S + SK2/2.),(U + UK2/2.),(B + BK2/2.))
      UK3 = STEP * FUN2((S + SK2/2.),(U + UK2/2.),(B + BK2/2.))
      BK3 = STEP * FUN3((S + SK2/2.),(U + UK2/2.),(B + BK2/2.))
C
      SK4 = STEP * FUN1((S + SK3),(U + UK3),(B + BK3))
      UK4 = STEP * FUN2((S + SK3),(U + UK3),(B + BK3))
      BK4 = STEP * FUN3((S + SK3),(U + UK3),(B + BK3))
C
      SNXT= S + (1. / 6.) * (SK1 + 2. * SK2 + 2. * SK3 + SK4)
      UNXT= U + (1. / 6.) * (UK1 + 2. * UK2 + 2. * UK3 + UK4)
      BNXT= B + (1. / 6.) * (BK1 + 2. * BK2 + 2. * BK3 + BK4)
C
      RETURN
      END
```

Reproduced with permission of the copyright owner. Further reproduction prohibited without permission.

APPENDIX E-2

Computer Code for Generating NO_3^-, NO_2^-, and Biomass Concentration Profiles in Sequencing Batch Reactors
[Modified from Sanyal, 1990]

Reproduced with permission of the copyright owner. Further reproduction prohibited without permission.

```
c*********************************************************************
c                                                                     *
c               THIS PROGRAM GIVES THE CONCENTRATIONS OF              *
c                                                                     *
c                    NITRATE, NITRITE, AND BIOMASS                    *
c                                                                     *
c                             IN A SBR                                *
c                                                                     *
c                         WITH RESPECT TO TIME.                       *
c                                                                     *
c              THE RUNGA KUTTA NUMERICAL METHOD IS USED               *
c                                                                     *
c                         TO SOLVE A SET OF                           *
c                                                                     *
c              NONLINEAR ORDINARY DIFFERENTIAL EQUATIONS.             *
c                                                                     *
c*********************************************************************
c
c---------------------------------------------------------------------
c
c          INITIALIZATION
c
c---------------------------------------------------------------------
c
      implicit double precision (a-h,o-z)
c
      common tm(100000),um(100000),xm(100000),pm(100000),
     &tmt(100000),umt(100000),xmt(100000),pmt(100000)
c
c
      open(10,file='[jxw7025.sbr.4]s4.dat',  status='old')
      open(20,file='[jxw7025.sbr.4]s41.dat', status='new')
      open(30,file='[jxw7025.sbr.4]s42.dat', status='new')
      open(40,file='[jxw7025.sbr.4]s43.dat', status='new')
c
c----------------INPUT DATA-----------------------------------
c
      read(10,*) delta,phi,gamma,w
      read(10,*) eta,rho,eps
      read(10,*) beta,uf,xf,pf
      read(10,*) u0,x0,p0
      read(10,*) n_pcycle,n_scycle
      read(10,*) step,last
      read(10,*) sigma1
      read(10,*) dif
      read(10,*) ans
c
c
      time3=(1.0-delta)*0.9
      np=time3/step
c
c
      u=u0
      x=x0
      p=p0
c
      u_init=u0
      x_init=x0
      p_init=p0
c
c
      if (ans.eq.0.0) then
          n_scycle=1
      endif
```

Reproduced with permission of the copyright owner. Further reproduction prohibited without permission.

```
c
c
      if (n_pcycle.gt.n_scycle) then
          ncycle=n_pcycle
      else
          ncycle=n_scycle
      endif
c
c
      do 100 icycle=1,ncycle,1
c
c
         tm(1)=0.0
         um(1)=u0
         xm(1)=x0
         pm(1)=p0
c
c
         call process(delta,phi,gamma,w,eta,rho,eps,ncycle,beta,last,
     &   u_init,x_init,p_init,np,icycle,step,time3,uf,xf,pf,u,x,p,
     &   sigma1,dif,n_pcycle,n_scycle,u_last,x_last,p_last)
c
c
         if (ncycle.eq.1) then
             goto 400
         endif
c
c
         if (icycle.eq.ncycle) then
             goto 100
         endif
c
c
         call new_values(u_last,x_last,p_last,u0,x0,p0)
c
c-------here u0,x0,p0 become the initial value for the next cycle-------
c
         u=u0
         x=x0
         p=p0
c
c-------------------------------------------------------------------------
c
         if (ans.eq.0.0) then
             goto 100
         endif
c
c
         if (icycle.eq.1) then
             goto 32
         endif
c
c
         do 31 ii=1,np,1
           if (abs(tmt(ii)-tm(ii)).gt.dif) then
               goto 32
           else
             if (abs(umt(ii)-um(ii)).gt.dif) then
                 goto 32
             else
               if (abs(xmt(ii)-xm(ii)).gt.dif) then
                   goto 32
               else
                  if (abs(pmt(ii)-pm(ii)).gt.dif) then
```

Reproduced with permission of the copyright owner. Further reproduction prohibited without permission.

```
                        goto 32
c
                     endif
c
c
          if (ii.eq.np) then
             call print_3(delta,phi,gamma,w,eta,rho,eps,uf,xf,pf,last,
     & tm,um,xm,pm,u_init,x_init,p_init,np,n_pcycle,beta,dif,step,
     & n_scycle,icycle,sigma1)
c
             goto 400
c
          endif
c
c
   31 continue
c
c
   32 do 33 jj=1,np,1
c
          tmt(jj)=tm(jj)
          umt(jj)=um(jj)
          xmt(jj)=xm(jj)
          pmt(jj)=pm(jj)
c
   33 continue
c
  100 continue
c
  400 stop
      end
c
c
c-------------------------END OF MAIN PROGRAM----------------------------
c
c--------------------SUBROUTINE PROCESS BEGINS HERE----------------------
c
c
      subroutine process(delta,phi,gamma,w,eta,rho,eps,ncycle,beta,last,
     &  u_init,x_init,p_init,np,icycle,step,time3,uf,xf,pf,u,x,p,
     &  sigma1,dif,n_pcycle,n_scycle,unxt,xnxt,pnxt)
c
c
      implicit double precision(a-h,o-z)
c
c
      common tm(100000),um(100000),xm(100000),pm(100000)
c
      j = 1
c
c
      do 30 time=0.0000000001,time3,step
c
        j = j + 1
c
c-------------here we check whether the fill period is over-------------
c
        b = 0.0
c
        if (time.le.(sigma1*(1.0-delta))) then
           b = 1.0
        endif
c
c----------------------------------------------------------------------
```

Reproduced with permission of the copyright owner. Further reproduction prohibited without permission.

```
c-----------here we determine the values of substrate,biomass-----------
c-----------                  and product                    -----------
c
        call RungaKutta1(b,delta,phi,gamma,w,eta,rho,eps,beta,
     &  sigma1,step,time,uf,xf,pf,u,x,p,unxt,xnxt,pnxt)
c
c-------------------------------------------------------------------------
c---------------here we store the instantaneous values-------------------
c
      um(j)=unxt
      xm(j)=xnxt
      pm(j)=pnxt
      tm(j)=time+step
c
c-------------------------------------------------------------------------
c
      u=unxt
      x=xnxt
      p=pnxt
c
   30 continue
c
c
      if (icycle.eq.1) then
         call print_1(delta,phi,gamma,w,eta,rho,eps,uf,xf,pf,last,
     & tm,um,xm,pm,u_init,x_init,p_init,np,n_pcycle,beta,dif,step,
     & n_scycle,sigma1)
      endif
c
c
  500 if(icycle.eq.n_pcycle) then
c
       call print_2(delta,phi,gamma,w,eta,rho,eps,uf,xf,pf,last,
     & tm,um,xm,pm,u_init,x_init,p_init,np,n_pcycle,beta,dif,step,
     & n_scycle,sigma1)
c2
      endif
c
c
  600 return
      end
c
c
c
c----------------SUBROUTINE_1 RUNGAKUTTA BEGINS HERE--------------------
c
c
c
      subroutine RungaKutta1(b,delta,phi,gamma,w,eta,rho,eps,beta,
     & sigma1,step,t,uf,xf,pf,u,x,p,unxt,xnxt,pnxt)
c
c
      implicit double precision (a-h,o-z)
c
c
      fun1(t1,u1,x1,p1)=(b/(t1+delta*sigma1))*(uf-u1)-
     &                  (beta*u1*x1)/(1.0+u1)
      fun2(t1,u1,x1,p1)=(-b/(t1+delta*sigma1))*x1+(beta*x1)*
     &    (u1/(1.0+u1))+(beta*phi*x1*p1)/(w+p1+gamma*(p1**2.))
     &   -eps*beta*x1*p1
      fun3(t1,u1,x1,p1)=(b/(t1+delta*sigma1))*(pf-p1)+(rho*beta*x1)*
     &    (u1/(1.0+u1))-(eta*phi*beta*p1*x1)/(w+p1+gamma*(p1**2.))
c
c
```

Reproduced with permission of the copyright owner. Further reproduction prohibited without permission.

```
      uk1=step*fun1(t,u,x,p)
      xk1=step*fun2(t,u,x,p)
      pk1=step*fun3(t,u,x,p)
c
c
      uk2=step*fun1((t+step/2.0),(u+uk1/2.0),(x+xk1/2.0),(p+pk1/2.0))
      xk2=step*fun2((t+step/2.0),(u+uk1/2.0),(x+xk1/2.0),(p+pk1/2.0))
      pk2=step*fun3((t+step/2.0),(u+uk1/2.0),(x+xk1/2.0),(p+pk1/2.0))
c
      uk3=step*fun1((t+step/2.0),(u+uk2/2.0),(x+xk2/2.0),(p+pk2/2.0))
      xk3=step*fun2((t+step/2.0),(u+uk2/2.0),(x+xk2/2.0),(p+pk2/2.0))
      pk3=step*fun3((t+step/2.0),(u+uk2/2.0),(x+xk2/2.0),(p+pk2/2.0))
c
      uk4=step*fun1((t+step),(u+uk3),(x+xk3),(p+pk3))
      xk4=step*fun2((t+step),(u+uk3),(x+xk3),(p+pk3))
      pk4=step*fun3((t+step),(u+uk3),(x+xk3),(p+pk3))
c
c
c
      unxt=u+(1.0/6.0)*(uk1+2.0*uk2+2.0*uk3+uk4)
      xnxt=x+(1.0/6.0)*(xk1+2.0*xk2+2.0*xk3+xk4)
      pnxt=p+(1.0/6.0)*(pk1+2.0*pk2+2.0*pk3+pk4)
c
      return
      end
c
c----------------------END OF RUNGAKUTTA SUBROUTINE----------------------
c
c------------------------------------------------------------------------
c
c---------------------SUBROUTINE NEW_VALUUES BEGINS HERE----------------
c
c
      subroutine new_values(u_last,x_last,p_last,u0,x0,p0)
c
c
      implicit double precision (a-h,o-z)
c
c
      u0=u_last
      x0=x_last
      p0=p_last
c
c
      return
      end
c
c---------------------SUBROUTINE NEW_VALUUES ENDS HERE------------------
c
c
c---------------------SUBROUTINE PRINT-1 BEGINS HERE--------------------
c
      subroutine print_1(delta,phi,gamma,w,eta,rho,eps,uf,xf,pf,last,
     &  tm,um,xm,pm,u_init,x_init,p_init,np,n_pcycle,beta,dif,step,
     &  n_scycle,sigma1)
c
c
      implicit double precision (a-h,o-z)
c
      dimension tm(100000),um(100000),xm(100000),pm(100000)
c
c-------PRINT INPUT DATA ON OUTPUT FILE-----------------------------
c
c
```

Reproduced with permission of the copyright owner. Further reproduction prohibited without permission.

```
      WRITE(20,140)
  140 FORMAT('**********************************
     &**************************************')
      WRITE(20,160)
  160 FORMAT(//10X,' S E Q U E N C I N G   B A T C H   R E A C T O R ')
      WRITE(20,150)
  150 FORMAT(//10X,'CONCENTRATION OF SUBSTRATE, BIOMASS AND
     &PRODUCT'//)
      WRITE(20,140)
      WRITE(20,151)
  151 FORMAT(//10X,'              DURING Ist CYCLE'//)
      WRITE(20,140)
      write(20,201)delta,phi,gamma,w
  201 format(/1x,'DELTA=',F10.5,4X,'PHI=',F10.5,4X,
     &GAMMA=',F12.5,4X,'W=',F10.5)
      write(20,202) eta,rho,eps,beta
  202 format(/1x,'ETA=',F10.4,4X,'RHO=',F10.5,4X,'EPS=',F10.5,4X,
     &'BETA=',F10.5)
      write(20,203)uf,xf,pf
  203 format(/1x,'UF=',F10.5,4X,'XF=',F10.5,4X,'PF=',F10.5)
      write(20,204)u_init,x_init,p_init
  204 format(/1x,'U0=',F10.5,4X,'X0=',F10.1,4X,'P0=',F10.5)
      write(20,205) np,step
  205 format(/1x,'NUMBER OF POINTS IN THE TIME DOMAIN=',I10,10X//
     &        1x,'STEP SIZE =',F10.6//)
      WRITE(20,140)
      write(20,206) sigma1
  206 format(//1x,'  SIGMA1 = ', F10.5//)
      WRITE(20,140)
      write(20,207)
  207 format(/1x,'TIME',15X,' U ',15X,' X  ',15X,'  P ')
c
c----------------PRINT COMPUTED DATA INTO OUTPUT FILE-------------------
c
c
      do 40 i=1,np+1,last
c
c
      write(20,210) tm(i),um(i),xm(i),pm(i)
  210 format(1X,f10.5,5x,f10.5,5x,f10.5,5x,f10.5)
   40 continue
c
c
      return
c
      end
c
c
c---------------------SUBROUTINE PRINT-1 ENDS HERE----------------------
c
c-----------------------------------------------------------------------
c
c---------------------SUBROUTINE PRINT-2 BEGINS HERE--------------------
c
c
      subroutine print_2(delta,phi,gamma,w,eta,rho,eps,uf,xf,pf,last,
     & tm,um,xm,pm,u_init,x_init,p_init,np,n_pcycle,beta,dif,step,
     & n_scycle,sigma1)
c
c
      implicit double precision (a-h,o-z)
c
      dimension tm(100000),um(100000),xm(100000),pm(100000)
c
```

Reproduced with permission of the copyright owner. Further reproduction prohibited without permission.

```
c
c-------------PRINT INPUT DATA ON THE SECOND OUTPUT FILE----------------
c
c
      WRITE(30,1400)
 1400 FORMAT('**********************************
     &**********************************')
      WRITE(30,1600)
 1600 FORMAT(//10X,' S E Q U E N C I N G   B A T C H   R E A C T O R ')
      WRITE(30,1500)
 1500 FORMAT(//10X,'CONCENTRATION OF SUBSTRATE, BIOMASS AND
     &PRODUCT'//)
      WRITE(30,1400)
      write(30,1550)n_pcycle
 1550 format(//10x,'             DURING ',I5,4x,'CYCLES'//)
      WRITE(30,1400)
      write(30,2010)delta,phi,gamma,w
 2010 format(/1x,'DELTA='F10.5,4X,'PHI=',F10.5,4X,
     &'GAMMA=',F12.5,4X,'W=',F10.5)
      write(30,2020) eta,rho,eps,beta
 2020 format(/1x,'ETA=',F10.4,4X,'RHO=',F10.5,4X,'EPS=',F10.5,4x,
     &'BETA=',F10.5)
      write(30,2030)uf,xf,pf
 2030 format(/1x,'UF=',F10.5,4X,'XF=',F10.5,4X,
     &'PF=',F10.5)
      write(30,2040)u_init,x_init,p_init
 2040 format(/1x,'U0=',F10.5,4X,'X0=',F10.5,4X,'P0=',F10.5)
      write(30,2050) np,step
 2050 format(/1x,'NUMBER OF POINTS IN THE TIME DOMAIN=',I5//
     &        1x,'STEP SIZE =',F10.6//)
      WRITE(30,1400)
      write(30,2055) sigma1
 2055 format(//1x,'  SIGMA1 = ', F10.5//)
      WRITE(30,1400)
      write(30,2060)
 2060 format(/1x,'TIME',15X,' U ',15X,' X  ',15X,'  P ')
c
c-------PRINT COMPUTED DATA INTO OUTPUT FILE-------------------------
c
c
      do 41 i=1,np+1,last
c
c
      write(30,2100) tm(i),um(i),xm(i),pm(i)
 2100 format(1X,f10.5,5x,f10.5,5x,f10.5,5x,f10.5)
   41 continue
c
c
      return
c
      end
c
c---------------------SUBROUTINE PRINT-2 ENDS HERE----------------------
c
c-----------------------------------------------------------------------
c
c---------------------SUBROUTINE PRINT-3 BEGINS HERE--------------------
c
c
      subroutine print_3(delta,phi,gamma,w,eta,rho,eps,uf,xf,pf,last,
     & tm,um,xm,pm,u_init,x_init,p_init,np,n_pcycle,beta,dif,step,
     & n_scycle,icycle,sigma1)
c
      implicit double precision (a-h,o-z)
```

Reproduced with permission of the copyright owner. Further reproduction prohibited without permission.

```
c
      dimension tm(100000),um(100000),xm(100000),pm(100000)
c
c
c-----------PRINT INPUT DATA ON OUTPUT FILE----------------------------
c
c
              WRITE(40,1401)
 1401 FORMAT('**********************************
     &**************************************')
      WRITE(40,1601)
 1601 FORMAT(//10X,' S E Q U E N C I N G   B A T C H   R E A C T O R ')
      WRITE(40,1501)
 1501 FORMAT(//10X,'CONCENTRATION OF SUBSTRATE, BIOMASS AND
     &                 PRODUCT'//)
      WRITE(40,1401)
      write(40,2052) icycle
 2052 format(//1x,'STEADY STATE IS REACHED AFTER',I6,4X,'CYCLES'//)
      WRITE(40,1401)
      write(40,2011)delta,phi,gamma,w
 2011 format(/1x,'DELTA='F10.5,4X,'PHI=',F10.5,4X,
     &'GAMMA=',F12.5,4X,'W=',F10.5)
      write(40,2021) eta,rho,eps,beta
 2021 format(/1x,'ETA=',F10.4,4X,'RHO=',F10.5,4X,'EPS=',F10.5,4X,
     & 'BETA=',F10.5)
      write(40,2031)uf,xf,pf
 2031 format(/1x,'UF=',F10.5,4X,'XF=',F10.5,4X,'PF=',F10.5)
      write(40,2041)u_init,x_init,p_init
 2041 format(/1x,'U0=',F10.5,4X,'X0=',F10.1,4X,'P0=',F10.5)
      write(40,2051) np,step
 2051 format(/1x,'NUMBER OF POINTS IN THE TIME DOMAIN=',I10//
     &        1x,'STEP SIZE =',F10.6//)
      WRITE(40,1401)
      write(40,2053) sigma1,dif
 2053 format(//1x,'  SIGMA1 = ',F10.5,10x,'DIF=',F10.5//)
      WRITE(40,1401)
      write(40,2061)
 2061 format(/1x,'TIME',15X,' U ',15X,' X  ',15X,'  P ')
c
c-------PRINT COMPUTED DATA INTO OUTPUT FILE-------------------------
c
      do 44 i=1,np+1,last
c
      write(40,2101) tm(i),um(i),xm(i),pm(i)
 2101 format(1X,f10.5,5x,f10.5,5x,f10.5,5x,f10.5)
c
   44 continue
c
      return
c
      end
c
c------------------END OF SUBROUTINE PRINT-3---------------------------
c
```

Reproduced with permission of the copyright owner. Further reproduction prohibited without permission.

APPENDIX E-3

Program for Analyzing the Dynamics of Biological Reduction of NO_3^-/NO_2^- in a Continuously Operated Sequencing Batch Reactor

Reproduced with permission of the copyright owner. Further reproduction prohibited without permission.

```
c       MULTIPLE NITROGEN LIMITATION IN AN SBR
c
c       This program does continuation (in the operating parameter
c       space) of periodic solutions computed as fixed points of the
c       Poincare map
c-----------------------------------------------------------------------
c-----------------------------------------------------------------------
c
      subroutine func(ndim,u,icp,par,ijac,f,dfdu,dfdp)
c     ---------- ----
c
      implicit double precision (a-h,o-z)
      dimension u(ndim),par(20),tmat(3,6)
      dimension f(ndim),dfdu(ndim,ndim),dfdp(ndim,20)
c
c       Call the subroutine that does integration of the
c       variational and the sensitivity equations.
c       The matrix tmat contains the result of the integration
c
      call fn(u,par,tmat)
c
      f(1)=tmat(1,1)
      f(2)=tmat(2,1)
      f(3)=tmat(3,1)
c
      if (ijac.eq.0) go to 10
c
      dfdu(1,1)=tmat(1,2)
      dfdu(1,2)=tmat(1,3)
      dfdu(1,3)=tmat(1,4)
      dfdu(2,1)=tmat(2,2)
      dfdu(2,2)=tmat(2,3)
      dfdu(2,3)=tmat(2,4)
      dfdu(3,1)=tmat(3,2)
      dfdu(3,2)=tmat(3,3)
      dfdu(3,3)=tmat(3,4)
c
      dfdp(1,4)=tmat(1,5)
      dfdp(2,4)=tmat(2,5)
      dfdp(3,4)=tmat(3,5)
      dfdp(1,5)=tmat(1,6)
      dfdp(2,5)=tmat(2,6)
      dfdp(3,5)=tmat(3,6)
c
 10 continue
c
      return
      end

      subroutine stpnt(ndim,u,par)
c     ---------- -----
c
c in this subroutine starting values for PAR and a corresponding
c fixed point U must be given (i.e., U must satisfy: U = F(U,PAR) ).
c (Used when not restarting from a previously computed solution).
c The problem parameters (PAR) may also be initialized in INIT.
c
c       NDIM   -   Dimension of F and U.
c       U           -   Vector of dimension NDIM.
c                         Upon return, U should contain a fixed point of
F
c                           corresponding to the values assigned to PAR.
c       PAR      -   Array of parameters in the differential equations.
c
```

Reproduced with permission of the copyright owner. Further reproduction prohibited without permission.

```
      implicit double precision (a-h,o-z)
c
      dimension u(ndim),par(20)
c
c Set the problem parameters.
c
c      delta    = v0/vmax
c      phi      = em1/em2
c      om       = ek2/ek1
c      sig1     = t1/t3
c      sig3     = (t3-t2)/t3
c      sig2     = 1.-sig1-sig3
c      eta      = y1/y2
c      gama1    = ek1/eki1
c      gama2    = ek1/eki2
c      e1       = ek21*ek1
c      e2       = ek12*ek1
c      elamda1 = emc1/em2 = 0.08387
c      elamda2 = emc2/em2 = 0.06540
c      rho      = alpha*y1/y1
c           = alpha = 0.616
c
      delta  = 0.5
      phi    = 0.71
      om     = 1.6488
      sig1   = 0.1
      eta    = 1.001
      gama1  = 0.4607
        gama2  = 0.898
      e1     = 0.0959
      e2     = 4.7960
c
       beta    =  6.
       uf      =  1.994
       vf      =  3.081
c
c      load parameter values in array par to carry them over
c      in the various subroutines.
c      par(1), par(2) and par(3) are dummy parameters
c      corresponding to the variational equations.
c      par(11) is not used because it is reserved by AUTO
c      par(15) is used later
c
      par(4)  = beta
      par(5)  = uf
      par(6)  = vf
      par(7)  = delta
      par(8)  = phi
      par(9)  = om
      par(10) = sig1
      par(12) = eta
      par(13) = gama1
      par(14) = gama2
      par(16) = e1
      par(17) = e2
c
c define the fixed point.
c
      u(1) = uf
      u(2) = vf
      u(3) = 0.
c
      return
      end
```

Reproduced with permission of the copyright owner. Further reproduction prohibited without permission.

```
c
c
c
      subroutine init
c     ---------- ----
c
      implicit double precision (a-h,o-z)
c
      common /blbcn/ ndim,ips,irs,ilp,icp(20),par(20)
      common /blcde/ ntst,ncol,iad,isp,isw,iplt,nbc,nint
      common /bldls/ ds,dsmin,dsmax,iads
      common /bltht/ thetal(20),thetau
      common /bleps/ epsl(20),epsu,epss
      common /bllim/ nmx,nuzr,rl0,rl1,a0,a1
      common /blmax/ npr,mxbf,iid,itmx,itnw,nwtn,jac
c
       do 13 i=1,20
       epsl(i)=1.d-5
 13   continue
       epsu   = 1.d-5
       epss   = 1.d-5
       thetal(1)=1.
       thetau= 1.
       ips    =-1
       ndim   = 3
c***
       icp(1)= 4
       icp(2)= 5
       irs    = 0
       isw    = 1
       ilp    = 1
c
       iplt   = 1
c
       nmx    =200
       rl0    =  0.
       rl1    = 10.
       a0     =  0.
       a1     = 10.
       ds     =  0.05
       dsmin  =  0.0001
       dsmax  =  1.
       npr    =  1
c
       return
       end
c
       function uszr(i,nuzr,par)
c      -------- ----
c
      implicit double precision (a-h,o-z)
c
      dimension par(20)
c
c This example has no functions of which zeroes are to be determined.
c (Since the default assignment NUZR=0 is used).
c
       uszr=0.0
c
      return
      end
c
c
c
```

Reproduced with permission of the copyright owner. Further reproduction prohibited without permission.

```
c*********************************************
      subroutine fn(u,par,y)
c
c      this subroutine does integration of the variational
c      and the sensitivity equations of the system
c*********************************************
      implicit double precision(a-h,o-z)
      external fun,dfun,jfun
      dimension u(3),par(20),y(3,6),atol(3,6),rtol(3,6),
     1          rwork(500),iwork(100),neq(2),iopt(3)
c
c   model parameters
c
      par(1) = 0.
      par(2) = 0.
      par(3) = 0.
c
      beta    = par(4)
      uf        = par(5)
      vf        = par(6)
      delta   = par(7)
      phi      = par(8)
      om      = par(9)
      sig1     = par(10)
      eta      = par(12)
      gama1 = par(13)
      gama2 = par(14)
      e1       = par(16)
      e2       = par(17)
c
c
c   initial conditions for odessa
c
      n        =3
      npar   =5
      neq(1)=n
      neq(2)=npar
      nsv     =npar+1
      do 10 i=1,n
      do 10 j=1,nsv
 10 y(i,j)=0.
      y(1,1)=u(1)
      y(2,1)=u(2)
      y(3,1)=u(3)
      y(1,2)=1.
      y(2,3)=1.
      y(3,4)=1.
c
c   error control
c
      err  = 1.d-7
      itol  = 4
      do 20 i=1,n
      do 20 j=1,nsv
      rtol(i,j)  =err
20 atol(i,j)=err
c
c   parameters of odessa
c
      itask   = 1
      iopt(1)= 0
      iopt(2)= 1
      iopt(3)= 1
      lrw = 500
```

Reproduced with permission of the copyright owner. Further reproduction prohibited without permission.

```
      liw = 100
      mf  =  21
      T   =   0.
c
c  set the time step to the period
c
      period = 1.-delta
c****
c   The following set of commands allows for a double call
c   to the integrator for the case of bang-bang forcing
c   The parameter PAR(15) is 1 for 0<t<sig1(1-delta)
c   and 0 for sig1(1-delta)<t<1-delta
c
      par(15)=1.
      tout  =sig1*period
 35 istate=1
        CALL ODESSA(fun,dfun,NEQ,Y,PAR,T,TOUT,ITOL,RTOL,ATOL,
    1    ITASK,ISTATE, IOPT,RWORK,LRW,IWORK,LIW,jfun,MF)
c
      if(istate.eq.-1) go to 35
      if(istate.lt.0) go to 45
c
c   ... and the second half of the integration
c
      par(15)=0.
      t=sig1*period
      tout=period
   36 istate=1
        CALL ODESSA(fun,dfun,NEQ,Y,PAR,T,TOUT,ITOL,RTOL,ATOL,
     1    ITASK,ISTATE, IOPT,RWORK,LRW,IWORK,LIW,jfun,MF)
c
      if(istate.eq.-1) go to 36
      if(istate.lt.0) go to 45
      return
 45 write(6,*) '  istate=  ',istate
      stop
      end
C**********************************************************************
      subroutine fun(neqn,t,y,par,ydot)
C**********************************************************************
c  this subroutine computes the vectorfield
c
      IMPLICIT DOUBLE PRECISION (A-H,O-Z)
      dimension y(neqn),ydot(neqn),par(20)
C*****
c
c   model parameters
c
      beta    = par(4)
      uf       = par(5)
      vf       = par(6)
      delta  = par(7)
      phi     = par(8)
      om     = par(9)
      sig1    = par(10)
      eta      = par(12)
      gama1 = par(13)
      gama2 = par(14)
      e1      = par(16)
      e2      = par(17)
      elamda1 = 0.08387
      elamda2 = 0.06540
      rho     = 0.616
c
```

Reproduced with permission of the copyright owner. Further reproduction prohibited without permission.

```
      If (u.gt.0.0) then
         delu = 1.0
      else
         delu = 0.0
      endif
c
      If (v.gt.0.0) then
         delv = 1.0
      else
         delv = 0.0
      endif
c
      If (v.lt.0.469) then
         e1 = 0.0
         e2 = 0.0
      endif
c
      u  = y(1)
      v  = y(2)
      x  = y(3)
c
      g1 = phi*u/(1.+u+gama1*u*u+e1*u*v)
      g2 =      v/(om+v+gama2*v*v+e2*u*v)
c
c  vectorfield
c
            ydot(1) = (uf-u)*par(15)/(delta*sig1+t)-beta*g1*x
     ydot(2) = (vf-v)*par(15)/(delta*sig1+t)+rho*beta*g1*x
     1                        -eta*beta*g2*x
     ydot(3) = -x*par(15)/(delta*sig1+t)+beta*g1*x+beta*g2*x
     1                      -elamda1*beta*x*delu-elamda2*beta*x*delv
c
C*****
      RETURN
      END
C*******************************************************************************
      subroutine jfun(neqn,t,y,par,ml,mu,pd,nrpd)
c*********************************************
c  this subroutine computes the jacobian
c  of the vectorfield
c***
      implicit double precision (a-h,o-z)
c
      dimension y(neqn),pd(nrpd,neqn),par(20)
C*****
      COMMON /PARAMC/ RPAR(20)
c
c   model parameters
c
      beta    = par(4)
      uf        = par(5)
      vf        = par(6)
      delta   = par(7)
      phi      = par(8)
      om      = par(9)
      sig1     = par(10)
      eta      = par(12)
      gama1 = par(13)
      gama2 = par(14)
      e1       = par(16)
      e2       = par(17)
      elamda1 = 0.08387
      elamda2 = 0.06540
      rho      = 0.616
```

Reproduced with permission of the copyright owner. Further reproduction prohibited without permission.

```
c
      If (u.gt.0.) then
         delu = 1.0
      else
         delu = 0.0
      endif
c
      If (v.gt.0.) then
         delv = 1.0
      else
         delv = 0.0
      endif
c
      If (v.lt.0.469) then
         e1 = 0.0
         e2 = 0.0
      endif
c
      u   = y(1)
      v   = y(2)
      x   = y(3)
c
      g1  = phi*u/(1.+u+gama1*u*u+e1*u*v)
      g2  =      v/(om+v+gama2*v*v+e2*u*v)
c
      r11 = phi*(1.-gama1*u*u)/(1.+u+gama1*u*u+e1*u*v)**2.
      r12 =-phi*e1*u*u/(1.+u+gama1*u*u+e1*u*v)**2.
      r21 =-e2*v*v/(om+v+gama2*v*v+e2*u*v)**2.
      r22 = (om-gama2*v*v)/(om+v+gama2*v*v+e2*u*v)**2.
c
c  jacobian of the vectorfield
c
      do 10 i = 1,neqn
      do 10 j = 1,neqn
 10 pd(i,j) = 0.
      pd(1,1) = -par(15)/(delta*sig1+t)-beta*x*r11
      pd(1,2) = -beta*x*r12
      pd(1,3) = -beta*g1
      pd(2,1) = rho*beta*x*r11-eta*beta*x*r21
      pd(2,2) = -par(15)/(delta*sig1+t)+beta*x*(rho*r12-eta*r22)
      pd(2,3) = rho*beta*g1-eta*beta*g2
      pd(3,1) = beta*x*r11+beta*x*r21
      pd(3,2) = beta*x*r12+beta*x*r22
      pd(3,3) = -par(15)/(delta*sig1+t)+beta*(g1+g2-elamda1*delu
     &             -elamda2*delv)
c
      RETURN
      END
c*****************************************
      subroutine dfun(neqn,t,y,par,dfdp,jpar)
c*****************************************
c   partial derivatives wrt. parameters of interest
c
      implicit double precision(a-h,o-z)
      dimension y(neqn),par(20),dfdp(20)
c
c   model parameters
c
      beta    = par(4)
      uf        = par(5)
      vf        = par(6)
      delta   = par(7)
      phi      = par(8)
      om      = par(9)
```

Reproduced with permission of the copyright owner. Further reproduction prohibited without permission.

```
      sig1     = par(10)
      eta      = par(12)
      gama1 = par(13)
      gama2 = par(14)
      e1       = par(16)
      e2       = par(17)
      elamda1 = 0.08387
      elamda2 = 0.06540
      rho      = 0.616
c
      If (u.gt.0.0) then
         delu = 1.0
      else
         delu = 0.0
      endif
c
      If (v.gt.0.0) then
         delv = 1.0
      else
         delv = 0.0
      endif
c
      If (v.lt.0.469) then
         e1 = 0.0
         e2 = 0.0
      endif
c
      u  = y(1)
      v  = y(2)
      x  = y(3)
c
      g1 = phi*u/(1.+u+gama1*u*u+e1*u*v)
      g2 =      v/(om+v+gama2*v*v+e2*u*v)
c
      go to (1,2,3,4,5) jpar
c
    1 return
c
    2 return
c
    3 return
c
    4 dfdp(1)=-g1*x
      dfdp(2)=rho*g1*x-eta*g2*x
      dfdp(3)=(g1+g2-elamda1*delu-elamda2*delv)*x
      return
c
    5 dfdp(1)=par(15)/(delta*sig1+t)
      dfdp(2)=0.
      dfdp(3)=0.
      return
      end
c-------------------------------------------------------
c     dummy subroutines
c-------------------------------------------------------
      subroutine bcnd
      return
      end
      subroutine fopt
      return
      end
      subroutine icnd
      return
      end
```

Reproduced with permission of the copyright owner. Further reproduction prohibited without permission.

APPENDIX E-4

Program for Searching the Kinetic Parameters in the Andrews-Herbert Kinetic Model by the Aid of a Statistical Computer Package -- SAS

Reproduced with permission of the copyright owner. Further reproduction prohibited without permission.

```
TITLE 'Andrews-Herbert Model: Y = A * X / (B+X+X**2/C) - D';
;
DATA;
   INPUT X Y @@;
   CARDS;
  6.90  0.030076    6.96  0.022722    9.16  0.063497
 10.28  0.059426   14.09  0.069754   17.20  0.105700
 21.76  0.108134   31.11  0.152641   32.07  0.149323
 44.13  0.154594   46.34  0.148988   54.29  0.143144
 54.55  0.144629   77.89  0.138392   85.22  0.127593
 90.91  0.129882  104.07  0.125402  108.64  0.118662
114.35  0.112052  126.23  0.099853  128.51  0.101797
140.08  0.100379  149.59  0.088163  168.70  0.078012
180.85  0.072950  191.63  0.063662  231.46  0.046784
;
PROC NLIN  BEST = 10 PLOT  METHOD = MARQUARDT;
   PARMS  A =  0.1 TO  10
          B = 10.0 TO 100
          C = 10.0 TO 100
;
   MODEL Y =  A * X / (B + X + X**2 / C) - 0.0586;
         DER.A =  X / (B + X + X**2 / C);
         DER.B = -A * X / (B + X + X**2 / C)**2;
         DER.C =  A * X**3 / (B + X + X**2 / C)**2 / C**2;
;
   OUTPUT OUT = B  P = YHAT  R = YRESID;
;
PROC PLOT  DATA = B;
   PLOT Y * X = 'A' YHAT * X = 'P' /OVERLAY  VPOS = 25;
   PLOT YRESID * X /VREF = 0  VPOS = 25;
;
PROC PRINT  DATA = B;
```

Reproduced with permission of the copyright owner. Further reproduction prohibited without permission.

APPENDIX E-5

Program for Searching the Parameters in the Non-competitive Model Expressing the Dependence of the Kinetics of pH. This Program Calls the Statistical Computer Package -- SAS

Reproduced with permission of the copyright owner. Further reproduction prohibited without permission.

```
TITLE 'Noncompetitive Model: Y=A/(1+B*(10**abs(7.35-X)-1))';
;
DATA;
   INPUT X Y @@;
   CARDS;
6.68  6.8210   6.82  9.3834   6.85 10.4736   7.06 14.0802
7.10 14.4629   7.12 14.7300   7.17 14.3144   7.40 13.8214
7.61 13.6532   7.99 10.6049   8.06  9.8474   8.29  4.9897
8.30  5.2774   8.34  6.8269   8.45  5.0423
;
PROC NLIN  BEST = 10 PLOT  METHOD = MARQUARDT;
   PARMS A = 0.1 TO 1.
         B = 0.1 TO 1.
;
   MODEL Y =  A * 100 / (1 + B * (10**abs(7.35 - X) - 1));
         DER.A =  100 / (1 + B * (10**abs(7.35 - X) - 1));
         DER.B = -A * 100 * (10**abs(7.35 - X) - 1) /
                   (1 + B * (10**abs(7.35 - X) - 1))**2;
;
   OUTPUT  OUT = B  P = YHAT  R = YRESID;
;
PROC PLOT  DATA = B;
   PLOT  Y * X = 'A'  YHAT * X = 'P' /OVERLAY  VPOS = 25;
   PLOT  YRESID * X  /VREF = 0  VPOS = 25;
;
PROC PRINT  DATA = B;
```

Reproduced with permission of the copyright owner. Further reproduction prohibited without permission.

REFERENCES

Abufayed, A. A. and E. D. Schroeder. 1986a. "Performance of SBR / Denitrification with a Primary Sludge Carbon Source." *J. WPCF*, **58**(5): 387-397.

Abufayed, A. A. and E. D. Schroeder. 1986b. "Kinetics and Stoichiometry of SBR / Denitrification with a Primary Sludge Carbon Source." *J. WPCF*, **58**(5): 398-405.

Alleman, J. E. and R. L. Irvine. 1980. "Storage-Induced Denitrification Using Sequencing Batch Reactor Operation." *Water Res.*, **14**: 1483-1488.

Andrews, J. F. 1968. "A Mathematical Model for the Continuous Culture of Microorganisms Utilizing Inhibitory Substrates." *Biotechnol. Bioeng.*, **10**: 707-723.

Antoniou, P., J. Hamilton, B. Koopman, R. Jain, B. Holloway, G. Lyberatos, and S. A. Svoronos. 1990. "Effect of Temperature and pH on the Effective Maximum Specific Growth Rate of Nitrifying Bacteria." *Water Res.*, **24**(1): 97-101.

Arora, M. L., E. F. Barth, and M. B. Umphres. 1985. "Technology Evaluation of Sequencing Batch Reactors." *J. WPCF*, **57**(8): 867-875.

ASTM Standards, Method: D 4815 - 89. 1989 "Standard Test Method for Determination of C_1 to C_4 Alcohols and MTBE in Gasoline by Gas Chromatography." ASTM Committee on Standards, Philadelphia, PA.

Atlas, R. M. 1988. *Microbiology: Fundamentals and Applications*. 2nd Edition, Macmillan Publishing Company, New York, New York

Bailey, J. E.. 1973. "Periodic Operation of Chemical Reactors: A Review." *Chem. Eng. Commun.*, **1**: 111-124.

Bailey, J. E., and D. F. Ollis. 1986. *Biochemical Engineering Fundamentals*. McGraw-Hill, New York, New York

Baltzis, B. C., G. A. Lewandowski, and S.-H. Chang. 1987. "A Dynamic Model of a Fill-And-Draw Reactor and its Implications for Hazardous Waste Treatment." presented at the AIChE National Conference, November, New York, New York

Baltzis, B. C., G. A. Lewandowski, and S. Sanyal. 1990. "Sequencing Batch Reactor Design in a Denitrifying Application." in *Am. Chem. Soc. Symp. Ser. 468: Emerging Technologies in Hazardous Waste Management II*, D. W. Tedder and F. G. Pohland (eds.), Chapter 14, June 4-7, Atlantic City, New Jersey.

Reproduced with permission of the copyright owner. Further reproduction prohibited without permission.

Beccari, M., R. Passino, R. Ramadori, and V. Tandoi. 1983. "Kinetics of Dissimilatory Nitrate and Nitrite Reduction in Suspended Growth Culture." *J. WPCF,* **55:** 58-64.

Betlach, M. R. and J. M. Tiedje. 1981. "Kinetic Explanation for Accumulation of Nitrite, Nitric Oxide, and Nitrous Oxide During Bacterial Denitrification." *Appl. and Environ. Microbiol.*, **42**(6)**:** 1074-1084.

Biswas, N. and R. G. Warnock. 1971. "Nitrogen Transformations and Fate of Other Parameters in Columnar Denitrification." *Water Res.*, **19**(8)**:** 1065-1071.

Bruno, J. B. and Paris D. N. Svoronos, *Basic Tables for Chemical Analysis.* National Bureau of Standards (NBS) Technical Note 1096, U. S. Department of Commerce, U. S. Government Printing Office, Washington D. C. (1986)

Bryan, B. A., G. Shearer, J. L. Skeeters, and D. H. Kohl. 1983. "Variable Expression of the Nitrogen Isotope Effect Associated with Denitrification of Nitrite." *J. Biol. Chem.*, **258**(14)**:** 8613-8617.

Chang, S.-H. 1987. *A Dynamic Model of a Fill-and-Draw Reactor and Its Implications for Hazardous Waste Treatment.* M.S. Thesis, New Jersey Institute of Technology.

Dahab, M. F. and Y. W. Lee. 1988. "Nitrate Removal from Water Supplies Using Biological Denitrification." *J. WPCF*, **60**(9)**:** 1670-1674.

Dawes, E. A., and D. W. Ribbons. 1962. "The Endogenous Metabolism of Micro-Organisms." *Ann. Rev. Microbiol.*, **16:** 241-264.

———. 1964. "Some Aspects of the Metabolism of Bacteria." *Bacteriol. Rev.*, **28**(2)**:** 126-149.

Dawson, R. N. and K. L. Murphy. 1972. "The Temperature Dependency of Biological Denitrification." *Water Res.*, **6:** 71-83.

Delwiche, C. C. 1959. "Production and Utilization of Nitrous Oxide by *Pseudomonas denitrificans.*" *J. Bacteriol.*, **77:** 55-59.

Dennis, R. W. and R. L. Irvine. 1979. "Effect of Fill:React Ratio on Sequencing Batch Biological Reactors." *J. WPCF*, **51**(2)**:** 255-263.

Dikshitulu, S. 1993. "Competition Between Two Microbial Populations in a Sequencing Fed-Batch Reactor and its Implications for Waste Treatment Applications." *Ph.D. Dissertation*, New Jersey Institute of Technology, Newark, N. J.

Reproduced with permission of the copyright owner. Further reproduction prohibited without permission.

Dikshitulu, S., B. C. Baltzis, G. A. Lewandowski, and S. Povlou. 1993. "Competition Between Two Microbial Populations in a Sequencing Fed-Batch Reactor: Theory, Experimental Verification, and Implications for Waste Treatment Applications." *Biotechnol. Bioeng.*, **42**: 643-656.

Dixon, M. and E.C. Webb. 1979. *Enzymes*. 3rd Edition, Academic Press, NewYork, New York

Doedel, E. J. 1986. *Auto 86 User Manual: Software for Continuation and Bifurcation Problems in Ordinary Differental Equations.* Second Printing, VAX/VMS, CIT Press, Pasadena, CA.

Drew, C. M. and J. R. McNesby. 1957. "Some Problems Encountered with the Application of Vapour Phase Chromatography to Kinetic Studies." in *Vapor Phase Chromatography*. Edited by D. H. Desty and C. L. A. Harbourn, Butterworths Scientific Publications, London.

Evans, P. J., W. Ling, N. J. Palleroni, and L. Y. Young. 1992. "Quantification of Denitrification by Strain T1 During Anaerobic Degradation of Toluene." *Appl. Microbiol. Biotech.*, **58:** 832-836.

Frame, K. K. and W.-S. Hu. 1990. "Cell Volume Measurement as An Estimation of Mammalian Cell Biomass." *Biotech. Bioeng.*, **36:** 191-197.

Francis, C. W. and J. B. Mankin. 1977. "High Nitrate Denitrification in Countinuous Flow-Stirred Reactors." *Water Res.*, **11:** 289-294.

Fredrickson, A. G. and H. M. Tsuchiya. 1977. "Microbial Kinetics and Dynamics." in *Chemical Reactor Theory: A Review.* edited by L. Lapidus and N. R. Amundson. Prentice-Hall, New Jersey.

Garber, E. A. E. and T. C. Hollocher. 1981. "^{15}N Tracer Studies on the Role of NO in Denitrification." *J. Biol. Chem.*, **256:** 5459-5465.

Gayle, B. P., G. D. Boardman, J. H. Sherrard, and R. E. Benoit. 1989. "Biological Denitrification of Water." *J. Environ. Eng.*, **115**(5): 930-943.

Grabinska-Loniewska, T. Slomczynski, and Z. Kanska. 1985. "Denitrification Studies with Glycerol as A Carbon Source." *Water Res.*, **19**(12): 1471-1477.

Grayson, M. (ed.). 1980. *Kirk-Othmer Encyclopedia of Chemical Technology*. 3rd Edition, **9**:99 John Wiley & Sons, New York, New York

Reproduced with permission of the copyright owner. Further reproduction prohibited without permission.

Hamilton, J., R. Jain, P. Antoniou, S. A. Svoronos, B. Koopman, and G. Lyberatos. 1992. "Modeling and Pilot-Scale Experimental Verification for Predenitrification Process." *J. Appl. Bact.*, **35:** 597-607.

Hartmann, L. and G. Laubenberger. 1968. "Toxicity Measurements in Activated Sludge." *Proc. Am. Soc. Civ. Eng., J. Sanit. Eng. Div.*, **94:**(SA 2) 247-256.

Henze, M. 1987. "Theories for Estimation of the Fraction of Denitrifiers in Combined Nitrifying-Denitrifying Treatment Plants." *Water Res.*, **21**(12): 1521-1524.

Herbert, D. 1958. "The Continuous Culture of Microorganisms; Some Theoretical Aspects." in "Continuous Cultivation of Microorganisms. A Symposium." I. Malek, ed. Publishing House of the Czechoslovak Academy of Sciences, Prague, 45-52.

Hernandez, D. and J. J. Rowe. 1987. "Oxygen Regulation of Nitrate Uptake in Denitrifying *Pseudomonas aeruginosa*." *Appl. and Environ. Microbiol.*, **53**(4): 745-750.

Hildebrand, J. H. and R. L. Scott. 1962. *Regular Solutions*. Chapter 2, p.23, Printice-Hall, Englewood, New Jersey

Hoepker, E. C. and E. D. Schroeder. 1979. "The Effect of Loading Rate on Batch-Activated Sludge Effluent Quality." *J. WPCF*, **51**(2): 264-273.

Hsu, E. H. 1986. "Treatment of a Petrochemical Wastewater in Sequencing Batch Reactors." *Environ. Prog.*, **5**(2): 71-81.

Ingraham, J. L. 1958. "Growth of Psychrophilic Bacteria." *J. Bacteriol.*, **76:** 75-80.

Irvine, R. L. and A. W. Busch. 1979. "Sequencing Batch Biological Reactor -- An Overview." *J. WPCF*, **51**(2): 235-243.

Irvine, R. L., L. H. Ketchum, R. Breyfogle, and E. F. Barth. 1983. "Municipal Application of Sequencing Batch Treatment." *J. WPCF*, **55**(5): 484-488.

Irvine, R. L., G. Miller, and A. S. Bhamrah. 1979. "Sequencing Batch Treatment of Wastewaters in Rural Areas." *J. WPCF*, **51**(2): 244-254.

Irvine, R. L., D. V. S. Murthy, M. L. Arora, J. L. Copeman, and J. A. Heidman. 1987. "Analysis of Full-Scale SBR Operation at Grundy Center, Iowa." *J. WPCF*, **59**(3): 132-138.

Iwasaki, H. and T. Mori. 1955. "Studies on Denitrification -- I. Nitrogen Production by a Strain of Denitrifying Bacteria Using Toluylene Blue as a Hydrogen Carrier." *J. Biochem.*, **42**(4): 375-380.

Reproduced with permission of the copyright owner. Further reproduction prohibited without permission.

Iwasaki, H., R. Matsubayashi, and T. Mori. 1956. "Studies on Denitrification -- II. Production of Nitric Oxide and Its Utilization in the n-n-Linkage Formation by Denitrifying Bacteria." *J. Biochem.*, **43**(3): 295-305.

Iwasaki, H. and T. Mori. 1958. "Studies on Denitrification -- III. Enzymatic Gas Production by the Reaction of Nitrite with Hydroxyamine." *J. Biochem.*, **45**(2): 133-140.

Iwasaki, H. 1960. "Studies on Denitrification -- IV. Participation of Cytochromes in the Denitrification." *J. Biochem.*, **47**(2): 174-184.

Iwasaki, H. and T. Mori. 1962. "Studies on Denitrification -- V. Purification of Denitrifying Enzyme by Means of Electrophoresis." *J. Biochem.*, **52**(3): 190-192.

Iwasaki, H., S. Shidara, H. Suzuki, and T. Mori. 1963. "Studies on Denitrification -- VII. Further Purification and Properties of Denitrifying Enzyme." *J. Biochem.*, **53**(4): 299-303.

Jain, R., G. Lyberatos, and S. A. Svoronos. 1992. "Operational Strategies for Predinitrification Process." *J. Environ. Eng.*, **118**(1): 56-67.

Johnson, F. J., and I. Lewin. 1946. *J. Cellular Comp. Physiol.*, **28:** 47.

Jones, W. L., E. D. Schroeder, and P. A. Wilderer. 1990a. "Denitrification in a Batch Wastewater Treatment System Using Sequestered Organic Substances." *J. WPCF*, **62**(3): 259-267.

Jones, W. L., P. A. Wilderer, and E. D. Schroeder. 1990b. "Operation of a Three-Stage SBR System for Nitrogen Removal from Wastewater." *J. WPCF*, **62**(3): 268-274.

Ju, L. -K., W. B. Armiger, X. Yang, and J. F. Lee. 1991. "On-Line Monitoring of Biological Activities in Wastewater Treatment Processes Based on the Culture Fluorescence." Presented at AIChE 1991 Summer National Meeting.

Ju, L. -K. and H. K. Trivedi. 1992 "Monitoring of Denitrification by Pseudomonas aeruginosa Using On-Line Fluorescence Technique." *Biotech. Tech.*, **6**(6): 549-554.

Ketchum, Jr. L. H., R. L. Irvine, and P. -C. Liao. 1979. "First Cost Analysis of Sequencing Batch Biological Reactors." *J. WPCF*, **51**(2): 288-297.

Ketchum, Jr. L. H. and P. -C. Liao. 1979. "Tertiary Chemical Treatment for Phosphorus Reduction Using Sequencing Batch Reactors." *J. WPCF*, **51**(2): 298-304.

Klapwijk, A., J. C. M. van der Hoeven and G. Lettinga. 1981. "Biological Denitrification in An Upflow Sludge Blanket Reactor." *Water Res.*, **15:** 1-6.

Reproduced with permission of the copyright owner. Further reproduction prohibited without permission.

Klingensmith, K. M. and V. Alexander. 1983. "Sediment Nitrification, Denitrification, and Nitrous Oxide Production in A Deep Arctic Lake." *Appl. and Environ. Microbiol.*, **46**(5): 1084-1092.

Knowles, R. 1982. "Denitrification." *Microbiol. Rev.*, **46**(1): 43-70.

Kodama, T., K. Shimada, and T. Mori. 1969. "Studies on Anaerobic Biphasic Growth of A Denitrifying Bacterium, *Pseudomonas stutzeri*." *Plant & Cell Physiol.*, **10**: 855-865.

Koike, I., and A. Hattori. 1975a. "Growth Yield of a Denitrifying Bacterium, *Pseudomonas denitrificans*, under Aerobic and Denitrifying Conditions." *J. gen. Microbiol.*, **88**: 1-10.

———. 1975b. "Energy Yield of Denitrification: An Estimate from Growth Yield in Continuous Cultures of *Pseudomonas denitrificans* under Nitrate-, Nitrite- and Nitrous Oxide-limited Conditions." *J. gen. Microbiol.*, **88**: 11-19.

Koopman, B., C. M. Stevens, C. A. Wonderlick. 1990. "Denitrification in a Moving Bed Upflow Sand Filter." *J. WPCF*, **62**(3): 239-245.

Krul, J. M. and R. Veeningen. 1977. "The Synthesis of the Dissimilatory Nitrate Reductase Under Aerobic Conditions in a Number of Denitrifying Bacteria, Isolated from Activated Sludge and Drinking Water." *Water Res.*, **11**: 39-43.

Kunerth, W. 1922. "Solubility of CO_2 and N_2O in Certain Solvents." *Phys. Rev.*, **19**: 512-524.

Lamanna, C. 1963. *Endogenous Metabolism with Special Reference to Bacteria.* edited by Harold E. Whipple, *Ann. N. Y. Acad. Sci.*, **102**: art. 3, 515-793.

Lee, Y. W. and M. F. Dahab. 1988. "Kinetics of Low Solids Bio-denitrification of Water Supplies." *J. WPCF*, **60**: 1857-1861.

Manoharan, R., S. Liptak, P. Parkinson, D. Mavinic, and C. W. Randall. 1989. "A Comparison of Glucose and Methanol as Carbon Sources for Denitrification in Biological Treatment of Leachate." *43rd Purdue Industrial Waste Conference Proceedings*, 196-202.

Marr, A. G., E. H. Nilson, and D. J. Clark. 1963. "The Maintenance Requirment of *Escherichia coli*." *Ann. N. Y. Acad. Sci.*, **102**: art. 3, 536-548.

Reproduced with permission of the copyright owner. Further reproduction prohibited without permission.

Marvillet, L. and J. Tranchant. 1960. "Qualitative and Quantitative Analysis by Gas-Solid Chromatography, of Mixtures containing Nitrogen Oxides." in *Proceedings of the Third Symposium on Gas Chromatography.* (Edinburgh). Page 321-332, Edited by R. P. W. Scott, Butterworths Scientific, Washington D. C.

Matsubara, T. and T. Mori. 1968. "Studies on Denitrification -- IX. Nitrous Oxide, Its Production and Reduction to Nitrogen." *J. Biochem.*, **64**(6): 863-871.

Matsubara, T. 1970. "Studies on Denitrification -- XII. Gas Production from Amines and Nitrite." *J. Biochem.*, **67**(2): 229-235.

———. 1971. "Studies on Denitrification -- XIII. Some Properties of the N_2O-Anaerobically Grown Cell." *J. Biochem.*, **69**(6): 991-1001.

McCarty, P. L., L. Beck, and P. St. Amant. 1969. "Biological Denitrification of Wastewaters by Addition of Organic Materials." *Proc. Ind. Waste Conf. Purdue Univ. Ext. Ser.*, **135**: 1271-1285.

Michaelis, L. 1922. *Die Wasserstoffionenkonzentration*, Springer-Verlag, Berlin.

Mindrup, R. 1978. "The Analysis of Gases and Light Hydrocarbons by Gas Chromatography." *J. Chromatogr. Sci.*, **16**: 380-389.

Miyata, M. and T. Mori. 1968. "Studies on Denitrification -- VIII. Production of Nitric Oxide by Denitrifying Reaction in the Presence of Tetramethyl-p-Phenylenediamine." *J. Biochem.*, **64**(6): 849-861.

Miyata, M. and T. Mori. 1969a. "Studies on Denitrification -- X. The "Denitrifying Enzyme as a Nitrite Reductase and the Electron Donating System for Denitrification." *J. Biochem.*, **66**(4): 463-471.

Miyata, M., T. Matsubara, and T. Mori. 1969b. "Studies on Denitrification -- XI. Some Properties of Nitric Oxide Reductase." *J. Biochem.*, **66**(6): 759-765.

Monod, J. 1942. *Recherches sur la croissance des cultures bactériennes.* Hermann et Cie., Paris.

Moore, S. F. and E. D. Schroeder. 1970. "An Investigation of the Effects of Residence Time on Anaerobic Bacterial Denitrification." *Water Res.*, **4**: 685-694.

Mulcahy, L. T. and W. K. Shieh. 1987. "Fluidization and Reactor Biomass Characteristics of the Denitrification Fluidized Bed Biofilm Reactor." *Water Res.*, **21**(4): 451-458.

Reproduced with permission of the copyright owner. Further reproduction prohibited without permission.

Nakajima, M., T. Hayamizu, and H. Nishimura. 1984a. "Effect of Oxygen Concentration on Rates of Denitratification and Denitritification in the Sediments of An Eutrophic Lake." *Water Res.*, **18**(3): 335-338.

———. 1984b. "Inhibitory Effect of Oxygen on Denitratification and Denitritification in Sludge from An Oxidation Ditch." *Water Res.*, **18**(3): 339-343.

Narkis, N., M. Rebhun, and Ch. Sheindore. 1979. "Denitrification at Various Carbon to Nitrogen Ratios." *Water Res.*, **13**: 93-98.

Ng, H. 1969. "Effect of Decreasing Growth Temperature on Cell Yield of *Escherichia coli*." *Am. Soc. Microbiol.*, **98**(1): 232-237.

Nozawa, T. and Y. Maruyama. 1988. "Denitrification by a Soil Bacterium with Phthalate and Other Aromatic Compounds as Substrates." *J. Bacteriol.*, **170**(6): 2501-2505.

Nurse, G. R. 1980. "Denitrification with Methanol: Microbiology and Biochemistry." *Water Res.*, **14**: 531-537.

Nyamapfene, K. W. and E. G. Mtetwa. 1987. "Biological Denitrification of A Highly Nitrogenous Industrial Effluent: A Case Study in Zimbabwe." *Environ. Pollut.*, **44**: 119-126.

Ohnishi, T. 1963. "Oxidative Phosphorylation Coupled with Nitrate Respiration with Cell Free Extract of *Pseudomonas denitrificans*." *J. Biochem.*, **53**(1): 71-79.

Painter, H. A. 1970. "A Review of Literature on Inorganic Nitrogen Metabolism in Microorganisms." *Water Res.*, **4**: 393-450.

Palis, J. C. and R. L. Irvine. 1985. "Nitrogen Removal in a Low-Loaded Single Tank Sequencing Batch Reactor." *J. WPCF*, **57**(1): 82-85.

Palumbo, S. A. and L. D.Witter. 1969. "Influence of Temperature on Glucose Utilization by *Pseudomonas fluorescens*." *Appl. Microbiol.*, **18**(2): 137-141.

Payne, W. J. 1981. *Denitrification*. John Wiley & Sons, Inc., New York, New York

Payne, W. J, P. S. Riley, and C. D. Cox, Jr. 1971. "Separate Nitrite, Nitric Oxide, and Nitrous Oxide Reducing Fractions from *Pseudomonas perfectomarinus*." *J. Bacteriol.*, **106**(2): 356-361.

Perry, J. H. and C. Chilton. 1973. *Chemical Engineer Handbook*. 5th Edition, McGraw-Hill, New York, New York

Reproduced with permission of the copyright owner. Further reproduction prohibited without permission.

Pirt S. J. 1965. "The Maintenance Energy of Bacteria in Growing Cultures." *Roy. Soc. Proc., B.*, **165:** 224-231.

Polprasert, C. and H. S. Park. 1986. "Effluent Denitrification With Anaerobic Filters." *Water Res.*, **20(8):** 1015-1021.

Przytocka-Jusiak, M., M. Blaszcyk, E. Kosinska, and A. Bisz-Konarzewska. 1984. "Removal of Nitrogen from Industrial Wastewaters with the Use of Algal Rotating Disks and Denitrification Packed Bed Reactor." *Water Res.*, **18**(9)**:** 1077-1082.

Rittmann, B. E. and W. E. Langeland. 1985. "Simultaneous Denitrification with Nitrification in Single-Channel Oxidation Ditches." *J. WPCF*, **57**(4)**:** 300-308.

Sacks, L. E. and H. A. Barker. 1949. "The Influence of Oxygen on Nitrate and Nitrite Reduction." *J. WPCF*, **58:** 11-22.

Sanyal, S. 1990. *Mathematical Modeling and Computer Simulations of Biodenitrification in Batch and Sequencing Batch Reactors.* M.S. Thesis, New Jersey Institute of Technology.

Schügerl, K. 1989. "Biofluidization: Application of the Fluidization Technique in Biotechnology." *Canadian J. Chem. Eng.*, **67:**178-184.

Schulze, K. L. and R. S. Lipe. 1964. *Arch. Mikrobiol.*, **48:**1.

Shuler, L M. and F. Kargi. 1992. *Bioprocess Engineering.* Prentice Hall. Englewoods Cliffs, New Jersey

Silverstein, JoAnn, and E. D. Schroeder. 1983. "Performance of SBR Activated Sludge Processes with Nitrification/Denitrification." *J. WPCF*, **55**(4)**:** 377-384.

Simpkin, T. J. and W. C. Boyle. 1988. "The Lack of Repression by Oxygen of the Denitrifying Enzymes in Activated Sludge." *Water Res.*, **22**(2): 201-206.

Smith, R. N., J. Swinehart, and D. G. Lesnini. 1958. "Chromatographic Analysis of Gas Mixtures Containing Nitrogen, Nitrous Oxide, Nitric Oxide, Carbon Monoxide, and Carbon Dioxide." *Anal. Chem.*, **30**(7): 1217-1218.

Strand, S. E., A. J. MocDonnell, and R. F. Unz. 1985. "Concurrent Denitrification and Oxygen Uptake in Microbial Films. 1985. " *Water Res.*, **19**(3): 335-344.

Streuli, C. A. and P. R. Averell. 1970. *The Analytical Chemistry of Nitrogen and Its Compounds.* Part 1. Chapter 4, A Series of *Chemical Analysis.* Volume 28, Wiley-Interscience, New York, New York

Reproduced with permission of the copyright owner. Further reproduction prohibited without permission.

Suzuki, H. and Iwasaki, H. 1962. "Studies on Denitrification -- VI. Preparations and Properties of Crystalline Blue Protein and Cryptocytochrome c, and Role of Copper in Denitrifying Enzyme from a Denitrifying Bacterium." *J. Biochem.*, **52**(3): 193-199.

Szulczewski, D. H. and T. Higuchi. 1957. "Gas Chromatographic Separation of Some Permanent Gases on Silica Gel at Reduced Temperatures." *Anal. Chem.*, **29**(10): 1541 - 1543

Thibodeaux, L. J. 1979. *Chemodynamics*. John Wiley & Sons, New York, NY

Timberlake, D. L., S. E. Strand, and K. J. Williamson. 1988. "Combined Aerobic Heterotrophic Oxidation, Nitrification and Denitrification in a Permeable-Support Biofilm." *Water Res.*, **22**(12): 1513-1517.

Timmermans, P. and A. Van Haute. 1983. "Denitrification with Methanol -- Fundamental Study of the Growth and Denitrification Capacity of *Hyphomicrobium sp.*" *Water Res.*, **17**(10): 1249-1255.

Topiwala, H. 1971. "Temperature Relationship in Continuous Culture." *Biotech. Bioeng.*, **13**: 795-831.

US Environmental Protection Agency (EPA). 1979. "Sequential Nitrification - Denitrification in a Plug Flow Activated Sludge System." EPA - 600 / 2 - 79 - 157, Municipal Environmental Research Laboratory. Cincinnati, Ohio

US National Research Council. 1928. *International Critical Tables of Numerical Data, Phisics, Chemistry and Technology*. First Edition, 3: 259 McGraw-Hill, New York, New York

US National Research Council. 1972. *Accumulation of Nitrate*. National Academy of Sciences, Washington, D. C.

van der Hoek, J. P., Paul J. M. Latour, and A. Klapwijk. 1987. "Denitrification with Methanol in the Presence of High Salt Concentrations and At High pH Levels." *Appl. Microbiol. Biotech.*, **27**: 199-205.

van der Hoek, J. P., Paul J. M. van der Ven, and A. Klapwijk. 1988. "Combined Ion Exchange/Biological Denitrification for Nitrate Removal from Ground Water under Different Process Conditions." *Water Res.*, **22**(6): 679-684.

Weeg-Aerssens, E., J. M. Tiedje, and B. A. Averill. 1987. "The Mechanism of Microbial Denitrification." *J. Am. Chem. Soc.*, **109**(11): 7214-7215.

———. 1988. "Evidence from Isotope Labeling Studies for a Sequential Mechanism for Dissimilatory Nitrite Reduction." *J. Am. Chem. Soc.*, **110**: 6851-6856.

Reproduced with permission of the copyright owner. Further reproduction prohibited without permission.

Wilderer, P. A., W. L. Jones, and U. Dau. 1987. "Competition in Denitrification Systems Affecting Reduction Rate and Accumulation of Nitrite." *Water Res.*, **21**(2): 239-245.

Reference Manual for MINICHROM. A Chromatography Data Handling System. Version 1.5, VG Data Systems Ltd. (1990)

Waters Ion Chromatography Cookbook. Millipore Co., Revision 0.0, Manual Number 20195, Waters Chromatography Division, Ion Chromatography Group. (1989)

Instructions for Models 111, 211 and 311 Analytical Gas Chromatographs. Part Number 30491, Division B, Carle Instruments, Inc. (1975)

Coulter® SAMPLE STAND II Product Reference Manual. Part Number 4235432B, Coulter® Instruments, Inc. (1984)

Operator's Manual for Masterflex® EASY - LOAD® PUMP HEADS Model 7518 Series. Manual Number A - 1299 - 335, Cole-Parmer Instrument Co. (1993)

Operating Manual for Masterflex® L/S "Unified" Drives Model 7520 - 35 Series. Manual Number A - 1299 - 168, Cole-Parmer Instrument Co. (1993)

Operating Manual for BioFlo II: the Microprocessor Controlled Laboratory - Scale Fermentor. Manual Number M1151 - 0050, New Brunswick Scientific Co., Inc. (1987)

Omron SYSMAC - 90 Sequence Controller User's Manual. Omron Tateisi Electronics Co. (1986)

Reproduced with permission of the copyright owner. Further reproduction prohibited without permission.